UNIVERSITÀ DEGLI STUDI DI CAMERINO

School of Advanced Studies

PhD Course in Chemical and Pharmaceutical Sciences and Biotechnology

Curriculum: Pharmaceutical, Nutraceutical and Food Sciences

XXXV Cycle

Impact of cold plasma processing on the phytochemical profiles and main bioactive compounds of antioxidant dietary plants: *Eruca sativa* Mill., *Fragaria* × *ananassa* & *Cucumis melo* L.

Coordinator:

Prof. Sauro Vittori

PhD Candidate:

Doaa Abouelenein

Supervisor:

Prof. Sauro Vittori

Co-supervisor

Prof. Giovanni Caprioli

Academic years 2022–2023

Index

Acknowledgements V

Publications included in the thesis. VI

Other publications during PhD period. VII

List of tables VIII

List of figures X

List of schemes XIV

List of abbreviations and symbols XV

Abstract XVI

1. literature review 1

1.1. Introduction 1

1.2. Cold plasma (CP) 3

1.2.1. Plasma generation 4

1.2.2. Plasma activated water (PAW) 7

1.3. Rocket-salad leaves (*Eruca sativa* Mill) 8

1.4. Strawberries (*Fragaria* × *ananassa*) 10

1.5. Melons (*Cucumis melo* L.) 12

1.6. Effect of CP processing on plant food bioactive components 14

1.6.1. Effect of CP processing on total phenolic content (TPC) 14

1.6.2. Effect of CP processing on individual phenolic compounds 17

1.6.3. Effect of CP processing on vitamins 22

1.6.4. Effect of CP processing on volatile organic compounds (VOCs) 26

1.6.5. Effect of CP processing on antioxidant activity 38

2. Materials and methods 40

2.1. Plant material 40

2.1.1. Rocket-salad leaves 40

2.1.2. Strawberries 40

2.1.3. Melons 40
2.2. Plasma treatment 41
2.2.1. Rocket-salad leaves treatment by PAW 41
2.2.2. Strawberries treatment by DBD 42
2.2.3. Fresh-cut melon treatment by sDBD 43
2.3. Sample extraction for LC-MS/MS and spectrophotometric analysis 44
2.4. HPLC-ESI-MS/MS analysis 44
2.4.1. HPLC-ESI-MS/MS 44
2.4.2. Optimization of the HPLC-MS/MS analytical method 45
2.4.3. Method validation 46
2.5. Spectrophotometric analysis 49
2.5.1. Total phenolic content (TPC) 49
2.5.2. Total flavonoid content (TFC) 49
2.5.3. Antioxidant activity (AOA) 50
2.6. Determination of ascorbic acid content using HPLC-DAD 50
2.6.1. Ascorbic acid extraction 50
2.6.2. HPLC-DAD analysis 50
2.7. Simultaneous quantification of riboflavin, nicotinamide and nicotinic acid by UHPLC MS/MS 52
2.7.1. Acidic hydrolysis extraction of riboflavin, nicotinamide and nicotinic acid 52
2.7.2. UHPLC-ESI–MS/MS analysis 52
2.8. Volatile Organic Compounds (VOCs) Analysis 53
2.8.1 Headspace Solid-Phase Microextraction (HS-SPME) 53
2.8.2. GC-MS Analysis 53
2.9. Phytosterol Analysis By HPLC-DAD 55
2.9.1. Extraction of phytosterols from rocket-salad leaves samples 55
2.9.2. HPLC-DAD Analyses 55

2.10. Determination Of β-carotene and lutein contents by HPLC-DAD 55
2.11. GC-MS analysis of silylated primary metabolites 57
2.11.1. Metabolome extraction and two-step derivatization 57
2.11.2. Metabolomic analysis. 58
2.11.3. GC data pre-processing and metabolomic identification 59
2.12. Statistical analysis 65
3. Results and discussion 66
3.1. Impact of Plasma activated water (PAW) treatment on bioactive compounds of rocket-salad leaves. 66
3.1.1. Impact of PAW treatment on the LC-MS/MS phenolic profile of rocket-salad leaves 66
3.1.2. Impact of PAW treatment on TPC, TFC and DPPH radical scavenging activity of rocket-salad leaves 71
3.1.3. Impact of PAW treatment on L-ascorbic acid content of rocket-salad leaves 73
3.1.4. Impact of PAW treatment on vitamins B (riboflavin, nicotinamide, and nicotinic acid) contents of rocket-salad leaves 74
3.1.5. Impact of PAW treatment on the main VOCs of rocket-salad leaves 76
3.1.6. Impact of PAW treatment on the main phytosterols of rocket-salad leaves 86
3.1.7. Impact of PAW treatment on β-Carotene and lutein contents of rocket-salad leaves 88
3.2. The effect of DBD processing on the bioactive compounds of cold-stored strawberries 90
3.2.1. The effect of DBD processing on the LC-MS/MS polyphenolic profile of cold-stored strawberries 90
3.2.2. The effect of DBD processing on TPC and DPPH radical scavenging activity of cold-stored strawberries 96
3.2.3. The effect of DBD processing on L-ascorbic acid content of cold-stored strawberries 97

3.2.4. The effect of DBD processing on GC-MS-based primary metabolites profile of cold-stored strawberries 98

3.3. Influence of DBD plasma treatment on the bioactive compounds of cut-melon fruit. 107

3.3.1. Influence of DBD plasma treatment on the LC-MS/MS phenolic profile of cut-melon fruit. 107

3.3.2. Influence of DBD plasma treatment on TPC and DPPH of cut-melon fruit. 114

3.3.3. Influence of DBD plasma treatment on L-ascorbic acid content of cut-melon fruit. 115

3.3.4. Influence of DBD plasma treatment on vitamins B (riboflavin, nicotinamide, and nicotinic acid) contents of cut-melon fruit. 117

4. Conclusion 119

Bibliography 122

Acknowledgements

I am greatly honored to express my deep feeling of gratitude and sincere appreciation to **Prof. Vittori**, for his kind supervision, valuable scientific guidance, directions, comments and especially, for the great independence he gave to me. I would like to acknowledge **Prof. Caprioli**. for his continuous academic guidance and inspiration, his encouragement and support throughout the course of this thesis.

Special thanks to my research team and to my colleagues, without whom my PhD would not have been the same. I would like to express my gratitude to all of them for helping me during my stay in Italy and for providing me a very comfortable atmosphere to work in. I am indebted to all of them for my entire life.

This work was supported by the research project, "PLASMAFOOD - Study and optimization of cold atmospheric plasma treatment for food safety and quality improvement" founded by MIUR - Ministero dell'Istruzione dell'Università e della Ricerca - **PRIN**: Progetti di Ricerca di Rilevante Interesse Nazionale, Bando 2017. So, I would like to thank all the members of the project for their continuous help.

Further I am grateful to **Prof. Andrej Frolov**, from the Leibniz Institute of Plant Biochemistry (IPB) for the successful collaboration in the past and, hopefully, also in the future. I appreciate the support of all my colleagues in the IPB during my stage period in Germany. Thank you to all of you.

Last but not the least, I would like to offer my deep feelings of love and gratitude to **my husband, Ahmed Mustafa** for his keen help, encouragement, and support throughout all the hard and exhausting times.

To them all
With my love
Doaa Abouelenein

Publications included in the thesis.

1. Mustafa, A.M.; Angeloni, S.; **Abouelenein, D.**; Acquaticci, L.; Xiao, J.; Sagratini, G.; Maggi, F.; Vittori, S.; Caprioli, G. A new HPLC-MS/MS method for the simultaneous determination of 36 polyphenols in blueberry, strawberry and their commercial products and determination of antioxidant activity. *Food Chem.* **2021**, 130743.
2. Laurita, R.; Gozzi, G.; Tappi, S.; Capelli, F.; Bisag, A.; Laghi, G.; Gherardi, M.; Cellini, B.; **Abouelenein, D.**; Vittori, S. Effect of plasma activated water (PAW) on rocket leaves decontamination and nutritional value. *Innovative Food Science & Emerging Technologies* **2021**, 102805.
3. **Abouelenein, D.**; Angeloni, S.; Caprioli, G.; Genovese, J.; Mustafa, A.M.; Nzekoue, F.K.; Petrelli, R.; Rocculi, P.; Sagratini, G.; Tappi, S. Effect of plasma activated water on selected chemical compounds of rocket-salad (*Eruca sativa* Mill.) leaves. *Molecules* **2021**,*26*, 7691.
4. **Abouelenein, D.**; Mustafa, A.M.; Nzekoue, F.K.; Caprioli, G.; Angeloni, S.; Tappi, S.; Castagnini, J.M.; Dalla Rosa, M.; Vittori, S. The impact of plasma activated water treatment on the phenolic profile, vitamins content, antioxidant and enzymatic activities of rocket-salad leaves. *Antioxidants* **2023**, *12*, 28.
5. **Abouelenein, D.**; Caprioli, G.; Mustafa, A.M. Exploring the impacts of novel cold plasma technology on the volatile profile, flavor, and aroma properties of fruits and vegetables—A review. *Food Safety and Health* **2023**.
6. **Abouelenein, D.**; Mustafa, A.M.; Caprioli, G.; Soboleva, A., Frolova, N., Frolov, A.; Tappi, S. Vittori, S. "Impact of dielectric barrier discharge (DBD) plasma on microbiological properties and the patterns of primary and secondary metabolites in cold-stored strawberries" [To be submitted].

Other publications during PhD period.

1. Angeloni, S.; Mustafa, A.M.; **Abouelenein, D.**; Alessandroni, L.; Acquaticci, L.; Nzekoue, F.K.; Petrelli, R.; Sagratini, G.; Vittori, S.; Torregiani, E. Characterization of the aroma profile and main key odorants of espresso coffee. *Molecules* **2021**,*26*, 3856.
2. Mustafa, A.M.; Angeloni, S.; Nzekoue, F.K.; **Abouelenein, D.**; Sagratini, G.; Caprioli, G.; Torregiani, E. An overview on truffle aroma and main volatile compounds. *Molecules* **2020**,*25*, 5948.
3. Mustafa, A.M.; **Abouelenein, D.**; Acquaticci, L.; Alessandroni, L.; Abd-Allah, R.H.; Borsetta, G.; Sagratini, G.; Maggi, F.; Vittori, S.; Caprioli, G. Effect of roasting, boiling, and frying processing on 29 polyphenolics and antioxidant activity in seeds and shells of sweet chestnut (*Castanea sativa* Mill.). *Plants* **2021**,*10*, 2192.
4. **Abouelenein, D.**; Mustafa, A.M.; Angeloni, S.; Borsetta, G.; Vittori, S.; Maggi, F.; Sagratini, G.; Caprioli, G. Influence of freezing and different drying methods on volatile profiles of strawberry and analysis of volatile compounds of strawberry commercial jams. *Molecules* **2021**,*26*, 4153.
5. Nzekoue, F.K.; Borsetta, G.; Navarini, L.; **Abouelenein, D.**; Xiao, J.; Sagratini, G.; Vittori, S.; Caprioli, G.; Angeloni, S. Coffee silverskin: Characterization of B-vitamins, macronutrients, minerals and phytosterols. *Food Chem.* **2022**,*372*, 131188.
6. Mustafa, A.M.; **Abouelenein, D.**; Angeloni, S.; Maggi, F.; Navarini, L.; Sagratini, G.; Santanatoglia, A.; Torregiani, E.; Vittori, S.; Caprioli, G. A New HPLC-MS/ms method for the simultaneous determination of quercetin and its derivatives in green coffee beans. *Foods* **2022**,*11*, 3033.
7. Mustafa, A.M.; Mazzara, E.; **Abouelenein, D.**; Angeloni, S.; Nunez, S.; Sagratini, G.; López, V.; Cespi, M.; Vittori, S.; Caprioli, G. Optimization of solvent-free microwave-assisted hydrodiffusion and gravity extraction of *Morus nigra* L. fruits maximizing polyphenols, sugar content, and biological activities using central composite design. *Pharmaceuticals* **2022**, *15*, 99.
8. Omer, H.A.; Caprioli, G.; **Abouelenein, D.**; Mustafa, A.M.; Uba, A.I.; Ak, G.; Ozturk, R.B.; Zengin, G.; Yagi, S. Phenolic Profile, antioxidant and enzyme inhibitory activities of leaves from two cassia and two Senna species. *Molecules* **2022**, *27*, 5590.
9. Mustafa, A.M.; **Abouelenein, D.**; Acquaticci, L.; Alessandroni, L.; Angeloni, S.; Borsetta, G.; Caprioli, G.; Nzekoue, F.K.; Sagratini, G.; Vittori, S. Polyphenols, saponins and phytosterols in lentils and their health benefits: An overview. *Pharmaceuticals* **2022**, *15*, 1225.
10. **Abouelenein, D.**; Mustafa, A.M.; Caprioli, G.; Ricciutelli, M.; Sagratini, G.; Vittori, S. Phenolic and nuntritional profiles, and antioxidant activity of grape pomaces and seeds from Lacrima di Morro d'Alba and Verdicchio varieties. *Food Bioscience* **2023**, 102808.
11. **Abouelenein, D**.; Mustafa, A.M.; Caprioli, G.; Ricciutelli, M.; Sagratini, G.; Vittori, S. Phenolic and nuntritional profiles, and antioxidant activity of grape pomaces and seeds from Lacrima di Morro d'Alba and Verdicchio varieties. Food Bioscience 2023, 102808.
12. **Abouelenein, D**.; Caprioli, G.; Mustafa, A.M. Phloridzin: Advances on Resources, Biosynthetic Pathway, Bioavailability, Bioactivity, and Pharmacology. In *Handbook of Dietary Flavonoids*, Springer: 2023; pp. 1-29.
13. **Abouelenein, D.**; Acquaticci, L.; Alessandroni, L.; Borsetta, G.; Caprioli, G.; Mannozzi, C.; Marconi, R.; Piatti, D.; Santanatoglia, A.; Sagratini, G. Volatile Profile of Strawberry Fruits and Influence of Different Drying Methods on Their Aroma and Flavor: A Review. *Molecules* **2023**, *28*, 5810.

List of tables

Table 1: Influence of plasma treatments on TPC of processed fruits and vegetables as reported by some studies. 16

Table 2: Effect of cold plasma treatment on vitamin contents in treated fruits and vegetables. 25

Table 3: Effect of cold plasma treatment on volatile profile of various fruits and vegetables as reported by **(Abouelenein, Caprioli, et al., 2023)**. 28

Table 4: HPLC–MS/MS acquisition parameters (dynamic MRM mode) used for the analysis of the 36 marker compounds. 48

Table 5: Ultra-high performance liquid chromatography/tandem mass spectrometry (UHPLC–MS/MS) acquisition parameters (MRM mode) used for the analysis of..... 53

Table 6: In-house library containing 150 primary metabolites detected by untargeted gas chromatography-electron ionization-quadrupole mass spectrometry (GC-EI-Q-MS). 60

Table 7: Phenolic compounds determined by HPLC-MS/MS in control and PAW treated rocket-salad leaves processed at different times..... 70

Table 8: Changes in the TPC, TFC and DPPH of control and PAW treated rocket-salad leaves processed at different times. 72

Table 9: Vitamin C, riboflavin, nicotinic acid and nicotinamide contents of control and PAW treated rocket-salad leaves processed at different times..... 75

Table 10: Relative abundance of volatile organic compounds detected by HPSE-GC–MS of control and PAW treated rocket-salad leaves processed at different times. 77

Table 11: Phenolic compounds determined by HPLC-MS/MS in control and and DBD treated strawberry samples stored at 4 °for 6 days. 92

Table 12: Changes in the ascorbic acid, TPC and DPPH in control and and DBD treated strawberry samples stored at 4 °for 6 days (mean values ± standard deviation)..... 97

Table 13: GC-MS-based primary metabolites profile of cold-stored strawberries 101

Table 14: Phenolic compounds determined by HPLC-MS/MS in control and and DBD treated melon samples, processed at different times in presence of two different ozone concentrations. Expressed as (mg.100g^{-1} DW). 110

Table 15: TPC and DPPH in control and and DBD treated melon samples, processed at different times in presence of two different ozone concentrations. Expressed as (mg.100g^{-1} DW). 114

Table 16: Content of vitamin C, riboflavin, nicotinic acid and nicotinamide in control and DBD treated melon samples, processed at different times in presence of two different ozone concentrations. Expressed as (mg.100g^{-1} DW)..... 118

List of figures

Figure 1: The four fundamental states of matter and the composition of cold plasma modified from **(Birania, et al., 2022)**. 3

Figure 2: Cold plasma generation systems. A) Corona discharge B) DBD discharge C) Atmospheric pressure plasma jet (APPJ) D) Gliding arc discharge; modified from **(Domonkos, et al., 2021)**. 6

Figure 3: Illustration of PAW generation. A) plasma discharge over water surface and B) plasma discharge beneath water as reported by **(Q. Wang, et al., 2021)**. 7

Figure 4: Classification and structures of flavonoid subgroups. 19

Figure 5: Reaction of various plasma-generated reactive species with phenol. A) Hydroxyl radical; B) Nascent oxygen; C) Ozone; D) Superoxide radical via single electron transfer; E) Nitric oxide; F) Superoxide radical via hydrogen atom abstraction as reported by **(Kumar, et al., 2023)**. 21

Figure 6: Ascorbic acid decay and regeneration cycle as reported by **(Fernandes, et al., 2021; B. Zhang, et al., 2022)** 24

Figure 7: Chemical reactions induced by plasma reactive species on different food volatile components. 27

Figure 8: Schematic presentation of the experimental setup of the corona source during the production of plasma activated water. 41

Figure 9: HPLC-MS/MS chromatogram of a standard mixture of 36 phenolic compounds plotted as overlapped multiple reaction monitoring (MRM) transition of each analyte. (1) Gallic acid, (2) Neochlorogenic acid, (3) Delphindin-3-galactoside, (4) (+)-Catechin, (5) Procyanidin B2, (6) Chlorogenic acid, (7) *p*-Hydroxybenzoic acid, (8) (-)-Epicatechin, (9) Cyanidin-3-glucoside, (10) Petunidin-3-glucoside, (11) 3-Hydroxybenzoic acid, (12) Caffeic acid, (13) Vanillic acid, (14) Pelargonidin-3-glucoside, (15) Pelagonidin-3-rutinoside, (16) Malvidin-3-galactoside, (17) Syringic acid, (18) Procyanidin A2, (19) *p*-Coumaric acid, (20) Ferulic acid, (21) 3,5-Dicaffeoylquinic acid, (22) Rutin, (23) Hyperoside, (24) Isoquercitrin, (25) Delphindin-3,5-diglucoside, (26) Phloridzin, (27) Quercitrin, (28) Myricetin, (29) Naringin, (30) Kaempferol-3-glucoside, (31) Hesperidin, (32) Ellagic acid, (33) Quercetin, (34) Phloretin, (35) Kaempferol, (36) Isorhamnetin. 47

Figure 10: Determination of TPC using Folin-Ciocalteu method. 49

Figure 11: Determination of AOA using DPPH method. 50

Figure 12: Extraction and analysis of VOCs using HS-SPME and GC-MS/MS analysis. 54
Figure 13: Experimental workflow of primary metabolome extraction and metabolites derivatisation. 58
Figure 14: Impact of PAW treatment on the LC-MS/MS phenolic profile of rocket-salad leaves 67
Figure 15: Content of phenolic acids determined by HPLC-MS/MS control and PAW treated rocket-salad leaves processed at different times. PAW-2, PAW-5, PAW-10, and PAW-20 refer to rocket samples subjected to plasma-activated water (PAW) treatment for 2, 5, 10, and 20 min, respectively. Concentrations detected in mg.kg-1, DW 68
Figure 16: Changes in the TPC, TFC and DPPH of control and PAW treated rocket-salad leaves processed at different times. 72
Figure 17: Changes in ascorbic acid content of control and PAW treated rocket-salad leaves processed at different times. Means that do not share letters differ significantly ($p < 0.05$) according to Tukey's test. Legends: PAW-2, PAW-5, PAW-10, and PAW-20 73
Figure 18: Riboflavin, nicotinic acid and nicotinamide contents of control and PAW treated rocket-salad leaves processed at different times. 75
Figure 19: Representative chromatogram of the control rocket samples showing the major detected VOCs. 76
Figure 20: Enzymatic hydrolysis of glucoerucin by myrosinase enzyme into erucin and erucin nitrile. 80
Figure 21: Major VOCs detected in control and PAW treated rocket-salad leaves. A) Relative abundance of erucin nitrile in control and PAW-treated samples, B) Relative abundance of erucin and erucin nitrile in control and PAW-5- treated sample. 80
Figure 22: Dendrogram obtained from hierarchical clustering analysis (HCA) based on relative compositions of 52 VOCs detected by HS-SPME GC/MS in the control and PAW-treated rocket-salad samples at different processing times. 85
Figure 23: Changes in β-sitosterol and campesterol content of control and PAW treated rocket-salad leaves processed at different times. Legends: PAW-2, PAW-5, PAW-10, and PAW-20 refer to rocket samples subjected to plasma-activated water (PAW) treatment for 2, 5, 10, and 20 min, respectively. 87
Figure 24: Changes in β-carotene and lutein contents of control and PAW treated rocket-salad leaves processed at different times. Legends: PAW-2, PAW-5, PAW-10, and PAW-20 refer to rocket samples subjected to plasma-activated water (PAW) treatment . 89

Figure 25: Effects of cold plasma on the different phenolic classes in strawberries during cold storage. A) Total phenolic acids, B) Total anthocyanins, C) Total flavan-3-ols, D) Total dihydrochalcones, E) Total flavanones and F) Total flavonols. Data were expressed as the means ± SD of three replications. Storage time in days was put on X-axis as T0, T1, T3 &T6, concentrations expressed as mg.kg^{-1} DW. 94

Figure 26: Significantly changed compounds in strawberries immediately post plasma processing. 95

Figure 27: Significantly changed compounds in strawberries during storage day 1. 95

Figure 28: Significantly changed compounds in strawberries during storage day 6. 96

Figure 29: Effects of cold plasma on the ascorbic acid content in control and and DBD treated strawberry samples stored at 4 °for 6 days. 98

Figure 30: Representative total ion chromatogram (TIC) of the control strawberry sample showing the major detected primary metabolites. 100

Figure 31: Primary metabolomic analyses of both control (C-0) and DBD treated strawberries (T-0) at day 0. A) Scores plot of Principal component analysis (PCA); B) partial least square discriminant analysis (PLS-DA). 100

Figure 32: Analysis of the metabolomics data acquired upon sampling at different storage days of control and CP treated strawberries with partial least square discriminant analysis (PLS-DA) and sparse partial least square discriminant analysis (sPLS-DA). A) Score plots obtained by PLS-DA and B) sPLS-DA 105

Figure 33: Top 10 metabolites with the highest variables in projection (VIP) scores of sPLS-DA 106

Figure 34: Box plots of different metabolites of strawberry samples obtained from both control and CP treated samples at different days according to the Fisher's Lsd test at $P < 0.05$. The bar plots show the original values (mean±SD). 106

Figure 35: Phenolic acids determined by HPLC-MS/MS in control and and DBD treated melon samples, processed at different times in presence of two different ozone concentrations. Expressed as (mg.100g^{-1} DW). 111

Figure 36: Flavonoids determined by HPLC-MS/MS in control and and DBD treated melon samples, processed at different times in presence of two different ozone concentrations. Expressed as (mg.100g^{-1} DW). 111

Figure 37: Major pathways for biosynthesis of phenolic compounds during ozonation. 112

Figure 38: Reaction of various plasma-generated ozone with phenol **(Kumar, et al., 2023)** Structure and degradation of polyphenols 112

Figure 39: Cinnamic acid determined by HPLC-MS/MS in control and and DBD treated melon samples, processed at different times in presence of two different ozone concentrations. Expressed as (mg.100g^{-1} DW). 113

Figure 40: Proposed degradation of cinnamic acid by high ozone concentrations during cold plasma treatment of melon. 113

Figure 41: *L*-ascorbic acid determined by HPLC-DAD in control and DBD treated melon samples, processed at different times in presence of two different ozone concentrations. Expressed as (mg.100g^{-1} DW). 116

Figure 42: Content of riboflavin, nicotinic acid and nicotinamide in control and DBD treated melon samples, processed at different times in presence of two different ozone concentrations. Expressed as (mg.100g^{-1} DW). 118

Figure 43: Major parameters responsible for changes of bioactive compounds after cold plasma treatment..... 119

List of schemes

Scheme 1: Classification of plasma types modified from **(Birania, et al., 2022)**. 4

Scheme 2: various analysis performed on control and plasma treated rocket-salad leaves, strawberries, and melons. 13

Scheme 3: Phenolic compounds classification 15

Scheme 4: Processing of strawberries resulting in eight groups with n = 3 replicates per group. C: untreated group (control); T: plasma treated, each stored for 0, 1, 3 & 6 days.. 42

Scheme 5: Processing of melon resulting in nine groups with n = 3 replicates per group. Control and plasma treated groups at four different times. 43

List of abbreviations and symbols

APPJ	Atmospheric pressure plasma jet
AOA	Antioxidant activity
CP	Cold plasma
CAP	Cold atmospheric pressure
DBD	Dielectric barrier discharge
DW	Dried weight
DPPH	2,2-diphenyl-1-picryl-hydrazyl-hydrate
GHPs	Glucosinolate hydrolysis products
GC	Gas chromatography
GAD	Gliding arc discharge
GDP	Glow discharge plasma
GAE	Gallic acid equivalent
HMCPT	High microwave density-cold plasma treatment
ITCs	Isothiocyanates
LPCP	Low pressure cold plasma
λ_{max}	Maximum emission wavelength
MRM	Multiple reaction monitoring
NTP	Non-thermal plasma
O_3	Ozone
PAL	phenylalanine ammonia-lyase
PAW	Plasma-Activated Water
RE	Rutin equivalents
ROS	Reactive oxygen species
RNS	Reactive nitrogen species
SDBD	Surface dielectric barrier discharge
TPC	Total phenolic content
TFC	Total flavonoid content
TMS	Trimethylsilyl
UV	Ultraviolet
VOCs	Volatile organic compounds

Abstract

Nowadays the consumers awareness about the consumption of healthy and safe food products has been increased. For this, experts in the food industry are continuously searching for products with prolonged shelf life without affecting or even improving the food quality. Consequently, novel processing methods are gaining popularity to obtain high-quality products without negatively affecting functional stability, nutritional or sensorial properties; a recently introduced approach is cold plasma (CP) processing. Many studies have been published on the food processing by CP, focused mainly on the potentials of CP technology for microbial decontamination, the induced chemical, physical and physiological quality attributes. However, the impact of this novel technology on the main bioactive compounds presents in the processed food, especially plant-based foods, is still lacking in the available literature.

Consumers can not directly assess the nutritional or functional composition of food products; at the same time, they can evaluate external attributes (appearance and textural quality) or eating quality. Instead, they rely on information available in specialized publications and databases or conveyed in outreach documents or in labelling. Consequently, this work will emphasize how CP processing impact the biologically active compounds present in different treated samples. Strawberry, melon and rocket-salad leaves were selected to be under study for their high nutritional values, being rich in various phenolic compounds and vitamins, in addition to their antioxidant capacities and potential in the nutraceutical and functional food market.

Qualitative and quantitative comparisons were performed between untreated, and CP treated samples using selected bioactive compounds, focusing mainly on the total phenolic content and individual phenolic profile of each sample, antioxidant activity, major vitamins (C, B2 & B3) and other secondary and primary metabolites.

The present work shows that the interaction of plasma-reactive species with plant food components depends mainly on various processing conditions. Preserving and improving the phenolic profile and vitamins content are among the most promising potentials of cold plasma. Even so, a thorough insight on the impact of cold plasma on functional and bioactive food constituents is still a subject of imminent research.


1
literature
review

1. literature review

1.1. Introduction

Food is indispensable for survival of all organisms, being the main responsible for providing energy as well as nutrition. The different bioactive compounds present in food include phenolic compounds, vitamins, carotenoids, phytosterols and other antioxidant compounds, which support the different mechanisms responsible for the body′s repair and growth. Functional compounds derived from plant-based food mainly fruits and vegetables, consist of non-toxic phytochemicals like phenolics (phenolic acids, flavanone, flavonols, flavan-3-ols, anthocyanins, dihydrochalcones,…etc.), carotenoids, and phytosterols **(Idehen, et al., 2017)**. Although phytochemical compounds are not considered drugs, they are now universally recognized for being important for a healthy diet and disease prevention **(Sruthi, et al., 2021)**.

Nowadays the consumers awareness about the consumption of healthy and safe food products has been increased. To attend this demand, experts and researchers in the food industry are continuously searching for products with prolonged shelf life together with preserving or even improving the food quality. As a result, it is critical to develop effective processing methods for prolonging the fresh state and maintaining the content and activity of bioactive compounds in these products. This would improve their marketability and have a positive impact on human health **(Gutiérrez, et al., 2018a; Nunes, et al., 2013)**. To date, thermal, chemical and mechanical processing are the most common food processing methods. However, it is noteworthy that they could lead to a shortfall in the nutritional value food components. Phenolic compounds, pigments, minerals, vitamins and other bioactive compounds are sensitive to severe process parameters such as high temperature leading to loss of nutrient bioavailability and organoleptic properties **(Galanakis, 2021)**.

Consequently, novel processing methods are gaining popularity to obtain high-quality products without negatively affecting functional stability, nutritional or sensorial properties. Among those methods are high-pressure processing **(Marszałek, et al., 2017)**, ultrasound processing **(Adekunte, et al., 2010)**, radiation processing **(Tremarin, et al., 2017)**, pulsed electric field **(Buckow, et al., 2013)** and cold plasma (CP) **(Kumar, et al., 2023)**.

Recently, cold plasma (CP) has become the centre of research for food processing and became among the inevitable and profitable food industry choices due to its short treatment time and minimal thermal effects on the food products with potential enzyme inactivation

(Misra, 2016), toxin removal **(Misra, 2015)**, food decontamination **(Misra, et al., 2011)** and packaging modification **(Mandal, et al., 2018; Shashi Kishor Pankaj, et al., 2014)**. Plasma is the fourth state of matter and CP has many applications in different industrial sectors, however recently, there is a great interest and growing research efforts in using the CP technique as an alternative food processing method **(Misra, 2016)**.

Many studies published on the food processing by CP, focused mainly on the potentials of CP technology for microbial decontamination **(Ekezie, et al., 2019; Misra, et al., 2017; Nwabor, et al., 2022; Punia Bangar, et al., 2022)**, the induced chemical, physical and physiological quality attributes **(Bourke, et al., 2018; Y.-Q. Chen, et al., 2020; Saremnezhad, et al., 2021)**. However, the impact of this novel technology on the main primary and secondary metabolites present in the processed food and the mechanism of the interaction between plasma particles and food bioactive compounds is still lacking in the available literature. In this context the aim of the present work is to better understand the changes happening in the major bioactive compounds present in the cold plasma treated samples. Strawberry, melon and rocket-salad leaves were selected to be under study for their high nutritional and antioxidant capacities. Qualitative and quantitative comparisons were performed between untreated, and CP treated samples using selected bioactive compounds focusing mainly on the total and individual phenolic profile of each sample, antioxidant activity, major vitamins (C, B2 & B3) and other metabolites.

1.2. Cold plasma (CP)

Plasma as an ionized or partially ionized gas is the fourth state of matter constitutes of highly excited ionic and reactive species **(Bußler, 2017; Misra, 2016; Misra, et al., 2016)**. Plasma contains plenty of charged particles (OH^-, H_2O^+, electrons), reactive oxygen species (ROS), reactive nitrogen species (RNS), excited molecules (excited O_2, N_2), UV photons, and positive and negative ions **(Liao, et al., 2019; Scholtz, et al., 2015)**. ROS include superoxide anion, atomic oxygen, singlet oxygen, hydroxyl radical, ozone (O_3). RNS including nitrogen, atomic nitrogen, nitric oxide, in addition to other species present in plasma as: UV photons, free electrons, and positive and negative ions (Figure 1).

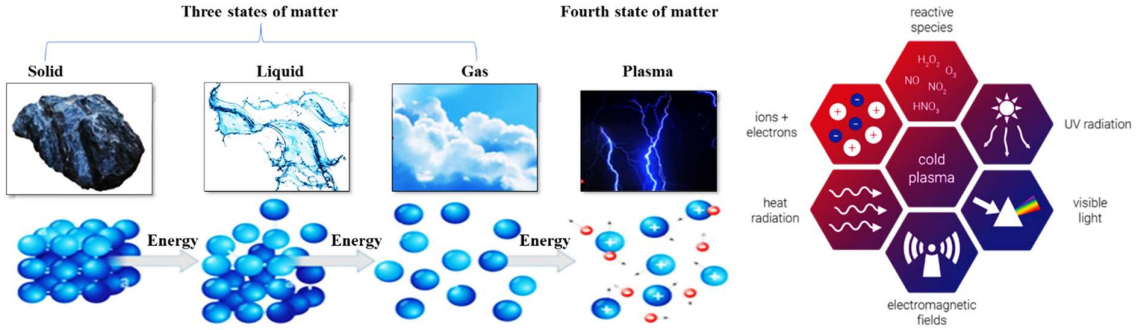

Figure 1: The four fundamental states of matter and the composition of cold plasma modified from **(Birania, et al., 2022)**.

As shown in scheme 1, plasmas are divided into high temperature and low temperature types, based on their mechanism of generation and the relative temperature between electrons, ions, and particles with no electric charge **(Puligundla, et al., 2020)**. High temperature plasma is achieved by heating gas in sufficiently high temperatures (around 20,000 K) to be ionized, resulting in the thermodynamic temperature equilibrium among all chemical species **(Misra, 2016)**. The low-temperature plasma is divided into thermal plasma (around 373.15 to 423.15 K), in which there is a local thermodynamic equilibrium among the species. The later type is the non-thermal plasmas (about 333.15 K) which is also called cold plasma and is produced by means of electrical discharges **(Misra, et al., 2016; Puligundla, et al., 2020; Sruthi, et al., 2021)**.

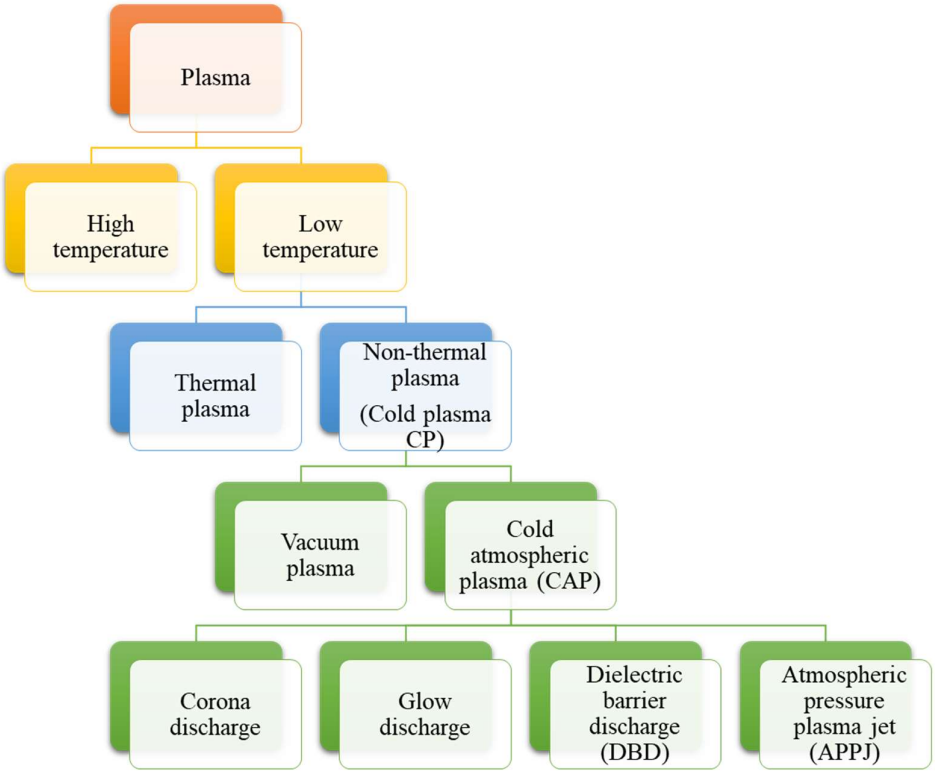

Scheme 1: Classification of plasma types modified from **(Birania, et al., 2022)**.

1.2.1. Plasma generation

Cold plasma can be achieved under atmospheric pressure or partial vacuum through ionization of different gas types. Different electrical discharge methods may be used for plasma generation such as corona discharge, dielectric barrier discharge (DBD), plasma jet, gliding arc discharge, etc. **(Domonkos, et al., 2021; Sakudo, et al., 2020; Sruthi, et al., 2021)**.

Corona discharge (Figure 2**A**) is usually created at atmospheric pressure, in which gas ionization occurs mainly in the sharp electrode. The system can work at the direct current or pulsed voltage mode and doesn't need a complex apparatus and large operating costs. It is generated by the application of high voltage between two or more sharp electrodes. The ionization process creates a crown around this active electrode. Coronas are very weak discharges, having very low electron and ion densities. Among the disadvantages of this system the non-uniformity of treatment and small sample area **(Domonkos, et al., 2021; Saremnezhad, et al., 2021)**.

As shown in figure 2**B**, in DBD devices two electrodes with dielectric covers (such as glass, plastic, silicon, or ceramic) are used for plasma generation. The insulators are

important to prevent an arc discharge and avoid the thermal plasma generation. DBD operates over a wide range of gas pressures and at frequencies between 0.05 and 500 kHz. A mong the advantages of this system the possibility of using different geometries for electrodes and wide variety of gases, the very short period of time for plasma generation, the homogenous discharge and the no need for gas flow **(Domonkos, et al., 2021; Sakudo, et al., 2020; Saremnezhad, et al., 2021)**.

The atmospheric pressure plasma jet (APPJ) shown in figure 2**C**, is a type of cold plasma discharge that produces a high velocity stream of highly reactive chemical species with weak emitted light. APPJs typically consist of two concentric cylindrical electrodes, where the inner electrode is connected to a power source at high frequency, inducing ionization of the working gas (mainly helium or argon). The gas exits through a nozzle, which gives a "jet-like" appearance **(Domonkos, et al., 2021)**.

Gliding arc discharge plasma reactors (Figure 2**D**) are known as hot plasma sources, however, under specific conditions they may also produce cold plasma. The gliding arc plasma can combine the advantages of both thermal and nonthermal plasmas (nonthermal plasma conditions at higher power). The discharge is formed by a high voltage at the spot where the distance between diverging electrodes is the shortest (~ in the range of millimeters). Electrodes are placed in a fast gas flow and the discharge increases its volume and length in the flow direction **(Domonkos, et al., 2021)**.

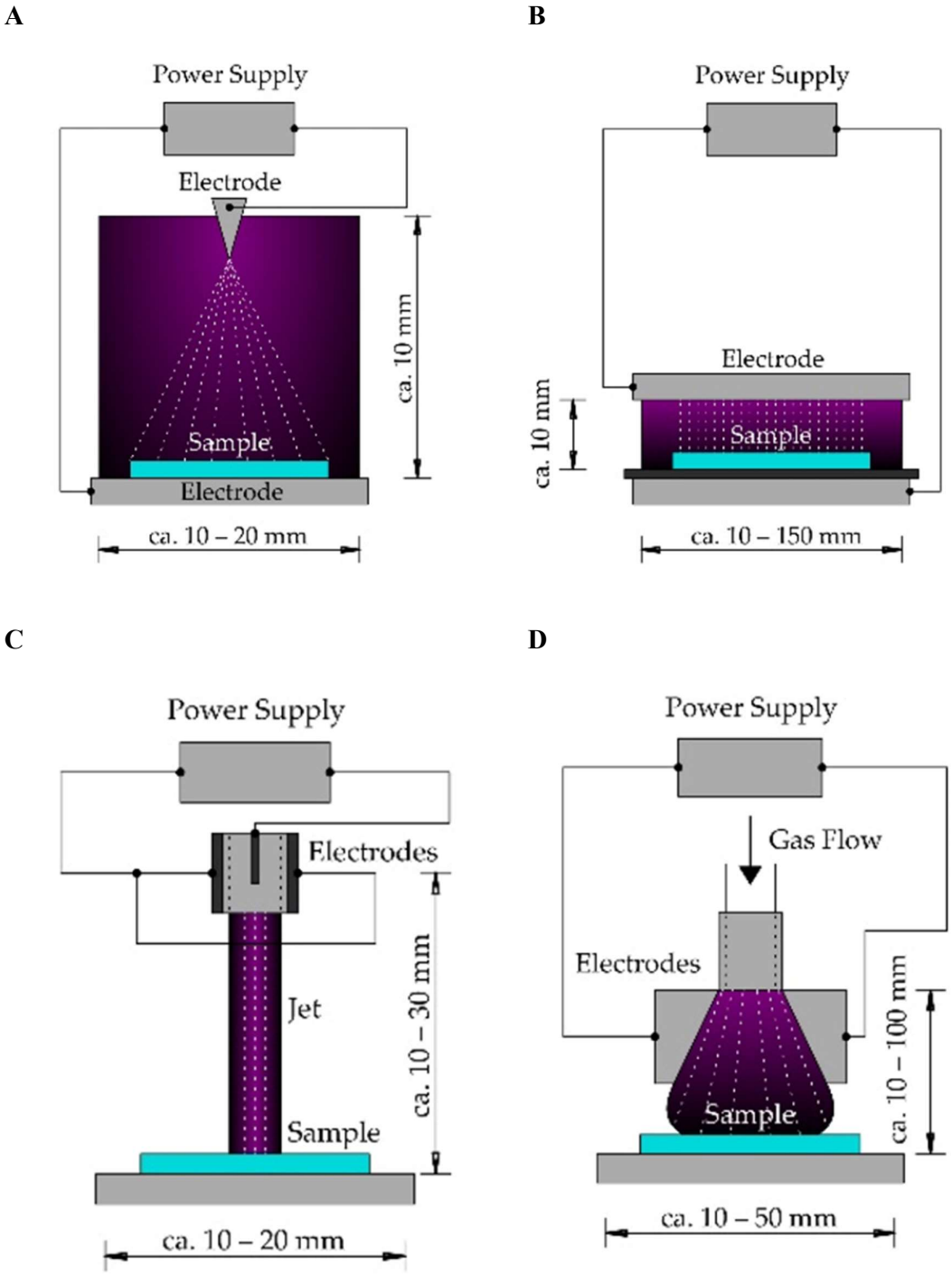

Figure 2: Cold plasma generation systems. A) Corona discharge B) DBD discharge C) Atmospheric pressure plasma jet (APPJ) D) Gliding arc discharge; modified from **(Domonkos, et al., 2021)**.

1.2.2. Plasma activated water (PAW)

In addition to directly exposing food to plasma discharges, using PAW as a delivery medium for plasma-generated reactive species has also shown a promising decontamination effect in recent years. Whereby the targeted product is not subjected directly to the plasma discharge, but is in contact with water which was pre-exposed to plasma discharge **(Q. Wang, et al., 2021)**. Compared to direct gas plasma treatment, PAW has the advantage that treated food become indirectly exposed to the harmful plasma reactive species **(Patra, et al., 2022)**.

1.2.2.1. PAW generation

As shown in figure 3, PAW is generated by applying plasma treatment to water with the plasma plume above or underneath water surface. Water molecules interact with the plasma-generated reactive particles and create several chemical reactions, which produce a mixture of biochemical reactive species called PAW. Depending on the chemical environment, generation mode, device set up and voltage, the ROS and RNS can be formed in the liquid and at the gas-liquid interface. There are several non-thermal plasma-water reaction systems, such as DBD, pulsed corona discharge, APPJ and gliding arc discharge **(Patra, et al., 2022)**..

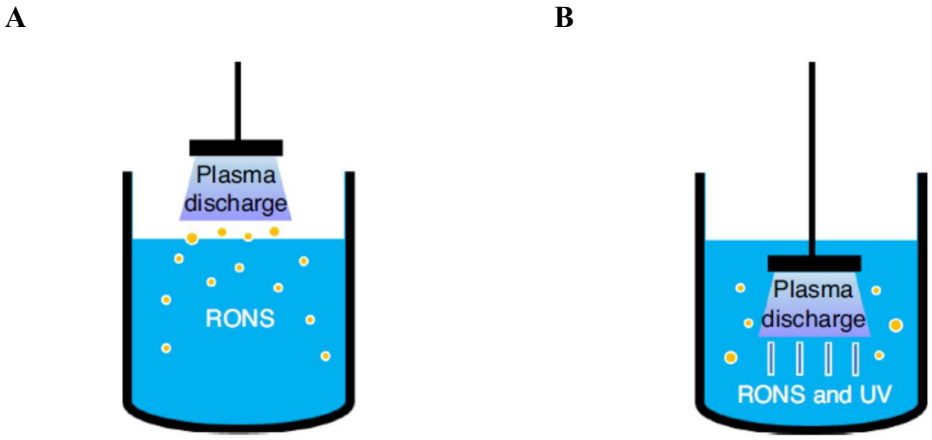

Figure 3: Illustration of PAW generation. A) plasma discharge over water surface and B) plasma discharge beneath water as reported by **(Q. Wang, et al., 2021)**.

1.3. Rocket-salad leaves (*Eruca sativa* Mill)

Eruca sativa Mill, also known as arugula salad, cultivated rocket, rucola, or roquette, is gaining popularity as a fresh cut ready-to-eat product. Plant leaves are commonly sold in whole bags, mixed salad bags or as gourmet micro-leaves **(Bell, et al., 2016)**. Its a vegetable of the Brassicaceae family which is characterized by its pleasant bitter taste. It is not only originated in the Mediterranean region, but also widely distributed all over the world **(Khoobchandani, et al., 2011)**. Vegetables of the Brassicaceae family are generally an excellent source of different bioactive compounds and vitamins. Rocket leaves contain high levels of vitamin C together with other vitamins as vitamin A, K and vitamins B-1, B-2, B-3 and B-6 **(Gutiérrez, et al., 2018b)**. It also contains a large number of bioactive constituents, mainly glucosinolates and polyphenolic compounds **(Sut, et al., 2018)**. Phenolic acids, including: ferulic, coumaric, ellagic and benzoic acids, were previously detected in rocket **(Sadiq, et al., 2014)**. Regarding flavonoids, quercetin, kaempferol and isorhamnetin are the main aglycones commonly isolated from Brassicaceae vegetables **(Avato, et al., 2015)**. Moreover, the major flavonoid glycosides found in different rocket species are quercetin, kaempferol and isorhamnetin glycosides **(Bell, et al., 2019; Khoobchandani, et al., 2011)**. Quercetin, kaempferol and isorhamnetin aglycons together with other quercetin glycosides were previously identified and quantified by LC-ESI-MS in freeze-dried rocket leaves **(Sut, et al., 2018)**. These compounds, due to their antioxidant properties ensure greater protection against disorders such as cancer and cardiovascular diseases **(Cory, et al., 2018)**. A common use for the plant was as an aphrodisiac, which was reported in ancient texts. It's also reported to have potential antioxidant, immune boosting and anti-inflammatory effects **(Bell, et al., 2019)**.

Rocket is also valued for its sensory and nutritional properties given by the volatile organic compounds (VOCs) found in the plant. VOCs comprise glucosinolate hydrolysis products (GHPs), alcohols, ketones, aldehydes, fatty acids, esters, and alkanes **(Bell, et al., 2016; Blažević, et al., 2008)**. It is widely accepted that the rocket distinctive aroma and flavour are produced by GHPs. This aroma could influence the sensory attributes perceived by the consumers and determine whether the product will be accepted or rejected, influencing the product re-purchase. **Azarenko, et al. (2014)** has focused on the application of erucin (a major compound in rocket) to human breast adenocarcinoma cells. Also, rocket leaves were previously reported to increase plasma nitrate and nitrite which could reduce the blood pressure significantly **(Jonvik, et al., 2016)**. The plant is also rich in other

nutrients such as phytosterols, carotenoids and fibers **(Bell, et al., 2014; Khoobchandani, et al., 2011; Martínez-Sánchez, et al., 2006; Spadafora, et al., 2016)** which are responsible for their health promoting effects.

The major post-harvesting problem of rocket vegetable is its rapid senescence, expressed primarily as yellowing and wilting **(Koukounaras, et al., 2007)**, which is accompanied also by a loss of ascorbic acid, glucosinolates and other bioactive compounds **(Force, et al., 2007)**. Therefore, it is very important to develop effective post-harvest processing methods to prolong its shelf-life as well as to preserve or even increase the content and the activity of these antioxidant compounds. This would improve the marketability of rocket and would have positive effects on its quality **(Gutiérrez, et al., 2018b)**. Among the known processing treatments for extending storage life of minimally processed rocket are cold storage **(Force, et al., 2007)**, and the use of food disinfectants such as chlorine, calcium oxide and acetic acid **(Agagunduz, et al., 2017)**. However, these methods have led to good inactivation of microorganisms but can alter the sensory and nutritional properties of foods. Therefore, new emerging technologies have been introduced to improve productivity by increasing the shelf life of rocket-salad without changing their nutritional and organoleptic properties **(de Castro, et al., 2020)**.

PAW has proven to be a promising strategy for the decontamination of rocket-salad leaves and is regarded as a promising alternative to hypochlorite treatment, with the advantage of having a less negative impact on the environment and the health of consumers. Shorter PAW treatments have shown a significant reduction in populations of Enterobacteriaceae and psychotropic bacteria, and higher inactivation were obtained for all studied microbial groups after 2 min of treatment **(Laurita, et al., 2021)**. However, little information on the effect of PAW on the content of the bioactive compounds of rocket-salad has been reported. For this reason, the present work aims to evaluate for the first time the effect of different processing times (2, 5, 10, and 20 min) of the PAW technique on the rocket-salad bioactive compounds phenolic composition, vitamins, volatile profile, phytosterols and carotenoids in order to evaluate the use of this technology as an alternative decontamination method and to provide a new insight for its utilization as a safe alternative for rocket-salad leaves decontamination.

1.4. Strawberries (*Fragaria* × *ananassa*)

Strawberries (*Fragaria* × *ananassa*) are among the most widely medicinal dietary planted fruit crops all over the world with global annual output exceeding nine million tons in 2017. This fruit is rich in natural antioxidants and other bioactive compounds and is recognized therefore for its pronounced anticancer, antioxidation, and anti-inflammatory properties **(Mustafa, Angeloni, et al., 2022)**. The nutritional value of strawberry fruits is mainly attributed to the high contents of multiple natural products, mostly represented by phenolics. Indeed, in the list of the 100 richest sources of dietary phenolics, strawberries are ranked as no. 9. The importance of dietary phenolics is to a large extent attributed to their high antioxidant activity **(Huang, et al., 2022; Mustafa, Angeloni, et al., 2022)**. The most frequently identified classes of phenolics in strawberries are represented by anthocyanins (being responsible for their bright red colour), phenolic acids and hydrolysable tannins. High contents of flavan-3-ols: epicatechin, and procyanidin derivatives were reported for this plant **(Mustafa, Angeloni, et al., 2022)**. Further phenolics present in strawberry in lower concentrations including flavonols, which dominate by glycosides of quercetin and kaempferol. Moreover, the presence of procyanidins in fruits resulting in an astringent and unfavourable taste was also reported **(Fernández-Lara, et al., 2015)**.

The organoleptic properties of strawberries depend mainly on the presence of a broad range of primary metabolites as amino acids, sugars and organic acids. Thereby, sugars define the sweetness of fruits, while organic acids influence their acidity. Importantly, these metabolites not only affect the quality of strawberries but also play an important role in the development and maturation of its fruits **(Huang, et al., 2022)**.

Noteworthily, strawberries have short postharvest shelf life, as their fruits are susceptible to mechanical injury, physiological deterioration and microbial decay during storage **(L. Li, et al., 2019)**. Therefore, their preservation is a challenging task. Consequently, improving the shelf life of the strawberry fruits by all means including their post-harvest treatments is absolutely mandatory. To control postharvest diseases of the strawberry fruits, conventional synthetic chemicals are routinely used. However, their application is associated with environmental and human health concerns, and, therefore, their use is strictly regulated **(Salazar-Orbea, et al., 2023)**. For example, fruit decontamination by chlorine-based washing, as well as washing fresh and fresh-cut products is currently prohibited in many countries **(Misra, Patil, et al., 2014)**. Thermal treatments to inactivate microorganisms and enzymes are also used to extend the shelf-life of fruits however, it could induce irreversible

losses of nutritional compounds and/or undesirable changes in physicochemical properties. It was reported earlier that thermal processing of strawberry fruits results in a significant reduction of antioxidant capacity (18%), ascorbic acid contents (36%), total phenolics and flavonoid contents (22% and 25%, respectively) **(Odriozola-Serrano, et al., 2008)**. Therefore, the evaluation of non-thermal technologies became essential for extending the shelf life of food products in general and for strawberry specifically without affecting their nutritional value.

In this context, being a novel dry and non-thermal chemical-free technology, atmospheric pressure cold plasma (ACP) offers distinct advantages for food decontamination and processing. Previous studies reported the positive effects of DBD on decontamination of both fresh **(Ahmadnia, et al., 2021; Misra, Moiseev, et al., 2014; Misra, Patil, et al., 2014)** or fresh-cut strawberries **(M. Li, et al., 2019)** and strawberry juice **(Mehta, et al., 2020)**. However, the effects of DBD on the nutritional quality, main bioactive compounds of whole fresh strawberry fruits are only minimally addressed so far.

Therefore, the objective of this study was to gain a deep understanding of the alterations in nutritional composition of strawberries associated with DBD treatment and to characterize the DBD-associated dynamics of primary and secondary metabolites in much detail. This knowledge would ensure the safety of the commercial application of this method in future. Therefore, HPLC-MS/MS was used for simultaneous quantitation of 38 bioactive phenolic compounds present in strawberries. In addition, the effects of the DBD treatment on the total contents of polyphenols and flavonoids contents, as well as the associated antioxidant activity, were also addressed. GC-MS-based analysis of primary metabolites was also accomplished and comprehensively analysed by multivariate and univariate statistics. This data will then be further employed as an important part of the ongoing research on optimizing and improving CP treatment parameters in strawberries processing.

1.5. Melons (*Cucumis melo* L.)

Melon (*Cucumis melo L.*) is one of the most consumed fruits all over the world due to its high nutritional value and pleasant flavour. It's rich in biologically active compounds that exert beneficial effect on human health including non-essential phytochemicals (e.g., polyphenols) and essential nutrients (e.g., vitamins) **(Amaro, et al., 2015; Ismail, et al., 2010)**. Due to the large size of the fruit, need for preparation and waste disposal of fresh-cut melons are more convenient for the modern consumer. However, crevices, cracks, and small fissures in melon fruit peel, provides an environment on which bacteria can strongly attach and transferred to the flesh during cutting. This complex netting peel will also prevent chlorine and other sanitizers from reaching the microorganisms. However, fresh-cut melon has been reported to be a vehicle for *Salmonella enterica* resulting in several salmonellosis outbreaks. The US Centres for Disease and Control and Prevention (CDC) has reported about 34 foodborne disease outbreaks in USA after melon consumption most of them were caused by *Salmonella* **(**CDC**2011)**. Moreover *Salmonella* melon outbreak in year 2019 resulted in 38 hospitalizations and 137 reported illnesses and in the USA **(**CDC**2019)**. Also, *Listeria monocytogenes* food poisoning was reported among the most common melon outbreaks which led to 32 deaths and 146 illnesses **(**CDC**2011)**. Therefore, more studies are required regarding fresh-cut melon preservation methods **(Burnett, et al., 2000; Richards, et al., 2004; Selma, et al., 2008)**.

Considering the consumers' demands for fresh-cut melon with improved shelf-life, microbial safety and high nutritional quality studies have well demonstrated many traditional techniques including UV-C light **(Chisari, et al., 2011; Kasim, et al., 2014; Manzocco, et al., 2011)** electron beam irradiation **(Palekar, et al., 2015)**, X-ray **(Mahmoud, 2012)**, edible coatings **(Martiñon, et al., 2014)**, gaseous ozone **(Selma, et al., 2008)** or modified atmosphere packaging **(Oms-Oliu, et al., 2008; B.-Y. Zhang, et al., 2013)**. Others have been focused on the use of sanitizers which is the currently used method at the industry **(Nicolau-Lapeña, et al., 2022; A. Silveira, et al., 2010; Ukuku, et al., 2015; L. Zhu, et al., 2022)**.

Consequently, the growing demand for fresh-cut products has pushed the researchers to develop new non-thermal treatments able to keep a desirable shelf-life, preserving the original fresh-like nutritional and sensory properties of the raw material. Among those the novel non-thermal plasma treatment where the impact of cold plasma treatment, on fresh-cut-melon microbiological aspects **(Tappi, et al., 2016)** and volatile profiles **(Zhou, et al.,**

2022) were previously reported. The results indicate that among all the different plasma constituents, the most important role in microbial inactivation and protein denaturation seems to be played by reactive species, however those are also responsible for the induced negative changes in the nutritional and sensorial qualities.

Compositional quality (nutritional and phytochemical profile) is built during melon production. The content of biologically active compounds results, in the end, from the interaction between a genotype and environmental factors, modulated by the horticultural techniques. A general understanding of how melon bioactive compounds and antioxidant activity are affected by cold plasma treatment parameters provides valuable information for understanding the impact of this novel technology on melon quality. In this context, the aim of this research was to evaluate the effects of cold plasma, generated by a sDBD device at two different operative conditions and four different treatment times each, on fresh-cut-melon phenolic profile and vitamins content.

In scheme 2 the various analysis performed on rocket-salad leaves, strawberries, and melons performed in the present work are shown.

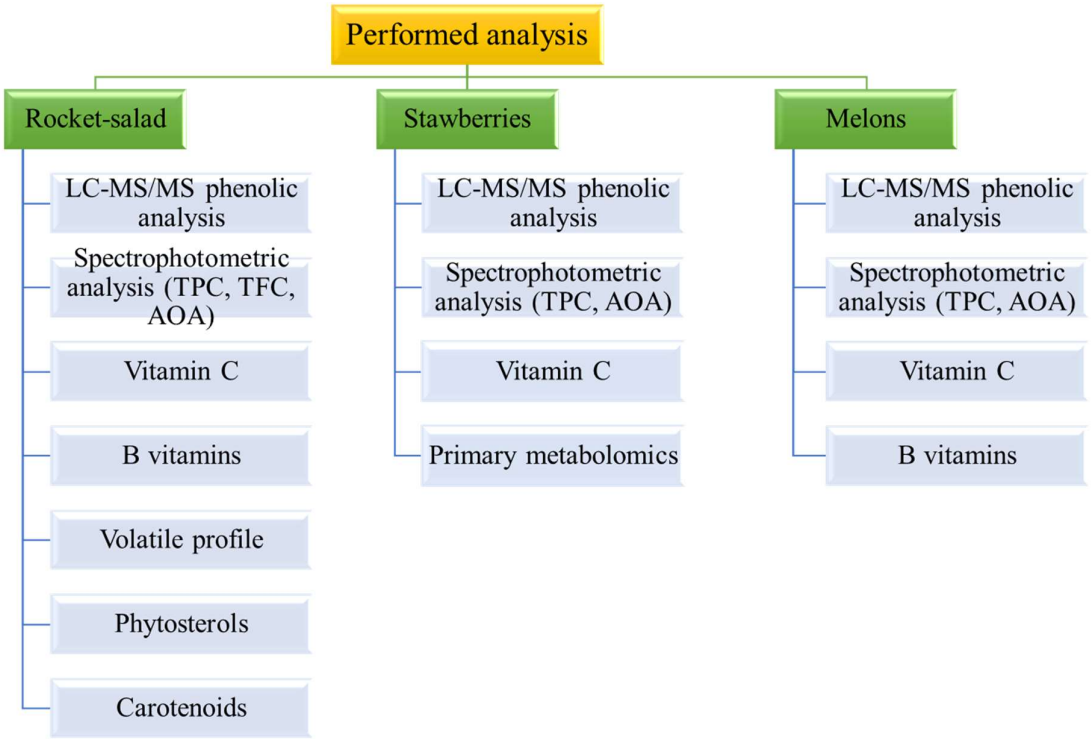

Scheme 2: various analysis performed on control and plasma treated rocket-salad leaves, strawberries, and melons.

1.6. Effect of CP processing on plant food bioactive components

Although plasma technology has matured in applications related to some sectors, it remains under-exploration in the food processing sector. While promising results have been documented in relation to some food applications, such as microbial decontamination, disinfection, germination enhancement, modification of food properties, and quality retention, a clear picture on the exact reactions, mechanisms and reactive components responsible for the changes in the food bioactive composition is still required **(Misra, 2016; Misra, et al., 2016)**. Though various reactive species are present in plasma, key reactive species with high reactivity, such as **.**OH, H, O_3 and NO are considered to be the major responsible for dominant changes in the food bioactive components **(Dharini, et al., 2022)**. Since the modifications in the chemical composition of the processed food depend mainly on the source of the plasma, to obtain a clear view of plasma-food interactions, investigating the interaction of reactive species with food must be prioritized **(Muhammad, et al., 2018)**. Consequently, this work aims to present a concise portrayal of cold plasma processing in the food industry and its effect on plant secondary metabolites (e.g., phenolic compounds, volatile organic compounds (VOCs) and phytosterols), primary metabolites (e.g., sugars, amino acids and fatty acids) and plant vitamins (mainly vitamin C).

1.6.1. Effect of CP processing on total phenolic content (TPC)

Phenolic compounds are one of the most important secondary bioactive metabolites in fruits and vegetables. They counteract oxidative stress and considered to be determinant of foods' antioxidant potentials **(Sruthi, et al., 2021)**. They contain at least one aromatic ring with one or more hydroxyl substituents and are mostly found in conjugated forms with mono and polysaccharides. They comprise flavonols, flavones, isoflavones, flavan-3-ols, lignans, anthocyanidins in addition to phenolic acids (Scheme 3). Many researchers have demonstrated the impact of CP treatment on phenolic compounds of food. Recently some review articles have been published focusing mainly on changes of polyphenolic profile after CP processing **(Kumar, et al., 2023; Muhammad, et al., 2018; Munekata, et al., 2020; Shashi K Pankaj, et al., 2018; Saremnezhad, et al., 2021; Sruthi, et al., 2021)**.

There are contradictory results about the effect of CP treatment on the total phenolic content of processed fruits and vegetables. Non-significant changes of the TPC were reported by some authors post plasma treatment, other studies showed significant increase in the TPC while others reported significant reductions after CP treatment. The effect of CP on TPC of fruits and vegetables has been summarized and illustrated in table 1.

Many hypothesis were done to explain the increase of TPC after cold plasma treatment. **X. Li, et al. (2019)** explained the accumulation of phenolic compounds post plasma treatment to be a defensive mechanism of plants against CP treatment which acts as an abiotic elicitor. They also hypothesized that CP could induce the increase of the ATP content and accelerate the utilization of sugars resulting in stimulating the biosynthesis of phenolic compounds. Other explanation was proposed by **Illera, et al. (2019)**, that reactive species of plasma can cause the degradation of the cell membrane and enhance the release of phenolic compounds. Consequently, the increase in TPC is due to the high extractability resulting from cellular structures disruption.

On the other hand, TPC reduction was observed in many studies and mainly related to the modification or inactivation of enzymes involved in the phenylpropanoid pathway which could affect the content of phenolics of a plant. Probable degradation of phenolics or inactivation of phenylalanine ammonia-lyase (PAL) has been introduced as the reasons for this reduction **(Zargarchi, et al., 2019)**. PAL is a key enzyme in the biochemical pathway of phenolics biosynthesis in plants which catalyse the non-oxidative deamination of *L*-phenylalanine to 7,8-unsaturated *trans*-cinnamic acid and an ammonium ion.

In brief, considering the results of different research, it seems that the type and variety of the plant and the condition of the CP treatment are of the most important and effective parameters in the content of phenolic compounds in the treated samples.

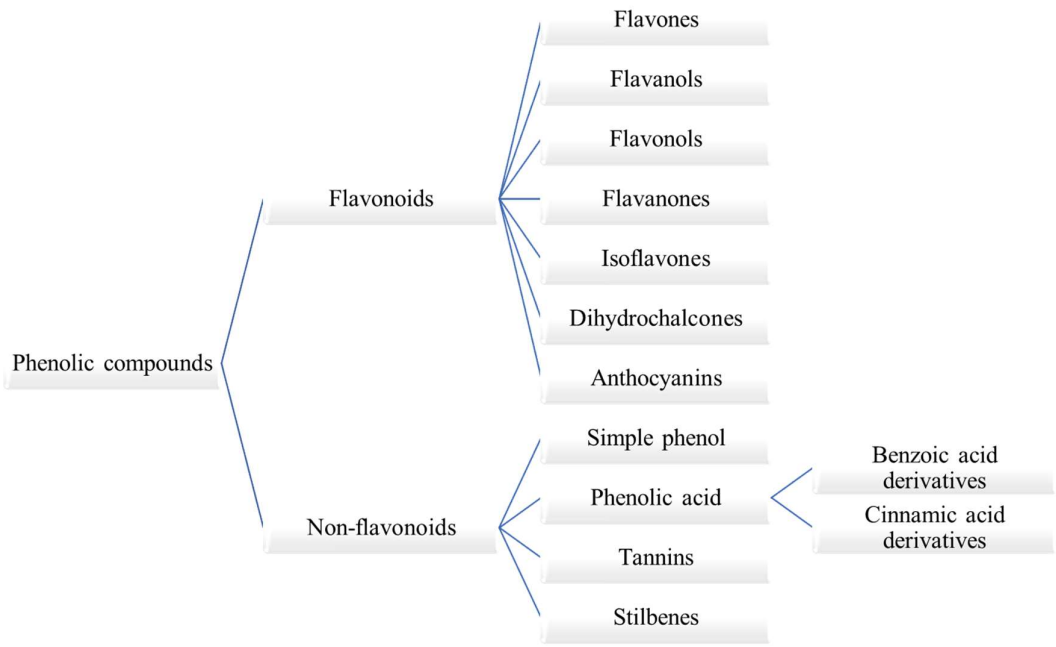

Scheme 3: Phenolic compounds classification

Table 1: Influence of plasma treatments on TPC of processed fruits and vegetables as reported by some studies.

Sample	Plasma treatment				Findings on TPC	Reference
	Plasma source	Power/voltage	Frequency	Exposure time		
Orange juice	Air (DBD)	70 kV	50 Hz	15–60 s	Non-significant change in TPC	**(Almeida, et al., 2015)**
Fresh and dried walnuts	Air (DBD)	15 kV	12 kHz		Non-significant change in TPC	**(Amini, et al., 2016)**
Whole strawberries	Air (DBD)	60 and 80 kV			Non-significant change in TPC	**(Misra, et al., 2015)**
Mandarin	Microwave	900 W	2.45 GHz	10 min	Non-significant change in TPC	**(Won, et al., 2017)**
Kiwi fruit	Air (DBD)				Increase by 5% at 15 kV and 40 min	**(Ramazzina, et al., 2015)**
Tomato juice	DBD	60 kV	50 Hz	10 and 15 min	Increase by 4% at 60 kV and 10 min; then decreased by 4% when treated for 15 min	**(Mehta, et al., 2019)**
Blueberries	Air (DBD)	60 and 80 kV	50 Hz	2 and 5 min	Increase by 10% at 80 kV and 1 min; decreased by 35% when treated for 5 min	**(Sarangapani, et al., 2017)**
Amazonian juice	Glow plasma		80 kHz	10, 20, and 30 min	Increase by 75% at 20 min & 10 ml/min.	**(Castro, et al., 2020)**
Sriguela juice	Glow plasma	80 W	50 kHz	5, 10, and 15 min	Increase by 58% at 20 L/min and 15 min.	**(Paixão, et al., 2019)**
Sour cherry juice	Gas phase plasma	4 W, 2.5 kV		3, 4, and 5 min	Increase by 74% at 1.25 L/min and 3 min.	**(Garofulić, et al., 2015)**
Banana slices	DBD plasma	4.8–6.9 kV	12–22 kHz	35–155 s	Increase by 134% at 5.87 kV and 180 s.	**(Pour, et al., 2022)**
Fresh cut Strawberries	Air (DBD, electric source)		45 kV	1 min.	Increase TPC, flavonoid, and anthocyanin contents up to day 5	**(M. Li, et al., 2019)**
Basmati rice flour	Air (DBD, RF source)	30 and 40 W	13.56 MHz	5 and 10 min	Increase TPC content by reducing time and power	**(Thirumdas, et al., 2016)**
Blueberries		549 W	47 kHz	15–120 s	Reduction of total anthocyanin content as treatment time increased	**(Lacombe, et al., 2015)**
White grape juice	DBD	80 kV		0–4 min	Decrease of TPC by 38% at 80 kV	**(Shashi Kishor Pankaj, et al., 2017)**
Pomegranate juice	Plasma jet Power	4 W	25 kHz	3, 5, and 7 min	Decrease of TPC by 49% at 1 L/min and 5 min	**(Herceg, et al., 2016)**

DBD, dielectric barrier discharge; AR: argon, He: helium, N_2: nitrogen, TPC: total phenolic content, MW: microwave, and RF: radio frequency.

1.6.2. Effect of CP processing on individual phenolic compounds

1.6.2.1. Phenolic acids

Phenolic acids: a family of chemical compounds with one carboxyl group linked to the benzene ring. As shown in scheme 3, they are separated into two groups: benzoic acid derivatives and cinnamic acid derivatives. Gallic acid, salicylic acid, 4- hydroxybenzoic acid and protocatechuic acid are examples of benzoic acid derivatives. On the other hand, coumaric acid, ferulic acid, caffeic acid, and sinapic acid are cinnamic acid derivatives.

Gallic acid is a common phenolic acid, the cold plasma treatment generally favoured the increase of gallic acid concentration to 4% in strawberry juice **(Mehta, et al., 2020)**. An increase in gallic acid was also reported in plasma-treated fresh-cut pitaya fruit **(X. Li, et al., 2019)** and plasma-treated green tea leaves **(Keshavarzi, et al., 2020)**, which was attributed to the conversion of epigallocatechin gallate into gallic acid during treatment.

Chlorogenic acid (3-caffeoylquinic acid) is an ester of quinic acid and caffeic acid, and very scarce literature is available regarding the effect of cold plasma on chlorogenic acid **(Kumar, et al., 2023)**. Following 10 and 15 min of treatment, the quantity of chlorogenic acid in a strawberry juice was raised by 39.85% and 46.5%, respectively **(Mehta, et al., 2020)**. **Herceg, et al. (2016)** also reported an increase in chlorogenic acid from 2.1 to 4.95 mg/ml in plasma-treated pomegranate.

Caffeic acid is 3, 4-dihydroxycinnamic acid, the cold plasma treatment probably decreased the caffeic acid content of food products **(Kumar, et al., 2023)**. The caffeic acid concentration in plasma-treated pitaya fruit was reduced by 16.7% after 36 h storage **(X. Li, et al., 2019)**. A similar decrease in caffeic acid was reported in plasma-treated pomegranate juice **(Herceg, et al., 2016)** and fresh lettuce leaves **(Grzegorzewski, et al., 2011)**. *p*-Coumaric acid is the precursor of caffeic acid, it has a similar structure to caffeic acid except for the absence of a hydroxyl group at the meta position. The concentration of *p*-coumaric acid increased by 108.8% in plasma-treated fresh-cut pitaya fruit **(X. Li, et al., 2019)**.

1.6.2.2. Flavonoids

Flavonoids have a diphenylpropane-based skeleton, two benzene rings (A and B) joined by a three-carbon chain, and a closed pyran ring on the benzene A ring (Figure 4). Flavonoids are classified further into flavonols, flavones, flavanones, flavanols, isoflavones, chalcones and anthocyanins. The structural difference in various flavonoids is shown in figure 4.

Diosmetin is a flavone which concentration increased significantly in CP treated lettuce leaves, while the other flavone luteolin was non significantly changed **(Grzegorzewski, et al., 2011)**. In another study, following plasma treatment, the level of both compounds increased significantly in CP treated lamb's lettuce rose **(Grzegorzewski, et al., 2010)**.

The CP treatment increased the concentrations of flavonols such as quercetin- 3-rutinoside and quercetin-3-glucoside of chokeberry juice **(Kovačević, Kljusurić, et al., 2016)**. Similarly, quercetin- 3-rutinoside increased significantly in CP treated strawberry juice **(Mehta, et al., 2020)**. Regarding flavanols, catechin content significantly increased in CP treated pomegranate juice **(Herceg, et al., 2016)** and green tea leaves **(Keshavarzi, et al., 2020)**. However, epicatechin and epigallocatechin gallate were decreased in green tea leaves, due to their degradation into gallic acid, by CP treatment **(Keshavarzi, et al., 2020)**.

Anthocyanins are plant pigments that give to flowers and fruits their red, purple, and blue colours. There are various types of anthocyanins including: cyanidin, pelargonidin, petunidin, malvidin, delphinidin and peonidin being the most common. They are unstable to traditional processing methods and are often found as glycosylated anthocyanins. Consequently, the CP process parameters: treatment time, sample volume, and gas flow rate, significantly affected anthocyanin concentration **(Kumar, et al., 2023)**.

Increase in the voltage and treatment time lead to anthocyanin reduction in CP treated chokeberry juice **(Kovačević, Kljusurić, et al., 2016)** and blueberry **(Lacombe, et al., 2015; Sarangapani, et al., 2017)**. This was attributed to the oxidative cleavage of chromophores by plasma hydroxyl radicals and ozone.

Similarly, sample volume and plasma treatment time significantly influence the anthocyanin concentrations, however the gas flow rate did not induce any effect in both pomegranate juice **(Kovačević, Putnik, et al., 2016)** and sour cherry marasca juice **(Garofulić, et al., 2015)**. Cyanidin-3-glucoside concentrations in CP treated pomegranate juice were highest at 5 min, while delphinidin-3-glucoside and pelargonidin-3, - 5-diglucoside concentrations were greatest at 3 min as compared to 5 min **(Kovačević, Putnik, et al., 2016)**.

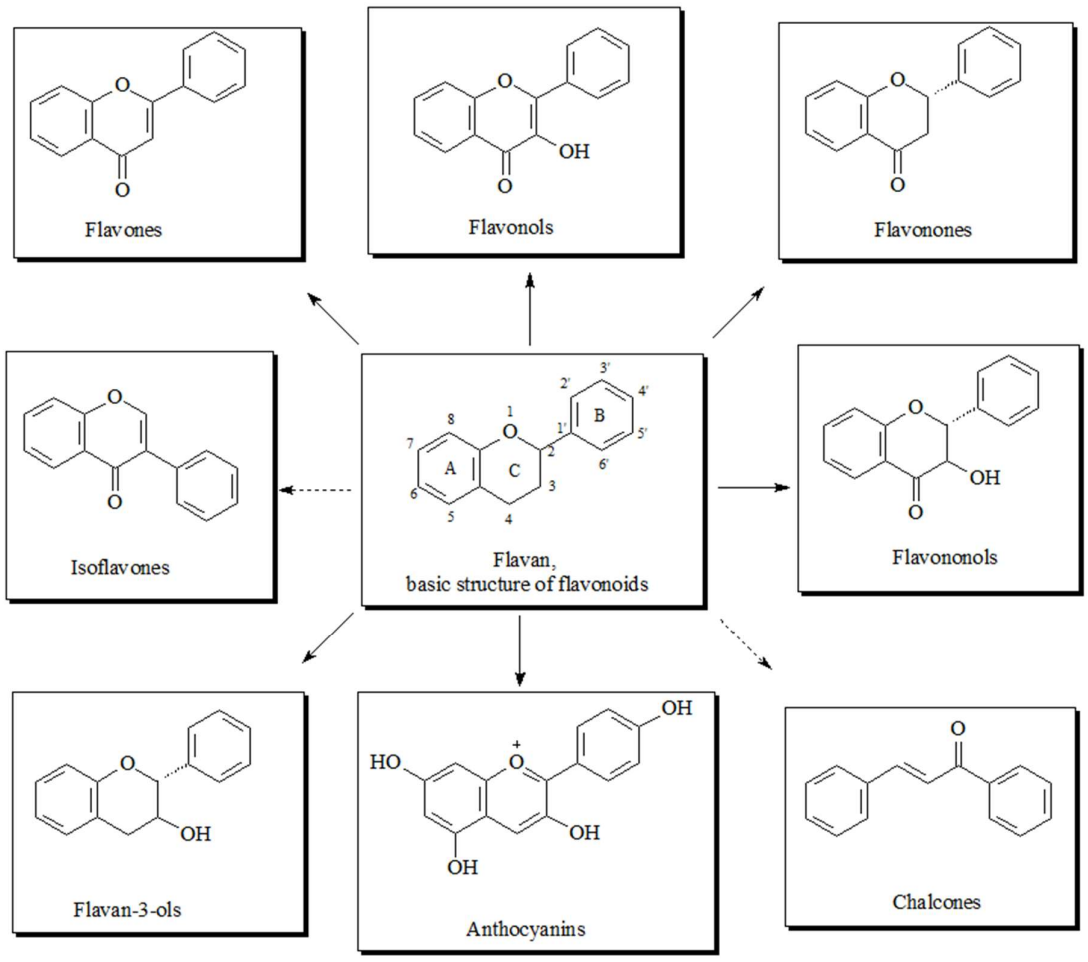

Figure 4: Classification and structures of flavonoid subgroups.

1.6.2.3. Reaction of individual plasma Species with polyphenols

Very few studies have been conducted to elucidate the mechanism of these reactive species on polyphenols. However, polyphenol contains one or more aromatic rings, the action of the plasma reactive species has been studied widely only on the aromatic ring of phenol, presented in figure 5 and discussed below as described by **(Kumar, et al., 2023)**.

The hydroxyl radical activates the aromatic ring of phenol via a resonance electron-donating effect. The reaction initiates with the formation of hydroquinone followed by the oxidation of hydroquinone into benzoquinone which then dispersed to form muconic acid, further decomposed to produce fumaric, maleic, and oxalic acids **(Alnaizy, et al., 2000; Kumar, et al., 2023)**.

Nascent oxygen (O) is a significant reactive oxygen species and a powerful oxidizing agent which reacts quickly with unsaturated compounds like phenolics. The atomic oxygen attacks the benzene ring of phenol and forms diols such as catechol, resorcinol, and

hydroquinone which further react with atomic oxygen to form triol pyrogallol **(Fernandes, et al., 2021; Kumar, et al., 2023)**.

Ozone (O_3) concentration depends on the oxygen concentration in the environment and the excitation frequency of the plasma. It induces hydroxylation of the benzene ring at the ortho or para position to form dihydric phenol (hydroquinone and catechol). The dihydric phenol undergoes ring cleavage rather than further hydroxylation or oxidation to quinones. After ring cleavage, the major intermediaries formed were glyoxal, glyoxalic acid, and oxalic acid. Further, the glyoxal was oxidized to glyoxalic acid, and then, ultimately, only oxalic and glyoxalic acid were left **(Alothman, et al., 2010)**.

Superoxide radicals (O_2^-) is very reactive but has poor permeability through membranes due to its charge. Therefore, it is mainly responsible for surface sanitization. The reaction of superoxide radicals and phenol can be mediated via two pathways: hydrogen atom transfer and single electron transfer forming various radicals and anions as shown in figure 5 D&F. Nitric oxide (NO) is the major RNS generated in atmospheric pressure plasma, it reacts with the phenolic compounds forming phenoxy radicals, producing nitric oxide adducts.

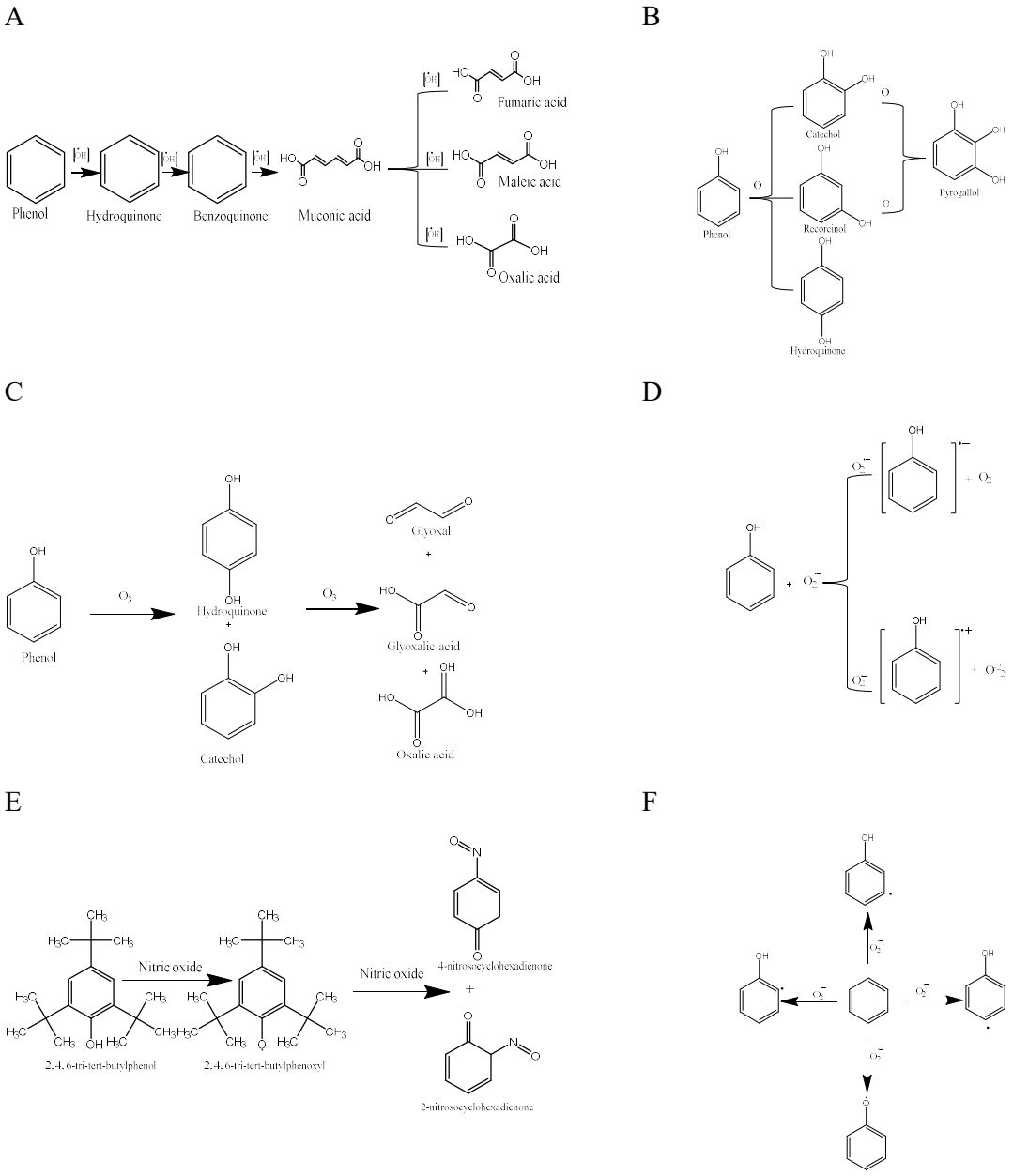

Figure 5: Reaction of various plasma-generated reactive species with phenol. A) Hydroxyl radical; B) Nascent oxygen; C) Ozone; D) Superoxide radical via single electron transfer; E) Nitric oxide; F) Superoxide radical via hydrogen atom abstraction as reported by **(Kumar, et al., 2023)**.

1.6.3. Effect of CP processing on vitamins

Vitamins are minor compounds, but one of the essential nutrients in food products especially fruits and vegetables. Their deficiency can result in hypovitaminosis and, if more severe, avitaminosis. Hence, it is very important to preserve them during the storage and processing of fruit and vegetables. Vitamins like biotin, riboflavin (B2), and pyridoxine (B6) are considered to be relatively stable, however others including thiamine (B1), folic acid (B9), and vitamins E, A, and C are thought to be unstable **(Sruthi, et al., 2021)**. Several studies have been developed to study the stability of vitamins in different foods post-harvest processing. These studies were mainly focused on the stability and changes of concentrations of the antioxidant *L*-Ascorbic acid (vitamin C).

1.6.3.1. Vitamin C

Vitamin C is an exogenous compound (not produced in the human body), so it must be supplied in food, where the greatest amounts of vitamin C can be found in fruits and vegetables. The recommended daily intake of vitamin C is about 110 mg/day for men and 95 mg/day for adult women **(Mieszczakowska-Frąc, et al., 2021)**. Vitamin C holds an efficient protecting function against coronary disease and known for being necessary as an enzyme cofactor for biochemical reactions catalysed by monooxygenases, dioxygenases, and mixed function oxygenase. Moreover, it contributes to maintaining the normal functioning of blood vessels, immune system, bones, cartilage, gums, skin, and the proper collagen formation in addition to the protection of cells from oxidative stress **(Mieszczakowska-Frąc, et al., 2021)**.

Vitamin C is characterized by low thermal stability and a tendency to oxidize easily; therefore, it is generally observed that when vitamin C is well retained, other nutrients are usually also well retained **(Mieszczakowska-Frąc, et al., 2021; Uddin, et al., 2002)**. Hence, it is important to follow how particular processing operations influence the quantity of this vitamin and to which extent it is detrimental for the final product quality. However, processing is an excellent possibility to prolong the shelf life, it is usually associated with significant losses of many pro-health ingredients, including vitamin C, which is the least stable of all vitamins. Very often, conventional processing methods involving the use of high temperatures, exposure to light and oxygen induce adverse changes in the vitamin C contents of processed fruits and vegetables due to the oxidation of Vitamin C to unstable *L*-dehydroascorbic acid **(Gamboa-Santos, et al., 2013)**. For this innovative low-temperature

techniques including CP treatment reported to show some advantages in vitamin C preservation compared to those traditional, high-temperature alternatives.

As shown in table 2, contradictory reports were found in the literature regarding the effect of cold plasma processing on the contents of vitamin C in fruits and vegetables. Most of the previous studies has reported non-significant reduction in ascorbic acid content after plasma treatment **(Oh, et al., 2017; Ramazzina, et al., 2015; Song, et al., 2015)**. However, other studies showed reduction in ascorbic acid content after plasma treatment of fruits and vegetables **(Misra, Moiseev, et al., 2014)**. The degradation of ascorbic acid was attributed to the reaction with ozone and other oxidizing plasma species and free radicals during the processing (Figure 6). In addition, vitamin C is light sensitive, so UV generated by plasma may also play an important role in the vitamin C degradation **(Shashi K Pankaj, et al., 2018)**.

Plentiful studies also narrated an improvement in ascorbic acid content owing to cold plasma treatment in blueberries, cashew apple, and prebiotic orange juice **(Dong, et al., 2019; Fernandes, et al., 2019; Rodríguez, et al., 2017; Sarangapani, et al., 2017; L. Xu, et al., 2017)**. Under mild plasma treatment conditions, the regeneration could exceed the degradation rate of ascorbic acid and the plasma treatment could induce an opposite mechanism where the reactive species in the medium could bring back the oxidized forms of ascorbic acid to the biologically active ascorbic acid form. For example, the NO generated by plasma can improve the activity of dehydroascorbate reductase. The degree of the rebuilding of ascorbic acid through the ascorbate–glutathione cycle, together with the degree of degeneration of ascorbic acid resulting from reactions with other plasma-generated species, will determine the level of ascorbic acid content in food products **(Hou, et al., 2019; Sruthi, et al., 2021)**. Consequently, process parameters such as gas type, input voltage and power, treatment time, food matrix and sample type (whole, cut, juice) can all affect the degradation &/or regeneration of vitamin C. Optimization of these process parameters should be considered to achieve the most ideal conditions required for keeping the vitamin C at a certain level. Thus, it can be concluded that CP has more positive effects than adverse effects on vitamin C stability in fruits and vegetables.

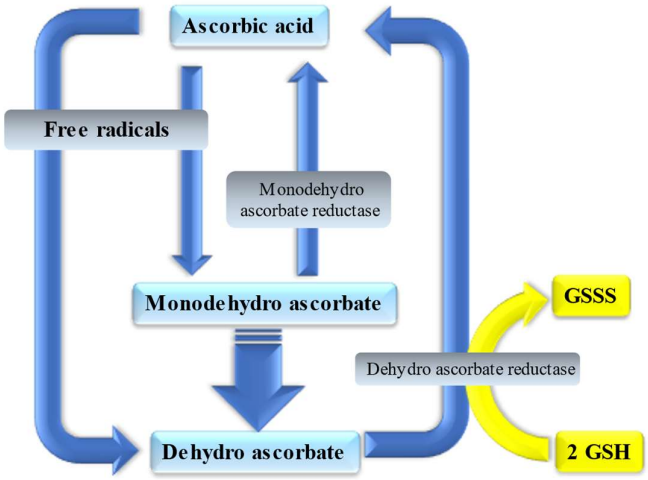

Figure 6: Ascorbic acid decay and regeneration cycle as reported by **(Fernandes, et al., 2021; B. Zhang, et al., 2022)**

1.6.3.2. Other vitamins

Reports on cold plasma effects on other vitamins like vitamins A, B, D, and K are scarce, and it is important to emphasize the need for further studies to analyse the effects of CP on other vitamins in the food products along with the mechanism of their reaction with plasma spieces **(Fernandes, et al., 2021)**. Previous study showed that glow discharge plasma application increased the contents of pro-vitamin A in acerola juice at mild treatment conditions (time and plasma flow). However, decay of this pro-vitamin was observed at higher fluences. An increase in vitamin B3 and B6 has been reported, but no decay was observed at higher fluences **(Fernandes, et al., 2019)**

Paixão, et al. (2019) explored the effects of glow discharge plasma on siriguela juice quality and found that elevated nitrogen gas flow rates and processing time more significant than 10 min pushed the degradation of pro-vitamin A. The same study showed increase in the concentrations of B3 and B6 vitamins.

Table 2: Effect of cold plasma treatment on vitamin contents in treated fruits and vegetables.

Matrix	Plasma treatment				Findings	Reference
	Plasma source	Power/voltage	Frequency	Exposure time		
Fresh Slices (pears, cucumbers And carrots)	PMJ			1 s	3.6%, 3.2% and 2.8% ↓ of vitamin C in cucumber, carrot and pear slice, respectively	**(R. Wang, et al., 2012)**
Orange juice	DBD	70 kV	50 Hz	5–60 s	Ascorbic acid ↑	**(Almeida, et al., 2015)**
Kiwifruit	DBD	15 kV		10–20 min	Vitamin C ↔	**(Ramazzina, et al., 2015)**
Orange juice	DBD	90 kV	60 Hz	0–120 s	Ascorbic acid ↓	**(L. Xu, et al., 2017)**
Blueberries	DBD	80 kV	50 Hz	0–5 min	Ascorbic acid↑	**(Sarangapani, et al., 2017)**
Mandarin flesh	MW	400, 650, 900 W	2.45 GHz	2–10 min	Ascorbic acid↔	**(Won, et al., 2017)**
Cashew apple juice			80 kHz	5–15 min	Decrease in vitamin C at higher flow rate	**(Rodríguez, et al., 2017)**
Radish sprouts	MW	900W		2.45 GHz	Ascorbic acid ↔	**(Oh, et al., 2017)**
Fresh-cut pears	PAW	6, 8, 10 kV		5 min	Ascorbic acid ↔	**(C. Chen, et al., 2019)**
Tomato juice	GAD	3.8 kV/40 W	50 Hz	30–300 s	Vitamin C ↓	**(Starek, et al., 2019)**
Siriguela juice	GDP	80 W	50 kHz	5–15 min	Vitamins C ↔	**(Paixão, et al., 2019)**
Acerola juice	GDP		80 kHz	5–15 min	Vitamin A↑ Vitamin C↔	**(Fernandes, et al., 2019)**
Tomato seedlings	PAW			15 and 30 min	Vitamin C ↓	**(Adhikari, et al., 2019)**
Tomato beverage				-	Vitamin C retention rate was the highest after 10 min of CP treatment, reaching	**(Mehta, et al., 2019)**
Siriguela juice	GDP	80 W	50 kHz	5–15 min	Pro-vitamin A Increase of 49% Increase of 19% B3 Increase of 56% B6 ↔ Vitamins C	**(Paixão, et al., 2019)**
Cashew apple juice	DBD	20 kV	200, 700 Hz	15 min	Vitamin C ↑	**(Leite, et al., 2021)**
Blueberry juice				-	Vitamin C ↓	
				-		
Strawberry				-	Vitamin C ↓	**Giannoglou, et al. (2021)**
Fresh-cut melon		40 kV		90 s	Vitamin C↔	**(Zhou, et al., 2022)**
Banana slices	DBD	4.8 to 6.9 kV		35-155 s	vitamin B6 ↑	**(Pour, et al., 2022)**

↓: Decrease in the level; ↑: increase in the level; ↔: insignificant change. PMJ: Atmospheric-pressure air cold plasma microjet; DBD: Dielectric Barrier Discharge; GAD: Gliding arc discharge; HMCPT: High microwave density-cold plasma treatment; MW: microwave; PAW: Plasma activated water; GDP: Glow discharge plasma; LPCP: Low pressure cold plasma.

1.6.4. Effect of CP processing on volatile organic compounds (VOCs)

Food processing methods including CP treatment induce chemical reactions between wide range of metabolites, leading to the production of volatile aromatic organic compounds. The influence on the quality characteristics of fruits and vegetables, including the VOCs profile, is also important. Unfortunately, treatment with the use of plasma is associated with the intensification of the fat oxidation process in the raw material, which results in the formation of secondary volatile and non-volatile compounds such as alcohols, aldehydes, carbonyls, furans, and hydrocarbons **(Wojtasik-Kalinowska, et al., 2023)**. **Kodama, et al. (2014)**, reported that plasma treatments had a significant effect on citrus essential oil composition, and limonene, γ-terpinene, and β-pinene in the essential oil were reduced **(Kodama, et al., 2014)**.

Shirani, et al. (2020) observed C5-C11 aldehydes in plasma-treated almond samples, which are the most common oleic and linoleic acid oxidation products. Hexanal, nonanal, and octane can result in odour that causes an undesirable effect on almond aroma and quality. These compounds further increase during storage and oxidation. **Chutia, et al. (2020)** reported a chemical change of odour in plasma-treated tender coconut water and suggested blending 1% orange juice to mask this flavor. Similar results were found on plasma-treated apple slices by **Schnabel, et al. (2015)**. However, the authors concluded that the noticed changes are probably not associated with the plasma treatment.

Figure 7 depicts the reported complex reactions induced by plasma reactive species such as rearrangements, hydrogenations, and dehydrogenation, which were observed in sesquiterpenes of camu-camu pulp treated by DBD plasma. DBD plasma at 420 & 700 Hz, and above 12000 Hz induced a reduction in β-caryophyllene concentration, and significant increase in the other dehydrogenated sesquiterpene compounds. However, processing at 200 & 900 Hz induced an inversed effect in which β-caryophyllene concentration was increase with a consequent decrease in the other sesquiterpene compounds **(Campelo, et al., 2020a)**. However, camu-camu pulp processing by glow discharge plasma induced the formation and thus, increase of α-pinene, limonene, terpinolene, and β-caryophyllene, α-fenchol, borneol, 4-terpineol, and α-terpineol concentrations. On the other hand, a reduction in the contents of α-humulene, α-bulnesene, γ-cadinene, cadina-1(2),4- diene, selina-3,7(11)-diene, α-calacorene, germacrene B, β-pinene, myrcene, and α-phellandrene was also observed **(Campelo, et al., 2020b)**.

The perception of active volatile compounds formed during chewing is responsible for feeling the flavour by help of taste receptors on the tongue **(Shirani, et al., 2020)**. The Flavors protection and stability are very crucial for the food industry to produce high-quality food products. Different fruit and vegetable juices each have their own distinct aromas. The main flavour components, which include esters, alcohols, aldehydes, and acids, also serve as an important evaluation indicator of product quality. It is challenging to prevent volatile substances from being destroyed during heat processes, which compromises flavour. Cold plasma treatment offers many benefits over thermal methods. Low processing temperatures, meanwhile, preserved product freshness while preserving the food's nutritional value, colour, flavour, and texture. The effects of cold plasma treatment on some major volatile organic compounds (VOCs) classes in different fruits and vegetables are illustrated in table 3.

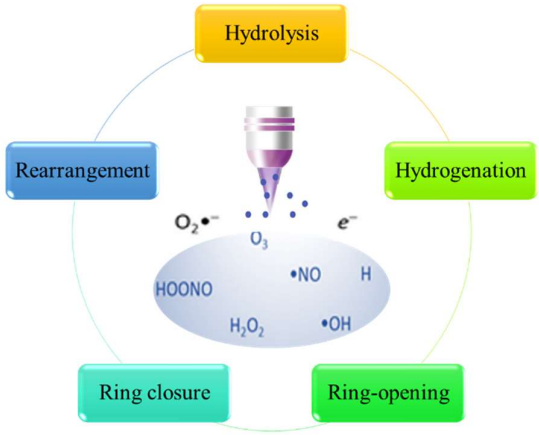

Figure 7: Chemical reactions induced by plasma reactive species on different food volatile components.

Table 3: Effect of cold plasma treatment on volatile profile of various fruits and vegetables as reported by **(Abouelenein, Caprioli, et al., 2023)**.

Class	Compounds	Sample	Plasma Treatment conditions				Findings	Ref.
			Plasma source	Power/voltage	Frequency	Exposure time		
Alcohols	**Glycerol**	Tomato Juice	Electric discharge	10 kV	-	5 min	↑After plasma treatment	**(T. Ma, et al., 2015)**
	***L*-Threitol**	Tomato Juice	Electric discharge	10 Kv	-	5 min	Produced by plasma treatment	**(T. Ma, et al., 2015)**
	1-Ethoxy-2-propanol	Tomato Juice	Electric discharge	10 Kv	-		↑ By 71.8 %	**(T. Ma, et al., 2015)**
	3-Methylbutan-1-ol	Camu- camu pulp	DBD plasma	voltage of a 10 & 20 kV	200, 420, 580, 700, 960, 12000, 30000 Hz	5 & 15 min.	Non-significant change with 200 Hz and Significant ↓ with all higher frequencies.	**(Campelo, et al., 2020a)**
		Camu- camu pulp	Glow discharge plasma	80 kV	50 kHz	(10, 20 and 30 min).	↑After plasma treatment	**(Campelo, et al., 2020b)**
	1-Heptanol	Fresh-cut cantaloupe	-	40 kV		90 s	↑After plasma treatment in all storage days.	**(Zhou, et al., 2022)**
	1-Octen-3-ol	Brown rice	DBD plasma	40 and 50 kV	-	1.5-3 min	↓ By T1: 40 kV-90 s; and disappeared by the other studied treatments (T2: 50 kV-90 s; T3: 40 kV-180 s; T4: 50 kV-180 s).	**(Q. Liu, et al., 2021)**
		Fresh-cut cantaloupe	-	40 kV		90 s	Exhibited first ↓trends but ↑ afterwards at days 6&8.	**(Zhou, et al., 2022)**
	1-Hexanol, 2-ethyl-	Fresh-cut cantaloupe	-	40 kV		90 s	↑After plasma treatment in all storage days.	**(Zhou, et al., 2022)**
	Phenylethyl alcohol	Brown rice	DBD plasma	40 and 50 kV	-	1.5-3 min	↑ in T1: 40 kV-90 s; and disappeared in the other studied treatments (T2: 50 kV-90 s; T3: 40 kV-180 s; T4: 50 kV-180 s).	**(Q. Liu, et al., 2021)**
	Hex-3-en-1-ol	Camu- camu pulp	DBD plasma	voltage of a 10 & 20 kV	200, 420, 580, 700, 960, 12000, 30000 Hz	5 & 15 min.	Non-significant change with 200 Hz and Significant ↓ with all higher frequencies	**(Campelo, et al., 2020a)**
		Camu- camu pulp	Glow discharge plasma	80 kV	50 kHz	10, 20 and 30 min	↑After plasma treatment	**(Campelo, et al., 2020b)**
	Hexan-1-ol	Camu- camu pulp	DBD plasma	voltage of a 10 & 20 kV	200, 420, 580, 700, 960, 12000, 30000 Hz	5 & 15 min.	Non-significant change with 200 Hz and Significant ↓ with all higher frequencies	**(Campelo, et al., 2020a)**
		Camu- camu pulp	Glow discharge plasma	80 kV	50 kHz	(10, 20 and 30 min).	↑After plasma treatment	**(Campelo, et al., 2020b)**
		Brown rice	DBD plasma	40 and 50 kV	-	1.5-3 min	↓ In all studied treatments	**(Q. Liu, et al., 2021)**
	1-Octanol	Fresh-cut cantaloupe	-	40 kV		90 s	Exhibited first ↑trends up to day 6.	**(Zhou, et al., 2022)**

Table 3: Continued

Class	Compounds	Sample	Plasma Treatment conditions				Findings	Ref.
			Plasma source	Power/voltage	Frequency	Exposure time		
	Benzyl Alcohol	Brown rice	DBD plasma	40 and 50 kV	-	1.5-3 min	↓ In all studied treatments	**(Q. Liu, et al., 2021)**
		Fresh-cut cantaloupe	-	40 kV		90 s	↑After plasma treatment in all storage days	**(Zhou, et al., 2022)**
	***(Z)*-2-Dodecenol**	Fresh-cut cantaloupe	-	40 kV		90 s	↑In all storage days, but significantly ↓ at days 4 &8.	**(Zhou, et al., 2022)**
Alcohols	***(Z)*-3-Nonen-1-ol**	Fresh-cut cantaloupe	-	40 kV		90 s	Treatment significantly inhibited the ↓ until day 2, but significantly stimulated the synthesis from 4 d to 8 d.	**(Zhou, et al., 2022)**
	3,6-Nonadien-1-ol	Fresh-cut cantaloupe	-	40 kV		90 s	Not detected in treated samples until day 4, but then ↑at days 4-8.	**(Zhou, et al., 2022)**
	***(E)*-2-Nonen-1-ol**	Fresh-cut cantaloupe	-	40 kV		90 s	↑After plasma treatment up to day 6 then ↓afterwards	**(Zhou, et al., 2022)**
	1-Nonanol	Fresh-cut cantaloupe	-	40 kV		90 s	↑After plasma treatment at days0, 4, 6&10	**(Zhou, et al., 2022)**
	1-Undecanol	Fresh-cut cantaloupe	-	40 kV		90 s	↑After plasma treatment at days 4, 6&8	**(Zhou, et al., 2022)**
	Dimethylcyclohexanol	Fresh-cut cantaloupe	-	40 kV		90 s	↑After plasma treatment at days0, 4, 6&10	**(Zhou, et al., 2022)**
	***n*-Heptadecanol**	Fresh-cut cantaloupe	-	40 kV		90 s	Not detected in almost all treated samples.	**(Zhou, et al., 2022)**
	Furfural	Brown rice	DBD plasma	40 and 50 kV	-	1.5-3 min	↓ In all studied treatments	**(Q. Liu, et al., 2021)**
	Hexanal	Tomato Juice	Electric discharge	10 Kv	-	5 min	↑ By 1.6 times	**(T. Ma, et al., 2015)**
		Brown rice	DBD plasma	40 and 50 kV	-	1.5-3 min	↓ In all studied treatments	**(Q. Liu, et al., 2021)**
		Fresh-cut cantaloupe	-	40 kV		90 s	Cold plasma significantly inhibited the ↓ until 6 days, but boosted the ↓ at 8 d and 10 d.	**(Zhou, et al., 2022)**
Aldehydes	***trans*-2-hexenal**	Tomato Juice	Electric discharge	10 Kv	-	5 min	↑ After plasma treatment	**(T. Ma, et al., 2015)**
	Heptanal	Brown rice	DBD plasma	40 and 50 kV	-	1.5-3 min	↓ In all studied treatments	**(Q. Liu, et al., 2021)**
		Fresh-cut cantaloupe	-	40 kV		90 s	↓ At 0, 4 & 10 days. ↑at 8 d and 10 days compared to the nontreated samples	**(Zhou, et al., 2022)**
	Acetal	Tomato Juice	Electric discharge	10 Kv	-	5 min	↑ After plasma treatment.	**(T. Ma, et al., 2015)**
	Benzaldehyde	Brown rice	DBD plasma	40 and 50 kV	-	1.5-3 min	↓ In all studied treatments	**(Q. Liu, et al., 2021)**
		Fresh-cut cantaloupe	-	40 kV		90 s	Significant higher contents in treated samples at days 0, 2, 6 and 10.	**(Zhou, et al., 2022)**
	***(E)*-2-Hexenal**	Fresh-cut cantaloupe	-	40 kV		90 s	Cold plasma significantly inhibited the ↓ until 6 days but boosted the ↓ at days 8 & 10.	**(Zhou, et al., 2022)**

Table 3: Continued

Class	Compounds	Sample	Plasma Treatment conditions				Findings	Ref.
			Plasma source	Power/voltage	Frequency	Exposure time		
Aldehydes	***(E)*-2-Pentenal**	Fresh-cut cantaloupe	-	40 kV		90 s	↑ After plasma treatment at all storage days up to day 10.	**(Zhou, et al., 2022)**
	Nonanal	Brown rice	DBD plasma	40 and 50 kV	-	1.5-3 min	↓ In all studied treatments	**(Q. Liu, et al., 2021)**
		Fresh-cut cantaloupe	-	40 kV		90 s	Generally, ↓during the storage, with the values ranging from 4.02 -2.14 µg/kg. Significantly higher contents identified in treated samples at days 2-4.	**(Zhou, et al., 2022)**
	***(E)*-2-Octenal**	Fresh-cut cantaloupe	-	40 kV		90 s	↑ After plasma treatment up to day 8 then ↓ at day 10.	**(Zhou, et al., 2022)**
	2-Dodecenal	Fresh-cut cantaloupe	-	40 kV		90 s	↑ After plasma treatment up to day 8 then ↓ at day 10	**(Zhou, et al., 2022)**
	Decanal	Brown rice	DBD plasma	40 and 50 kV	-	1.5-3 min	↓ By T1: 40 kV-90 s; T2: 50 kV-90 s; T4: 50 kV-180 s). ↑ byT3: 40 kV-180 s.	**(Q. Liu, et al., 2021)**
		Fresh-cut cantaloupe	-	40 kV		90 s	Maintained or ↑ after plasma treatment up to day 8.	**(Zhou, et al., 2022)**
	2,4-Nonadienal	Fresh-cut cantaloupe	-	40 kV		90 s	↑ After plasma treatment up to day 8 then ↓ at day 10	**(Zhou, et al., 2022)**
	***(E)*-2-Nonenal**	Brown rice	DBD plasma	40 and 50 kV	-	1.5-3 min	↓ In all studied treatments	**(Q. Liu, et al., 2021)**
	***β*-cyclocitral**	Fresh-cut cantaloupe	-	40 kV		90 s	↑ After plasma treatment at day 2 storage, then↓ or even lost with other storage times.	**(Zhou, et al., 2022)**
	4-Oxononanal	Fresh-cut cantaloupe	-	40 kV		90 s	Treatment inhibited the ↓ until 6 days but boosted the ↓ at days 8 & 10.	**(Zhou, et al., 2022)**
Ketones	**3-Octanone**	Fresh-cut cantaloupe	-	40 kV		90 s	↑ After plasma treatment at all storage days up to day 10	**(Zhou, et al., 2022)**
	Farnesyl acetone	Fresh-cut cantaloupe	-	40 kV		90 s	↑ After plasma treatment at all storage days up to day 10 but not detected at day 8.	**(Zhou, et al., 2022)**
	Geranyl acetone	Brown rice	DBD plasma	40 and 50 kV	-	1.5-3 min	Produced by only T1: 40 kV-90 s; and T4: 50 kV-180 s treatments.	**(Q. Liu, et al., 2021)**
		Fresh-cut cantaloupe	-	40 kV		90 s	Not detected at day 0, but ↑ after plasma treatment up to day 10	**(Zhou, et al., 2022)**
	***β*-ionone**	Fresh-cut cantaloupe	-	40 kV		90 s	↓at day 0, but ↑ afterwards up to day 10	**(Zhou, et al., 2022)**
Esters	**Octyl formate**	Tomato Juice	Electric discharge	10 Kv	-	5 min	Lost by plasma treatment	**(T. Ma, et al., 2015)**
	Nonyl chloroformate	Brown rice	DBD plasma	40 and 50 kV	-	1.5-3 min	↓ In all studied treatments	**(Q. Liu, et al., 2021)**
		Brown rice	DBD plasma	40 and 50 kV	-	1.5-3 min	↓ In all studied treatments	**(Q. Liu, et al., 2021)**

Table 3: Continued

Class	Compounds	Sample	Plasma Treatment conditions				Findings	Ref.
			Plasma source	Power/voltage	Frequency	Exposure time		
Esters	**2-Methylpropyl acetate**	Fresh-cut cantaloupe	-	40 kV		90 s	Significant ↑ after plasma treatment In control samples increased up to the peak value at day 2 and at day 8 in treated ones.	**(Zhou, et al., 2022)**
	2-Methylbutyl acetate	Fresh-cut cantaloupe	-	40 kV		90 s	↑After plasma treatment	**(Zhou, et al., 2022)**
	Bis(2-ethylhexyl) maleate	Fresh-cut cantaloupe	-	40 kV		90 s	Not detected at day 0, afterwards ↑after plasma treatment	**(Zhou, et al., 2022)**
	Hexyl acetate	Fresh-cut cantaloupe	-	40 kV		90 s	Fluctuating changes in control and treated samples, but CP ↑ hexyl acetate production compared to control.	**(Zhou, et al., 2022)**
	Isobutyl nonyl carbonate	Fresh-cut cantaloupe	-	40 kV		90 s	Fluctuating changes in control and samples	**(Zhou, et al., 2022)**
	Benzyl dodecanoate	Fresh-cut cantaloupe	-	40 kV		90 s	↑After plasma treatment except for day 6.	**(Zhou, et al., 2022)**
	Heptyl Acetate	Fresh-cut cantaloupe	-	40 kV		90 s	↑After plasma treatment	**(Zhou, et al., 2022)**
	Ethyl laurate	Tomato Juice	Electric discharge	10 Kv	-	5 min	Lost by plasma treatment.	**(T. Ma, et al., 2015)**
	Ethyl butanoate	Camu- camu pulp	DBD plasma	voltage of a 10 & 20 kV	200, 420, 580, 700, 960, 12000, 30000 Hz	5 & 15 min.	Significant ↓ with all frequencies	**(Campelo, et al., 2020a)**
	Ethyl butanoate	Camu- camu pulp	Glow discharge	80 kV	50 kHz	(10, 20 and 30 min).	↑After plasma treatment	**(Campelo, et al., 2020b)**
	Hydroxymandelic acid ethyl ester	Fresh-cut cantaloupe	-	40 kV		90 s	Non-significant differences between treated a control sample	**(Zhou, et al., 2022)**
	Benzyl acetate	Fresh-cut cantaloupe	-	40 kV		90 s	↑After plasma treatment	**(Zhou, et al., 2022)**
	Tetradecadienyl acetate	Fresh-cut cantaloupe	-	40 kV		90 s	Not detected in most control and plasma treated samples	**(Zhou, et al., 2022)**
	Phenethyl acetate	Fresh-cut cantaloupe	-	40 kV		90 s	Not detected at day 0, then ↑ after wards up to day 8	**(Zhou, et al., 2022)**
	Octyl heptafluorobutyrate	Fresh-cut cantaloupe	-	40 kV		90 s	↑After plasma treatment up to day 6, then ↓ afterwards	**(Zhou, et al., 2022)**
	***cis*-Non-3-en-1-yl acetate**	Fresh-cut cantaloupe	-	40 kV		90 s	↑After plasma treatment	**(Zhou, et al., 2022)**
	***cis*-6-Nonenyl Acetate**	Fresh-cut cantaloupe	-	40 kV		90 s	↑After plasma treatment	**(Zhou, et al., 2022)**
	Nonenyl Acetate	Fresh-cut cantaloupe	-	40 kV		90 s	↑After plasma treatment	**(Zhou, et al., 2022)**
	Pentadecyl hexanoate	Fresh-cut cantaloupe	-	40 kV		90 s	Fluctuating changes in control and samples	**(Zhou, et al., 2022)**
	Butyl butanoate	Fresh-cut cantaloupe	-	40 kV		90 s	↑After plasma treatment	**(Zhou, et al., 2022)**
	Heptadecanoic acid heptadecyl ester	Fresh-cut cantaloupe	-	40 kV		90 s	Fluctuating changes in control and samples	**(Zhou, et al., 2022)**

Table 3: Continued

Class	Compounds	Sample	Plasma Treatment conditions				Findings	Ref.
			Plasma source	Power/voltage	Frequency	Exposure time		
	2-Tetradecyl methoxy acetate	Fresh-cut cantaloupe	-	40 kV		90 s	↑After plasma treatment except for day 8 where its not detected	**(Zhou, et al., 2022)**
Terpenes	***α*-pinene**	Camu- camu pulp	DBD plasma	voltage of a 10 & 20 kV	200, 420, 580, 700, 960, 12000, 30000 Hz	5 & 15 min.	Significant ↑ with 200Hz, non-significant change with 420 Hz, then Significant ↓ with all higher frequencies	**(Campelo, et al., 2020a)**
		Camu- camu pulp	Glow discharge	80 kV	50 kHz	(10, 20 and 30 min).	↑After plasma treatment	**(Campelo, et al., 2020b)**
		Lemon verbena shrubs (EO)	LPCP system	1200W	2.45 GHz	0, 1, 3, & 5 min.	↑ After plasma treatment at all time points.	**(Ebadi, et al., 2019)**
	Camphor	Fresh-cut cantaloupe	-	40 kV		90 s	↑ At day6, but non-significant changes with other time points	**(Zhou, et al., 2022)**
	***β*-pinene**	Camu- camu pulp	DBD plasma	voltage of a 10 & 20 kV	200, 420, 580, 700, 960, 12000, 30000 Hz	5 & 15 min.	Significant ↑ with all frequencies	**(Campelo, et al., 2020a)**
		Camu- camu pulp	Glow discharge	80 kV	50 kHz	(10, 20 and 30 min).	↓ After plasma treatment	**(Campelo, et al., 2020b)**
	Sabinene	Lemon verbena shrubs (EO)	LPCP system	1200W	2.45 GHz	0, 1, 3, & 5 min.	↓ After plasma treatment at all time points.	**(Ebadi, et al., 2019)**
	Myrcene	Camu- camu pulp	DBD plasma	voltage of a 10 & 20 kV	200, 420, 580, 700, 960, 12000, 30000 Hz	5 & 15 min.	Significant ↓ with all frequencies.	**(Campelo, et al., 2020a)**
		Camu- camu pulp	Glow discharge	80 kV	50 kHz	(10, 20 and 30 min).	↓ After plasma treatment	**(Campelo, et al., 2020b)**
	***α*-Phellandrene**	Camu- camu pulp	DBD plasma	voltage of a 10 and 20 kV	200, 420, 580, 700, 960, 12000, 30000 Hz	5 & 15 min.	Non-significant change with 200 & 580Hz, Significant ↑ with 420, 700 & 960 Hz and significant ↓ with higher frequencies	**(Campelo, et al., 2020a)**
	***α*-Phellandrene**	Camu- camu pulp	Glow discharge	80 kV	50 kHz	(10, 20 and 30 min).	↓ After plasma treatment	**(Campelo, et al., 2020b)**
	1, 8 Cineole	Lemon verbena shrubs (EO)	LPCP system	1200W	2.45 GHz	0, 1, 3, & 5 min.	↑ After plasma treatment at all time points.	**(Ebadi, et al., 2019)**
	Citronellal	Lemon verbena shrubs (EO)	LPCP system	1200W	2.45 GHz	0, 1, 3, & 5 min.	↑ After plasma treatment at all time points	**(Ebadi, et al., 2019)**
	Geranial	Lemon verbena shrubs (EO)	LPCP system	1200W	2.45 GHz	0, 1, 3, & 5 min.	↓ After plasma treatment at all time points	**(Ebadi, et al., 2019)**

Table 3: Continued

Class	Compounds	Sample	Plasma Treatment conditions				Findings	Ref.
			Plasma source	Power/voltage	Frequency	Exposure time		
Terpenes	**Limonene**	Camu- camu pulp	DBD plasma	voltage of a 10 and 20 kV	200, 420, 580, 700, 960, 12000, 30000 Hz	5 & 15 min.	Non-significant change with 420, 580 & 700 Hz, Significant ↑ with 200 & 960 Hz and significant ↓ with higher frequencies	**(Campelo, et al., 2020a)**
		Camu- camu pulp	Glow discharge	80 kV	50 kHz	(10, 20 and 30 min).	↑After plasma treatment	**(Campelo, et al., 2020b)**
		Lemon verbena shrubs (EO)	LPCP system	1200W	2.45 GHz	0, 1, 3, & 5 min.	↑after plasma treatment at all time points.	**(Ebadi, et al., 2019)**
	***γ*-Terpinene**	Camu- camu pulp	DBD plasma	voltage of a 10 & 20 kV	200, 420, 580, 700, 960, 12000, 30000 Hz	5 & 15 min.	Significant↑ with all frequencies	**(Campelo, et al., 2020a)**
		Camu- camu pulp	Glow discharge	80 kV	50 kHz	(10, 20 and 30 min).	↑ at10 ml/min& 10min treatment time ↑ at 20 ml/min& 20,30 min treatment ↑ at 30 ml/min& 10,20 min treatment ↓ with other conditions.	**(Campelo, et al., 2020b)**
		Lemon verbena shrubs (EO)	LPCP system	1200W	2.45 GHz	0, 1, 3, & 5 min.	↑ After plasma treatment at all time points but lost at 3 min. treatment.	**(Ebadi, et al., 2019)**
	Terpinolene	Camu- camu pulp	DBD plasma	voltage of a 10 & 20 kV	200, 420, 580, 700, 960, 12000, 30000 Hz	5 & 15 min.	Significant ↓ with all frequencies except for 960Hz that showed significant↑.	**(Campelo, et al., 2020a)**
		Camu- camu pulp	Glow discharge	80 kV	50 kHz	(10, 20 and 30 min).	↑After plasma treatment	**(Campelo, et al., 2020b)**
		Lemon verbena shrubs (EO)	LPCP system	1200W	2.45 GHz	0, 1, 3, & 5 min.	↓ After plasma treatment at all time points, and lost at longest treatment time 5 min.	**(Ebadi, et al., 2019)**
	Neral	Lemon verbena shrubs (EO)	LPCP system	1200W	2.45 GHz	0, 1, 3, & 5 min.	↓ After plasma treatment at all time points	**(Ebadi, et al., 2019)**
	Neryl acetate	Lemon verbena shrubs (EO)	LPCP system	1200W	2.45 GHz	0, 1, 3, & 5 min.	↓ After plasma treatment at all time points	**(Ebadi, et al., 2019)**
	***α*-Fenchol**	Camu- camu pulp	DBD plasma	voltage of a 10 & 20 kV	200, 420, 580, 700, 960, 12000, 30000 Hz	5 & 15 min.	Significant ↓ with all frequencies	**(Campelo, et al., 2020a)**
		Camu- camu pulp	Glow discharge	80 kV	50 kHz	(10, 20 and 30 min).	↑After plasma treatment	**(Campelo, et al., 2020b)**
	***trans*-pino carveol**	Lemon verbena shrubs (EO)	LPCP system	1200W	2.45 GHz	0, 1, 3, & 5 min.	Lost after plasma treatment at all time points.	**(Ebadi, et al., 2019)**

Table 3: Continued

Class	Compounds	Sample	Plasma Treatment conditions				Findings	Ref.
			Plasma source	Power/voltage	Frequency	Exposure time		
Terpenes	***cis*- Sabinol**	Lemon verbena shrubs (EO)	LPCP system	1200W	2.45 GHz	0, 1, 3, & 5 min.	Lost after plasma treatment at all time points.	**(Ebadi, et al., 2019)**
	Borneol	Camu- camu pulp	DBD plasma	voltage of a 10 & 20 kV	200, 420, 580, 700, 960, 12000, 30000 Hz	5 & 15 min.	Significant ↓ with all frequencies	**(Campelo, et al., 2020a)**
		Camu- camu pulp	Glow discharge	80 kV	50 kHz	(10, 20 and 30 min).	↑After plasma treatment	**(Campelo, et al., 2020b)**
	4-Terpineol	Camu- camu pulp	DBD plasma	voltage of a 10 & 20 kV	200, 420, 580, 700, 960, 12000, 30000 Hz	5 & 15 min.	Non-significant change with 200 Hz and Significant ↓ with all higher frequencies	**(Campelo, et al., 2020a)**
		Camu- camu pulp	Glow discharge	80 kV	50 kHz	(10, 20 and 30 min).	↑After plasma treatment	**(Campelo, et al., 2020b)**
	***α*-Terpineol**	Camu- camu pulp	DBD plasma	voltage of a 10 & 20 kV	200, 420, 580, 700, 960, 12000, 30000 Hz	5 & 15 min.	Non-significant change with 200, 960 &12000 Hz and Significant ↓ with all other frequencies	**(Campelo, et al., 2020a)**
		Camu- camu pulp	Glow discharge	80 kV	50 kHz	(10, 20 and 30 min).	↑After plasma treatment	**(Campelo, et al., 2020b)**
		Lemon verbena shrubs (EO)	LPCP system	1200W	2.45 GHz	0, 1, 3, & 5 min.	↑ After plasma treatment at all time points	**(Ebadi, et al., 2019)**
	***E*-Caryophyllene**	Lemon verbena shrubs (EO)	LPCP system	1200W	2.45 GHz	0, 1, 3, & 5 min.	↓ After plasma treatment at all time points.	**(Ebadi, et al., 2019)**
	***α*-Copaene**	Lemon verbena shrubs (EO)	LPCP system	1200W	2.45 GHz	0, 1, 3, & 5 min.	↓ After short plasma treatment then lost with longer treatment times	**(Ebadi, et al., 2019)**
	***γ*-Elemene**	Lemon verbena shrubs (EO)	LPCP system	1200W	2.45 GHz	0, 1, 3, & 5 min.	↑ After plasma treatment at all time points	**(Ebadi, et al., 2019)**
	***α*-Gurjunene**	Lemon verbena shrubs (EO)	LPCP system	1200W	2.45 GHz	0, 1, 3, & 5 min.	Lost after plasma treatment at all time points	**(Ebadi, et al., 2019)**
	***β*-Caryophyllene**	Camu- camu pulp	DBD plasma	voltage of a 10 & 20 kV	200, 420, 580, 700, 960, 12000, 30000 Hz	5 & 15 min.	Non-significant change with 420, Hz, Significant ↑ with 200 & 960 Hz & significant ↓ with other frequencies	**(Campelo, et al., 2020a)**
		Camu- camu pulp	Glow discharge	80 kV	50 kHz	(10, 20 and 30 min).	↑After plasma treatment	**(Campelo, et al., 2020b)**
	Nerol	Lemon verbena shrubs (EO)	LPCP system	1200W	2.45 GHz	0, 1, 3, & 5 min.	↑ After short plasma treatment then lost with longer treatment times	**(Ebadi, et al., 2019)**

Table 3: Continued

Class	Compounds	Sample	Plasma Treatment conditions				Findings	Ref.
			Plasma source	Power/voltage	Frequency	Exposure time		
Terpenes	***α*-Humulene**	Camu- camu pulp	DBD plasma	voltage of a 10 & 20 kV	200, 420, 580, 700, 960, 12000, 30000 Hz	5 & 15 min.	Non-significant change with 960 Hz, Significant ↑ with all other frequencies except for 700Hz that showed significant ↓	**(Campelo, et al., 2020a)**
		Camu- camu pulp	Glow discharge	80 kV	50 kHz	(10, 20 and 30 min).	↓ After plasma treatment	**(Campelo, et al., 2020b)**
		Lemon verbena shrubs (EO)	LPCP system	1200W	2.45 GHz	0, 1, 3, & 5 min.	↑ After 3min. treatment and ↓ with other treatments	**(Ebadi, et al., 2019)**
	***α*-Bulnesene**	Camu- camu pulp	DBD plasma	voltage of a 10 & 20 kV	200, 420, 580, 700, 960, 12000, 30000 Hz	5 & 15 min.	Significant↑ with all frequencies	**(Campelo, et al., 2020a)**
		Camu- camu pulp	Glow discharge	80 kV	50 kHz	(10, 20 and 30 min).	↓ After plasma treatment	**(Campelo, et al., 2020b)**
	***γ*-Cadinene**	Camu- camu pulp	DBD plasma	voltage of a 10 & 20 kV	200, 420, 580, 700, 960, 12000, 30000 Hz	5 & 15 min.	Significant ↑ with 420, 580, 700 &12000. significant ↓ with other frequencies	**(Campelo, et al., 2020a)**
		Camu- camu pulp	Glow discharge	80 kV	50 kHz	(10, 20 and 30 min).	↓ After plasma treatment	**(Campelo, et al., 2020b)**
	Cadina-1(2),4-diene	Camu- camu pulp	DBD plasma	voltage of a 10 & 20 kV	200, 420, 580, 700, 960, 12000, 30000 Hz	5 & 15 min.	Significant ↑ with all other frequencies except for 700Hz that showed significant ↓	**(Campelo, et al., 2020a)**
		Camu- camu pulp	Glow discharge	80 kV	50 kHz	(10, 20 and 30 min).	↓ After plasma treatment	**(Campelo, et al., 2020b)**
	Selina-3,7(11)-diene	Camu- camu pulp	DBD plasma	voltage of a 10 & 20 kV	200, 420, 580, 700, 960, 12000, 30000 Hz	5 & 15 min.	Non-significant change with 1200 Hz, Significant ↑ with 420, 580, 700 & 30000 Hz except for 200 & 960 Hz that showed significant ↓	**(Campelo, et al., 2020a)**
		Camu- camu pulp	Glow discharge	80 kV	50 kHz	(10, 20 and 30 min).	↓ After plasma treatment	**(Campelo, et al., 2020b)**
	***α*-Calacorene**	Camu- camu pulp	DBD plasma	voltage of a 10 & 20 kV	200, 420, 580, 700, 960, 12000, 30000 Hz	5 & 15 min.	Non-significant change with 1200 Hz, Significant ↑ with 420, 580, 700 & 30000 Hz except for 200 & 960 Hz that showed significant ↓	**(Campelo, et al., 2020a)**
		Camu- camu pulp	Glow discharge	80 kV	50 kHz	(10, 20 and 30 min).	↓ After plasma treatment	**(Campelo, et al., 2020b)**

Table 3: Continued

Class	Compounds	Sample	Plasma Treatment conditions				Findings	Ref.
			Plasma source	Power/voltage	Frequency	Exposure time		
Terpenes	**Spathulenol**	Lemon verbena shrubs (EO)	LPCP system	1200W	2.45 GHz	0, 1, 3, & 5 min.	↑ After plasma treatment at all time points	**(Ebadi, et al., 2019)**
	Globulol	Lemon verbena shrubs (EO)	LPCP system	1200W	2.45 GHz	0, 1, 3, & 5 min.	↑ After plasma treatment at all time points	**(Ebadi, et al., 2019)**
	Epi-*a*-cadinol	Lemon verbena shrubs (EO)	LPCP system	1200W	2.45 GHz	0, 1, 3, & 5 min.	↑ After plasma treatment at all time points	**(Ebadi, et al., 2019)**
	Longicyclene	Brown rice	DBD plasma	40 and 50 kV	-	1.5-3 min	Produced by only T3: 40 kV-180 s; T4: 50 kV-180 s.	**(Q. Liu, et al., 2021)**
	Germacrene B	Camu- camu pulp	DBD plasma	voltage of a 10 & 20 kV	200, 420, 580, 700, 960, 12000, 30000 Hz	5 & 15 min.	Significant ↑ with 420, 580, 700, 12000 & 30000 Hz except for 200 & 960 Hz that showed significant ↓	**(Campelo, et al., 2020a)**
		Camu- camu pulp	Glow discharge	80 kV	50 kHz	(10, 20 and 30 min).	↓ After plasma treatment	**(Campelo, et al., 2020b)**
Benzene dv.	**Longifolene**	Brown rice	DBD plasma	40 and 50 kV	-	1.5-3 min	↓ In all studied treatments	**(Q. Liu, et al., 2021)**
		Fresh-cut cantaloupe	-	40 kV		90 s	Fluctuating changes in control and samples	**(Zhou, et al., 2022)**
	***m*-Xylene**	Tomato Juice	Electric discharge	10 Kv	-	5 min	Produced by plasma treatment	**(T. Ma, et al., 2015)**
	***o*-Xylene**	Tomato Juice	Electric discharge	10 Kv	-	5 min	Produced by plasma treatment	**(T. Ma, et al., 2015)**
	3-Methyl-4-isopropylphenol	Fresh-cut cantaloupe	-	40 kV		90 s	↑ After plasma treatment at all time points	**(Zhou, et al., 2022)**
	3-*tert*-Butylphenol	Brown rice	DBD plasma	40 and 50 kV	-	1.5-3 min	Lost by all studied treatments	**(Q. Liu, et al., 2021)**
	Styrene	Brown rice	DBD plasma	40 and 50 kV	-	1.5-3 min	↓ In all studied treatments	**(Q. Liu, et al., 2021)**
Hydrocarbons	**2-Ethoxy propane**	Tomato Juice	Electric discharge plasma	10 Kv	-	5 min	↑ After plasma treatment	**(T. Ma, et al., 2015)**
	2-Ethoxy-pentane	Tomato Juice	Electric discharge	10 Kv	-	5 min	Decreased by plasma treatment	**(T. Ma, et al., 2015)**
	Pentadecane	Brown rice	DBD plasma	40 and 50 kV	-	1.5-3 min	Lost by all studied treatments	**(Q. Liu, et al., 2021)**
	Hexadecane	Brown rice	DBD plasma	40 and 50 kV	-	1.5-3 min	↑ By T2: 50 kV-90 s; T3: 40 kV-180 s; ↓ By T1: 40 kV-90 s; T4: 50 kV-180 s	**(Q. Liu, et al., 2021)**
	2,3-Dimethyldodecane	Fresh-cut cantaloupe	-	40 kV		90 s	↑ or at least not changed after plasma treatment	**(Zhou, et al., 2022)**
	Dodecane	Brown rice	DBD plasma	40 and 50 kV	-	1.5-3 min	↓ In all studied treatments	**(Q. Liu, et al., 2021)**
		Fresh-cut cantaloupe	-	40 kV		90 s	↑ or at least not changed after plasma treatment	**(Zhou, et al., 2022)**
	Tridecane	Brown rice	DBD plasma	40 and 50 kV	-	1.5-3 min	Produced by only T4: 50 kV-180 s.	**(Q. Liu, et al., 2021)**

Table 3: Continued

Class	Compounds	Sample	Plasma Treatment conditions				Findings	Ref.
			Plasma source	Power/voltage	Frequency	Exposure time		
Hydrocarbons	**Tetradecane**	Brown rice	DBD plasma	40 and 50 kV	-	1.5-3 min	↓ By T1: 40 kV-90 s; ↑ By T2: 50 kV-90 s; T3: 40 kV-180 s; T4: 50 kV-180 s.	**(Q. Liu, et al., 2021)**
		Fresh-cut cantaloupe	-	40 kV		90 s	↑ or at least not changed after plasma treatment	**(Zhou, et al., 2022)**
	Undecylcyclopentane	Brown rice	DBD plasma	40 and 50 kV	-	1.5-3 min	↓ By T1: 40 kV-90 s; T4: 50 kV-180 s. ↑ By T2: 50 kV-90 s; T3: 40 kV-180 s; T4: 50 kV-180 s.	**(Q. Liu, et al., 2021)**
	3-Methylheptadecane	Brown rice	DBD plasma	40 and 50 kV	-	1.5-3 min	↓ In all studied treatments	**(Q. Liu, et al., 2021)**
	5-Butylhexadecane	Brown rice	DBD plasma	40 and 50 kV	-	1.5-3 min	↓ In all studied treatments	**(Q. Liu, et al., 2021)**
	5-Methylundecane	Brown rice	DBD plasma	40 and 50 kV	-	1.5-3 min	Produced by only T3: 40 kV-180 s.	**(Q. Liu, et al., 2021)**
	7-Hexyl-tridecane	Brown rice	DBD plasma	40 and 50 kV	-	1.5-3 min	↓ In all studied treatments	**(Q. Liu, et al., 2021)**
	Nonylcyclopentane	Brown rice	DBD plasma	40 and 50 kV	-	1.5-3 min	↑ By T1: 40 kV-90 s; T2: 50 kV-90 s; ↓ By T3: 40 kV-180 s; T4: 50 kV-180 s	**(Q. Liu, et al., 2021)**
	8-Hexylpentadecane	Brown rice	DBD plasma	40 and 50 kV	-	1.5-3 min	↓ In all studied treatments	**(Q. Liu, et al., 2021)**
	9-Methylnonadecane	Brown rice	DBD plasma	40 and 50 kV	-	1.5-3 min	↓ In all studied treatments	**(Q. Liu, et al., 2021)**
	10-Methylnonadecane	Brown rice	DBD plasma	40 and 50 kV	-	1.5-3 min	Produced by only T3: 40 kV-180 s; T4: 50 kV-180 s.	**(Q. Liu, et al., 2021)**
	***(E,E,E)*-2,4,6-Octatriene**	Fresh-cut cantaloupe	-	40 kV		90 s	↑ Up to day 4, then not detected afterwards	**(Zhou, et al., 2022)**
Lactones	***γ*-Heptalactone**	Brown rice	DBD plasma	40 and 50 kV	-	1.5-3 min	Produced by T1: 40 kV-90 s;, T2: 50 kV-90 s; and T3: 40 kV-180 s).	**(Q. Liu, et al., 2021)**
		Fresh-cut cantaloupe	-	40 kV		90 s	↓at day 0, but ↑ afterwards up to day 10	**(Zhou, et al., 2022)**
	Dihydroactinidiolide	Fresh-cut cantaloupe	-	40 kV		90 s	Non-significant changes up to day 2 then ↑ afterwards.	**(Zhou, et al., 2022)**
Pyrazines	**2,5-Dimethylpyrazine**	Brown rice	DBD plasma	40 and 50 kV	-	1.5-3 min	↑ By T3: 40 kV-90 s. ↓ By T4: 50 kV-180 s. Lost by T1: 40 kV-90 s; T2: 50 kV-90 s.	**(Q. Liu, et al., 2021)**

↓: Decrease in the level; ↑: increase in the level; DBD: Dielectric Barrier Discharge; LPCP: Low pressure cold plasma.

1.6.5. Effect of CP processing on antioxidant activity

The significant antioxidants and scavenging compounds present in fruits and vegetables are phenolic compounds, vitamin C, and vitamin E. Though antioxidant activity is not an exact indication of quality in the food industries, it closely points to the various polyphenols, flavanols, and flavonoids present in foods **(Shashi K Pankaj, et al., 2018)**. These bioactive compounds show the ability to scavenge free radicals accountable for infections and diseases often triggered by oxidative stress and thus minimize their threat. The modification of radical-scavenging capabilities of functional compounds present in food throughout plasma processing might be of advantage or disadvantage.

The antioxidant potentials of food products are primarily evaluated employing 1,1-diphenyl-2-picrylhydrazyl (DPPH) scavenging activity, oxygen radical absorbance capacity (ORAC) 2,2′ -azino-bis-3-ethylbenzothiazoline 6 sulfonic acid (ABTS) radical scavenging activity, and ferric reducing antioxidant power (FRAP) assay **(Sruthi, et al., 2021)**.

There are contradictory outcomes regarding the impact of CP on antioxidant activities of CP processed food. For example, an increase in the antioxidant activity after CP treatment has been documented for treated brown rice **(H. H. Chen, et al., 2016)**, cloudy apple juice **(Illera, et al., 2019)** and fresh-cut pitaya **(Illera, et al., 2019)**. On the other hand, a reduction in the antioxidant power of CP treated *Indica* rice paddies **(Zargarchi, et al., 2019)** and white grape juice **(Shashi Kishor Pankaj, et al., 2017)** by low-pressure plasma and high voltage atmospheric CP treatment respectively, was previously reported. This reduction in the antioxidant activity was attributed it to the decrease in the total phenolics content and the decomposition of antioxidant phenolic compounds. It was illustrated that low and limited exposure to plasma increased the antioxidant activity, whereas exposure for extended times at elevated flow rates directed a drop in the antioxidant activity.

de Castro, et al. (2020) showed the correlation between the excitation frequency of DBD-CP and the antioxidant activity of processed camu-camu juice. They found that the antioxidant activity increased at low frequency (200 Hz), while intermediate frequencies (420–628 Hz) had negative effects on the antioxidants power. Higher frequencies (960 Hz) improved the antioxidant activity.

Several studies showed non-significant differences in the antioxidant activity after cold plasma processing **(Amini, et al., 2016; Ramazzina, et al., 2015; Song, et al., 2015; Yodpitak, et al., 2019)**.

Generally, most researchers have limited their investigation to either narrating an increase or reduction in the antioxidant potential of plasma-treated products. Additional

examinations are thus recommended to elucidate the reaction chemistry between the plasma reactive species and the antioxidants in the treated foods.

2 Materials and methods

2. Materials and methods

2.1. Plant material

All samples: rocket-salad leaves: *Eruca sativa* (L.) Mill., strawberries fruit: *Fragaria* × *ananassa* and melon: *Cucumis melo* L. were purchased at the local market in Cesena, Italy and stored in a refrigerated cell at 2 ± 1 °C for maximum 24 h before processing.

2.1.1. Rocket-salad leaves

For rocket samples, intact leaves free of defects were selected and divided into sub-samples to be subjected to the different treatments.

2.1.2. Strawberries

The selected strawberries had a consistent physiological and mature state without any damage. As described in scheme 3, twelve trays were selected randomly to be treated with DBD-Cold Plasma (named "T group") while the remaining 12 trays (named "C group") with no treatment were used as the control group. After the treatments, the trays were stored at 4 °C for six days and then collected on day 0, 1, 3 or 6 d. Fruit after harvest without treatment was used as control at 0 d. At each time point, six trays (3 trays in C group and 3 trays in T group) were selected for further determinations. This to obtain eight different groups control (CT0, CT1, CT3 and CT6) and the treated (TT0, TT1, TT3 and TT6) groups; respectively. Fresh fruits stored at each time point in a freezer at −80 °C then all samples were freeze-dried and then extracted before analysis.

2.1.3. Melons

Regarding melons, they were washed in the surface with abrasive sponge to remove dirt, then dipped for 2 min in sodium hypochlorite solution. Then each melon was first cut in half, the final parts were discarded, and the central one was cut into slices. From each slice, 4-5 pieces of 8-10 g were obtained and from each, rind and seeds were removed with a stainless-steel knife.

2.2. Plasma treatment

2.2.1. Rocket-salad leaves treatment by PAW

PAW was produced using a corona discharge plasma source (AlmaPlasma s.rl., Bologna, Italy) using distilled water as described in **(Laurita, et al., 2021)**. A microsecond pulse generator (AlmaPulse, AlmaPlasma s.r.l.) is connected to a stainless-steel pin electrode, held 5mmfrom the surface. of 450 mL of distilled water which is stirred continuously (Figure 8). Operating parameters were 9 kV peak voltage and 5 kHz frequency. PAW was created by exposing distilled water to plasma for 4 min. The measured concentrations of H_2O_2, NO_2, and dissolved O_3 after 4 min were 4.5 ± 0.1, 30.4 ± 0.9, and 0.3 ± 0.1 mg/L, respectively, and the pH of the PAW was 3.3. Following the water treatment, rocket samples were soaked in PAW for 2, 5, 10, and 20 min at room temperature in a product: liquid ratio of 1:20 (w:v), to obtain five different samples control, PAW-2, PAW-5, PAW-10 & PAW-20. In an orbital agitator, materials were continually stirred during immersion. Rocket leaves were taken from PAW after dipping and wiped with absorbent paper to remove excess liquid. Two separate treatments were carried out for each treatment time. Fresh rocket leaves (untreated) were used as control. Rocket samples from both washing replicates were promptly freeze-dried (freeze dryer model LIO2000P, 5Pascal, Milan, IT, Italy) after each treatment period, and the resulting samples were kept at -20 °C until analysis (about 2 weeks).

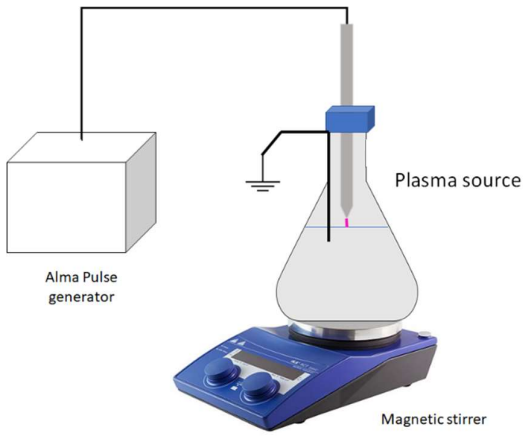

Figure 8: Schematic presentation of the experimental setup of the corona source during the production of plasma activated water.

2.2.2. Strawberries treatment by DBD

Cold Atmospheric Plasma (CAP) was generated by a surface dielectric barrier discharge (SDBD) placed at the top of a closed chamber, defining a confined atmosphere. A high voltage generator produced a sinusoidal waveform with a peak voltage of 6 kV and a repetition frequency of 23 kHz; the power density absorbed by the plasma source was of 425.35 ± 25.79 W, resulting in a surface power density of 2.6 W/cm^2. The distance measured from the surface of SDBD, and the top surface of the fruit sample was 10 cm. Treatments were carried out at room temperature (26 ± 1 °C) for 30 min. After treatment, samples were packed in plastic macroforated trays and subjected to storage at 2°C for 1,3 and 6 days (Scheme 4).

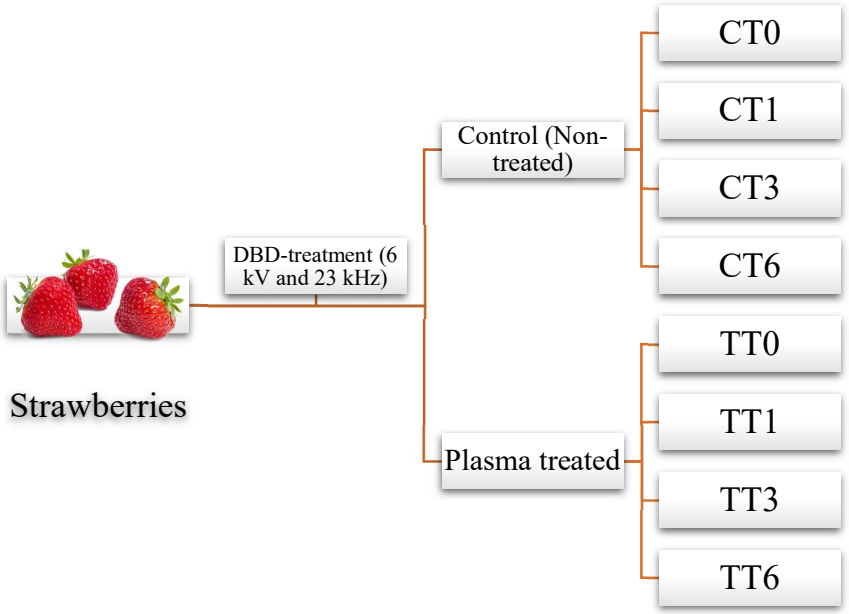

Scheme 4: Processing of strawberries resulting in eight groups with n = 3 replicates per group. C: untreated group (control); T: plasma treated, each stored for 0, 1, 3 & 6 days.

2.2.3. Fresh-cut melon treatment by sDBD

Melons were randomly divided into subsamples for the CAP treatment. An SDBD plasma source operated in ambient air **(Capelli, et al., 2021)** was used for sample treatments. Two different operative conditions were investigated, both working with sinusoidal high voltage signal having a peak voltage of 6.6 kV and a frequency of 23 kHz, varying the duty-cycle (DC), i.e., the ratio of time in which the signal was turned on over the treatment time. The ozone concentrations were measured using the optical absorption spectroscopy technique that exploits the Lambert–Beer law, resulting in low (300 ppm, O_3) or high (800 ppm, O_3(+)) ozone concentrations using 10% DC or 100%DC, respectively. For each condition 5, 10, 20 and 30 min were used as treatment time. The untreated sample was kept as a control (Scheme 5).

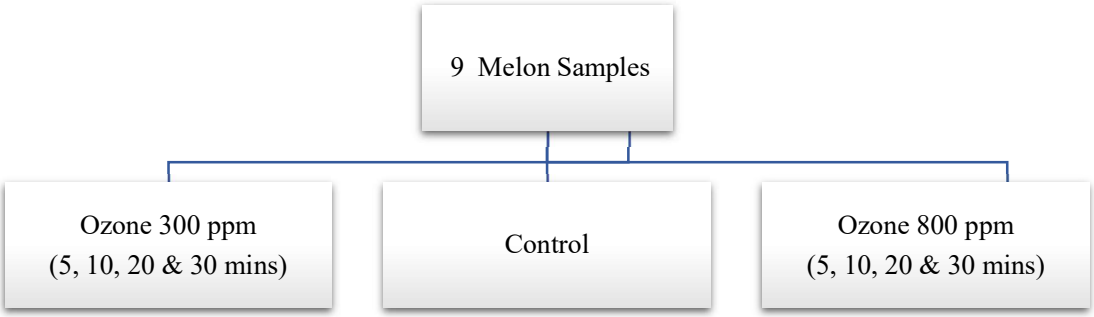

Scheme 5: Processing of melon resulting in nine groups with n = 3 replicates per group. Control and plasma treated groups at four different times.

2.3. Sample extraction for LC-MS/MS and spectrophotometric analysis

Freeze-dried rocket, strawberry and melon powders (10 $mg.ml^{-1}$ each) were extracted using aqueous ethanol 70% acidified with 1.5 % formic acid, The suspension was shaken vigorously for 3 min and then put in the sonicator using a FALC ultrasonic bath (FALC, Treviglio, Italy) for 60 min at a frequency of 40 kHz, and a temperature of 30 °C. After extraction, centrifugation for 10 min at 5000 rpm was performed. The clear supernatant was filtered through a 0.2-µm syringeless filter before injection. Triplicate analysis was done for each sample and was used for both HPLC-MS/MS analysis and spectrophotometric analysis.

2.4. HPLC-ESI-MS/MS analysis

2.4.1. HPLC-ESI-MS/MS

HPLC-MS/MS studies were performed using an Agilent 1290 Infinity series and a Triple Quadrupole 6420 from Agilent Technology (Santa Clara, CA) equipped with an electrospray ionization (ESI) source operating in negative and positive ionization modes. In fact, the instrument allowed to perform a one run with polarity switching without any problems. MS/MS parameters of each analyte were optimized in flow injection analysis (FIA) (1 µl of a 10 mg L^{-1} individual standard solution) by using Optimizer Software (Agilent). The separation of target compounds was achieved on a Synergi Polar–RP C18 analytical column (250 mm x 4.6 mm, 4 µm) from Phenomenex (Chesire, UK). The column was preceded by a Polar RP security guard cartridge (4 mm x 3 mm ID). The mobile phase was a mixture of (a) water and (b) methanol, both with formic acid 0.1% at a flow rate of 0.2 ml min^{-1} in gradient elution mode. The composition of the mobile phase varied as follows: 0–1 min, isocratic condition, 20% B; 1–25 min, 85% B; 25–26 min, isocratic condition, 85% B; 26–32 min, 20% B. All solvents and solutions were filtered through a 0.2-µm polyamide filter from Sartorius Stedim (Goettingen, Germany). The injection volume was 2 µl. The temperature of the column was 30 ºC, and the temperature of the drying gas (nitrogen) in the ionization source was 350 ºC. The gas flow was 12 L/min, the nebulizer pressure was 55 psi, and the capillary voltage was 4000 V. Detection was performed in the dynamic-multiple reaction monitoring (dynamic-MRM) mode, and the dynamic-MRM peak areas were integrated for quantification. The most abundant product ion was used for quantitation, and the other for qualification. The selected ion transitions and the mass spectrometer parameters including the specific time window for each compound (Δ retention time) are reported in table 4**.**

2.4.2. Optimization of the HPLC-MS/MS analytical method

To correct the unambiguous identification of the analyzed compounds, the high-performance liquid chromatography tandem mass spectrometry (HPLC–MS/MS) analysis was performed with electrospray ionization (ESI) mode. The simultaneous analysis of the 36 analytes was performed in dynamic-MRM mode that permitted to monitor a specific transition at a specific time according to the retention time of the analytes. Analytes were characterized by their MS/MS spectra and retention time.

The selection of the chromatographic conditions was guided by the need to obtain chromatograms with the best resolution of adjacent peaks in a short time of analysis. Two different columns namely, Synergi Polar–RP C18 (250 mm x 4.6 mm, 4 µm) and Kinetex PFP (100 mm × 2.1mm, 2.6 µm) were tested and Synergi Polar–RP C18 was the ideal column for the analysis and separation of this complex mixture of molecules.

We also studied the effect of column temperature at 25 and 30 °C. At 25 °C, the column demonstrated a partial coelution of the peaks of some compounds, but when the column temperature was kept at 30 °C, all peaks were well separated. Several attempts have been performed to enhance the separation process in a reasonable run time. For this purpose, we injected a standard mixture of 36 analytes at concentration of 1 mg L^{-1} using different mobile phases (water/acetonitrile, water/methanol; both with and without formic acid). The best separation was achieved with water/methanol containing 0.1% of formic acid, flowing at 0.8 ml min^{-1}.

Moreover, considering the different and wide degrees of polarity of the 36 standards belonging to the chemical classes of anthocyanins (delphindin-3,5-diglucoside, delphindin-3-galactoside, cyanidin-3-glucoside, petunidin-3-glucoside, pelargonidin-3-rutinoside, pelargonidin-3-glucoside, malvidin-3-galactoside), flavonols (quercetin, rutin, isoquercitrin, quercitrin, hyperoside, isorhamnetin, myricetin, kaempferol, kaempferol-3-glucoside), flavan-3-ols ((+)-Catechin, (-)-Epicatechin, Procyanidin A2, Procyanidin B2), flavanones (hesperidin, naringin), dihydrochalcones (phlorizin, phloretin) and phenolic acids (neochlorogenic acid, chlorogenic acid, gallic acid, *p*-hydroxybenzoic acid, 3-hydroxybenzoic acid, caffeic acid, vanillic acid, syringic acid, *p*-coumaric acid, ferulic acid, 3,5-dicaffeoylquinic acid, ellagic acid), gradient elution was used to achieve better separation (Figure 9). Under the optimum gradient conditions (0–1 min, 20% B; 1–25 min, 20–85% B; 25–26 min, 85% B; 26–32 min, 85–20% B), the baseline separation of the peaks of these 36 compounds was achieved with good peak symmetry and all compounds were eluted within 25 min. However, other gradient conditions caused poor separation of some

peaks or extended run time. Figure 9 shows the HPLCMS/MS chromatogram of a standard mixture of the 36 analytes plotted as overlapped MRM transition of each monitored compound.

For optimum MS results, ionization was performed in both negative and positive ESI modes and the precursor ions were corresponding to the deprotonated $[M - H]^-$ or protonated $[M + H]^+$ adducts; respectively. Whereas for delphindin-3-galactoside, cyanidin-3-glucoside, petunidin-3-glucoside, pelargonidin-3-rutinoside, pelargonidin-3-glucoside and malvidin-3-galactoside, the precursor ions were the molecules positively charged $[M]^+$ in positive polarity. The MRM mode was applied to monitor the transitions of the parent-to-daughter ions of all standards except for procyanidin A2, procyanidin B2 and ellagic acid which were studied using single ion monitoring (SIM). Precursor ions were subjected to MS/MS experiments by testing various values of fragmentor and collision energy and choosing the optimum values which showed the highest sensitivity. Quantification of target compounds was performed after optimizing the acquisition parameters (Table 4).

2.4.3. Method validation

After optimizing the chromatographic conditions, the HPLC–MS/MS method was validated in terms of linearity, limits of detection (LODs), limits of quantification (LOQs), repeatability, specificity and recovery (Table 4). Calibration curves were constructed by injecting standard mixture solutions at the eight concentrations of 0.005, 0.01, 0.05, 0.1, 0.5, 1, 5 and 10 µg/mL and the 36 analytes demonstrated good linearity ($R^2 \geq 0.9943$) in a wide concentration range. The LODs and LOQs were obtained by injecting serial dilutions of the corresponding standard solutions, taking the signal-to-noise (S/N) ratio of 3 and 10 as criteria, respectively. The signal-to-noise (SNR) ratio was measured using Mass Hunter Software from Agilent Technology (Santa Clara, CA). The LODs ranged from 0.0004 to 0.0033 µg/mL, while the LOQs were defined in the range of 0.0012 to 0.01 µg/mL, indicating an excellent sensitivity. The intraday precision (intraday repeatability or run-to-run precision) of the HPLC-MS/MS method was validated with the injection of the standard mixture solution under the selected optimal conditions five times a day. For interday precision (interday repeatability or day-to-day precision), measurements were conducted once a day on three consecutive days. All the precision measurements were expressed as relative standard deviations (RSDs). The method revealed a very good precision with inter and intraday variations where RSD (%) ranged from 0.34 to 4.73 and 0.12 to 2.62; respectively. High specificity was obtained using HPLC-MS/MS working in dynamic-MRM mode. The method specificity was evaluated by measuring retention time stability

and setting multiple pairs of precursor/product ions. Retention time stability for each molecule was studied three times over a period of 3 days and expressed by RSDs % which was in all cases ≤ 1.0 %.

Accuracy was evaluated by recovery study. Recovery percent (R %) was determined by spiking the blueberry and strawberry matrices with two concentrations of standard compounds. For this purpose, known amounts of the standard mixture solution were added to the fresh plant material, which was then extracted and assayed as described before. The percentage of recovery was evaluated by calculating the ratio of detected amount versus the added amount; the mean recovery of each compound in matrices of blueberry and strawberry is shown in table 4.

In LC-MS/MS analysis, the quantification or total polyphenols content is based on different references and not by one single reference and presented as gallic acid equivalents as in the spectrophotometric method. The spectrophotometric method is non-specific and usually overestimates the polyphenolic content with respect to the chromatographic method, mainly because of non-phenolic materials present in the extracts interfered in the spectrophotometric analysis.

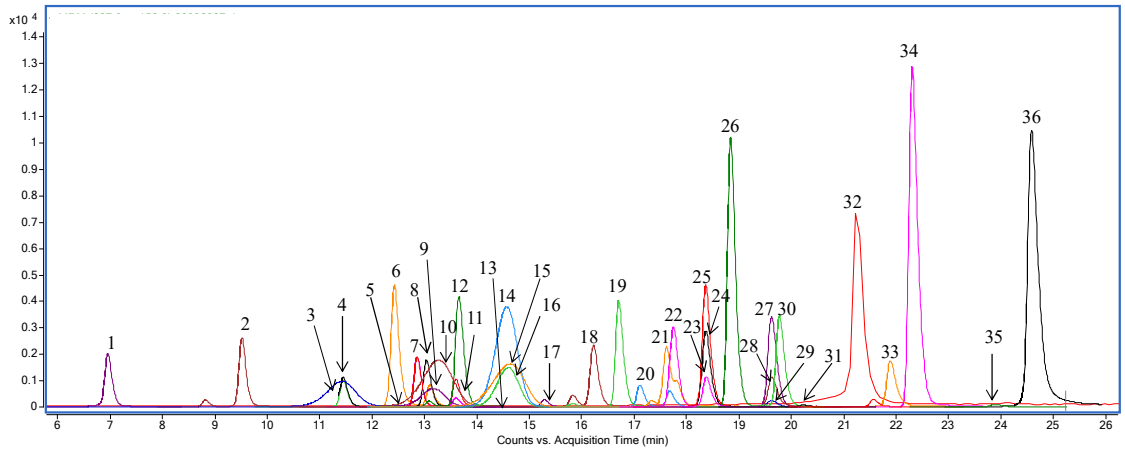

Figure 9: HPLC-MS/MS chromatogram of a standard mixture of 36 phenolic compounds plotted as overlapped multiple reaction monitoring (MRM) transition of each analyte. (1) Gallic acid, (2) Neochlorogenic acid, (3) Delphindin-3-galactoside, (4) (+)-Catechin, (5) Procyanidin B2, (6) Chlorogenic acid, (7) *p*-Hydroxybenzoic acid, (8) (-)-Epicatechin, (9) Cyanidin-3-glucoside, (10) Petunidin-3-glucoside, (11) 3-Hydroxybenzoic acid, (12) Caffeic acid, (13) Vanillic acid, (14) Pelargonidin-3-glucoside, (15) Pelagonidin-3-rutinoside, (16) Malvidin-3-galactoside, (17) Syringic acid, (18) Procyanidin A2, (19) *p*-Coumaric acid, (20) Ferulic acid, (21) 3,5-Dicaffeoylquinic acid, (22) Rutin, (23) Hyperoside, (24) Isoquercitrin, (25) Delphindin-3,5-diglucoside, (26) Phloridzin, (27) Quercitrin, (28) Myricetin, (29) Naringin, (30) Kaempferol-3-glucoside, (31) Hesperidin, (32) Ellagic acid, (33) Quercetin, (34) Phloretin, (35) Kaempferol, (36) Isorhamnetin.

Table 4: HPLC–MS/MS acquisition parameters (dynamic MRM mode) used for the analysis of the 36 marker compounds.

No.	Compounds	Precursor ion, *m/z*	Product ion, *m/z*	Fragmentor, V	Collision energy, V	Polarity	(Rt, min)	(ΔRt)
1	**Gallic acid**	169	125.2	97	12	Negative	6.96	3
2	**Neochlorogenic acid**	353	191.2, 179	102	12, 12	Negative	9.52	3
3	**Delphindin-3-galactoside**	465.01	303	121	20	Positive	11.36	3
4	***(+)*-Catechin**	289	245.2,109.2,123.2	131	8, 20, 24	Negative	11.44	3
5	**Procyanidin B2**	576.99	576.99, 321.2	160	0, 32	Negative	12.41	3
6	**Chlorogenic acid**	353	191.2, 127.5	82	12, 20	Negative	12.42	3
7	***p*-Hydroxybenzoic acid**	137	93.2	92	16	Negative	12.86	3
8	***(-)*-Epicatechin**	289	245.1, 109.1, 123.1	126	8, 20, 24	Negative	13.03	3
9	**Cyanidin-3-glucoside**	449	287.3, 255.6	121	20, 20	Positive	13.14	3
10	**Petunidin-3-glucoside**	479.01	317, 302, 186.2	121	20, 44, 50	Positive	13.26	3
11	**3-Hydroxybenzoic acid**	137	93.2	88	8	Negative	13.59	3
12	**Caffeic acid**	179	135.2, 134.1	92	12, 24	Negative	13.65	3
13	**Vanillic acid**	167	152.4, 108.1	88	12, 20	Negative	14.32	3
14	**Pelargonidin-3-glucoside**	433.01	271, 121	116	24, 50	Positive	14.52	3
15	**Pelagonidin-3-rutinoside**	579.01	271	145	32	Positive	14.56	3
16	**Malvidin-3-galactoside**	493.01	331, 315.1, 287	121	20, 50, 50	Positive	14.64	3
17	**Syringic acid**	196.9	182.2, 121.2	93	8, 12	Negative	15.28	3
18	**Procyanidin A2**	575	575, 285, 321.7	170	0, 20, 50	Negative	16.18	3
19	***p*-Coumaric acid**	163	119.2, 93.2	83	12, 36	Negative	16.70	3
20	**Ferulic acid**	193	134.2, 131.6	83	12, 8	Negative	17.10	3
21	**3,5-Dicaffeoylquinic acid**	514.9	353.1, 191	117	8, 28	Negative	17.61	3
22	**Rutin**	609	300.2, 271.2	170	32, 50	Negative	17.73	3
23	**Hyperoside**	465.01	303, 61.1, 85	97	8, 50, 24	Positive	18.33	3
24	**Isoquercitrin**	463	271.2, 300.2	155	44, 24	Negative	18.36	3
25	**Delphindin-3,5-diglucoside**	462.9	300.1	165	24	Negative	18.38	3
26	**Phloridzin**	435.39	273, 167, 123	155	8, 28, 40	Negative	18.83	3
27	**Quercitrin**	446.99	300.2, 301.2, 271.2	160	24, 16, 44	Negative	19.61	3
28	**Myricetin**	316.99	179.1, 182, 102	150	16, 24, 28	Negative	19.61	3
29	**Naringin**	578.99	271.3, 151.3	170	32, 44	Negative	19.62	3
30	**Kaempferol-3-glucoside**	447	284.2,255.2, 227.3	170	24, 40, 48	Negative	19.77	3
31	**Hesperidin**	611.01	303, 334.8, 352.1	112	20, 12, 48	Positive	20.19	3
32	**Ellagic acid**	301	301, 229	170	0, 24	Negative	21.41	3
33	**Quercetin**	300.99	151.2, 179.2, 107.2	145	16, 12, 24	Negative	21.87	3
34	**Phloretin**	272.99	167, 123, 81	116	8, 20, 28	Negative	22.30	3
35	**Kaempferol**	287.01	153, 69.1, 121	60	36, 50, 36	Positive	23.84	3
36	**Isorhamnetin**	314.99	300.2, 196.1	145	16, 4	Negative	24.57	3

Delta retention time (ΔRt), Retention time (Rt, min)

2.5. Spectrophotometric analysis

2.5.1. Total phenolic content (TPC)

As shown in figure 10, TPC was determined using a previously reported Folin-Ciocalteu method **(Mustafa, Mazzara, et al., 2022)**, in which 0.5 mL of the extract was mixed with 2.5 mL of diluted Folin-Ciocalteu reagent and 7 mL of Na_2CO_3 (7.5% aqueous solution), then left for 2 h in dark at room temperature; the absorption was measured spectrophotometrically at 765 nm. Results were expressed as gallic acid equivalents (GAE).

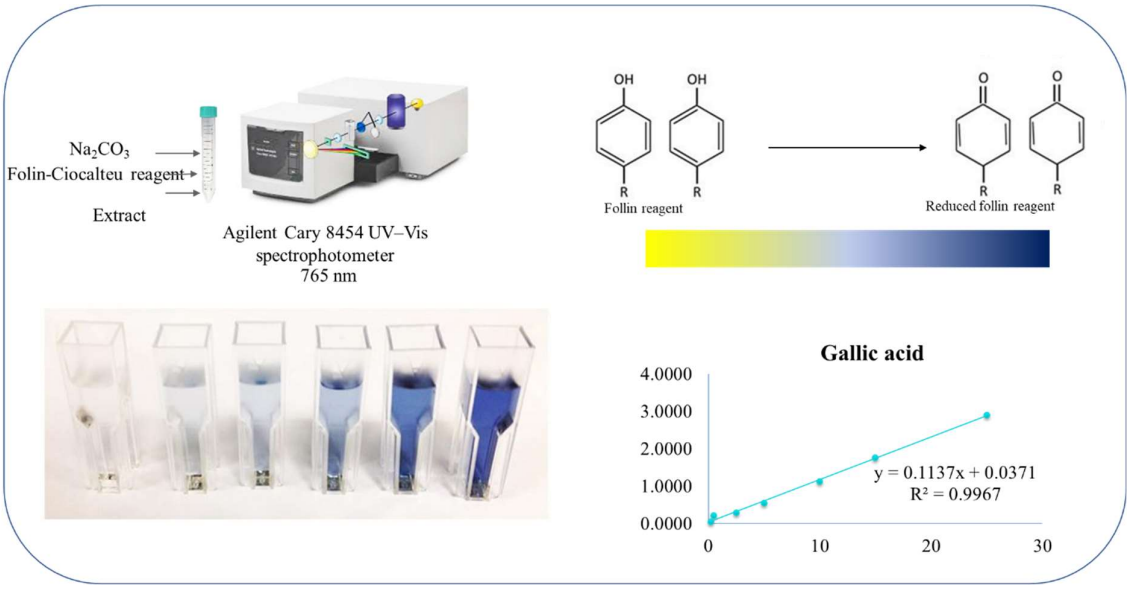

Figure 10: Determination of TPC using Folin-Ciocalteu method.

2.5.2. Total flavonoid content (TFC)

The TFC was determined using $AlCl_3$ method for flavonoids, based on the formation of a flavonoid-aluminum complex **(Mustafa, Mazzara, et al., 2022)**, in which 500 µL of the extract, 150 µL $NaNO_2$ (0.5 M), 3.2 mL methanol (30%v/v) and 150 µL $AlCl_3$ (0.3 M) were mixed. After 6 min, 1 mL of NaOH (1 M) was added to the mixture. The absorbance was measured using UV spectrophotometer at 506 nm. Results were expressed as rutin equivalents (RE).

2.5.3. Antioxidant activity (AOA)

As shown in figure 11, Antioxidant activity was determined in vitro by evaluation of the free radical scavenging activity using 2,2-diphenyl-1-picrylhydrazyl (DPPH) **(Mustafa, Mazzara, et al., 2022)**, in which 4.5 ml of a 0.1 mM DPPH ethanolic solution were added to 0.5 ml of the sample. The reaction mixture was measured at 517 nm after an incubation time of 30 min under dark conditions. The inhibition of free radical DPPH was expressed as trolox equivalents (TE).

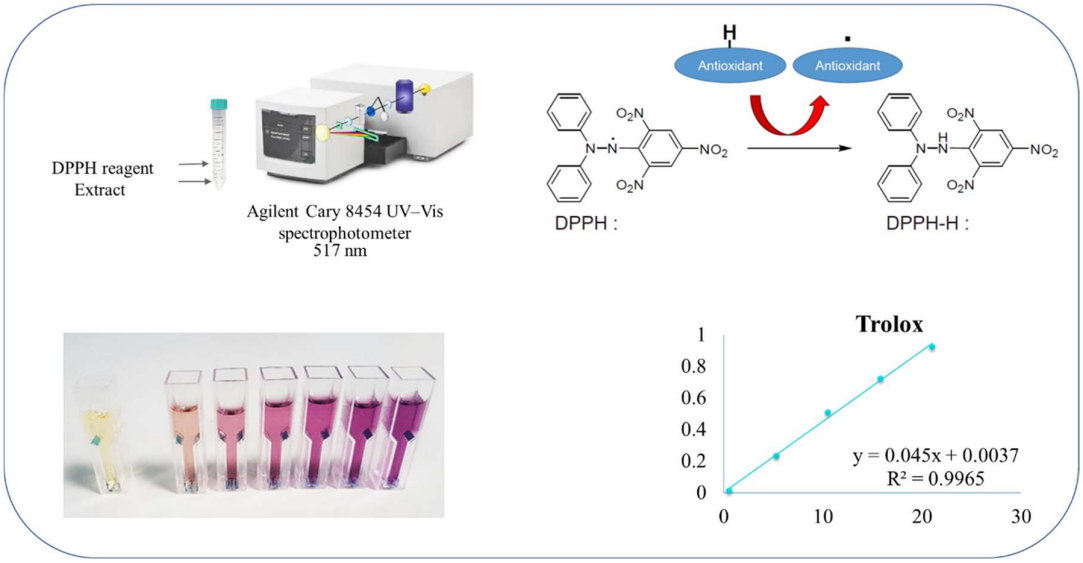

Figure 11: Determination of AOA using DPPH method.

2.6. Determination of ascorbic acid content using HPLC-DAD

2.6.1. Ascorbic acid extraction

The content of ascorbic acid was determined by an HPLC-DAD method previously described by **(Caprioli, et al., 2014)**. In which 100 mg freeze-dried samples were immersed in a 5ml extraction solution of water containing 5% metaphosphoric acid (MPA). The extraction was done for 4 h in darkness using a magnetic stirrer. Then, the samples were centrifuged for 10 min at 5000 rpm. The clear supernatant was filtered using a 0.45 mm membrane filter before analysis.

2.6.2. HPLC-DAD analysis

Hewlett Packard (Palo Alto, CA, USA) HP-1090 Series II was used for HPLC analysis. The series is composed of an autosampler and a binary solvent pump, together with a diode-array detector (DAD). Water with 0.1% formic acid (90 %) was utilized as mobile phase A

and methanol with 0.1% formic acid (10 %) was used as mobile phase B. The used flow rate was 0.5 mL/min in isocratic conditions. The injection volume was 10 µl. The used analytical column was Synergi Polar-RP C18 (4.6 mm x 150 mm, 4 µm) from Phenomenex (Chesire, UK). UV spectra were recorded (from 210 to 400 nm), and 245 nm was used for quantification.

2.7. Simultaneous quantification of riboflavin, nicotinamide and nicotinic acid by UHPLC MS/MS

2.7.1. Acidic hydrolysis extraction of riboflavin, nicotinamide and nicotinic acid

The contents of riboflavin (vitamin B2), two forms of vitamin B3; nicotinamide, and nicotinic acid were detected. The analysis was carried out using the method of **(Caprioli, et al., 2018)**. 0.1 N hydrochloric acid (10 mL) was used to hydrolyze 200 mg of each sample for 30 min at 100 °C with magnetic stirring. The liquid was allowed to cool to 25 °C before being adjusted to a pH of 4.0–4.5 using 2 M sodium acetate. After that, a 1 mL sample was diluted to 5 mL with deionized water before being filtered through Whatman No. 40 filter paper. Before injection, the supernatant was filtered again using a 0.2 m membrane filter (Gelman Sciences Inc., USA).

2.7.2. UHPLC-ESI–MS/MS analysis

A previous approach was used to measure riboflavin, nicotinic acid, and nicotinamide levels **(Caprioli, et al., 2018)**. An Agilent 1290 Infinity series and a Triple Quadrupole 6420 from Agilent Technology (Santa Clara, CA) were used to perform the analysis, which used an electrospray (ESI) source in the positive ionization mode. A Kinetex Hilic analytical column (100 mm 4.6 mm i.d., particle size 2.6 m) from Phenomenex was used to separate B vitamins (riboflavin, nicotinic acid, and nicotinamide) (Torrance, CA, USA).

For UHPLC–MS/MS analysis, the mobile phase was a combination of water (A, 95%) and acetonitrile (B, 5%), both containing formic acid 0.1%, and flowed at 0.8 mL/min with isocratic elution. The injection was 2 µL in volume. The column temperature was 30 °C, while that of the drying gas in the ionization source was 300 °C. The gas flow rate was set to 12 L/min, the nebulizer pressure was set to 50 psi, and the capillary voltage was set to 4000 V.

The data was collected in MRM mode, with the most abundant transitions chosen for quantification and the others for qualifying. The mobile phase used for analysis was a mixture of 95% water with 0.1 % formic acid (mobile phase A) and 5% acetonitrile with formic acid 0.1% (mobile phase B). Isocratic elution was done at a flow rate of 0.8 mL/min.

The samples injection volume was 2 µL and the gas flow was set at 12 L/min. The temperature of the column was kept at 30 °C while the temperature of the drying gas in the ionization source was kept at 300 °C. The acquisition was performed in MRM mode and the most abundant transitions were used for quantitation (Table 5).

Table 5: Ultra-high performance liquid chromatography/tandem mass spectrometry (UHPLC–MS/MS) acquisition parameters (MRM mode) used for the analysis of

Compound name	Precursor Ion	Product Ion	Fragmentor	Collision Energy	Rit. Time	Polarity
Nicotinic acid	124.06	80.1	92	21	1.58	Positive
Nicotinic acid	124.06	53.2	92	33	1.58	Positive
Nicotinamide	123.06	80.1	92	21	1.70	Positive
Nicotinamide	123.06	53.2	92	33	1.70	Positive
Riboflavin	377.15	243.1	131	21	2.14	Positive
Riboflavin	377.15	172.1	131	41	2.14	Positive

2.8. Volatile Organic Compounds (VOCs) Analysis

2.8.1 Headspace Solid-Phase Microextraction (HS-SPME)

As shown in figure 12, 400 mg of lyophilized rocket samples were weighted into a 20 mL vial sealed with a screw cap with a PTFE septum and equilibrated at 80 °C for 30 min. The incubation of the sample was done under agitation (250 rpm, 5 s of on-time and 2 s of off-time) and extracted using PDMS/DVB 65 µm SPME fibre coatings.

The fibre was conditioned for 15 min at 250 ºC and then exposed to the sample headspace at a penetration depth of 45 mm with a speed of 20 mm/s. The temperature was kept at 80 °C throughout the extraction of the volatile compounds for 15 min without agitation. After the extraction, the volatiles were directly desorbed on the GC liner and maintained at 250 °C for 2 min for fibre reconditioning.

2.8.2. GC-MS Analysis

Samples were analysed using an 8890-gas chromatograph (GC) from Agilent equipped with a PAL RTC 120 autosampler and a 5977B mass spectrometer (MSD) Agilent (Santa Clara, CA, USA). The ionization was obtained by using an electron ionization source (EI). The injector temperature was set at 250 ºC, and the liner used was recommended for SPME injection, namely, Inlet liner, Ultra Inert, splitless, straight, 0.75 mm id, from Agilent.

The gas carrier was helium at a flow rate of 1.0 mL/min. The separation of target molecules was established onto on a DB-Wax column (60 m, 250 µm i.d., 0.25 µm film thickness). The oven temperature program started at 35 ºC for 3 min, before increasing to 180 ºC at 3 ºC/min and from 180 to 210 ºC at 15 ºC/min, the final temperature (250 °C) was held for 10 min. The acquisition was carried out in SCAN mode (35–450 m/z).

The compounds identification was performed by comparison of their mass spectra and their experimental retention indices (RI) with data of the NIST library (US National Institute of Standards and Technology) and with those available in the literature **(Bell, Methven, et al., 2017; Bell, et al., 2016; Blažević, et al., 2008; Raffo, et al., 2018)**. The relative percentages of the individual components were calculated based on GC peak area, which was obtained by dividing the area of each component by the total area of all separated components. Percentage values were the means of two replicates for each sample. Data results were managed using MSD ChemStation Software (Agilent, Version G1701DA D.01.00, Santa Clara, CA, USA).

Figure 12: Extraction and analysis of VOCs using HS-SPME and GC-MS/MS analysis.

2.9. Phytosterol Analysis By HPLC-DAD

2.9.1. Extraction of phytosterols from rocket-salad leaves samples

The extraction was done as proposed previously by **Nzekoue, et al. (2020)** with slight modifications. Where 100 mg of each sample were mixed with 1N HCl (1 ml) and water (3 mL) then sonicated for 10 min (59 Hz). After sonication, the samples were saponified for 40 min and extracted after cooling with hexane (10 mL X 3), then collected and dried with a rotary evaporator. Subsequently, the dry extracts were dissolved in 1 mL of hexane. Dansylating was used to derivatize the extracted phytosterols in which, 1 mL of the hexane extract was mixed with 20 µL of hexaconazole (500 µg/ mL) then dried under nitrogen and redissolved with 2 mL of dichloromethane containing dansyl chloride and DMAP, both at a concentration of 8 mg /mL. Then, the sample was dried under nitrogen and dissolved in 1 mL of acetonitrile. Samples were sonicated and filtered for HPLC analysis.

2.9.2. HPLC-DAD Analyses

The dansylated phytosterols were detected using a 1260 Infinity liquid chromatography system (Agilent Technologies, Santa Clara, CA, USA), with an autosampler, quaternary pump and a diode array detector (DAD). The sample injection volume was 20 µL and the separation of analytes was performed on a Gemini C18 analytical column (250 × 3.0 mm, 5 µm) preceded by a security guard column C18 (4 × 3 mm, 5 µm), (Phenomenex, Torrance, CA, USA). Methanol (100%) was used as a mobile phase at a flow rate of 0.5 mL/ min. The elution was done in isocratic mode and phytosterols were detected and quantified at λ 254 nm **(Nzekoue, et al., 2020)**.

2.10. Determination Of *β*-carotene and lutein contents by HPLC-DAD

Both carotenoids were extracted according to the method described by **(Villatoro - Pulido, et al., 2013)** with slight modifications. Where 50 mg of lyophilized rocket sample were rehydrated with 5 mL ethanol containing 1 mg/ mL of butylated hydroxytoluene (BHT). 1 ml of a 50% (w/v) methanolic KOH solution was added and rocket extracts were saponified for 10 min at 85 ºC (in the dark). Samples were cooled in an ice bath and 2 mL of ice-cold water was added. The suspensions had been extracted two times with 2 mL of hexane by vigorous shaking then centrifuged at 5000 rpm for 10 min at room temperature. The upper hexane layers were separated and evaporated to dryness. Dried extracts were redissolved in 1 mL of an acetonitrile–methanol–dichloromethane solution (60:30:10 v/v) and filtered before injection. Carotenoid concentrations were determined by HPLC Agilent 1260 infinity II series (Santa Clara, CA, USA) using the method of **(Caprioli, et al., 2020)**

with some modifications. The analyses were carried out on a Chromolith RP-18e analytical column (100 x 3 mm I.D., macropore size 2 µm, mesopore size 13 nm) from Merck (Darmstadt, Germany). A gradient was used with a mobile phase composed of MilliQ water (A) and acetonitrile (B) and 2-propanol (C), the solvent composition is changed as follows: 0–2 min, 30:70 A/B (v/v); 2–5 min, 100% B (v/v); 5– 11 min, 80:20 B/C (v/v); 11–10 min, 100% B (v/v); 12– 14 min, 30:70 A/B (v/v). at a flow rate of 0.8 mL/ min. The detection of carotenoids was carried out at a wavelength of 450 nm.

2.11. GC-MS analysis of silylated primary metabolites

2.11.1. Metabolome extraction and two-step derivatization

As shown in figure 12, metabolites were extracted from strawberry samples according to the method reported by **Dai, et al. (2019)** with some modifications. Extraction solution was prepared by dissolving adonitol (internal standard; IS) into methanol preparing 50 µmol mL^{-1} solution. Freez-dried samples (20 mg each) were suspended in 800 µL extraction solvent, vortex-mixed then incubated in an ultrasonic bath for 10 min followed by centrifugation at 15,000 g for 10 min. The supernatant was collected, and the extraction was repeated with 400 µL water to obtain a total 110 µL extract. 300 µL hexane were added to remove the unwanted lipids then samples were vortexed shortly and centrifuged 5 min at 2,000 g. The lower layer containing the metabolites was transferred into a new microcentrifuge tube.

Pooled extracts were prepared to be used as quality controls (QC) and prepared by mixing equal aliquots of samples. Process/extraction blanks were also prepared by following the same extraction procedure described above without including the samples.

For derivatisation, 20 µL of each metabolomic extract was evaporated using a vacuum evaporator (Eppendorf Concentrator Vacufuge® plus, AG, Germany no. 022820168). In the first step, 30 µL of methoxamine (MEOX) hydrochloride (20 mg/mL in pyridine) were added to each samples then incubated at 30°C for 90 min under shaking. In the second step, metabolites were converted into trimethylsilyl (TMS) derivatives using 55 µL of MSTFA (*N*-trimethylsilyl-*N*-methyl trifluoroacetamide) then samples were Shaked for 30 min at 37°C with speed 750 rpm according to the earlier established procedure **(Leonova, et al., 2019)**. Finally, a mixture containing *n*-alkanes (C8 to C40, 5 µg mL−1) were added to the vials and injected to further calculate retention indices (RI) and to evaluate instrument performance, respectively.

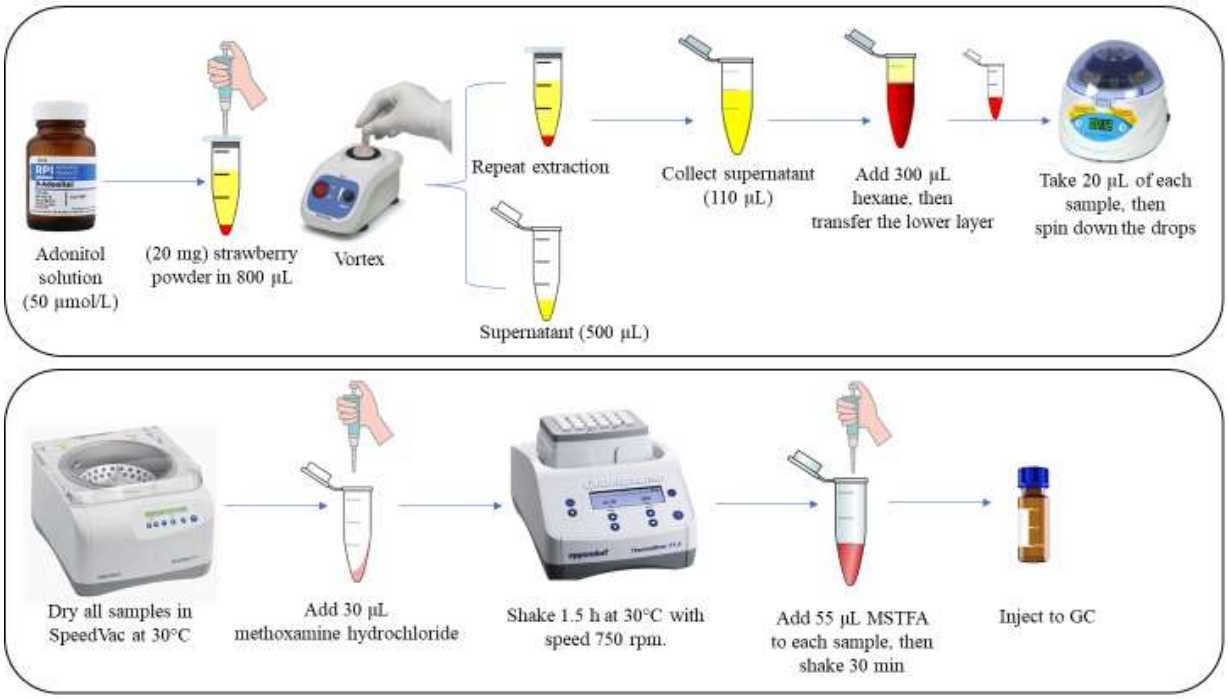

Figure 13: Experimental workflow of primary metabolome extraction and metabolites derivatisation.

2.11.2. Metabolomic analysis.

Derivatised samples were analysed using a gas chromatography-electron ionization-quadrupole-mass spectrometry (GC-EI-Q-MS) using a GC2010 gas chromatography coupled online to a quadrupole mass selective detector Shimadzu GCMS QP2010, equipped with a CTC GC PAL Liquid Injector (Shimadzu Deutschland GmbH, Duisburg, Germany). Samples were randomly separated and injected together with five quality control (QC) samples, a process/extraction blank, and a derivatisation control. The derivatisation control is a mixture of the derivatisation reagents added following the same derivatisation procedure to that of samples which used to allow further exclusion of features related to the derivatisation reagents.

The GC was equipped with HP-5 capillary column (30 m × 0.25 mm ID, 0.25 μ m film thickness, Thermo Fisher Scientific, Bremen, Germany). The oven temperature was held at 40 °C for 1 min and increased to 70 °C at 15 °C min^{-1} and held for 1 min then increased to to 320 °C at 6 °C min^{-1} and held for 10 min. Helium was used as a carrier gas at 1 mL min^{-1}. The MS detector was operated in EI positive mode (scan range of *m/z* 50–500, resolution of 60,000). The transfer line and ion source were maintained at 250 °C. Injection (1 µL) was performed in splitless mode (90 s splitless time).

2.11.3. GC data pre-processing and metabolomic identification

The pre-processing steps were performed on Automated Mass Spectral Deconvolution and Identification System (AMDIS, version 2.66 from 08.08.2008, free available via www.amdis.net) and Xcalibur ™ (version 2.0.7) in order to perform peak deconvolution and alignment of features from samples. The pre-processing procedure included importing raw files (. mzML data), followed by mass detection and construction of extracted ion chromatograms, to build a separate chromatogram – EIC – to each *m*/*z* that was detected by the instrument. Then, peak detection and deconvolution were applied to integrate peaks from EIC and to construct mass spectra of features by combining peaks from different EIC, respectively, thereby resulting in a list of RT-*m*/*z* to generate a table with all features detected. A filtering step was further applied to remove features associated to extraction blank and derivatisation controls.

The mass spectra of all detected compounds were identified by comparison with available spectral libraries – National Institute of Standards and Technology (NIST), Golm Metabolome Database (GMD), Human Metabolome Database (HMDB) and in-house library containg 150 standards (Table 6). (Partly with Kovats retention time indices, calculated by retention times of alkane standards. Quantitation relied on integration of the corresponding extracted ion chromatograms (XICs, ± 0.5 Da) at specific retention times (t_R).

Table 6: In-house library containing 150 primary metabolites detected by untargeted gas chromatography-electron ionization-quadrupole mass spectrometry (GC-EI-Q-MS).

	Name	t_{R1}	RI1	t_{R2}	RI2	m/z1 (quant)
n.1	*L*-Alanine, *N*-(trimethylsilyl)-, trimethylsilyl ester	10.13	1114.30	10.30	1121.60	116
n.2	*DL*-Malic acid, O-trimethylsilyl-, bis(trimethylsilyl) ester	18.57	1483.40			233
n.3	*N*-Acetyl glucosamine methoxime, tetrakis(trimethylsilyl)	28.92	2065.90	29.02	2072.50	319
n.4	d-Glucose, 2,3,4,5,6-pentakis-O-(trimethylsilyl)-, o-methyloxyme, (1E)-	26.08	1888.50	26.38	1906.70	319
n.5	D-Fructose, 1,3,4,5,6-pentakis-O-(trimethylsilyl)-, O-methyloxime	25.65	1863.40	25.82	1873.30	307
n.6	Octadecanoic acid, trimethylsilyl ester/stearic acid	31.58	2244.50			341
n.7	Fumaric acid/2-Butenedioic acid *(E)*-, bis(trimethylsilyl) ester	15.68	1350.40			245
n.8	*γ*-Aminobutyric acid (= GABA)/Butanoic acid, 4-[bis(trimethylsilyl)amino]-, trimethylsilyl ester	19.38	1523.40			174
n.9	*L*-(-)-Arabitol, pentakis(trimethylsilyl) ether	22.75	1697.70			217
n.10	d-Mannose, 2,3,4,5,6-pentakis-O-(trimethylsilyl)-, o-methyloxyme, (1E)-	26.13	1891.40			319
n.11	Hexadecanoic acid, trimethylsilyl ester (Palmitic Acid, TMS derivative)	28.61	2046.30			313
n.12	Oleonitrile	29.33	2092.40			122
n.13	Octadecanoic acid, trimethylsilyl ester/stearic acid	31.61	2246.40			341
n.14	Hexanedioic acid, bis(2-ethylhexyl) ester	33.76	2400.00			129
n.15	Valine (1TMS)	10.05	111.20			72
n.16	*L*-Valine, *N*-(trimethylsilyl)-, trimethylsilyl ester	12.67	1221.50			144
n.17	Butanedioic acid, bis(trimethylsilyl) ester/succinic acid	14.87	1314.80			247
n.18	d-Arabinose, 2,3,4,5-tetrakis-O-(trimethylsilyl)-, O-methyloxime	21.96	1655.90			307
n.19	Glycerol phosphate disodium salt hydrate	23.16	1720.60	23.85	1759.50	357
n.20	Hexadecanoic acid, trimethylsilyl ester	28.62	2046.40			313
n.21	Sucrose	36.72	2629.10			361
n.22	Oxalic acid, 2TMS derivative	11.10	1155.40			220
n.23	*L*-Proline, trimethylsilyl ester	11.90	1189.20			70
n.24	Malonic acid, bis(trimethylsilyl) ester	12.45	1212.10			73
n.25	*L*-Glutamine, tris(trimethylsilyl) deriv.	18.33	1472.10			155
n.26	*L*-5-Oxoproline, 2TMS derivative	19.21	1514.80			156
n.27	D-Sorbitol, 6TMS	26.73	1928.00			319
n.28	Trimethylsilyl ether of glycerol	13.97	1276.40			205

n.29	Octanoic acid	13.81	1269.70			201
n.30	*L*-(-)-Sorbose	25.63	1862.30	25.73	1867.80	307
n.31	Maleic acid	14.64	1304.60			245
n.32	Citric acid, tetrakis(trimethylsilyl) deriv	24.77	1811.50			273
n.33	Mucic acid (=Galactaric acid)	28.43	2034.60			333
n.34	*L*-Aspartic acid, bis(trimethylsilyl) ester	17.25	1421.40			116
n.35	*L*-Aspartic acid, *N*-(trimethylsilyl)-, bis(trimethylsilyl) ester			19.22	1515.20	232
n.36	*D-(+)*-Galactose2,3,4,5,6-pentakis-O-(trimethylsilyl)-, o-methyloxyme, (1E)-	25.97	1882.30			319
n.37	Glycerol (=1,2,3-Propanetriol)	13.96	1275.90			205
n.38	*D (+)*- Xylose	21.63	1638.40			307
n.39	*D (+)*- Xylose			21.83	1648.80	307
n.40	Stearic acid, TMS derivative	31.62	2247.30			117
n.41	*L*-Ascorbic acid, 2,3,5,6-tetrakis-O-(trimethylsilyl)-	26.97	1942.90			332
n.42	Tryptamine, 2TMS	31.10	2211.20			174
n.43	Tryptamine, 3TMS			31.18	2216.70	174
n.44	d-Ribose, 2,3,4,5-tetrakis-O-(trimethylsilyl)-, O-methyloxime	22.24	1670.50			307
n.45	Melibiose, octakis(trimethylsilyl)-	38.28	2757.90			361
n.46	Maltose, octakis(trimethylsilyl)-	44.67	3351.30			361
n.47	Glycine, *N*-(trimethylsilyl)-, trimethylsilyl ester	10.72	1139.50			102
n.48	Glycine, *N, N*-bis(trimethylsilyl)-, trimethylsilyl ester			14.66	1304.40	248
n.49	*L*-Methionine, trimethylsilyl ester	17.00	1409.50			104
n.50	*L*-Methionine, *N*-(trimethylsilyl)-, trimethylsilyl ester			19.19	1513.40	176
n.51	glutaric acid/Pentanedioic acid, 2-(methoxyimino)-, bis(trimethylsilyl) ester	19.89	1548.80			221
n.52	glutaric acid/Pentanedioic acid, 2-(methoxyimino)-, bis(trimethylsilyl) ester			20.37	1572.70	198
n.53	*D-(+)*-Turanose, octakis(trimethylsilyl) ether	39.48	2860.90			361
n.54	D-Mannitol, 6TMS derivative	26.62	1921.10			319
n.55	Sucrose, 8TMS derivative	44.93	3377.90			361
n.56	Serine, bis(trimethylsilyl)-	13.67	1263.90			116
n.57	Serine tri-TMS			15.87	1358.80	116
n.58	Erythrose, O-methyloxime, tris-O-(trimethylsilyl)-	17.55	1435.20			205
n.59	Erythrose, O-methyloxime, tris-O-(trimethylsilyl)-			17.86	1450.00	205
n.60	4-Ketoglucose, bis(O-methyloxime), tetrakis(trimethylsilyl)	18.20	1466.00			103

n.61	*L- (+)*-Tartaric acid (=*L*-Threaric acid)	21.51	1631.60			292
n.62	Myo-Inositol	29.17	2082.00			318
n.63	Palmitic acid (Hexadecanoic acid)	28.60	2045.30			313
n.64	D-(-)-Isoascorbic acid (=erythorbic acid, D-araboascorbic acid, D-erythro-2-enoic acid γ-lactone	27.12	1952.10			332
n.65	Oxalic acid, 2TMS derivative (Ethanedioic acid, bis(trimethylsilyl) ester)			11.09	1155.00	133
n.66	Niacin, TMS derivative (=Nicotinic acid-TMS)	14.46	1297.00			180
n.67	Salicylic acid, 2TMS derivative	18.95	1501.60			267
n.68	*L*-Homoserine, 2TMS derivative	15.81	1356.30			146
n.69	β-Alanine	17.27	1422.20			248
n.70	*DL*-Norvaline (= (±)-2-Aminopentanoic acid)	13.21	1244.30			144
n.71	*L*-Rhamnose monohydrate (= 6-Deoxy-*L*-mannose)	23.95	1708.70			117
n.72	Glycolic acid	9.81	1100.80			177
n.73	Decanoic acid (=Capric acid, C10:0)	18.04	1458.40			229
n.74	meso-Erythritol (=1,2,3,4-Butanetetrol)	18.94	1501.30			217
n.75	D-Glucuronic acid	26.70	1926.30			333
n.76	D-Glucuronic acid			26.94	1941.30	333
n.77	α-Lactose monohydrate (= 4-O-β-D-Galactopyranosyl-α-D-glucose)	37.33	2678.90			361
n.78	α-Lactose monohydrate (= 4-O-β-D-Galactopyranosyl-α-D-glucose)			37.54	2695.50	204
n.79	*DL*-Glyceraldehyde	12.46	1212.60			103
n.80	*DL*-Glyceraldehyde			12.78	1226.20	103
n.81	*L*-Leucine	13.89	1273.10			158
n.82	*L*-Threonine	14.41	1294.70			219
n.83	*L*-Threonine			16.42	1383.20	218
n.84	*D-(+)*-Galacturonic acid monohydrate	26.83	1934.60			333
n.85	*D-(+)*-Galacturonic acid monohydrate			27.14	1953.30	333
n.86	*DL*-Lysine-monohydrochloride	25.35	1845.50			174
n.87	*DL*-Lysine-monohydrochloride			26.51	1914.40	156
n.88	Glyoxylic acid monohydrate	7772.00	1004.20			160
n.89	Valeric acid (=Pentanoic acid) (2-Hydroxy-3-methylvaleric_acid)					
n.90	Glyceric acid, tris(trimethylsilyl) deriv.	15.20	1329.30			189
n.91	*L*-Pyroglutamic acid (=(S)-(−)-2-Pyrrolidone-5-carboxylic acid) (=5-oxoproline)	19.20	1514.20			156
n.92	*L*-Cysteine	19.88	1548.00			220

n.93	*L*-Isoleucine, 2TMS derivative	14.39	1293.80			158
n.94	*L*-Isoleucine, TMS derivative			11.92	1189.90	86
n.95	Gallic acid (=3,4,5-trihydroxybenzoic acid)	27.09	1950.40			281
n.96	D-Erythronic acid potassium salt	19.64	1536.10			292
n.97	Vanillin	21.78	1646.10			223
n.98	*L*-(-)-Fucose (= 6-Deoxy-*L*-galactose)	23.08	1716.10			117
n.99	*L*-(-)-Fucose (= 6-Deoxy-*L*-galactose)			23.30	1728.40	117
n.100	*L*-Glutamic acid, 3TMS derivative	21.17	1613.80			246
n.101	*DL*-Ornithine hydrochloride anhyrous	23.64	1747.80			174
n.102	Glutaric acid	16.84	1401.90			261
n.103	*trans*-Caffeic acid (= 2-propenoic acid)	29.95	2133.60			219
n.104	*cis*-Caffeic acid (= 2-propenoic acid)	27.47	1974.00			219
n.105	*DL*-Tryptophan	30.91	2198.00			202
n.106	Adenine	25.59	1859.80			264
n.107	2-Phenylglycine (= (±)-*α*-Aminophenylacetic acid)	19.16	1512.30			178
n.108	*L*-Arginine monohydrochloride	23.50	1739.50			184
n.109	Glutaric acid (=pentanedioic acid)	16.84	1401.90			261
n.110	Cinnamic acid	19.80	1544.00			220
n.111	Shikimic acid	24.65	1804.70			255
n.112	*cis*-Ferulic acid	26.51	1914.80			338
n.113	*trans*-Ferulic acid	29.29	2089.70			338
n.114	Putrescine (= 1.4-butanediamine)	23.28	1727.30			174
n.115	Vanillic acid	23.83	1758.30			297
n.116	Quinic acid	25.43	1850.40			345
n.117	*D-(+)*-Trehalose α,α' dihydrate	38.00	2734.30			361
n.118	*D*-Glucaric acid calcium salt (Calcium D-saccharate tetrahydrate)	27.92	2001.30			333
n.119	*D*-Ribose-5-phosphate disodium hydrate	29.20	2083.80			315
n.120	*D*-Ribose-5-phosphate disodium hydrate			29.50	2103.30	315
n.121	*D(-)*-Erythrulose	18.16	1464.10			173
n.122	*D(-)*-Erythrulose			18.39	1474.90	173
n.123	*D-(+)*-Maltose monohydrate	37.93	2728.80			361
n.124	*D-(+)*-Maltose monohydrate			38.26	2756.00	361

n.125	Erythrose-4-phosphate sodium	26.30	1901.70			357
n.126	Erythrose-4-phosphate sodium			26.47	1912.20	357
n.127	Ribulose	22.23	1670.30			263
n.128	Mannose-1-phosphate	32.61	2316.60			387
n.129	Galactinol	40.79	2977.30			204
n.130	Fructose-6-phosphate	32.38	2300.10			315
n.131	Isomaltose	39.52	2864.20			361
n.132	Isomaltose			39.88	2895.60	361
n.133	Dulcitol (=Galactitol)	26.81	1932.90			319
n.134	Glucose-6-phosphate	33.37	2372.10			387
n.135	Glucose-6-phosphate			33.54	2384.00	387
n.136	*D-(+)*-Turanose, octakis(trimethylsilyl) ether	37.63	2702.90			361
n.137	*D-(+)*-Turanose, octakis(trimethylsilyl) ether, methyloxime	38.11	2743.50			307
n.138	*D-(+)*-Turanose, octakis(trimethylsilyl) ether, methyloxime			38.45	2772.20	307
n.139	*D*-glyceraldehyde-3-phosphate	22.89	1705.40			328
n.140	*D*-glyceraldehyde-3-phosphate (gap)_3Hpeak	23.13	1718.90			328
n.141	*D(-)*-Phospho-glyceric acid (gip)	24749.00	1800.50			299
n.142	Raffinose	45.03	3387.60			437
n.143	Melibiose	39.39	2853.20			361
n.144	Melibiose	39.49	2862.00			361
n.145	Galactitol (=Dulcitol)	26.82	1933.80			219
n.146	Gluconic acid	27.74	1990.50			333
n.147	Gluconic acid-1,4-lactone	26.09	1889.30			217
n.148	Myo-inositol	29.17	2082.10			318
n.149	*D-(+)*-Gluconic acid δ-lactone (=gluconolactone)	25.90	1877.90			319
n.150	Gulonic acid, γ-lactone	27935.00	1990.30			189

t_R: retention time (min); RI: Kovats retention Index.

2.12. Statistical analysis

For untargeted primary metabolic analysis, data matrix exported using excel (Excel 365, Microsoft®, Redmond, WA, USA) for all samples, including their replicates. The data set was then modelled, the processing and statistical interpretation of the acquired data relied on MetaboAnalyst 5.0 online platform (free available via www.metaboanalyst.ca). Where features were filtered if their RSDs are > 30 % in quality controls and samples were Pareto scaled (mean-centered and divided by the square root of the standard deviation of each variable. Principal component analysis (PCA) was applied for checking the general trend in an unsupervised way. Then, Partial least squares discriminate analysis (PLS-DA) was used to maximize the fitness of variables discriminating between the two groups in a supervised way. The PLS-DA model was tested by cross-validation, and the validated model was further considered in sparse PLS-DA (sPLS-DA). In cross-validation, R2 indicates the fitness of the PLS-DA model with the whole data set, while Q2 is an estimate of the predictive ability of the model. High Q2 values indicate good prediction **(L. C. Lee, et al., 2018)**. Based on the high number of features in the untargeted metabolome, sPLS-DA was chosen to select the most predictive or discriminative features in the data that help classify the samples **(L. C. Lee, et al., 2018; Worley, et al., 2013)**.

For other analysis, a one-way analysis of variance (ANOVA) followed by the Tukey post hoc test were used to analyze statistical significance ($p < 0.05$). Hierarchical Clustering Analysis (HCA) was used to process data from HSPME-GC/MS analysis. Statistical analysis was performed using Minitab ver. 19.0 and Microsoft Excel 365 software. Measurements were made in triplicates and data from all chemical assays are presented as the mean ± SD.

3 Results and discussion

3. Results and discussion

3.1. Impact of Plasma activated water (PAW) treatment on bioactive compounds of rocket-salad leaves.

3.1.1. Impact of PAW treatment on the LC-MS/MS phenolic profile of rocket-salad leaves

A total of 18 phenolic compounds were detected in control and PAW treated rocket samples. The contents of individual and total phenolic compounds are given in table 7.

Since high temperatures used usually in food processing are able to degrade polyphenols, non-thermal technologies (especially, cold plasma technology) have become one of the best alternatives for an increased shelf life with improved polyphenol retention **(Z. H. Zhang, et al., 2019)**. Therefore, the phenolic profiles of control and PAW-treated rocket samples were analyzed by HPLC-MS/MS (Figure 14 & Table 7). The phenolic profile of the control rocket sample, consisted mainly of quercetin and quercetin glycosides (around 57 % of the total) which is consistent with the previous study of **(Villatoro-Pulido, et al., 2013)** who reported that quercetin derived compounds were the major flavonoids in rocket samples. However, previous studies have shown variability in rocket's phenolic profile that could be due to several factors, including extraction, chromatographic method together with quantification tools as well as the origin, and condition of the sample **(Bell, et al., 2019)**. In the current study, the extracts of the rocket leaves treated by PAW for 2, 5, 10 and 20 min were compared with the control.

The treatment time was found to promote a general increase in the total phenolic content of rocket for all treatment times with a maximum increase of 27.1 % in the samples treated with PAW-20. However, this increase in total phenolic content was not statistically significant. On the other side, analyzing the singular content of the different compounds, various significant differences were found, mostly at the longer treatment times (Table 7).

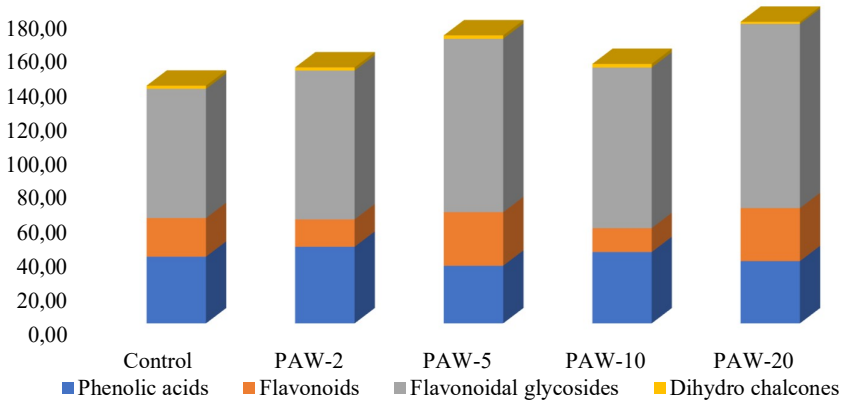

Figure 14: Impact of PAW treatment on the LC-MS/MS phenolic profile of rocket-salad leaves

As shown in table 7 & figure 15, among the phenolic acids, the extracts of rocket samples treated by PAW-20 min showed significant increase in ferulic, caffeic and coumaric acids concentrations compared to the control. Also, a significant increase in the concentration of chlorogenic acid was observed, but only in samples treated for 2 and 5 min. However, the concentration of 3,5-dicaffeoylquinic acid (isochlorogenic acid) was significantly decreased after PAW treatment, while ellagic acid concentration was constant in all treated samples. An increase in hydroxycinnamic acids have been observed by various authors after cold plasma exposure. **Herceg, et al. (2016)** reported a higher content of chlorogenic, ellagic and ferulic acid together with an increase in the catechin content of pomegranate juice processed by gas phase plasma. The authors attributed this increase to an effect of cell membrane breakdown, hydrolysis and depolymerization due to the reactive species of plasma. Also, a 30 % increase in the content of chlorogenic acids was observed after 10 min treatment in fresh-cut apples **(Tappi, et al., 2018)**. However, in this case, authors suggested an increase in gene expressions of enzymes involved in the biosynthesis of phenolic compounds from the phenylpropanoid pathway including: cinnamate-4-hydroxylase, 4-coumarate coenzyme A ligase, and phenylalanine ammonium lyase enzymes, as it occurs after wounding of vegetable tissue. The exposure to highly reactive species generated by plasma discharges in PAW represents a physiological stress for the tissue and can act as abiotic elicitors participating in the regulation of stress responses in plants, which explains the stimulating effect of plasma treatments on polyphenol biosynthesis in plant tissues **(M. Li, et al., 2019)**.

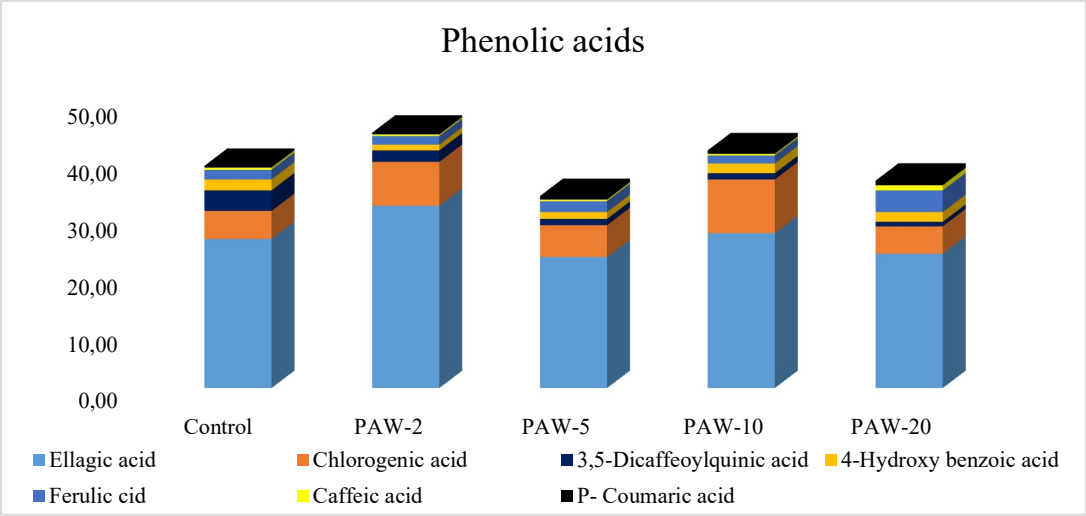

Figure 15: Content of phenolic acids determined by HPLC-MS/MS control and PAW treated rocket-salad leaves processed at different times. PAW-2, PAW-5, PAW-10, and PAW-20 refer to rocket samples subjected to plasma-activated water (PAW) treatment for 2, 5, 10, and 20 min, respectively. Concentrations detected in mg.kg-1, DW

Compared to the control, the extracts of rocket samples treated by PAW-20 showed a significant increase in quercetin, quercetin-3-O-galactoside, kaempferol-3-O-glucoside and hesperidin concentrations (79.8%, 58.6%, 113.0% and 33.3%, respectively). Non-significant increase in the concentration of quercetin-3-O-glucoside was found with PAW-treated samples. On the contrary, a reduction of the concentrations of quercetins-3-O-rutinoside and -3-O-rhamnoside was observed after 5 min of processing time for both compounds. Similarly, a significant increase in quercetin concentration was reported in grape pomace treated by high voltage cold atmospheric plasma in samples treated for 15 min **(Bao, et al., 2020)**. Also, an increase in the content of both quercetin and quercetin glycoside after 10 min treatment of fresh-cut apples was reported by **(Tappi, et al., 2018)**, which suggested to be a result of the cell wall hydrolysis **(Zheng, et al., 2009)**. On the other hand, a reduction in the concentration of quercetin and kaempferol glycosides was found in *Pisum sativum* treated by cold atmospheric plasma **(Bußler, et al., 2015)**.

The content of dihydrochalcone derivative phlorizin showed a significant increase (25 %) after 10 min (PAW-10), followed by a significant reduction in PAW-20 samples. Similarly, a 40% increase in phlorizin concentration was previously reported after 10 min treatment with cold plasma in fresh cut apples which was suggested to be synthesized after the increase in the activity of the enzymes involved in the phenyl-propanoid biosynthetic pathway like chalcone synthase and phenylalanine ammonia lyase enzymes **(Tappi, et al., 2018)**. On the other hand, a significant decrease in phloretin levels was observed only in

PAW-2 samples and remained unchanged over a longer treatment period. In general, it can be assumed that reactive species of the plasma can interact with the surface of the food, causing a physiological response that converts these reactive particles into compounds that are less harmful to plant cells **(Munekata, et al., 2020)**. Also, this response was associated by the significant increase in the activity and genes expression of some enzymes responsible for polyphenol preservation **(M. Li, et al., 2019)**. Some authors also reported that after a stimulation of the phenolic compounds production, increasing treatment time led to a following reduction, attributed to oxidative or polymerization reactions **(Ramazzina, et al., 2015; Ramazzina, et al., 2016)**. However, this effect was observed for prolonged exposition times (more than 40 min), that were not reached in the present study.

Nevertheless, it is important to consider that most of the previous literature findings are based on the exposure of fruit and vegetable tissues to gas phase plasma. Hence, while both plasma phases contain highly reactive species, their specific composition may vary quite substantially.

Table 7: Phenolic compounds determined by HPLC-MS/MS in control and PAW treated rocket-salad leaves processed at different times.

Class	Compound	Treatment condition (Time)				
		Control	**PAW-2**	**PAW-5**	**PAW-10**	**PAW-20**
	Ellagic acid	26.2±7.8a	32.0±1.6a	23.0±5.2a	27.2±4.6a	23.6±2.5a
Phenolic acids	**Chlorogenic acid**	4.9±0.7a	7.7±0.5b	5.6±0.1a	9.4±0.4c	4.8±0.1a
	3,5-Dicaffeoylquinic acid	3.6±0.2a	2.0±0.2b	1.1±0.2c	1.1±0.2c	0.8±0.2c
	4-Hydroxy benzoic acid	1.9±0.0a	1.0±0.0b	1.2±0.0b	1.7±0.1a	1.7±0.2a
	Ferulic acid	1.7±0.2a	1.5±0.2a	1.9±0.2a	1.4±0.2a	3.8±0.3b
	Caffeic acid	0.4±0.0a	0.3±0.0a	0.3±0.0a	0.3±0.0a	0.9±0.1b
	***P*- Coumaric acid**	0.3±0.0a	0.3±0.1a	0.6±0.1a	0.6±0.1a	0.8±0.0b
Flavonol aglycons	**Quercetin**	11.4±3.4a	9.3±2.1a	16.6±2.7ab	9.9±0.6a	20.5±0.9b
	Isorhamnetin	10.5±0.9ab	6.3±0.9bc	13.5±1.0a	3.7±0.0c	9.5±1.8ab
	Kaempferol	0.7±0.1ab	0.4±0.0a	1.2±0.2c	0.4±0.0a	1.0±0.1bc
Flavonol glycosides	**Quercetin-3-O-galactoside**	37.0±2.9a	43.0±0.8ab	52.5±0.4ab	50.6±0.5ab	58.7±6.7b
	Quercetin -3-O-glucoside	26.4±4.7a	32.2±0.3a	32.7±6.0a	31.9±1.4a	33.6±5.7a
	Quercetin-3-O-rutinoside	2.7±0.0a	2.5±0.2a	1.0±0.2b	0.6±0.0b	0.9±0.0b
	Quercetin-3-O-rhamnoside	1.8±0.3a	1.9±0.2a	1.0±0.2b	0.8±0.2b	0.7±0.0b
	Kaempferol-3-O-glucoside	4.6±0.1a	5.1±0.7ab	9.3±2.3bc	6.2±0.3abc	9.8±0.5c
Flavanone glycoside	**Hesperidin**	3.0±0.3ab	2.3±0.1a	4.9±1.3b	3.8±0.1ab	4.0±0.1ab
Dihydro-chalcones	**Phloretin**	0.3±0.0a	0.1±0.0b	0.1±0.0b	0.1±0.0b	0.1±0.0b
	Phlorizin	1.6±0.0a	1.8±0.0ab	1.9±0.1b	2.0±0.1b	1.2±0.1c
Total phenolics		138.8±13.3a	149.7±1.8a	168.5±9.6a	151.7±10.3a	176.4±18.1a

All the data are expressed as mean ± standard deviations. Means that do not share letters in each row differ significantly ($p < 0.05$) according to Tukey's test. Legends: PAW-2, PAW-5, PAW-10, and PAW-20 refer to rocket samples subjected to plasma-activated water (PAW) treatment for 2, 5, 10, and 20 min, respectively. Values calculated in mg kg^{-1}, DW.

3.1.2. Impact of PAW treatment on TPC, TFC and DPPH radical scavenging activity of rocket-salad leaves

Table 8 shows the time dependent changes in the total phenolic content (TPC), total flavonoid content (TFC) and DPPH radical scavenging activity of control and PAW treated rocket-salad leaves. According to the obtained results, all PAW treated samples showed non-significant differences in the TPC ($p > 0.05$) compared to the control samples, except for the 5 min treatment which induced a slight reduction. These results are in good accordance with the previous findings reported by **Fan, et al. (2020)**, in which the PAW treatment did not induce any significant change in the total phenolic content of mung bean sprouts.

A significant variation in total flavonoid content was observed for PAW treated rocket samples with higher values for 10 and 20 min (3098.85 ± 53.20 and 3046.88 ± 38.58 mg GAE/ 100 g, respectively) compared to the control samples (2524.88 ± 39.53 mg RE/ 100 g).

Vitamins as C and E together with the phenolic compounds are able to scavenge free radicals which are the cause of many diseases resulted by oxidative stress. Thus, changes in AOA are thought to be associated with the changes in these compounds. Here, PAW treatment affected the antioxidant activity of the rocket leaves. The AOA was increased in PAW-20 and PAW-10 samples and decreased in PAW-5 and PAW-2 samples. PAW-20 showed the highest AOA, while PAW-5 demonstrated the lowest activity. As shown in Fig. 3, a reduction in the AOA (20.36 %), measured as radical scavenging ability, was observed in the PAW-5 sample, which might be due to the observed decrease in the ascorbic acid content (by 35.56 %), which has been proven to have strong antioxidant properties. On the other side, a significant increase compared to the untreated sample was observed for the PAW-20 sample, reflecting what was observed for the polyphenol and partly the *L*-ascorbic acid content. In polyphenols, the anti-free radical activity depends on the specific structure (presence of phenolic hydrogens) and on the stabilizing capacity of the resulting phenoxy radicals (Figure 16 and Table 8).

Generally, while increasing the hydroxyl groups and decreasing the glycosylation led to higher antioxidant activity **(Heredia, et al., 2009)**, it is quite difficult to precisely predict the antioxidant capacity of a mixture of polyphenols. Previous reports on button mushroom showed an increase in the antioxidant activity with increase in PAW treatment time with the best antioxidant activity with PAW-15 **(Y. Xu, et al., 2016)**.

Although there is little data on the effect of PAW treatment on the functional and nutritional characteristics of foods **(Muhammad, et al., 2018)**, antioxidant activities generally follow a similar trend to the bioactive compounds.

Table 8: Changes in the TPC, TFC and DPPH of control and PAW treated rocket-salad leaves processed at different times.

Treatment conditions	TPC (mg Gallic acid/kg DW)	TFC (mg rutin/kg DW)	DPPH (mg trolox/g DW)
Control	3343.58 ± 2.59^{a}	2524.88 ± 1.57^{a}	8.48±0.59^{b}
PAW-2	3259.70 ± 2.44^{a}	2763.17 ± 0.49^{b}	8.13±0.35^{b}
PAW-5	2683.68 ± 7.81^{b}	2501.65 ± 2.45^{a}	6.50±0.10^{c}
PAW-10	3297.40 ±1.74^{a}	3098.85 ± 1.72^{c}	9.67±0.12^{a}
PAW-20	3397.08 ± 0.41^{a}	3046.88 ± 1.27^{c}	11.29±0.96^{a}

All the data are expressed as mean ± standard deviations. Means that do not share letters in each row differ significantly ($p < 0.05$) according to Tukey's test. Legends: PAW-2, PAW-5, PAW-10, and PAW-20 refer to rocket samples subjected to plasma-activated water (PAW) treatment for 2, 5, 10, and 20 min, respectively

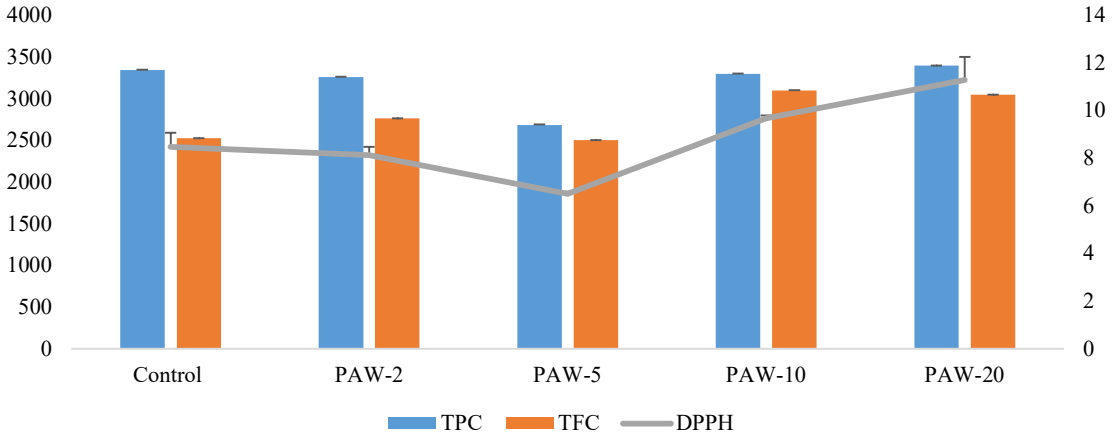

Figure 16: Changes in the TPC, TFC and DPPH of control and PAW treated rocket-salad leaves processed at different times.

3.1.3. Impact of PAW treatment on L-ascorbic acid content of rocket-salad leaves

L-ascorbic acid has high antioxidant capacity which inactivates free radicals and other reactive substances that cause oxidative damage to biomolecules such as proteins, lipids and DNA **(de Castro, et al., 2020)**. Researchers used *L*-ascorbic acid as as an indicator of food quality because it is a very sensitive bioactive compound that provides a valid mark for the loss of vitamins and other nutritional components **(Barba, et al., 2012)**. The contents of ascorbic acid of the non-treated and PAW treated samples are shown in figure 17 and table 9. It can be observed that treatment time has a significant influence ($p < 0.05$) on the content of ascorbic acid. The highest *L*-ascorbic acid concentration (382.76 ± 15.24 mg.100g^{-1} DW) was found in the product subjected to intermediate processing time (10 min). Longer treatment (20 min) resulted in a non-significant increase of *L*-ascorbic acid content (363.14 mg.100g^{-1}), compared with control sample (337.73 ± 7.35 mg.100g^{-1} DW).

A decrease in the content of ascorbate in the roots of tomato seedlings was observed in PAW-15 and PAW-30 samples **(Adhikari, et al., 2019)** and in orange juice **(L. Xu, et al., 2017)**. However, the ascorbic acid contents of blueberry samples and guava-flavored whey beverages were significantly enhanced post plasma treatment **(Sarangapani, et al., 2017; M. R. Silveira, et al., 2019)**.

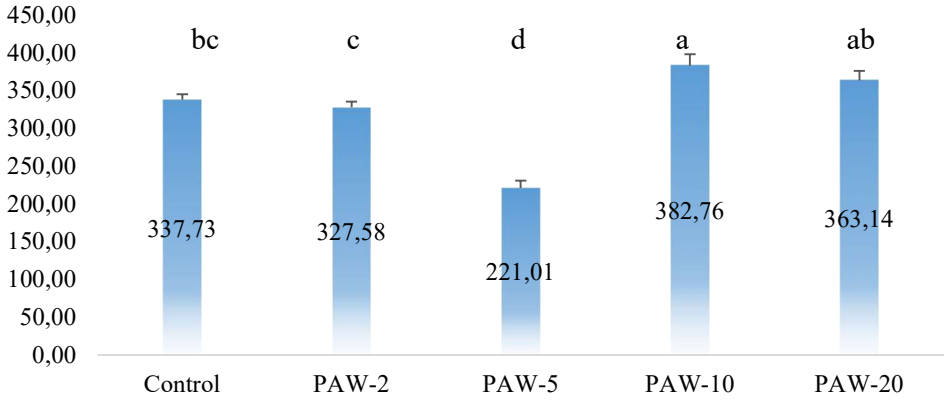

Figure 17: Changes in ascorbic acid content of control and PAW treated rocket-salad leaves processed at different times. Means that do not share letters differ significantly ($p < 0.05$) according to Tukey's test. Legends: PAW-2, PAW-5, PAW-10, and PAW-20

3.1.4. Impact of PAW treatment on vitamins B (riboflavin, nicotinamide, and nicotinic acid) contents of rocket-salad leaves

In this study, the contents of different forms of vitamin B were evaluated using UHPLC-ESI–MS/MS system. The contents of the untreated (control) and the PAW treated rocket samples are shown in table 9. Compared to the control sample (0.32 ± 0.00 mg.100g-1), PAW-2, PAW-5**,** and PAW-10 exhibited non-significant changes of riboflavin (B2) content. On the contrary, PAW-20 sample showed a significant increase in riboflavin content with a value of 0.53 ± 0.02 mg.100g^{-1} (Table 9 & Figure 18). Since riboflavin has a pH dependent stability, being more stable under acidic conditions **(Dionísio, et al., 2009)**, the acidic environment provided by PAW- treatment may be responsible for the retention of this vitamin after treatment.

Two forms of Vit. B3, niacin (or nicotinic acid) and nicotinamide, that have the same vitaminic activity were quantified. A non-significant change ($p > 0.05$) was observed in the nicotinamide content of all PAW treated samples, while a significant enhancement of nicotinic acid content was observed with PAW-20 (1.26 ± 0.02 mg.100g-1 DW), compared with control sample (0.61 ± 0.01mg.100g^{-1} DW). Previous reports indicated that an increase in the concentration of niacin after food thermal processing may be due to the change of bound niacin to the free form (nicotinic acid and nicotinamide) **(Okmen, et al., 1999)**. However, being PAW a non-thermal treatment, this effect might be considered negligible. Moreover, to our knowledge, the production of newly formed riboflavin and nicotinic acid has never been observed as a consequence to metabolic stress, therefore, the observed increase in the longer processing time could be related to a higher extraction capacity due to the alteration of the integrity of the cell membrane promoted by the reactive species of the plasma **(Tappi, et al., 2018)**.

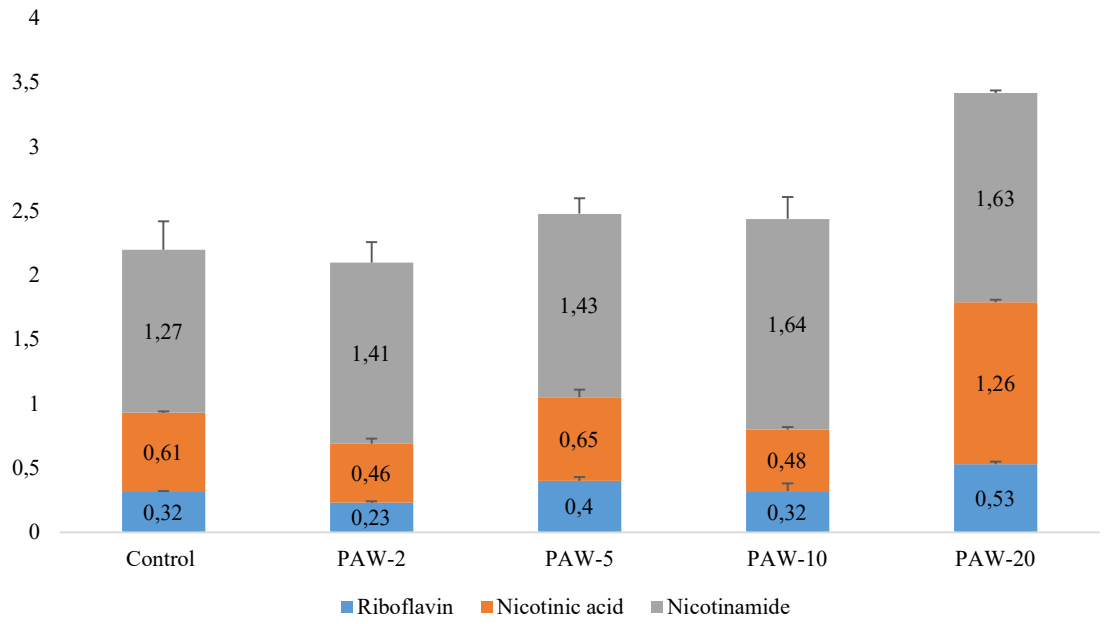

Figure 18: Riboflavin, nicotinic acid and nicotinamide contents of control and PAW treated rocket-salad leaves processed at different times.

Table 9: Vitamin C, riboflavin, nicotinic acid and nicotinamide contents of control and PAW treated rocket-salad leaves processed at different times.

Treatment conditions	Riboflavin	Nicotinic acid	Nicotinamide	Vitamin C
Control	0.32 ± 0.00^{bc}	0.61 ± 0.01^{bc}	1.27 ± 0.22^{a}	337.73 ± 7.3^{bc}
PAW-2	0.23 ± 0.01^{c}	0.46 ± 0.04^{d}	1.41 ± 0.16^{a}	327.58 ± 7.7^{c}
PAW-5	0.40 ± 0.03^{ab}	0.65 ± 0.06^{b}	1.43 ± 0.12^{a}	221.01 ± 9.8^{d}
PAW-10	0.32 ± 0.06^{bc}	0.48 ± 0.02^{cd}	1.64 ± 0.17^{a}	382.76 ± 15.2^{a}
PAW-20	0.53 ± 0.02^{a}	1.26 ± 0.02^{a}	1.63 ± 0.02^{a}	363.14 ± 13.1^{ab}

All the data are expressed as mean ± standard deviations. Means that do not share superscript letters in each column differ significantly ($p < 0.05$) according to Tukey's test with $p < 0.05$. Note: PAW-2, PAW-5, PAW-10, and PAW-20 refer to plasma-activated water (PAW) subjected to plasma treatment for 2, 5, 10, and 20 min respectively. Data expressed in $mg.100g^{-1}$ DW.

3.1.5. Impact of PAW treatment on the main VOCs of rocket-salad leaves

Detection of the main volatile compounds in rocket samples was performed, which is illustrated by the chromatogram presented in figure 19. Table 10 describes the VOCs identified in the control and PAW-treated rocket samples, their relative abundances together with their experimental retention indices (RI) **(Abouelenein, et al., 2021)**.

The volatile composition of rocket samples was in a good agreement with previously published data **(Bell, Methven, et al., 2017; Bell, et al., 2016; Blažević, et al., 2008; Raffo, et al., 2018)**. In total, 52 compounds were identified, and the most predominant class was Glucosinolate hydrolysis products (GHPs) (7 compounds) followed by other sulphur containing metabolites (6 compounds). In addition, 13 ketones, 13 aldehydes, 4 fatty acids and esters, 8 alcohols and 1 compound of the class of alkanes were identified.

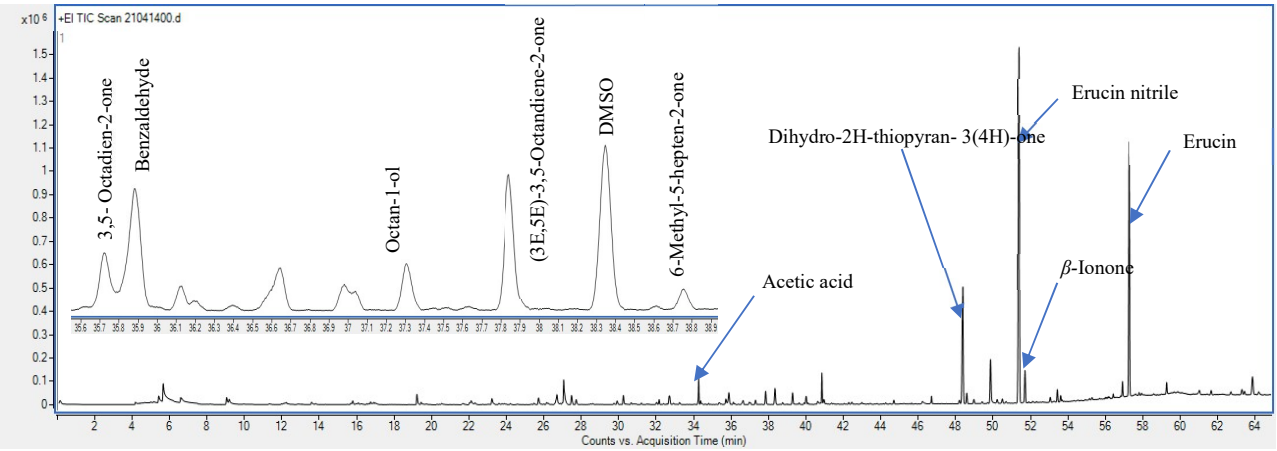

Figure 19: Representative chromatogram of the control rocket samples showing the major detected VOCs.

Table 10: Relative abundance of volatile organic compounds detected by HPSE-GC–MS of control and PAW treated rocket-salad leaves processed at different times.

	Compounds	Control	PAW-2	PAW-5	PAW-10	PAW-20	RI
	Glucosinolate hydrolysis products (GHPs)	**54.58 ± 1.48^{a}**	**57.02 ± 0.08^{a}**	**49.61 ± 3.85^{a}**	**53.87 ± 4.44^{a}**	**60.44 ± 3.15^{a}**	
1	Methyl thiocyanate	0.04 ± 0.01^{c}	0.09 ± 0.01^{bc}	0.17 ± 0.04^{a}	0.07 ± 0.01^{bc}	0.12 ± 0.01^{ab}	1282
2	5-Methyl Hexanenitrile	0.09 ± 0.01^{a}	0.10 ± 0.01^{a}	Nd ± 0.00^{c}	0.11 ± 0.00^{a}	0.03 ± 0.00^{b}	1362
3	Heptanonitrile	0.18 ± 0.04^{a}	0.18 ± 0.01^{a}	Nd ± 0.00^{c}	0.15 ± 0.01^{a}	0.07 ± 0.00^{b}	1403
4	1-Butene 4-isothiocyanate	0.07 ± 0.01^{b}	0.14 ± 0.02^{b}	0.56 ± 0.10^{a}	0.13 ± 0.04^{b}	0.42 ± 0.04^{a}	1452
5	4-Methylthio butanenitrile	0.35 ± 0.11^{ab}	0.38 ± 0.08^{ab}	Nd ± 0.00^{c}	0.45 ± 0.08^{a}	0.11 ± 0.00^{bc}	1784
6	Erucin nitrile	37.52 ± 2.54^{a}	34.52 ± 1.60^{a}	4.71 ± 0.27^{c}	36.91 ± 5.41^{a}	21.74 ± 0.06^{b}	1935
7	Erucin	16.35 ± 4.16^{b}	21.63 ± 0.74^{b}	44.17 ± 4.19^{a}	16.06 ± 0.82^{b}	37.96 ± 3.27^{a}	2143
	Sulphur compounds	**19.15 ± 0.81^{a}**	**13.23 ± 0.05^{bc}**	**10.08 ± 1.51^{c}**	**15.02 ± 1.03^{b}**	**10.57 ± 1.11^{c}**	
8	Methyl disulphide	0.92 ± 0.11^{b}	0.62 ± 0.05^{c}	1.47 ± 0.01^{a}	0.54 ± 0.00^{c}	1.14 ± 0.05^{b}	746
9	Dimethyl sulphide	3.30 ± 1.56^{a}	3.32 ± 0.35^{a}	3.22 ± 1.20^{a}	3.57 ± 0.01^{a}	3.82 ± 0.57^{a}	760
10	Dimethyl trisulphide	0.18 ± 0.04^{a}	0.08 ± 0.01^{a}	0.33 ± 0.05^{a}	0.14 ± 0.04^{a}	0.07 ± 0.01^{a}	1385
11	Dimethyl Sulfoxide	1.37 ± 0.19^{a}	1.86 ± 0.18^{a}	1.91 ± 0.21^{a}	1.77 ± 0.13^{a}	1.66 ± 0.11^{a}	1577
12	Dihydro-2H-thiopyran- 3(4H)-one	13.09 ± 2.64^{a}	6.98 ± 0.56^{bc}	2.79 ± 0.12^{c}	8.76 ± 0.82^{ab}	3.49 ± 0.37^{c}	1845
13	Dimethyl sulfone	0.31 ± 0.01^{a}	0.39 ± 0.04^{a}	0.38 ± 0.04^{a}	0.25 ± 0.05^{a}	0.40 ± 0.03^{a}	1899
	Ketones	**10.20 ± 0.81^{b}**	**13.85 ± 0.73^{ab}**	**15.48 ± 1.66^{a}**	**11.64 ± 0.72^{ab}**	**11.36 ± 0.58^{b}**	
14	2,5-Dimethyl-3-hexanone	0.04 ± 0.00^{bc}	Nd ± 0.00^{d}	0.20 ± 0.01^{a}	0.12 ± 0.02^{b}	0.10 ± 0.04^{b}	1188
15	3-Hydroxybutan-2-one	0.06 ± 0.01^{a}	0.05 ± 0.00^{a}	0.07 ± 0.01^{a}	0.05 ± 0.01^{a}	0.05 ± 0.00^{a}	1297
16	1-Hydroxypropan-2-one	0.08 ± 0.02^{ab}	0.05 ± 0.00^{ab}	0.13 ± 0.04^{a}	0.03 ± 0.00^{b}	0.06 ± 0.02^{ab}	1309
17	6-Methyl-5-hepten-2-one	0.41 ± 0.01^{b}	0.95 ± 0.10^{a}	0.46 ± 0.05^{b}	0.52 ± 0.09^{b}	0.39 ± 0.07^{b}	1344
18	3-Octen-2-one	0.05 ± 0.01^{b}	0.12 ± 0.01^{b}	0.28 ± 0.04^{a}	0.10 ± 0.02^{b}	0.09 ± 0.00^{b}	1409
19	3,5- Octadien-2-one	0.20 ± 0.07^{b}	0.74 ± 0.01^{ab}	0.82 ± 0.21^{a}	0.64 ± 0.09^{ab}	0.85 ± 0.23^{a}	1514
20	(3E,5E)-3,5-Octandiene-2-one	0.79 ± 0.41^{a}	1.27 ± 0.08^{a}	1.30 ± 0.15^{a}	1.00 ± 0.07^{a}	1.28 ± 0.11^{a}	1565
21	6-Methyl-3,5-heptadien-2-one	0.18 ± 0.04^{a}	0.24 ± 0.00^{a}	0.34 ± 0.08^{a}	0.24 ± 0.08^{a}	0.15 ± 0.01^{a}	1587
22	*(E)*-*β*-Ionone	2.73 ± 0.30^{b}	2.96 ± 0.21^{b}	3.70 ± 0.02^{a}	2.75 ± 0.07^{b}	3.11 ± 0.04^{ab}	1945
23	*β*-Ionone-5,6-epoxide Norisoprenoid	0.97 ± 0.04^{c}	1.21 ± 0.06^{ab}	1.27 ± 0.07^{ab}	1.40 ± 0.04^{a}	1.12 ± 0.04^{bc}	1999
24	6,10,14-Trimethylpentadecan-2-one	1.61 ± 0.54^{b}	1.75 ± 0.04^{ab}	3.12 ± 0.59^{a}	1.27 ± 0.07^{b}	1.39 ± 0.01^{b}	2129
25	*(E)*-geranylacetone	0.99 ± 0.25^{ab}	1.64 ± 0.24^{a}	1.09 ± 0.08^{ab}	1.00 ± 0.09^{ab}	0.85 ± 0.01^{b}	1852
26	Dihydroactinidiolide Norisoprenoid	2.12 ± 0.13^{ab}	2.87 ± 0.24^{a}	2.73 ± 0.32^{ab}	2.56 ± 0.06^{ab}	1.95 ± 0.10^{b}	2371

	Aldehydes	**6.48 ± 0.13^{b}**	**6.84 ± 0.30^{b}**	**12.71 ± 0.07^{a}**	**7.75 ± 0.96^{b}**	**8.00 ± 0.88^{b}**	
27	2-Methyl propanal	0.87 ± 0.10^{b}	1.14 ± 0.08^{b}	2.26 ± 0.14^{a}	1.20 ± 0.17^{b}	1.22 ± 0.22^{b}	810
28	2-Methyl butanal	0.77 ± 0.00^{b}	0.56 ± 0.02^{c}	1.53 ± 0.03^{a}	0.64 ± 0.05^{bc}	0.69 ± 0.06^{bc}	911
29	3-Methyl butanal	0.77 ± 0.15^{ab}	0.34 ± 0.04^{c}	0.79 ± 0.02^{a}	0.45 ± 0.10^{bc}	0.47 ± 0.03^{bc}	915
30	Pentanal	0.11 ± 0.01^{b}	0.12 ± 0.01^{b}	0.19 ± 0.02^{a}	0.16 ± 0.01^{ab}	0.11 ± 0.02^{b}	976
31	Hexanal	0.15 ± 0.04^{b}	0.19 ± 0.01^{b}	0.33 ± 0.05^{a}	0.18 ± 0.04^{b}	0.10 ± 0.00^{b}	1088
32	2-hexenal (E)	0.41 ± 0.02^{a}	0.44 ± 0.06^{a}	0.78 ± 0.32^{a}	0.65 ± 0.21^{a}	0.32 ± 0.13^{a}	1236
33	Octanal	0.11 ± 0.01^{bc}	0.15 ± 0.01^{bc}	0.29 ± 0.02^{a}	0.23 ± 0.05^{ab}	0.23 ± 0.01^{ab}	1299
34	Nonanal	0.83 ± 0.10^{bc}	0.62 ± 0.03^{c}	0.92 ± 0.02^{ab}	0.61 ± 0.02^{c}	1.12 ± 0.10^{a}	1395
35	3-Furfural	0.17 ± 0.04^{c}	0.18 ± 0.03^{c}	0.85 ± 0.05^{a}	0.16 ± 0.10^{c}	0.55 ± 0.08^{b}	1459
36	Benzaldehyde	1.15 ± 0.05^{c}	1.62 ± 0.01^{bc}	2.33 ± 0.01^{a}	1.79 ± 0.05^{ab}	1.28 ± 0.33^{bc}	1518
37	*β*-cyclocitral	0.59 ± 0.01^{b}	0.81 ± 0.05^{ab}	1.00 ± 0.07^{a}	0.74 ± 0.17^{ab}	0.73 ± 0.01^{ab}	1619
38	Benzene acetaldehyde	0.39 ± 0.02^{a}	0.49 ± 0.19^{a}	0.66 ± 2.16^{a}	0.42 ± 0.11^{a}	0.58 ± 0.06^{a}	1635
39	2- Methyl benzaldehyde	0.20 ± 0.04^{a}	0.22 ± 0.09^{a}	0.83 ± 0.32^{a}	0.55 ± 0.13^{a}	0.63 ± 0.06^{a}	1643
	Fatty acids and esters	**2.16 ± 0.07^{b}**	**1.66 ± 0.13^{b}**	**3.99 ± 0.34^{a}**	**1.96 ± 0.30^{b}**	**2.52 ± 0.11^{b}**	
40	Acetic acid	1.23 ± 0.31^{b}	1.09 ± 0.04^{b}	2.37 ± 0.25^{a}	1.23 ± 0.23^{b}	1.71 ± 0.07^{ab}	1447
41	Propanoic acid	0.05 ± 0.01^{b}	0.06 ± 0.00^{ab}	0.11 ± 0.02^{a}	0.08 ± 0.02^{ab}	0.08 ± 0.01^{ab}	1530
42	Hexanoic acid	0.24 ± 0.04^{b}	0.33 ± 0.04^{ab}	0.54 ± 0.11^{a}	0.23 ± 0.04^{b}	0.44 ± 0.05^{ab}	1840
43	Methyl palmitate	0.65 ± 0.21^{ab}	0.19 ± 0.05^{c}	0.99 ± 0.04^{a}	0.43 ± 0.01^{bc}	0.30 ± 0.01^{bc}	2221
	Alcohols	**1.14 ± 0.10^{b}**	**1.61 ± 0.08^{a}**	**1.23 ± 0.08^{ab}**	**1.57 ± 0.13^{a}**	**1.39 ± 0.11^{ab}**	
44	Pent-1-en-3-ol	0.12 ± 0.00^{b}	0.31 ± 0.02^{a}	0.14 ± 0.00^{b}	0.25 ± 0.07^{ab}	0.17 ± 0.01^{b}	1180
45	pentan-1-ol	0.06 ± 0.01^{b}	0.10 ± 0.00^{a}	0.08 ± 0.01^{ab}	0.06 ± 0.01^{b}	0.07 ± 0.00^{ab}	1267
46	*(Z)*-2-penten-1-ol	0.04 ± 0.01^{c}	0.10 ± 0.01^{b}	0.07 ± 0.01^{bc}	0.16 ± 0.03^{a}	0.06 ± 0.01^{bc}	1329
47	Hexan-1-ol	0.05 ± 0.01^{b}	0.09 ± 0.00^{ab}	0.11 ± 0.01^{a}	0.08 ± 0.01^{ab}	0.10 ± 0.01^{a}	1360
48	Hex-3-ene -1-ol	0.27 ± 0.10^{b}	0.38 ± 0.01^{ab}	0.26 ± 0.02^{b}	0.51 ± 0.00^{a}	0.20 ± 0.04^{b}	1388
49	Octan-1-ol	0.40 ± 0.04^{b}	0.34 ± 0.02^{b}	0.50 ± 0.03^{ab}	0.36 ± 0.04^{b}	0.65 ± 0.07^{a}	1552
50	Nonan-1-ol	0.08 ± 0.00^{ab}	0.11 ± 0.01^{a}	0.09 ± 0.01^{a}	0.07 ± 0.01^{ab}	0.04 ± 0.01^{b}	1654
51	Phenylethyl alcohol	0.14 ± 0.02^{b}	0.20 ± 0.01^{a}	Nd ± 0.00^{c}	0.09 ± 0.02^{b}	0.10 ± 0.01^{b}	1913
	Alkanes	**0.16 ± 0.01^{c}**	**0.12 ± 0.06^{c}**	**0.95 ± 0.00^{a}**	**0.40 ± 0.03^{b}**	**0.47 ± 0.05^{b}**	
52	Undecane	0.16 ± 0.01^{c}	0.12 ± 0.06^{c}	0.95 ± 0.00^{a}	0.40 ± 0.03^{a}	0.47 ± 0.05^{b}	1094

3.1.5.1. Glucosinolate Hydrolysis Products (GHPs)

Glucosinolates (GSLs) in rocket leaves are not only the major class in terms of their concentration, but also the main contributors to the bitter and pungent taste, which is quickly formed when the rocket leaf tissues are crushed. GSLs are hydrolysed normally by the brassica enzyme myrosinase, into GHPs: Isothiocyanates (ITCs) or nitriles which are generally considered to be responsible for the pungency and Brassicaceae-like aroma **(Bell, et al., 2021; Raffo, et al., 2018)**. However, the GHPs of whether ITCs or nitriles, retain the R group of GSLs, which has an impact on their bioactivity **(Mullaney, et al., 2013)**. Therefore, monitoring of GHPs could be of use as a marker for nutritional composition and sensorial quality of rocket.

As shown in table 10, seven kinds of hydrolysates were detected in the control rocket sample, including: methyl thiocyanate, 2 ITCs (1-butene 4-isothiocyanate, 4-methylthio-butyl isothiocyanate) and 4 nitriles (4-methylthio butanenitrile, 5-methyl hexanenitrile, heptanenitrile, 5-methylthiopentanonitril). All these compounds have been reported before in rocket leaves **(Bell, et al., 2021; Blažević, et al., 2008; Jirovetz, et al., 2002; Raffo, et al., 2018)**. As shown in figure 19, erucin nitrile (5-methylthiopentanenitrile) and erucin (4-methylthiobutyl isothiocyanate) were the major compounds detected in the chromatogram of the control rocket sample. As reported by **(Leng, et al., 2019; Melchini, et al., 2010)** erucin and erucin nitrile are the degradation products of glucoerucin (one of the major GSLs found in rocket leaves) (Figure 20). Besides being the major VOC in rocket leaves **(Jirovetz, et al., 2002; Raffo, et al., 2018)**, erucin has been reported as one of the most potent odor-active compounds in rocket being associated with radish and typical rocket aroma **(Bell, et al., 2021; Raffo, et al., 2018)**. However, erucin nitrile, was reported as a major compound in samples obtained from dried plant material **(Blažević, et al., 2008)**. This suggests that drying of the plant material in our case contributed to the degradation of glucoerucin towards erucin nitrile being the major VOC in the control sample followed by the erucin (Table 10).

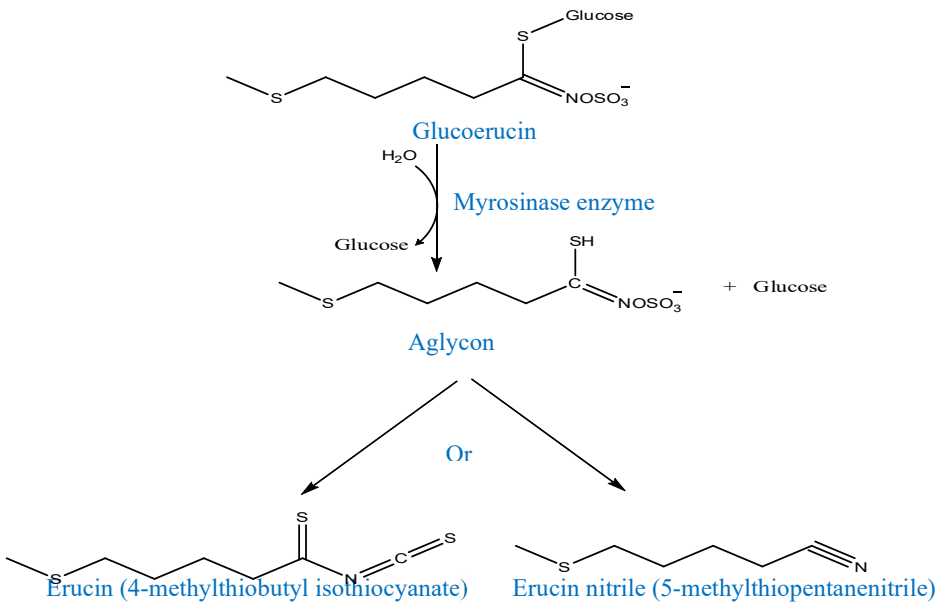

Figure 20: Enzymatic hydrolysis of glucoerucin by myrosinase enzyme into erucin and erucin nitrile.

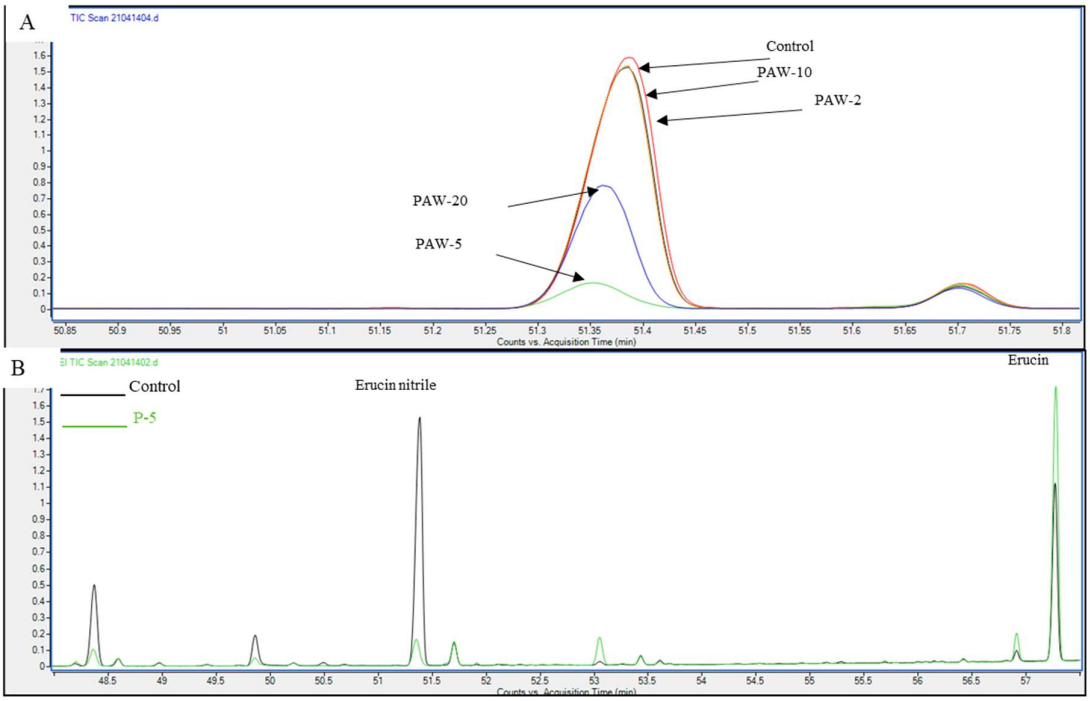

Figure 21: Major VOCs detected in control and PAW treated rocket-salad leaves. A) Relative abundance of erucin nitrile in control and PAW-treated samples, B) Relative abundance of erucin and erucin nitrile in control and PAW-5- treated sample.

Non-significant changes in the total relative abundance of this class in all PAW treated samples were observed. Also, the process carried out at 2 and 10 min did not show any significant changes in the individual contents of this class. On the other hand, a significant qualitative and quantitative changes were observed for both PAW-5 and 20 samples. Regarding PAW-5, three compounds Could not be identified which are 5-methyl hexanenitrile, heptanonitril, 4-methylthio butanenitrile. A significant decrease in the former two compounds was also observed in PAW-20.

As shown in figure 21, a significant decrease in the major VOC erucin nitrile was also observed in both PAW-5 and PAW-20 samples, which was accompanied by a significant increase in the relative % of erucin when compared to control. Interestingly, it can be concluded that the abandonment of nitrile production in favor of ITCs occurred in these two samples. It was previously reported that different factors could affect the yield and abundance of GHPs from rocket leaves. These may include pH, the solvent used for extraction, method for leaf homogenization, liquid or headspace extraction, and sample state (e.g., fresh or dried). As GHPs profiles change rapidly, it is difficult to compare absolute quantities between various studies **(Bell, et al., 2019)**. One study reported that the amount of erucin and erucin nitrile produced during this hydrolysis is a pH dependant **(Vaughn, et al., 2005)**. **Bell, Yahya, et al. (2017)** also reported a low amount of nitrile compounds detected in rocket leaves after processing which was suggested to be a cause of the acidity of hydrolysis conditions. Another study on the hydrolysis of the GSLs to their nitriles using beneficial bacteria, confirmed that aerobic and anaerobic conditions favored the production of erucin nitrile, but for Enterobacteriaceae aerobic only trace amounts of erucin nitrile were produced **(Mullaney, et al., 2013)**. This may explain the reciprocal transformation among erucin and erucin nitrile during glucoerucin hydrolysis in PAW treated samples. However, this effect did not seem to be time dependent.

Despite the low content in terms of the overall volatile profile, the compound 1-butene 4-isothiocyanate was reported to have descriptions of typical pungency in rocket at high intensities **(Bell, et al., 2021)**. The compound also showed a significant increase in both PAW-5 and 20 samples. Generally, along with their contribution to the rocket aroma, ITCs are suggested to have cytotoxic activity against the most common cancer types **(Melchini, et al., 2010)**. Our data infer that whether the retention of ITCs in PAW-2 and PAW-10 samples, or their significant increase in PAW-5 and PAW-20 will have important implications for health benefits to the consumer. Cold plasma treatment has also previously been reported to increase total ITC content in green mustard seeds **(Saengha, et al., 2021)**.

Since ITCs can survive during PAW processing, this may suggest that PAW processing can enhance this property of rocket leaves.

3.1.5.2. Sulphur Compounds

Together with the ITCs, other sulphur containing compounds has been detected in rocket leaves, including a high content dihydro-2H-thiopyran- 3(4H)-one which has also been detected before in rocket-salad by **(Bell, et al., 2021)**. Generally, positive correlations have been reported between ITCs and sulphur compounds detected in rocket with bitterness, peppery, mustard, and initial heat mouthfeel characters **(Bell, Methven, et al., 2017)**.

A significant reduction in the relative abundance of the sulfur-containing compound is also evident in the reduction of dihydro-2H-thiopyran- 3(4H)-one in all samples after treatment without significant differences among treatment times. **Bußler (2017)** has reported that sulphur-containing compounds, including sulphur containing aromatic amino acids, are preferred for attacks of ROS released from the plasma treatment, hence it is possible to hypothesise oxidation of these components due to the reactive species present in PAW.

3.1.5.3. Ketones

Ketones are reported to have an important role in plant defense. They are previously reported to contribute to the sensory characters of rocket as they are correlated with the pleasant odours **(Bell, Methven, et al., 2017)**. Among the identified ketones, 3,5- Octadien-2-one and (3E,5E)-3,5-Octandiene-2-one were described to impart a pungent green aroma of medium intensity in Brassicaceae species **(Bell, et al., 2021)**; 6-Methyl-5-hepten-2-one which was previously identified in rocket leaves by **(Bell, et al., 2021; Raffo, et al., 2018)** and hexahydrofarnesyl acetone (phytone), a very common ketone in brassicaceae plants that resulted from the oxidative degradation of the diterpene alcohol *(E)*-phytol, that occurs as a side chain of chlorophyll a **(Taviano, et al., 2021)** were detected.

Among the identified ketones, another group, called volatile norisoprenoids was also identified in rocket samples such as *(E)-β*-ionone, *β*-ionone-5,6-epoxide, *(E)*-geranylacetone and dihydroactinidiolide, that were detected in all rocket samples. **Bell, et al. (2021)** has reported the presence of geranylacetone (0.1 %) in rocket leaves. The major ketone in all rocket samples was *β*-ionone, also previously detected in rocket leaves by **(Blažević, et al., 2008; Raffo, et al., 2018)**. Moreover, dihydroactinidiolide was detected in brassicacea by Oulad El Majdoub *et al.* **(Oulad El Majdoub, et al., 2020)**.

Except for PAW-5, which showed a significant increase in the total relative abundance of ketones, other PAW treatments showed non-significant changes compared to the untreated sample. Our results are in good agreement with some previous results as those of **Korachi, et al. (2015)**, who reported non-significant changes in the total composition of ketones in milk following cold plasma treatment. Regarding the individual compounds, PAW-20 and PAW-10 did not induce any significant changes except for the *β*-ionone-5,6-epoxide, which increased significantly in PAW-10 samples.

Moreover, a significant increase was observed in the relative abundance of 6-methyl-5-hepten-2-one and *β*-ionone-5,6-epoxide in PAW-2 samples however 2,5-dimethyl-3-hexanone Could not be identified. PAW-5 showed a significant increase of 2,5-dimethyl-3-hexanone, 3-octen-2-one, 3,5-octadien-2-one, *(E)*-*β*-ionone and *β*-ionone-5,6-epoxide which led consequently to the significant increase in the total ketone content of this sample. Also, **Q. Liu, et al. (2021)** detected higher contents of geranylacetone in brown rice upon processing with cold plasma. A reason for the increase of total content of ketones in PAW-5 could be the lipid oxidation that may have occurred in this sample, which can lead to further formation of secondary lipid oxidation products epoxides, aldehydes, dimers or ketones **(Pérez-Andrés, et al., 2020)**.

3.1.5.4. Aldehydes

The aldehydes which were detected in the rocket samples were 2-methyl propanal, 2-methyl butanal, 3-methyl butanal, pentanal, hexanal, 2-hexenal, octanal, nonanal, 3-furfural, benzaldehyde, *β*-cyclocitral, benzenacetaldehyde and 2- methyl benzaldehyde. It is worth mentioning that aldehydes showed a high degree of association with taste, flavour, and mouth-feel traits in rocket **(Bell, Methven, et al., 2017)**. *(E)*-2-hexenal and hexanal were associated with the green aroma impression of the rocket-salad. Also, herbal aromas are caused by *(E)*-2-hexenal. Floral-fruity odor notes can be associated with nonanal. At the same time, nutty and almond-like odor impressions are known from furfural and benzaldehyde. Hexanal and nonanal compose the fatty side-notes **(Jirovetz, et al., 2002)**.

Overall, non-significant changes were observed in the total content of aldehydes in PAW-2, 10 and 20. However, A significant increase ($P < 0.05$) in the level of total aldehydes was observed only in PAW-5 samples. A significant increase was observed in the content of 2-methyl propanal, 2-methyl butanal, pentanal, hexanal, octanal, 3-furfural, benzaldehyde, and *β*-cyclocitral ($P \leq 0.05$). Also, a non-significant increase was revealed for all the other detected aldehydes ($P \geq 0.05$). The results evidenced that plasma treated

cells in PAW-5 accumulated higher amounts of several aldehydes compared to the control ones.

Previous studies have also reported an increase in aldehyde content in guava-flavored whey beverages **(M. R. Silveira, et al., 2019)** and milk **(Korachi, et al., 2015)** after plasma treatment. This increase in these aldehydes could be attributed to the degradation of several unsaturated fatty acids found in rocket **(Bell, et al., 2016)**, by auto-oxidation and/or the spontaneous decomposition of hydroperoxides. Such degradation could be the result of the damaging effect of reactive species produced by the plasma which can initiate lipid peroxidation and produce hydroperoxide, which can then be converted to secondary oxidation products such as aldehydes or shorter fatty acyl compounds. **(Benedetti, et al., 1984; Mead, 1976)**. However, further studies are needed to confirm these assumptions.

3.1.5.5. Alcohols

Alcohols may be formed by the decomposition of fatty acids hydroperoxides or the reduction of aldehydes **(J. Liu, et al., 2015)**. They are used as a defensive mechanism of plants and often responsible for the 'cut grass' aroma found in leafy vegetables **(Bell, et al., 2016; Ruther, et al., 2005)**. In this study, a significant increase was observed in total relative abundance of alcohol with PAW-2 and PAW-10 samples. The content of hex-3-en-1-ol which was detected as a major alcohol in Eruca spp **(Bell, Methven, et al., 2017; Blažević, et al., 2008; Jirovetz, et al., 2002)** increased after PAW application. Also, PAW treatment increased the content of hexan-1-ol. These two compounds are typical green leaves volatiles (GLVs) produced naturally in plants. They are derived from linoleic acid through the lipoxygenase (LOX) enzymatic route **(Hu, et al., 2018; Tawfik, et al., 2017)**. The pathway produces hexanal and hex-3-enal by the oxygenation of linoleic acid through the catalysis of LOX, which by further reduction of the aldehydes producing hexan-1-ol and hex-3-en-1-ol.

According to our results, an increase in both compounds was observed with all PAW treatments when compared to control, with a non-significant decrease in hex-3-en-1-ol in PAW-5 and 20. These results agreed with the previous study that reported the increase in the contents of hexan-1-ol and hex-3-en-1-ol observed in camu-camu pulp. The results were explained that either the LOX enzyme was activated by plasma application or the oxidation of linoleic acid was catalysed by the reactive oxygen species formed during plasma generation **(Campelo, et al., 2020b)**. Also, 1-penten-3-ol which is significantly correlated with sweet attributes in rocket **(Bell, Methven, et al., 2017)** was increased in all PAW-treated samples with a significant increase in PAW-2. Moreover, the significant increase in

the content of pentan-1-ol and phenylethyl alcohol in PAW-2 samples was also observed. Octan-1-ol was significantly increased in PAW-20 samples. On the other hand, phenylethyl alcohol was not detected in PAW-5 samples.

Interestingly, profiles of VOCs in all four PAW-treated rocket samples showed some differences. So that, hierarchical clustering analysis (HCA) was performed on the data of the 52 compounds detected in all samples: control, PAW-2, PAW-5, PAW-10 and PAW-20 to have a concluded idea about the effect of PAW treatment on the volatile profile. As shown in the dendrogram (Figure 22), the five samples were sorted into 3 logical classes. PAW-10 was first grouped with the control sample with a 99.7% similarity level. The PAW-2 sample was then isolated but still grouped closely with a high similarity level (99.1%) which confirms that PAW did not induce significant changes in the volatile profile of these two samples. On the other hand, the profiles of PAW-5 and PAW-20 samples were grouped together but were distinct from that of the control (similarity level 82.7%). However, the results indicated a non-significant effect of the PAW-treatment on rocket-salad volatile profile, further research is needed to better understand the effect of PAW-processing time on the volatile profile of rocket samples.

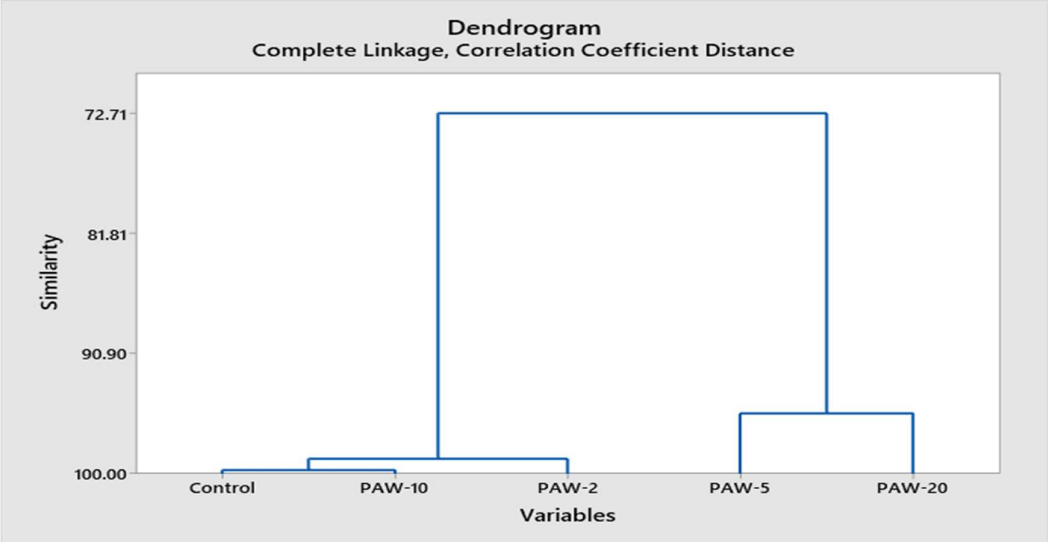

Figure 22: Dendrogram obtained from hierarchical clustering analysis (HCA) based on relative compositions of 52 VOCs detected by HS-SPME GC/MS in the control and PAW-treated rocket-salad samples at different processing times.

3.1.6. Impact of PAW treatment on the main phytosterols of rocket-salad leaves

Phytosterols are a class of lipids which refer to steroidal compounds, physiologically and structurally similar to cholesterol. They are naturally present in foods of plant origin and exhibit blood LDL cholesterol-lowering properties. Moreover, they exert anticancer, hepato-protective and anti-inflammatory properties **(da Silva Marineli, et al., 2015)**. Recently, the oxidation of food lipids due to plasma reactive species has received much attention, since literature reveals that cold plasma could induce lipid oxidation in different types of foods, including rice **(K. H. Lee, et al., 2018)**, wheat flour **(Bahrami, et al., 2016)** and olive oil **(Van Durme, et al., 2016)** via the action of reactive species.

The problem of lipid oxidation severely affects the quality of food products and sometimes limits their shelf-life. It also causes loss of flavor or development of off- flavors, loss of color, nutrient value, and the accumulation of compounds, which may be detrimental to health **(Wąsowicz, et al., 2004)**. For this reason, it is important to study the impact of a novel technology such as PAW on the content of these micronutrients *β*-sitosterol and campesterol are the main phytosterols reported in rocket leaves **(Khoobchandani, et al., 2011)**. The content of each compound was determined by HPLC-DAD in control and PAW-treated samples and the results are summarized graphically in figure 23. Results demonstrate that PAW treatment induced a significant reduction of both *β*-sitosterol and campesterol contents in all treatments, except for PAW-10 that showed a non-significant decrease.

It is noteworthy that no one studied the effect of PAW treatment on phytosterols in rocket, but relatively little information exists on the effect of plasma treatment on phytosterols content in other plants. For example, **Yodpitak, et al. (2019)** reported a significant decrease in total phytosterol content in one of the brown rice cultivars while the other cultivars showed non-significant changes after cold plasma treatment. This significant reduction in both *β*-sitosterol and campesterol contents could be due to an autoxidation process promoted by the plasma reactive species, as also confirmed by the increase of the aldehydes, alcohols, and ketones as the main volatile compounds generated in the lipid oxidation process **(Wąsowicz, et al., 2004)**. However, also in this case, the changes are not strictly proportional to treatment time.

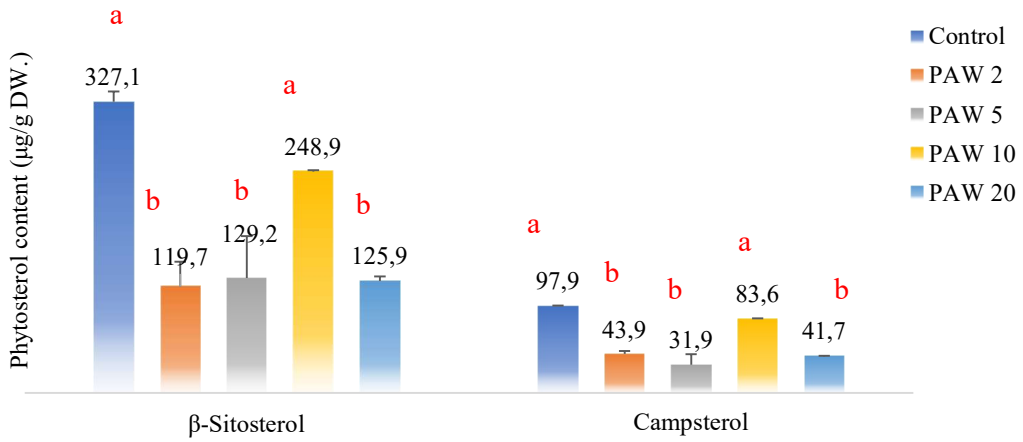

Figure 23: Changes in *β*-sitosterol and campesterol content of control and PAW treated rocket-salad leaves processed at different times. Legends: PAW-2, PAW-5, PAW-10, and PAW-20 refer to rocket samples subjected to plasma-activated water (PAW) treatment for 2, 5, 10, and 20 min, respectively.

3.1.7. Impact of PAW treatment on β-Carotene and lutein contents of rocket-salad leaves

Carotenoids are lipophilic compounds with several conjugated double bonds and 40 carbon molecules. They are classified chemically as xanthophylls, which have one or more oxygen groups (e.g., lutein and zeaxanthin), and carotenes, which are non-oxygenated (e.g., lycopene and *β*-carotene). Long-chain carotenoids are significantly more susceptible to oxidation and isomerization, which can happen during processing and storage. **(López-Gámez, et al., 2021)**. Lutein and *β*-carotene have been reported to be the most abundant carotenoids in rocket leaves **(Dvorakova, et al., 2021; Keyata, et al., 2021; Villatoro-Pulido, et al., 2013; Žnidarčič, et al., 2011)**. Higher content of *β*-carotene than that of lutein in both garden and wild rocket samples has been previously reported **(Žnidarčič, et al., 2011)**, however lutein was reported at higher concentrations in rocket leaves **(Dvorakova, et al., 2021; Villatoro-Pulido, et al., 2013)**. The content of lutein in control rocket samples was 37.40 mg/100g DW, as shown in figure 24. The β-carotene content was 36.31 ± 3.41 mg/100g DW, which is consistent with the findings of **(Keyata, et al., 2021)**, who reported a β-carotene content of 36.00 ± 0.01 mg/100g in dried rocket leaves. However, both *β*-carotene and lutein contents found in this study were higher than the values reported by previous studies **(Dvorakova, et al., 2021; Villatoro-Pulido, et al., 2013; Žnidarčič, et al., 2011)**.

Figure 24 shows the effect of PAW treatment on the carotenoid content of control and treated samples. Similar behaviour was observed for the content of both carotenoids (*β*-carotene and lutein) after short PAW treatment, in which an increase in the contents of both carotenoids was observed after PAW treatment with PAW-2,5 &10, this increase was significant for both carotenoids after the shortest treatment time (PAW-2), subjecting the samples longer processing time (PAW-20) lead to a non-significant reduction ($p \geq 0.05$) in lutein content. Generally, carotenoids are stored in chromoplasts, which are together with the cell walls and cell membranes, and act as natural barriers to their release. Disrupting or weakening of these natural barriers was previously reported as crucial for increasing the bio-accessibility of carotenoids. As a result, food processing has been regarded as an important tool for this purpose **(López-Gámez, et al., 2021)**. The exact biochemical pathway that leads to a rise in the carotenoid content is still unknown, but reactive plasma species have previously been reported to react by breaking the bond between carotenoid molecules and cell membranes, resulting in an increase in the concentration of free carotenoids **(Fernandes, et al., 2019)**. Exposure to electrically charged species from cold

plasma has also been reported to lead to a certain degree of electroporation **(Fernandes, et al., 2019)**, that, in turn, can promote changes to the hydrophobic and hydrophilic properties of the membrane and contributes to the release of fat-soluble compounds bound to the cell pulp membrane **Martínez, et al. (2018)**. The longer processing times tended to cause a non-significant reduction in lutein content due to the higher concentration of reactive species that may have accumulated in the samples **(Fernandes, et al., 2019)**. Thus, it could be assumed that the carotenoids radical scavenging behaviour may contribute to their breakdown in the presence of higher content of free radicals and ions **(Di Mascio, et al., 1989)**. Contrary to our results, a reduction in the content of carotenoids was previously reported in kiwi **(Ramazzina, et al., 2015)**, pumpkin puree **(Santos Jr, et al., 2018)**, guava beverages **(M. R. Silveira, et al., 2019)** and tomato **(Adhikari, et al., 2019)** post plasma treatment. However, the plasma generation systems, sources and modes of application were different compared to those used in the present research.

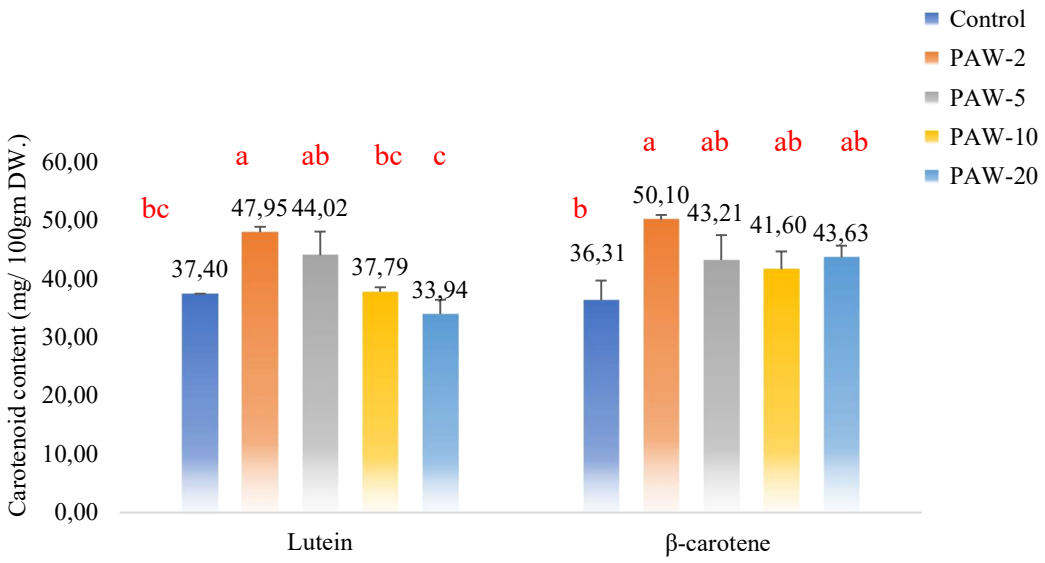

Figure 24: Changes in *β*-carotene and lutein contents of control and PAW treated rocket-salad leaves processed at different times. Legends: PAW-2, PAW-5, PAW-10, and PAW-20 refer to rocket samples subjected to plasma-activated water (PAW) treatment

3.2. The effect of DBD processing on the bioactive compounds of cold-stored strawberries

3.2.1. The effect of DBD processing on the LC-MS/MS polyphenolic profile of cold-stored strawberries

3.2.1.1. LC-MS/MS phenolic profile of strawberries – time zero

Different classes of phenolic compounds were identified in strawberry samples. A total of 25 phenolic compounds were identified and quantified: 7 phenolic acids, 7 flavonols, 4 anthocyanins, 3 flavan-3-ols, 2 dihydrochalcones and 1 flavanone in addition to the *trans*-cinnamic acid. Table 11 shows the phenolic compounds identified in control and plasma treated strawberry samples at different time points. As can be observed, anthocyanins are the most abundant phenolic group in all samples followed by flavan-3-ols. The phenolic profiles of the analysed strawberry samples were consistent with literature **(Mustafa, Angeloni, et al., 2022)**.

As shown in table 11 and figure 25, a preservation of the phenolic profile was observed immediately after processing, where non-significant differences ($p > 0.05$) were observed in the total phenolic contents and total contents of each class at time zero. Regarding individual compounds, only the contents of two phenolic acids have been changed significantly at time zero. Where, significant increase ($P < 0.05$) in *p*-hydroxy benzoic acid (155 %) and in caffeic acid (49 %) contents was observed immediately after treatment. To our knowledge the effect of plasma treatment on the individual phenolic compounds of whole fruits hasn't been reported so far. Previous studies also reported an increase in other phenolic acids post plasma treatment including chlorogenic acid **(Mehta, et al., 2020)** and caffeic acid **(Abouelenein, Mustafa, et al., 2023)** in both strawberry juice and rocket-salad respectively. *p*-Coumaric acid is the precursor of caffeic and *p*-hydroxybenzoic acids (Figure 26). The increase of these acids in strawberry could be explained by an increase in the biosynthesis of *p*-coumaric acid via the phenylpropanoid pathway catalysed by PAL (Phenylalanine ammonia-lyase) and C_4H (cinnamate 4-hydroxylase) enzymes after plasma treatment **(Kumar, et al., 2023)**. Generally, accumulation of phenolic compounds in the tissues is a defensive mechanism of plants against stress induced by reactive species of plasma **(M. Li, et al., 2019)**.

Its noteworthy that anthocyanins seemed not to be affected by the processing at zero time, as non-significant differences were observed between the control and processed samples. Anthocyanins are pigments responsible for the strawberries red colour, and being

very sensitive, their stability usually affected by traditional processing methods **(Civello, et al., 1997; Stübler, et al., 2020)**.

3.2.1.2. LC-MS/MS phenolic profile of strawberries– during storage

DBD treatment effect on quality characteristics of the strawberries was also evaluated during cold storage at 4 °C for six days. Unprocessed strawberries (control) were also assessed at same time points. The change in phenolic profile of the control and processed strawberries during storage at 4°C, is depicted in table 11 and figures 25-28. The total phenolic content of the strawberries followed a specific trend during storage, with an increase up to a maximum value at day 1 followed by a non-significant decrease up to day 6. Processed samples however showed non-significant differences compared to control sample at time zero ($p > 0.05$) and maintained the total phenolic content of strawberries during storage.

Regarding individual phenolic compounds, processed strawberries almost maintained the quantity of different compounds during storage. However, pairwise comparison between processed and control samples at each time point showed a significant reduction in some compounds in DBD treated samples compared to the control. As shown in figure 27, after 1 day storage a significant increase in the contents of the anthocyanins (pelargonidin-3-glucoside & cyanidin-3-glucoside), flavonols (kaempferol-3-glucoside & quercetin), flavan-3-ols (catechin & epicatechin) and chlorogenic acid contents was observed in control strawberry samples. A significant reduction in kaempferol was also observed at treated samples at day 3. However, those reductions are non-significant compared to the control sample at day 0.

On the other hand, at day 6 a significant increase in the three quercetin glycosides (quercetin-3-o-rutinoside, quercetin-3-o-glucoside & quercetin-3-o-galactoside) was observed in both control and treated samples (Figure 28). The concentration of both quercetin and kaempferol derivatives in strawberries during storage was previously reported **(Gil, et al., 1997)**. And plasma treatment seemed to preserve this property. A significant increase in the content of the flavanone hesperidin was also observed at day 6 only in the processed samples, which could be explained by the inactivation of polyphenol oxidase (PPO) in strawberries following nonthermal plasma treatments **(Misra, et al., 2015)**.

Table 11: Phenolic compounds determined by HPLC-MS/MS in control and and DBD treated strawberry samples stored at 4 °for 6 days.

	C0	**T0**	**C1**	**T1**	**C3**	**T3**	**C6**	**T6**
Gallic acid	11.90±2.72b	16.60±4.70ab	16.78±2.11ab	12.07±1.09b	15.98±2.54ab	15.04±1.63ab	17.87±2.48a	13.53±5.65ab
Neochlorogenic acid	n.d	n.d	n.d	n.d	n.d	n.d	n.d	n.d
Chlorogenic acid	2.75±0.92b	3.76±0.89ab	4.90±1.13a	3.15±0.74b	3.58±1.10ab	3.32±0.68b	2.97±0.80b	3.68±0.94ab
Hydroxy benzoic acid	10.29±2.10b	26.26±2.74a	12.20±3.58b	12.70±4.88b	14.75±3.00b	14.35±4.37b	15.10±3.51b	12.31±2.42b
Caffeic acid	3.84±0.74bcd	5.74±1.54a	3.09±0.38d	3.31±1.07cd	4.46±1.30abcd	4.81±1.01abcd	5.21±0.39ab	5.03±1.13abc
Vanillic acid	n.d	n.d	n.d	n.d	n.d	n.d	n.d	n.d
Syringic acid	n.d	n.d	n.d	n.d	n.d	n.d	n.d	n.d
P-Coumaric acid	113.84±31.96ab	128.36±23.98a	93.95±13.39ab	83.29±18.77b	103.78±11.09ab	127.20±20.84a	122.55±23.96a	112.17±11.29ab
Ferulic acid	1.33±0.11a	1.44±0.24a	1.21±0.17a	1.34±0.11a	1.20±0.21a	1.29±0.14a	1.23±0.22a	1.36±0.25a
3,5-Dicaffeoylquinic acid	n.d	n.d	n.d	n.d	n.d	n.d	n.d	n.d
Ellagic acid	470.26±175.46a	602.29±158.41a	669.24±15.24a	475.08±40.64a	664.18±97.44a	536.30±112.53a	643.25±162.26a	509.48±183.43a
Total phenolic acids	**614.20±185.40b**	**784.44±167.08a**	**801.37±25.74a**	**590.95±29.50b**	**807.93±98.76a**	**702.30±90.46ab**	**808.19±176.51a**	**657.58±180.27ab**
Delphidin 3,5 diglucoside	47.87±13.15a	55.03±13.16a	64.06±9.36a	38.14±3.58a	52.88±12.47a	42.40±9.21a	49.80±12.44a	51.07±19.01a
Delphidin3-galactoside	n.d	n.d	n.d	n.d	n.d	n.d	n.d	n.d
Cyanidin-3-glucoside	106.28±22.21bc	90.47±29.40c	163.92±21.54a	97.21±14.38c	149.06±20.70ab	120.42±59.89abc	116.34±24.09abc	132.33±23.19abc
Petunidin-3-glucoside	n.d	n.d	n.d	n.d	n.d	n.d	n.d	n.d
Pelargonidin-3-rutinoside	591.21±90.64ab	502.07±159.43b	682.89±45.74a	519.69±22.82ab	631.00±107.73ab	595.44±132.38ab	674.37±96.39a	641.02±39.69ab
Pelargonidin-3-glucoside	4862.94±1050.91ab	4694.33±1391.04b	6599.08±1736.32a	4633.84±678.93b	5743.00±612.39ab	5446.27±1133.82ab	6020.59±946.62ab	5569.89±802.44ab
Malvidin-3-galactoside	n.d	n.d	n.d	n.d	n.d	n.d	n.d	n.d
Total anthocyanins	**5608.30±1146.88ab**	**5341.90±1580.82b**	**7509.95±1782.76a**	**5288.89±713.01b**	**6575.94±689.68ab**	**6204.53±1325.12ab**	**6861.11±954.73ab**	**6394.32±880.45ab**
Phloridzin	65.82±12.52a	67.06±17.91a	80.76±18.13a	59.81±12.39a	73.72±15.84a	78.79±21.07a	67.29±13.42a	77.51±10.16a
Phloretin	0.12±0.02ab	0.10±0.03ab	0.14±0.03a	0.10±0.02ab	0.11±0.01ab	0.11±0.03ab	0.09±0.01b	0.08±0.01b
Total Dihydro chalcones	**65.93±12.54a**	**67.16±17.93a**	**80.89±18.17a**	**59.91±12.38a**	**73.83±15.84a**	**78.90±21.09a**	**67.38±13.42a**	**77.59±10.16a**
Catechin	1030.12±244.08b	987.53±247.95b	1634.49±351.49a	950.05±167.78b	1323.98±180.57ab	1336.76±194.92ab	1095.54±289.68b	1355.80±167.19ab
Epicatechin	8.97±2.15ab	7.87±1.637ab	11.30±3.38a	7.00±1.55b	10.77±2.24ab	10.42±2.75ab	9.69±1.32ab	11.14±1.60a
Procyanidin A2	n.d	n.d	n.d	n.d	n.d	n.d	n.d	n.d

procyanidin B2	136.33±14.28bc	125.44±26.37bc	239.90±55.19a	97.67±26.96c	167.50±22.51b	141.16±22.62bc	149.26±35.14bc	144.91±15.34bc
Total Flavan-3-ols	**1175.42±259.11b**	**1120.84±274.8b**	**1885.69±404.08a**	**1054.72±196.12 b**	**1502.24±195.72a b**	**1488.34±217.67ab**	**1254.49±320.10b**	**1511.85±180.45a b**
Quercetin-3-o-rutinoside	2.39±0.82c	3.29±0.51ab	2.51±0.59bc	2.45±0.24bc	2.55±0.30bc	2.79±1.24bc	3.59±0.73ab	4.04±0.44a
Quercetin-3-o-glucoside	7.07±1.50cd	9.78±1.37ab	9.23±0.88abcd	6.56±1.01d	9.56±0.97abcd	8.37±2.20bcd	10.65±1.01b	11.74±3.84a
Quercetin-3-o-rhamnoside	n.d	n.d	n.d	n.d	n.d	n.d	n.d	n.d
Myricetin	n.d	n.d	n.d	n.d	n.d	n.d	n.d	n.d
Kaempferol-3-glucoside	126.23±36.9b	169.76±54.53a	217.97±65.47a	121.27±45.49b	231.34±68.22a	152.33±36.27ab	188.44±36.01a	172.96±50.50a
Quercetin	0.65±0.15bc	0.74±0.01abc	1.00±0.24a	0.62±0.02c	0.94±0.13ab	0.74±0.14abc	0.88±0.25abc	0.96±0.28ab
Isorhamnetin	0.13±0.04ab	0.10±0.02ab	0.14±0.04a	0.09±0.01ab	0.14±0.04ab	0.09±0.01ab	0.12±0.03ab	0.09±0.02b
Quercetin 3-o-galactoside	5.67±1.17c	7.98±1.54ab	7.10±0.57bc	5.42±1.25c	8.58±1.26a	7.13±1.66bc	8.85±0.96a	9.97±2.81a
Kampferol	3.05±0.61b	4.70±1.24a	3.59±1.07b	3.51±0.30b	5.54±1.71a	3.53±0.54b	4.16±0.72ab	3.43±0.96b
Total Flavonols	**145.19±40.16b**	**196.36±53.11a**	**241.54±66.99a**	**139.93±46.80b**	**258.65±69.78a**	**174.98±37.28a**	**216.69±38.56a**	**203.20±57.86a**
Naringin	n.d	n.d	n.d	n.d	n.d	n.d	n.d	n.d
Hesperidin	2.10±0.31bc	2.28±0.06abc	2.37±0.62abc	2.18±0.54bc	2.08±0.30c	2.10±0.28bc	2.94±0.68ab	3.11±0.72a
Total Flavanone	**2.10±0.31bc**	**2.28±0.06abc**	**2.37±0.62abc**	**2.18±0.54bc**	**2.08±0.30c**	**2.10±0.28bc**	**2.94±0.68ab**	**3.11±0.72a**
Trans-cinnamic acid	104.90±47.63a	110.07±63.49a	56.78±22.26a	64.99±32.24a	82.61±0.89a	66.67±8.63a	93.21±13.49a	94.52±3.84a
Total phenolics	**7716.0±1620.0b**	**7623.1±1949.3b**	**10578.6±2225.6a**	**7201.6±850.7b**	**9303.3±492.2ab**	**8717.8±1612.1ab**	**9304.0±1439.4**	**8942.2±1220.9ab**

All the data are expressed as mean ± standard deviations. Means that do not share letters in each row differ significantly ($p < 0.05$) according to Tukey's test. Legends: C0, C1, C3 & C6 refer to control strawberry samples stored for 0, 1, 3 & 6 days respectively; T0, T1, T3 & T6 refer to DBD-treated strawberry samples stored for 0, 1, 3 & 6 days, respectively.

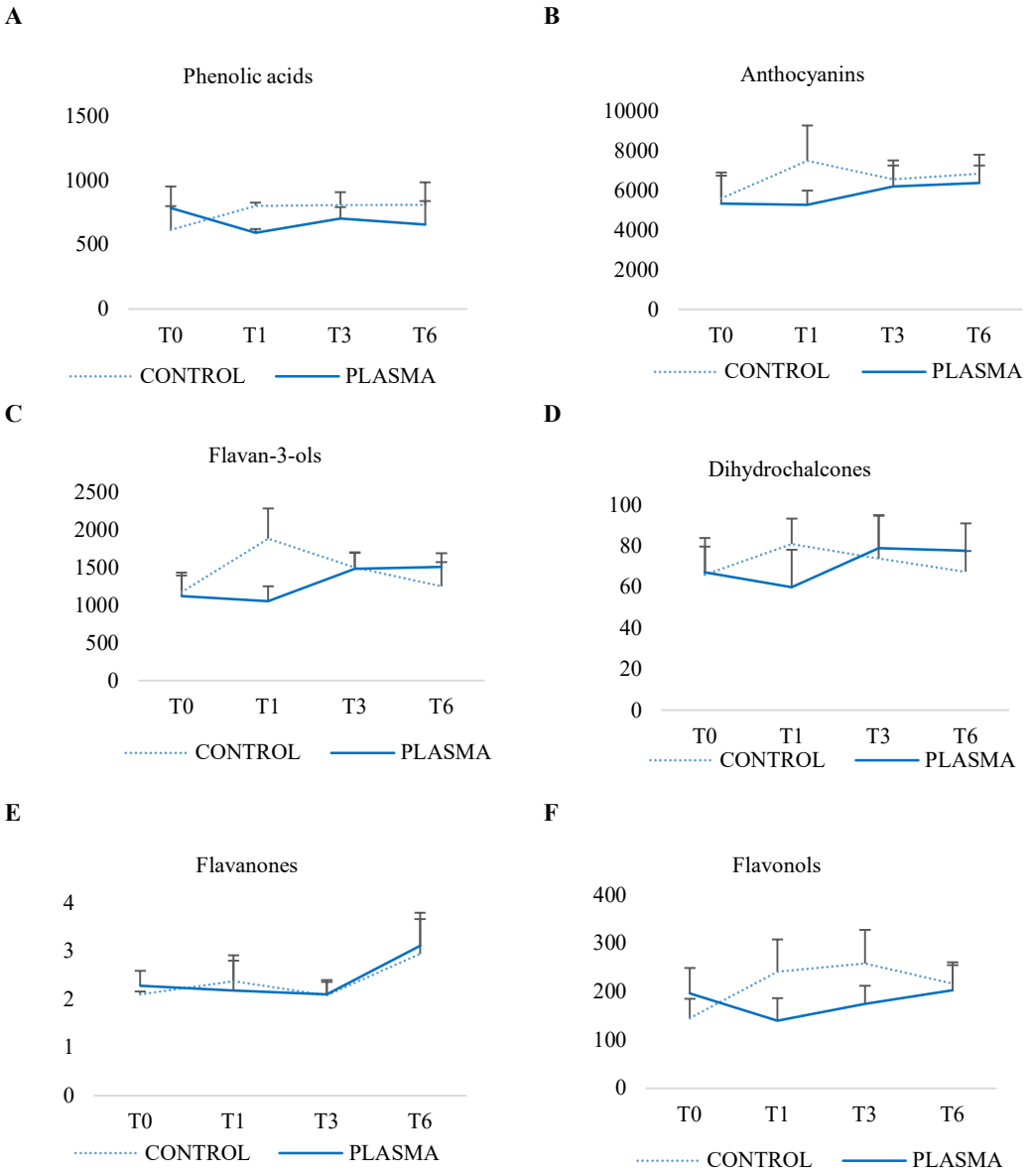

Figure 25: Effects of cold plasma on the different phenolic classes in strawberries during cold storage. A) Total phenolic acids, B) Total anthocyanins, C) Total flavan-3-ols, D) Total dihydrochalcones, E) Total flavanones and F) Total flavonols. Data were expressed as the means ± SD of three replications. Storage time in days was put on X-axis as T0, T1, T3 &T6, concentrations expressed as $mg.kg^{-1}$ DW.

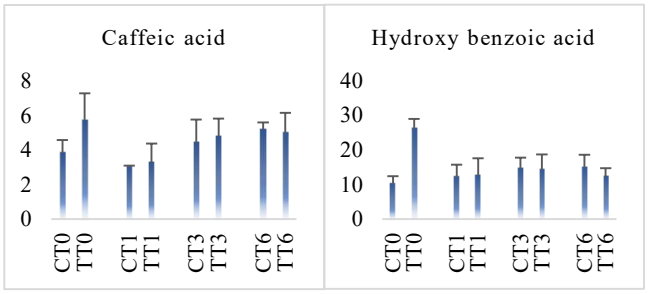

Figure 26: Significantly changed compounds in strawberries immediately post plasma processing.

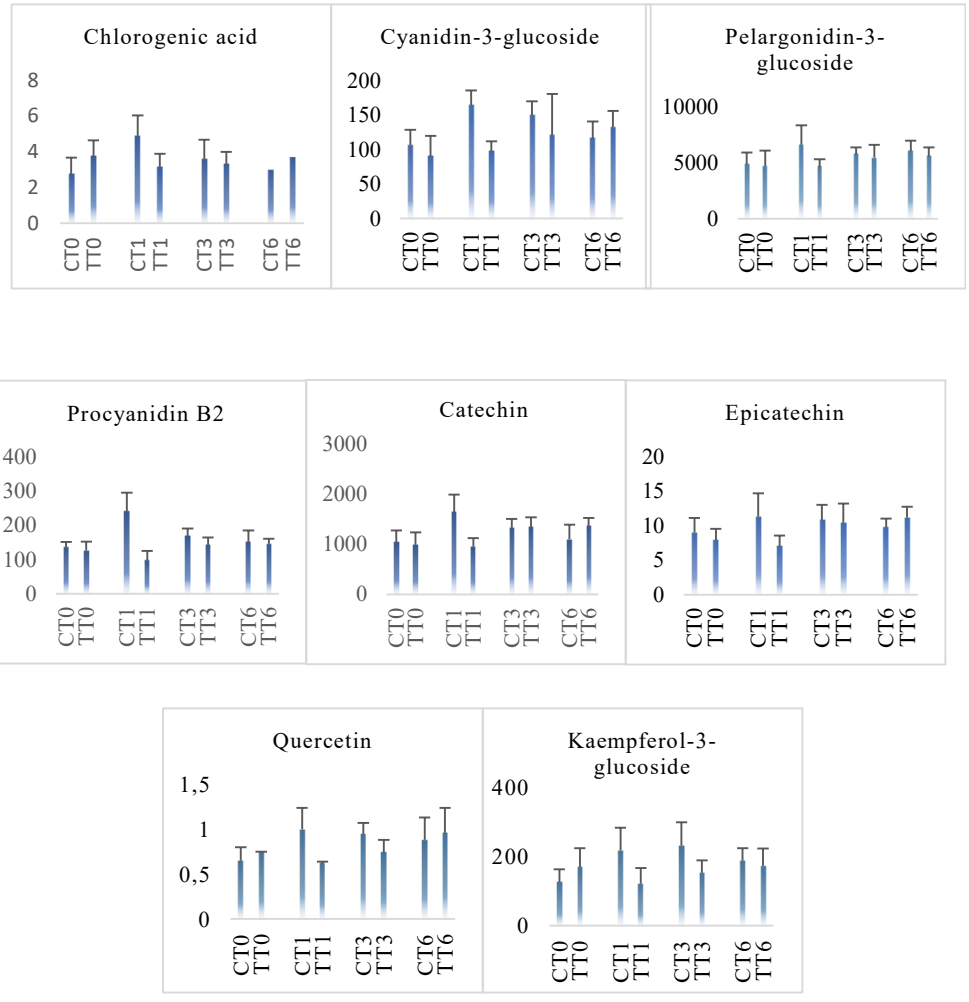

Figure 27: Significantly changed compounds in strawberries during storage day 1.

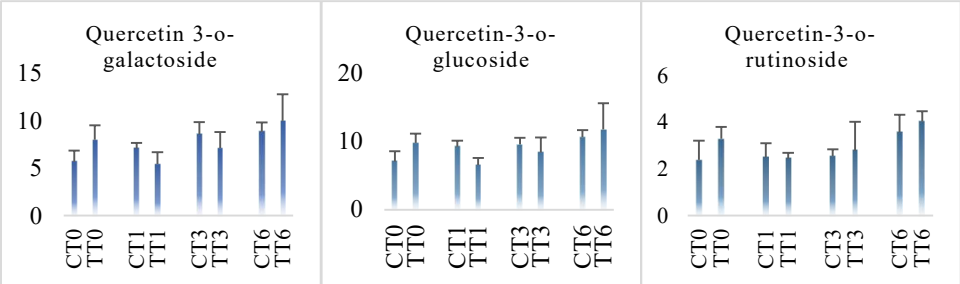

Figure 28: Significantly changed compounds in strawberries during storage day 6.

3.2.2. The effect of DBD processing on TPC and DPPH radical scavenging activity of cold-stored strawberries

3.2.2.1. TPC and DPPH radical scavenging activity of strawberries – time zero

As shown in table 12, the total phenolic content (TPC) and the free-radical scavenging activity (DPPH) were non-significantly affected in the DBD-processed strawberries compared to the control ones ($p > 0.05$), which confirms the stability of phenolic profile to the processing parameters and goes in a good accordance with the LC-MS/MS results. DPPH reducing activity slightly increased immediately post processing, however this is increase wasn't statistically significant ($p > 0.05$).

3.2.2.2. TPC and DPPH radical scavenging activity of strawberries – during storage

During storage TPC seems to be non-significantly changed, however the DPPH activity was significantly increased by time in the processed samples (Table 12). This increase in the antioxidant activity could be related to the observed increase in the ascorbic acid and some individual phenolic compounds contents. Generally, traditional thermal processing methods such as blanching, pasteurization, and sterilization, can lead to the oxidation and degradation of polyphenols in strawberries. **Garzoli, et al. (2020)** reported reductions in both total phenolic content and antioxidant activity of strawberries by 46% and 64%, respectively, following pasteurization. Enzymatic and mechanical treatments can also affect the polyphenol content of strawberries, consequently alternative processing techniques that could preserve polyphenols and antioxidant activity in strawberries should be considered **(Sruthi, et al., 2021)**.

Table 12: Changes in the ascorbic acid, TPC and DPPH in control and and DBD treated strawberry samples stored at 4 °for 6 days (mean values ± standard deviation).

Quiality index	**Samples**	**Storage time (days) 0**			
		T0	T1	T3	T6
TPC ***(mg gallic acid/g DW)***	Control	22.98± 3.5bc	29.29±4.0a	26.27±1.3ab	25.49±5.1ab
	Plasma-treated	22.64±3.9bc	21.07±1.8c	24.83±2.3bc	24.93±2.9bc
DPPH ***(mg trolox/g DW)***	Control	24.55±2.14b	30.43±4.1a	28.31±3.5b	24.10±2.8b
	Plasma-treated	25.37± 6.46b	24.18± 2.3b	29.07±4.1a	29.67±5.3a
Ascorbic acid ***(mg/g DW)***	Control	3.82±0.1b	4.16±0.4 bc	4.36±0.2bc	4.06±0.5bc
	Plasma-treated	2.78±0.7c	4.23±0.3bc	5.02±0.7a	4.87±0.6a

3.2.3. The effect of DBD processing on L-ascorbic acid content of cold-stored strawberries

3.2.3.1. Ascorbic acid content of strawberries – time zero

As shown in table 12 and figure 29, DBD processing seemed to induce a significant decrease (27.2%) of ascorbic acid in the strawberries at zero time of storage compared to the untreated fruits. According to the literature, both applied voltage and treatment time were reported to significantly affect the ascorbic acid content of strawberries **(Misra, et al., 2015)**, DBD treatment for 30 min could explain the ascorbic acid reduction in our study. The reaction of the plasma reactive species with ascorbic acid is proposed to be the major reason for the observed loss. **Giannoglou, et al. (2021)** have reported slight but not statistically significant decrease ($p > 0.05$) in contents of ascorbic acid entire strawberry fruits post plasma processing for 10 minutes. Similar results were reported for fresh cut strawberries post plasma treatment **(M. Li, et al., 2019)**.

3.2.3.2. Ascorbic acid content of strawberries– during storage

However, the content of ascorbic acid was decreased immediately after processing, higher stability during storage was observed. As shown in table 12 and figure 29, processed strawberries showed higher ascorbic acid contents compared to the unprocessed samples during the whole storage period, possibly due to an increase in cell membranes permeabilization caused by the processing leading to an increase in the extractability of the ascorbic acid as previously reported **(Giannoglou, et al., 2021)**. Those results are in a good accordance with **(Zhou, et al., 2023)**, who reported a higher ascorbic acid concentration in blueberries during storage post plasma processing.

The storage conditions are very important for *L*-Ascorbic acid stability, where any damage in the surface of fruit could induce major losses of ascorbic acid. Fruits which have a low pH (citrus fruits) have smaller losses of ascorbic acid and fruit with a soft consistency, such as strawberries are more sensitive to external influences **(Pavlovska, et al., 2015)**.

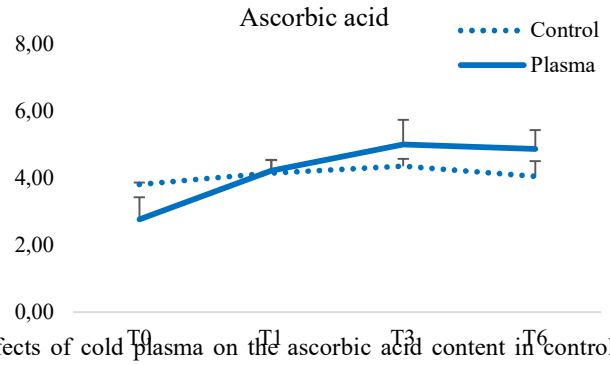

Figure 29: Effects of cold plasma on the ascorbic acid content in control and and DBD treated strawberry samples stored at 4 °for 6 days.

3.2.4. The effect of DBD processing on GC-MS-based primary metabolites profile of cold-stored strawberries

3.2.4.1. GC-MS-based primary metabolites profile of strawberries– time zero

The changes in qualitative and quantitative contents of primary metabolites (specifically sugars and acids) in the strawberry fruits can be used as an essential index to evaluate their flavour, taste and quality **(Pedrosa, et al., 2021)**. Primary metabolic response associated with food processing is very complex and varies essentially depending on the duration, type and level of stress occurred during the process, in addition to the type of food matrix, its species origin, and plethora of other factors. **(Pedrosa, et al., 2021)**. Traditional processing techniques, which include high temperatures, enzymatic or mechanical treatment, can lead to the destruction or degradation of sugars and amino acids in strawberries **(Civello, et al., 1997; Villarreal, et al., 2010)**. For this, selecting appropriate processing techniques and optimizing processing conditions could minimize degradation of valuable sugars, acids and other metabolites preserving the sweetness and nutritional value of the fruit.

Studies on the effect of nonthermal plasma on primary metabolomic profile of fruits and vegetables are scarce. Further research is needed to fully understand the effects of cold plasma treatment on primary metabolites and to optimize treatment conditions to ensure maximum health benefits **(Sruthi, et al., 2021)**. Previous studies reported that chemically active plasma species emerged by cold plasma cause cleavage of certain bonds inducing chemical modifications at the side chains of some amino acids that could considerably affect

their function. Amino acids with aromatic and sulphur-residues are specifically sensitive to these attacks **(Pal, et al., 2016; Sruthi, et al., 2021)**. Direct exposure to argon plasma reported to induce a degradation of both carboxylic and amino groups in *L*-alanine **(Setsuhara, et al., 2013)**. Most studies showed that, the soluble sugar content often remains unaffected upon plasma treatment showing that CP treatment can be effectively used to process foods without negatively affecting the major quality parameters **(Porto, et al., 2020; Y. Wang, et al., 2020; L. Xu, et al., 2017)**. Other studies documented a significant decrease in sugar content as in Chinese bayberries **(R. Ma, et al., 2016)** or considerable rise as in fresh-cut pears **(C. Chen, et al., 2019)**.

As shown in table 13 and figure 30, GC-EI-Q-MS approach focused on identification and relatively quantification of thermally stable primary metabolites revealed 122 compounds, in the form of their methyl oxime trimethylsilyl (MO-TMS) derivatives annotated in the aqueous methanolic extracts of control strawberry samples under DBD treated samples (Table 13). In this group, 107 individual compounds were identified as primary metabolites by spectral similarity search against available libraries and/or co-elution with authentic standards. Some metabolites appeared as several isomers and/or methoxamine-trimethylsilyl derivatives; therefore, the total number of metabolites identified was only 104 compounds. The identified metabolites represented 7 amino acids, 29 acids and esters, 21 sugars and 9 compounds of other classes. Unidentified 8 metabolites were partially annotated to a certain chemical class by the presence of characteristic signals (*m/z* values): for example, unknown cinnamic acids, carboxylic acids, amino acids, primary alcohols derivatives (Table 13). 27 unidentified metabolites are labelled with the word Unknown, and their annotation contains the retention time (t_R) and retention index (RI). Monosaccharides were found to predominate, with glucose and fructose, which yielded the most abundant signals (Figure 30). This was in a good agreement with earlier studies **(L. Li, et al., 2019; Mikulic-Petkovsek, et al., 2013)**.

To compare the changes in the relative metabolite contents observed before (C0) and immediately after DBD treatment (T0) were analysed. Based on this combined data, we were not able to observe a clear separation between control and treated samples using both PCA (Figure 31). Further, the PLS-DA model presented in figure 32, also showed poor performance, reflected by its negative Q2 revealed by cross-validation which means that the model was not predictive or it was overfitted **(W. Xu, et al., 2021)**. The poor performance of the PLS-DA model suggested that the changes occurred between variables in different

control and CP treated samples were non-significant or below the detectable limit with the current sample size (n =3).

The observed ambiguous separation between control and plasma-treated samples suggesting that there were no discernible differences between the metabolite profiles of control and DBD-treated strawberry samples immediately post treatment.

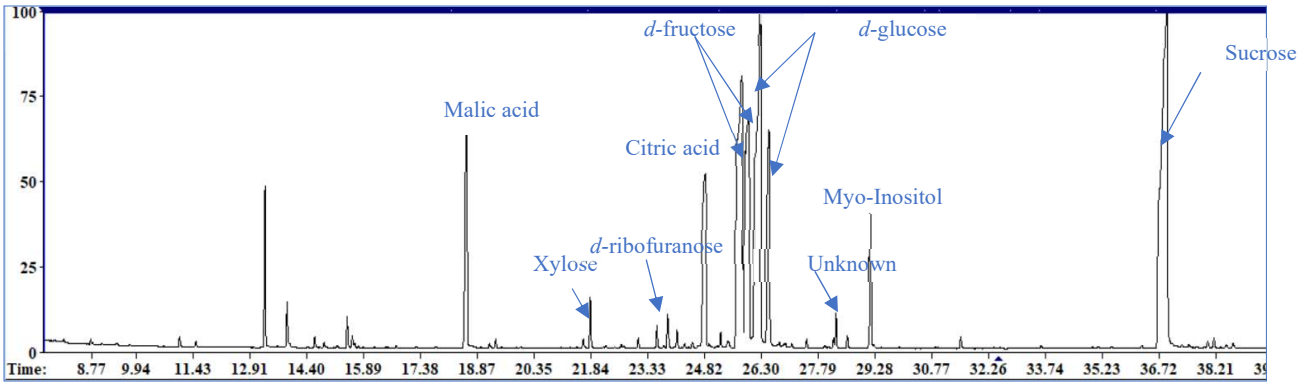

Figure 30: Representative total ion chromatogram (TIC) of the control strawberry sample showing the major detected primary metabolites.

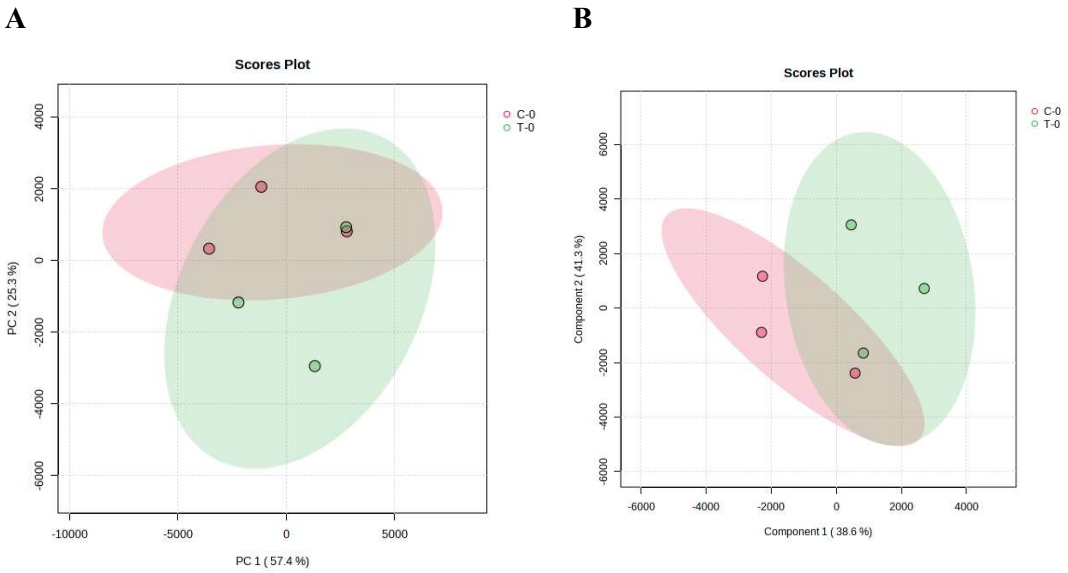

Figure 31: Primary metabolomic analyses of both control (C-0) and DBD treated strawberries (T-0) at day 0. A) Scores plot of Principal component analysis (PCA); B) partial least square discriminant analysis (PLS-DA).

Table 13: GC-MS-based primary metabolites profile of cold-stored strawberries

	Acids	**t_R**	**RI**
N.1	Boric acid-3TMS	**7.7**	**1011.7**
N.2	Lactic acid-2TMS	**9.5**	**1087.5**
N.3	Glycolic acid-2TMS	**9.8**	**1101.6**
N.4	Oxalic acid-2TMS	**11.1**	**1156.0**
N.81	phosphoric acid-TMS	**13.9**	**1274.0**
N.5	Maleic acid	**14.6**	**1304.6**
N.6	Butanedioic acid-2TMS	**14.9**	**1315.3**
N.7	Itaconic acid-2TMS	**15.5**	**1342.1**
N.8	Itaconic acid-2TMS	**15.6**	**1348.1**
N.9	Fumaric acid-2TMS	**15.7**	**1350.7**
N.10	Nonanoic acid-TMS	**15.9**	**1362.1**
N.11	Methylmaleic acid-2TMS	**16.8**	**1398.5**
N.12	Pentanedioic acid-2TMS	**16.9**	**1403.7**
N.13	Malic acid-3TMS	**18.6**	**1485.6**
N.14	4-Coumaric acid-2TMS	**26.9**	**1939.6**
N.15	Gluconic acid-6TMS	**27.8**	**1991.7**
N.16	Gluconic acid-6TMS	**28.0**	**2006.2**
N.17	Hexanedioic acid, bis(2-ethylhexyl) ester	**33.7**	**2392.7**
N.18	4-Aminobutanoic acid-3TMS	**19.4**	**1522.6**
N.19	3-Hydroxybenzoic acid-2TMS	**20.2**	**1562.9**
N.20	Erythronic acid-4TMS	**20.0**	**1555.3**
N.21	Aconitic acid-3TMS	**23.6**	**1744.7**
N.22	Shikimic acid-4TMS	**24.7**	**1807.1**
N.23	Citric acid-4TMS	**24.8**	**1813.1**
N.24	Dehydroascorbic acid dimer, 2MEOX	**25.3**	**1839.9**
N.25	Quininic acid-5TMS	**25.4**	**1851.3**
N.26	Hexadecanoic acid-3TMS	**28.6**	**2043.8**
N.27	Galactaric acid-6TMS	**28.4**	**2035.5**
N.28	Ribonic acid-5-TMS	**22.5**	**1683.7**
N.29	Ascorbic acid-4TMS	**27.0**	**1942.2**
N.30	Stearic acid-TMS	**31.6**	**2242.6**
	Amino acids		
N.31	*L*-Alanine-2TMS	**10.1**	**1114.2**
N.32	*L*-Valine -TMS	**10.2**	**1115.9**
N.33	*L*-Alanine-2TMS	**10.3**	**1123.4**
N.34	*L*-Threonine-2TMS	**14.4**	**1296.4**
N.35	Uracil-2TMS	**15.4**	**1337.1**
N.36	Alanine-3TMS	**15.8**	**1355.2**
N.37	*L*-Threonine-3TMS	**16.4**	**1382.7**
N.38	*β*-Alanine-3TMS	**17.3**	**1423.0**
N.39	*L*-5-Oxoproline-2TMS	**19.2**	**1514.4**
	Sugars		
N.40	Xylose-4TMS, MEOX	**21.7**	**1639.8**
N.41	Xylose-4TMS, MEOX	**21.8**	**1649.7**
N.42	Arabinose, 4TMS	**22.0**	**1656.4**
N.43	d-Ribose-4TMS, MEOX	**22.0**	**1656.4**

N.44	Xylose, 4TMS	**22.3**	**1671.4**
N.45	Xylitol, 5TMS derivative	**22.4**	**1677.7**
N.46	Myo-Inositol, 6TMS derivative	**22.9**	**1703.8**
N.47	Arabitol, 5TMS derivative	**23.0**	**1712.6**
N.48	Ribofuranose, 4TMS	**23.9**	**1760.5**
N.49	Ribofuranose, 4TMS	**24.1**	**1774.4**
N.50	D-Fructose-5TMS, MEOX	**25.7**	**1866.2**
N.51	D-Fructose-5TMS, MEOX	**26.0**	**1882.8**
N.52	D-Glucose-5TMS, MEOXe	**26.2**	**1894.2**
N.53	D-Glucose-5TMS, MEOXe	**26.5**	**1915.1**
N.54	D-Glucopyranose, 5TMS	**27.5**	**1976.4**
N.55	Myo-Inositol, 6TMS	**29.2**	**2083.8**
N.56	Galactose-5TMS	**29.9**	**2127.5**
N.57	Galactose-5TMS	**29.9**	**2133.1**
N.58	D-Ribose-5-phosphate MEOX 5TMS	**31.1**	**2210.2**
N.59	Fructose-6-phosphate-6TMS	**32.4**	**2302.3**
N.60	Mannose-6-phosphate-6TMS	**32.6**	**2314.4**
N.61	Glucose-6-phosphate-6TMS	**32.8**	**2332.8**
N.62	Myo-Inositol-5-phosphate MEOX 5TMS	**33.8**	**2406.3**
N.63	Sucrose-8TMS	**35.3**	**2515.7**
N.64	Sucrose-8TMS	**36.1**	**2581.5**
N.65	Sucrose-8TMS	**36.7**	**2629.6**
N.66	*D-(+)*-Trehalose α,α' dihydrate	**38.0**	**2735.8**
N.67	Melibiose-8TMS	**38.4**	**2766.1**
N.68	Maltose-4TMS, MEOX	**38.5**	**2777.3**
N.69	Galactinol-9TMS	**40.5**	**2946.9**
N.70	Galactinol-9TMS	**40.8**	**2982.2**
N.71	Galactinol-9TMS	**41.5**	**3041.9**
N.72	Glucopyranose-5TMS	**42.1**	**3097.0**
N.73	Sucrose, 8TMS derivative	**44.6**	**3347.2**
N.74	Sucrose, 8TMS derivative	**44.8**	**3366.3**
N.75	Sucrose, 8TMS derivative	**45.0**	**3382.8**
N.76	Raffinose, 11TMS	**45.1**	**3390.4**
	Others		
N.77	Decamethyltetrasiloxane	**8.7**	**1052.8**
N.78	Methyltris(trimethylsiloxy)silane	**9.0**	**1068.6**
N.79	Pentasiloxane, dodecamethyl-	**11.5**	**1173.0**
N.80	Diethylene glycol-2TMS	**13.3**	**1249.7**
N.82	Glycerol-3TMS	**14.0**	**1276.5**
N.83	Glycerol-3TMS	**14.6**	**1301.0**
N.84	Levoglucosan-3TMS	**22.7**	**1696.2**
N.85	Adonitol-5TMS peak2	**23.1**	**1717.5**
N.86	1.4-butanediamine-4TMS	**23.3**	**1728.3**
N.87	Catechine-5TMS	**39.7**	**2883.1**
	Unknowns		
N.88	Unknown (Carboxylic acid dv.)	**15.9**	**1358.9**
N.89	Unknown (carbonyl group)	**16.2**	**1373.3**
N.90	Unknown (carbonyl group)	**16.3**	**1377.0**

N.91	Unknown (cinnamic acid dv.)	**20.0**	**1552.0**
N.92	Unknown (carboxylic acid dv.)	**21.5**	**1630.9**
N.93	Unknown (alpha amino acid)	**22.4**	**16.81.8**
N.94	Unknown (Carboxylic acid dv.)	**24.3**	**1785.3**
N.95	Unknown (primary alcohol)	**41.8**	**3072.8**
N.96	Unknown	**17.8**	**1447.4**
N.97	Unknown	**19.9**	**1550.5**
N.98	Unknown	**22.7**	**1692.9**
N.99	Unknown	**28.2**	**2020.6**
N.100	Unknown	**28.3**	**2025.0**
N.101	Unknown	**30.9**	**2197.1**
N.102	Unknown	**33.1**	**2353.8**
N.103	Unknown	**33.3**	**2369.6**
N.104	Unknown	**33.5**	**2381.0**
N.105	Unknown	**33.6**	**2387.2**
N.106	Unknown	**34.0**	**2418.2**
N.107	Unknown	**34.2**	**2432.5**
N.108	Unknown	**34.3**	**2437.7**
N.109	Unknown	**34.4**	**2449.5**
N.110	Unknown	**34.9**	**2485.9**
N.111	Unknown	**35.0**	**2493.4**
N.112	Unknown	**35.2**	**2505.3**
N.113	Unknown	**35.5**	**2532.6**
N.114	Unknown	**36.0**	**2569.7**
N.115	Unknown	**36.3**	**2593.8**
N.116	Unknown	**36.4**	**2600.5**
N.117	Unknown	**37.3**	**2679.8**
N.118	Unknown	**37.5**	**2695.2**
N.119	Unknown	**37.9**	**2729.0**
N.120	Unknown	**38.183**	**2749.8**
N.121	Unknown	**38.693**	**2792.6**
N.122	Unknown	**39.199**	**2836.4**

3.2.4.2. GC-MS-based primary metabolites profile of strawberries – during storage

To compare the changes in the relative metabolite contents observed before and after CP treatment, samples at different storage days, i.e., before (C-0 to C-6) and after treatment (T0 to T-6), were analysed. For better feature selection and data reduction a supervised partial least square–discriminant analysis (PLS-DA) and sparse partial least square discriminant analysis (sPLS-DA) were applied and statistically analysed. A trend of separation in the metabolome profiles based only on the consideration of the storage period was observed. where a clear separation in the s-PLSDA between samples treated at day 6 grouped in on the left side of the scores plot and almost all other samples clustered separately in the right sector (Figure 32). Metabolic features significantly affected by the storage time, were presented in figures 33 & 34, they found to have a relatively high variable importance in projection (VIP) score in the sPLS-DA and were also determined by two-way ANOVA ($p<0.05$) box plots fisher Lsd.

Storage of fruits can have various effects on their chemical composition, including changes in the levels of sugars and other metabolites **(Uarrota, et al., 2019)**. In the present study, mannose, glucose phosphates and other sugars were increased during storage in both control and treated samples. Cold plasma treatment using the present parameters did not induce any significant changes in the strawberry primary metabolome up to day 6 of storage. The increase of sugars in strawberries can enhance the sweetness and flavour, making them more desirable to consumers. However, on the negative side, it can also lead to browning and softening of fruits, which can reduce their shelf life and overall quality.

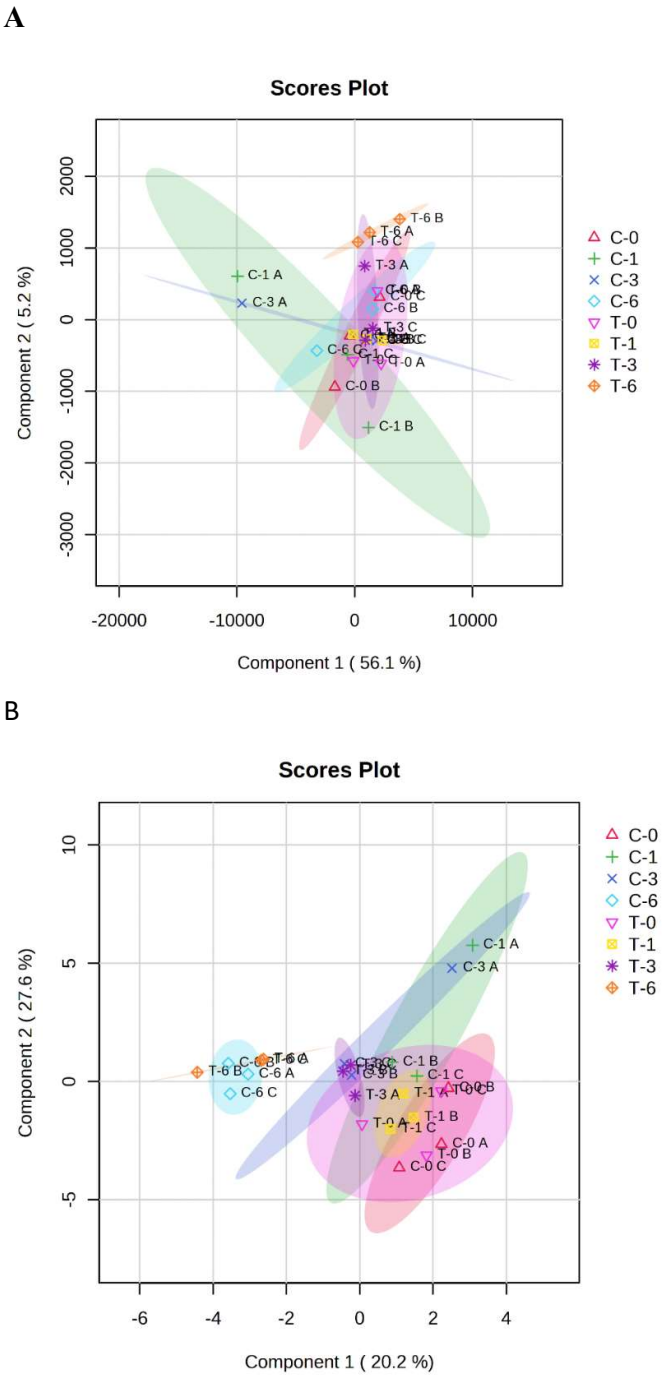

Figure 32: Analysis of the metabolomics data acquired upon sampling at different storage days of control and CP treated strawberries with partial least square discriminant analysis (PLS-DA) and sparse partial least square discriminant analysis (sPLS-DA). A) Score plots obtained by PLS-DA and B) sPLS-DA

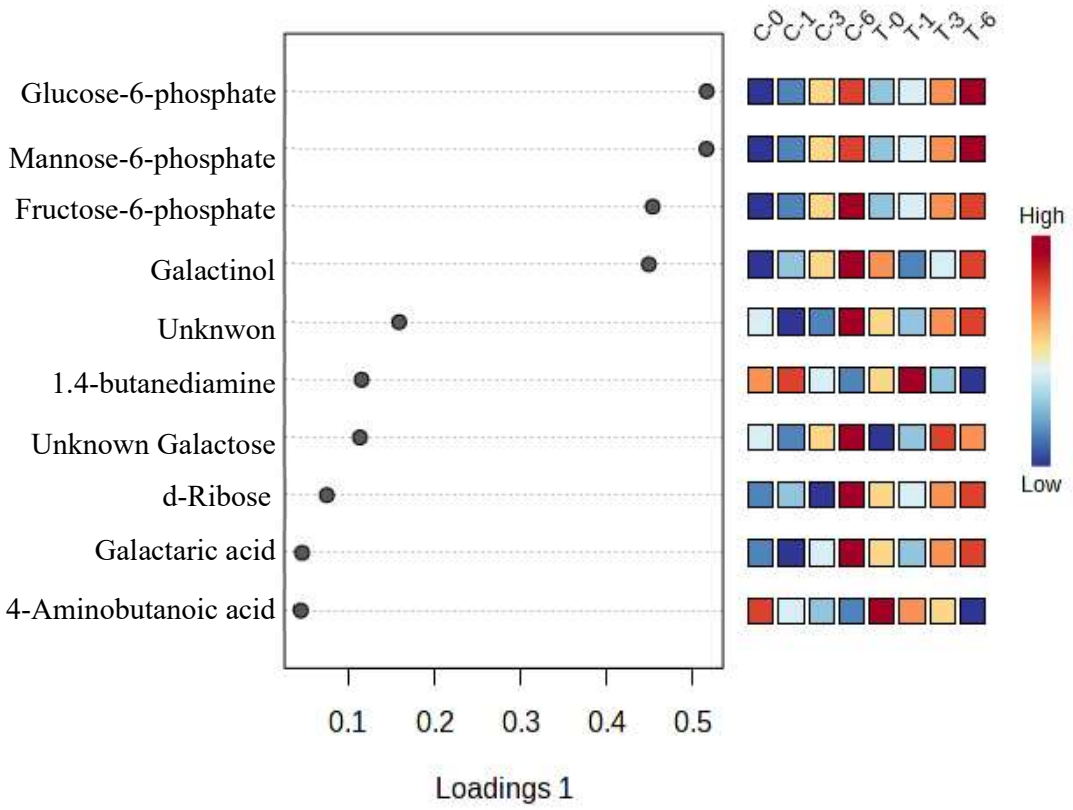

Figure 33: Top 10 metabolites with the highest variables in projection (VIP) scores of sPLS-DA

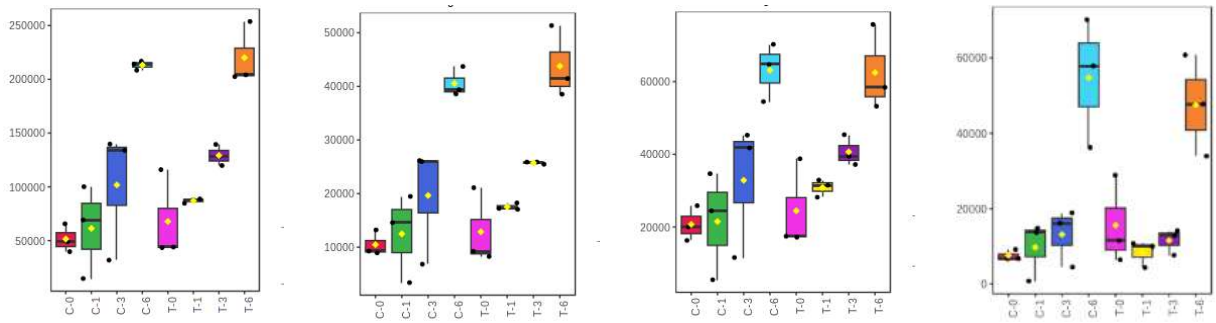

Figure 34: Box plots of different metabolites of strawberry samples obtained from both control and CP treated samples at different days according to the Fisher's Lsd test at $P < 0.05$. The bar plots show the original values (mean±SD).

3.3. Influence of DBD plasma treatment on the bioactive compounds of cut-melon fruit.

3.3.1. Influence of DBD plasma treatment on the LC-MS/MS phenolic profile of cut-melon fruit.

Even though melon fruit does not rank particularly highly in phenolic content **(Amaro, et al., 2015)**, phenolics remains one the most important biologically active phytochemicals due to their redox properties allowing them to act as reducing agents and free radical scavengers. As shown in table 14 a total of 14 phenolic compounds were identified and quantified: eight phenolic acids, six flavonoids in addition to the *trans*- cinnamic acid. Table 14 shows the phenolic compounds identified in control and treated melon samples. As can be observed, hesperidin is the most abundant phenolic compound in control samples followed by *p*-hydroxybenzoic, *p*-coumaric and neochlorogenic acids. Other compounds as gallic acid, chlorogenic acid, quercetin, and quercetin glycosides are found in small amounts in consistent with literature **(Kolayli, et al., 2010)**. In this study the impact of ozone concentration and plasma treatment time on different phenolic compounds have been studied and presented in table 14 and figures 35 &36.

Ozone (O_3) is produced by the collision of electrons with the oxygen molecules in the plasma discharge and its concentration varies according to the environmental oxygen concentration and the plasma excitation frequency. In which higher oxygen concentration and excitation frequency results in higher O_3 concentration **(Fang, et al., 2008)**. As previously reported by **(Kumar, et al., 2023)**, the generation of ozone during cold plasma treatment might cause a decrease in phenolic content due to the hydroxylation of the benzene ring to form dihydric phenol which then undergoes ring cleavage forming intermediate by-products including glyoxal, glyoxalic acid, and oxalic acid (Figure 38). Phenolic compounds in fruit may also react with reactive oxygen species present in cold plasma and produced during ozonation and increase the transfer of antioxidant metabolites from the placenta to the pericarp, this will prevent damage of macromolecules as DNA, lipids and proteins, and in turn results in decreased phenol concentrations **(Kaur, et al., 2022)**.

On the contrary, other studies reported that ozone exposure may cause cell wall modification delignified the guard and subsidiary cell walls, eventually enhancing the non-lignin phenolic compounds and consequently enhancing flavonoid and phenolic compounds **(Alothman, et al., 2010)**. According to **Maier-Maercker, et al. (1992)**, plasma non-ionic

species (ozone and UV- rays) can penetrate deep into the mesocarp activating the fruits' defensive mechanism triggering several metabolic reactions producing phenolic compounds **(Fernandes, et al., 2021)**.

As shown in table 14, total phenolic compounds analysed by LC-MS/MS, were statistically not changed in short treatment times (5 minutes) for both low and high ozone concentrations. However longer treatment times at higher ozone concentrations induced significant reduction in the total content of detected phenolic compounds where a 57.7 % reduction was observed in samples treated for 30 minutes at high ozone concentration (800ppm).

Phenolic acids were well preserved in samples treated for short times regardless of the ozone concentration (Figure 35). However, a gradual reduction in the contents of each phenolic acid and consequently the total phenolic acids content was observed with samples treated for longer times. Regarding flavonoids, six compounds were detected and quantified in all melon samples. Significant reduction in the concentration of the major flavonone (hesperidin) was also observed in presence of high ozone concentration for all treatment times. Non-significant changes were observed in hesperidin contents at lower ozone concentration which could be explained by the sensitivity of hesperidin to higher ozone concentrations. Quercetin -3-O- glucoside showed a similar trend where a significant reduction was observed only in presence of higher ozone concentration at long treatment times. On the other hand, a significant increase in the rutin (quercetin3-O-rutionside) concentration was observed at higher ozone concentration but only in samples treated for a short time (5 minutes). Which goes in a good accordance with **X. Zhu, et al. (2019)**, who reported a significant increase of rutin in mandarin samples after ozone treatment. Other flavonoids, quercetin and kaempferol glucoside did not show any significant changes after treatment when compared to the control samples.

As shown in figure 37, In the phenylpropanoid biosynthetic pathway, enzymes such as phenylalanine ammonia-lyase (PAL) play an important role in the production of phenolic compounds including phenolic acids, flavonoids and flavonoid glycosides. The concomitant stimulation of these enzymes induced by the increased oxidative stress triggered by ozone results in increased phenolic compound production. This could explain the significant increase in gallic acid, caffeic acid and quercetin3-O-rutionside that was observed only in samples treated for short time (5 min).

High dose or longer exposure to ozone, on the other hand, may cause a significant drop in the phenolic content due to various reactions between fruit and ozone **(Kaur, et al., 2022)**.

Like what was observed in the phenolic acids (gallic, chlorogenic, neochlorogenic, *p*-coumaric, 3-hydroxybenzoic & 4-hydroxy benzoic acids) and the flavonoid glycoside Quercetin -3-O- glucoside.

(Liao, et al., 2018) reported a reduction in phenolic content of apple juice and explained this by the destruction of the aromatic ring in the compounds which are most vulnerable to ozone assault. The reduction in the anthocyanin in blueberries post plasma treatment was previously attributed to the oxidative cleavage of chromophores due to hydroxyl radicals and ozone **(Lacombe, et al., 2015)**. Further increase in treatment time to 6 min decreased the concentration of anthocyanin and antioxidant activity in blueberries juice by 37.49% and 19.15%, respectively, due to hydroxyl radicals, reactive atomic oxygen, metastable oxygen molecules, and ozone **(Hou, et al., 2019)**.

Table 14: Phenolic compounds determined by HPLC-MS/MS in control and and DBD treated melon samples, processed at different times in presence of two different ozone concentrations. Expressed as (mg.100g^{-1} DW).

		Plasma treatment conditions								
		Ozone.800 PPM					**Ozone.300 PPM**			
	class	**5 min.**	**10 min.**	**20 min.**	**30 min.**	**Control**	**5 min.**	**10 min.**	**20 min.**	**30 min.**
1. **Quercetin**		0.06 ± 0.01^{a}	0.06 ± 0.01^{a}	0.06 ± 0.01^{a}	0.06 ± 0.01^{a}	**0.06 ± 0.01^{a}**	0.06 ± 0.01^{a}	0.06 ± 0.01^{a}	0.06 ± 0.01^{a}	0.06 ± 0.01^{a}
2. **Quercetin-3-O-rutinoside**		0.29 ± 0.01^{a}	0.06 ± 0.01^{bc}	0.06 ± 0.01^{bc}	0.07 ± 0.01^{bc}	**0.13 ± 0.03^{b}**	0.10 ± 0.01^{bc}	0.07 ± 0.01^{bc}	0.08 ± 0.02^{bc}	0.06 ± 0.02^{c}
3. **Quercetin 3-glucoside**	**Flavonoids**	0.12 ± 0.01^{a}	0.04 ± 0.01^{bc}	0.03 ± 0.01^{bc}	0.02 ± 0.01^{c}	**0.11 ± 0.03^{a}**	0.05 ± 0.01^{abc}	0.08 ± 0.01^{ab}	0.07 ± 0.01^{ab}	0.05 ± 0.01^{abc}
4. **Kaempferol-3-glucoside**		0.19 ± 0.01^{b}	0.29 ± 0.01^{ab}	0.26 ± 0.05^{ab}	0.24 ± 0.02^{ab}	**0.28 ± 0.06^{ab}**	0.32 ± 0.01^{a}	0.27 ± 0.01^{ab}	0.27 ± 0.06^{ab}	0.21 ±0.02^{ab}
5. **Hesperidin**		0.76 ± 0.13^{b}	0.81 ± 0.16^{b}	0.76 ± 0.08^{b}	0.80 ± 0.03^{b}	**1.57 ± 0.08^{a}**	1.43 ± 0.03^{a}	1.48 ± 0.10^{a}	1.54 ± 0.08^{a}	1.26 ± 0.10^{a}
6. **Catechin**		0.16 ± 0.04^{a}	0.12 ± 0.02^{ab}	0.13 ± 0.04^{ab}	0.07 ±0.02^{b}	**0.08 ± 0.00^{ab}**	0.09 ± 0.02^{ab}	0.09 ± 0.02^{ab}	0.12 ± 0.02^{ab}	0.07 ± 0.02^{b}
7. **Gallic acid**		0.17 ± 0.05^{a}	0.05 ± 0.01^{b}	0.05 ± 0.01^{b}	0.03 ± 0.01^{b}	**0.05 ± 0.01^{b}**	0.07 ±0.02^{b}	0.06 ± 0.01^{b}	0.06 ± 0.01^{b}	0.05 ± 0.01^{b}
8. **Neochlorogenic acid**		0.53 ± 0.00^{abc}	0.59 ± 0.09^{a}	0.39 ± 0.03^{bcd}	0.26 ± 0.03^{d}	**0.58 ± 0.04^{ab}**	0.51 ± 0.07^{abc}	0.38 ± 0.02^{cd}	0.44 ± 0.08^{abcd}	0.43 ± 0.01^{abcd}
9. **Chlorogenic acid**		0.10 ± 0.02^{bc}	0.11 ± 0.01^{abc}	0.12 ± 0.01^{ab}	0.03 ± 0.00^{c}	**0.15 ± 0.03^{ab}**	0.20 ± 0.04^{a}	0.11 ± 0.03^{abc}	0.08 ± 0.01^{bc}	0.03 ± 0.00^{c}
10. **4-Hydroxy benzoic acid**		1.26 ± 0.33^{a}	0.74 ± 0.01^{ab}	0.50 ± 0.10^{b}	0.37 ± 0.08^{b}	**0.90 ± 0.10^{a}**	0.64 ± 0.17^{b}	0.64 ± 0.16^{b}	0.49 ± 0.06 ^{b}	0.43 ± 0.07^{b}
11. **3-Hydroxy benzoic acid**		0.26 ± 0.02^{ab}	0.23 ± 0.02^{abc}	0.21 ± 0.06^{bc}	0.16 ± 0.04^{bc}	**0.18 ± 0.02^{bc}**	0.36 ± 0.04^{a}	0.27 ± 0.04^{ab}	0.21 ± 0.02^{bc}	0.11 ± 0.04^{c}
12. **Caffeic acid**	**Phenolic acids**	0.20 ± 0.06^{a}	0.22 ± 0.04^{a}	0.16 ± 0.03^{a}	0.09 ± 0.00^{a}	**0.19 ± 0.06^{a}**	0.13 ± 0.01^{a}	0.17 ± 0.02^{a}	0.09 ± 0.00^{a}	0.13 ± 0.01^{a}
13. ***P*-Coumaric acid**		0.93 ± 0.18^{a}	0.98 ± 0.02^{a}	0.72 ± 0.06^{ab}	0.45 ± 0.02^{b}	**0.85 ± 0.03^{a}**	0.78 ± 0.03^{a}	0.74 ± 0.12^{ab}	0.84 ±0.04^{a}	0.94 ± 0.02^{a}
14. **3,5-Dicaffeoylquinic acid**		0.02 ± 0.01^{a}	0.02 ± 0.01^{a}	0.03 ± 0.01^{a}	0.02 ± 0.01^{a}	**0.04 ± 0.01^{a}**	0.04 ± 0.01^{a}	0.04 ± 0.01^{a}	0.04 ± 0.01^{a}	0.02 ± 0.01^{a}
Total phenolics		5.04 ± 0.03^{ab}	4.33 ± 0.15^{cd}	3.49 ± 0.16^{e}	2.68 ± 0.06^{f}	**5.18 ± 0.01^{a}**	4.78 ± 0.21^{abc}	4.47 ± 0.16^{bcd}	4.38 ± 0.36^{bcd}	3.84 ± 0.06^{de}
***Trans*-cinnamic acid**		5.40 ± 0.02^{cde}	4.07 ± 0.10^{ef}	3.26 ± 0.14^{f}	2.74 ± 0.37^{f}	**6.51 ±0.56^{abc}**	7.14 ± 0.03^{ab}	5.85 ± 0.60^{bcd}	4.94 ± 0.13^{cde}	7.31^{a}± 0.03^{a}

All the data are expressed as mean ± standard deviations. Means that do not share letters in each row differ significantly ($p < 0.05$) according to Tukey's test.

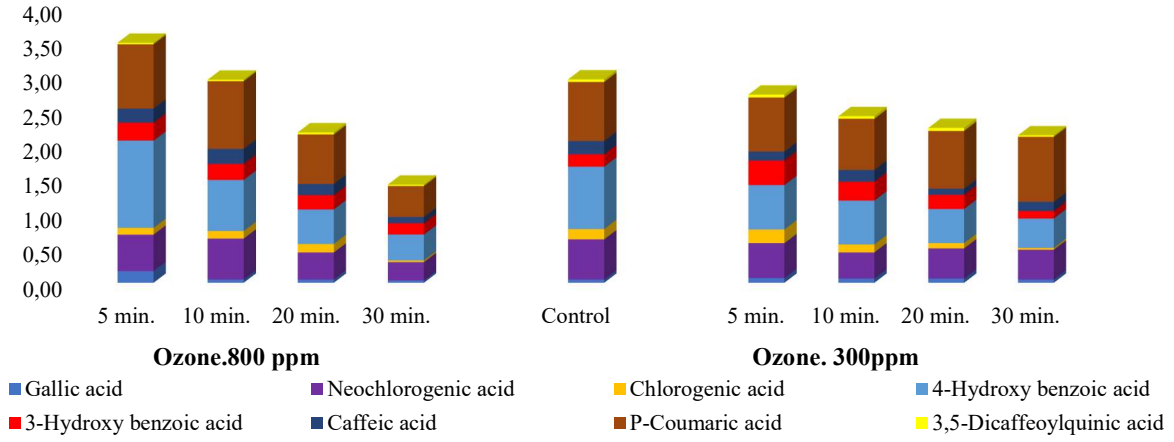

Figure 35: Phenolic acids determined by HPLC-MS/MS in control and and DBD treated melon samples, processed at different times in presence of two different ozone concentrations. Expressed as (mg.100g^{-1} DW).

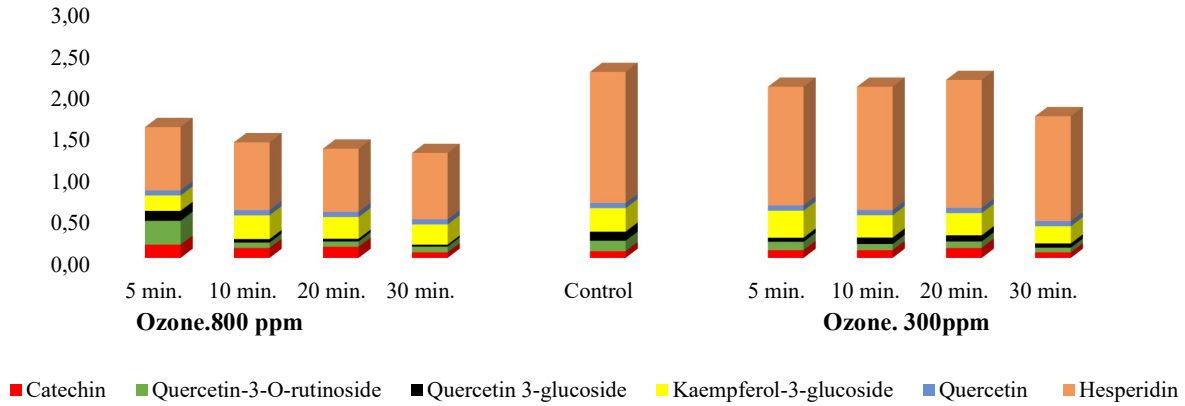

Figure 36: Flavonoids determined by HPLC-MS/MS in control and and DBD treated melon samples, processed at different times in presence of two different ozone concentrations. Expressed as (mg.100g^{-1} DW).

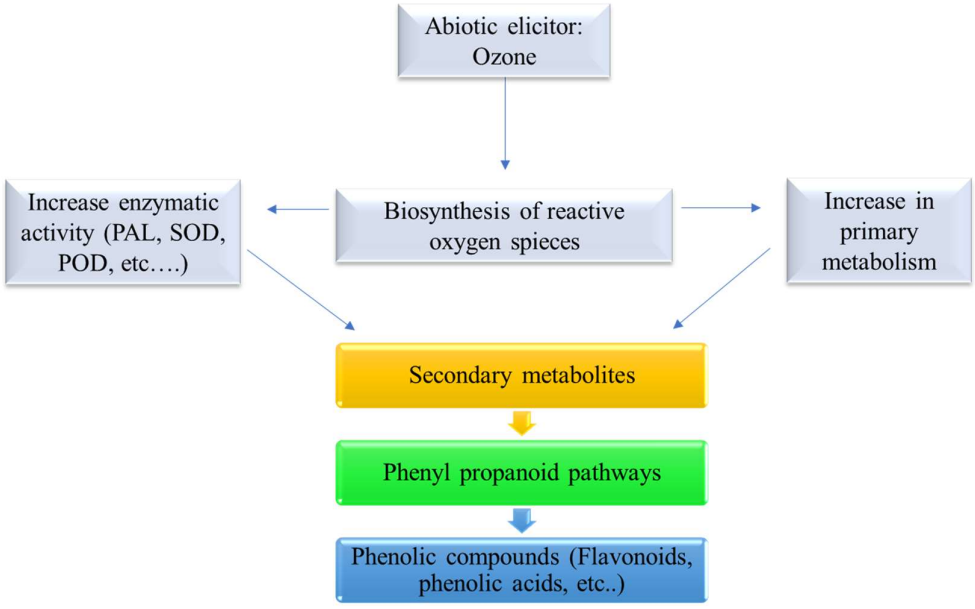

Figure 37: Major pathways for biosynthesis of phenolic compounds during ozonation.

Figure 38: Reaction of various plasma-generated ozone with phenol **(Kumar, et al., 2023)** Structure and degradation of polyphenols

Cinnamic acid ($C_9H_8O_2$) is an organic acid play key roles in the formation of other more complex phenolic compounds. Chlorogenic acid (5-caffeoylquinicacid) is perhaps the most important cinnamic acid derivative observed in fruits. Other cinnamic acid derivatives including: neochlorogenic, *P*-coumaric, caffeic, ferulic, etc…… **(Kuchi, et al., 2018)**. As shown in figure 39, the contents of *trans*-cinnamic acid decreased significantly in presence of higher ozone concentrations (Ozone.800 ppm) except for samples treated for short time (5 min). As shown in figure 40, a degradation mechanism involves the reaction of ozone with cinnamic acid forming glyoxylic acid, H_2O_2 and the corresponding benzaldehydes was previously proposed by **(Leitzke, et al., 2001)**.

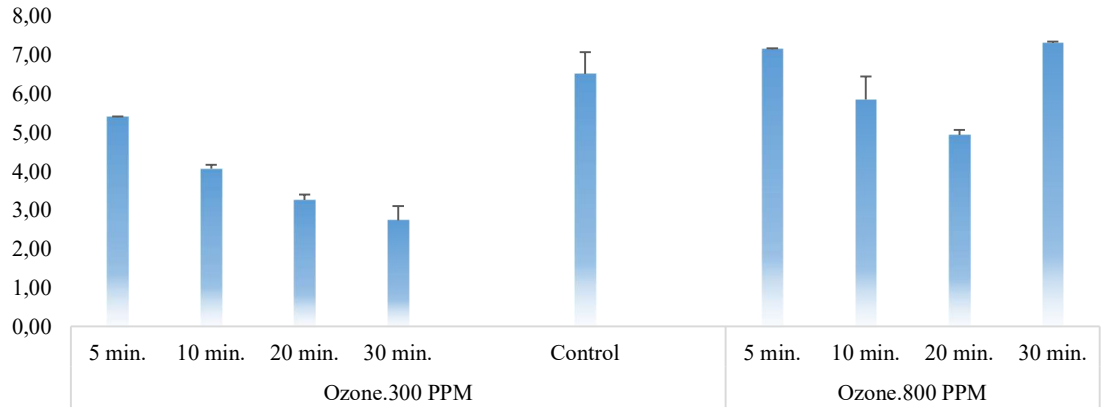

Figure 39: Cinnamic acid determined by HPLC-MS/MS in control and and DBD treated melon samples, processed at different times in presence of two different ozone concentrations. Expressed as (mg.100g^{-1} DW).

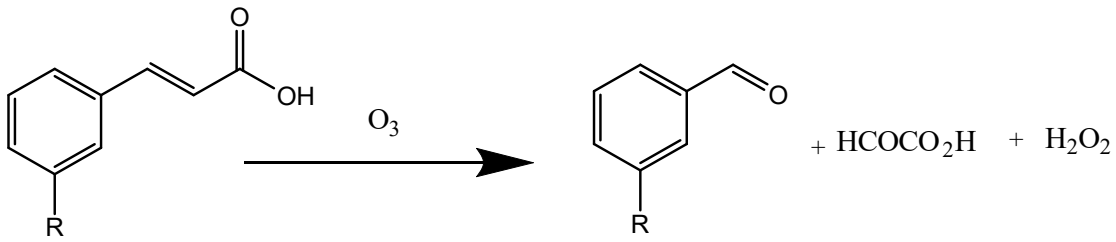

Figure 40: Proposed degradation of cinnamic acid by high ozone concentrations during cold plasma treatment of melon.

3.3.2. Influence of DBD plasma treatment on TPC and DPPH of cut-melon fruit.

Table 15 shows the time and ozone concentration dependent changes in the total phenolic content (TPC) and antioxidant activity (AOA) in melon samples post plasma treatment. According to the obtained results, all CP- treated samples showed non-significant differences in both TPC and AOA ($p > 0.05$) compared to the control samples. Non-significant elevation in both contents was observed for samples treated for shorter times (5 &10 min).

Those results confirm the results obtain by LC-MS/MS analysis and confirmed the safety of short time cold plasma treatment on the phenolic profile of cut-melon fruit. To our knowledge the effect of plasma treatment on the individual and the total phenolic contents of melon hasn't been reported so far.

Table 15: TPC and DPPH in control and and DBD treated melon samples, processed at different times in presence of two different ozone concentrations. Expressed as ($mg.100g^{-1}$ DW).

		Total phenolics mg gallic acid equivalent /kg	**AOA mg trolox equivalent (TE)/g**
Ozone 800 ppm	5 min.	8.45 ± 0.3^{a}	10.00 ± 0.3^{a}
	10 min.	8.37 ± 0.9^{a}	9.91 ± 0.3^{ab}
	20 min.	7.79 ± 0.7^{a}	7.20 ± 0.1^{c}
	30 min.	8.22 ± 0.6^{a}	7.13 ± 0.2^{c}
	Control	7.97 ± 0.3^{a}	8.51 ± 0.6^{abc}
Ozone.300 ppm	5 min.	7.79 ± 0.6^{a}	7.52 ± 0.3^{c}
	10 min.	7.66 ± 0.3^{a}	9.94 ± 0.7^{a}
	20 min.	7.35 ± 0.8^{a}	8.19 ± 0.9^{bc}
	30 min.	7.72 ± 0.2^{a}	8.56 ± 0.7^{abc}

All the data are expressed as mean ± standard deviations. Means that do not share letters in each column differ significantly ($p < 0.05$) according to Tukey's test.

3.3.3. Influence of DBD plasma treatment on L-ascorbic acid content of cut-melon fruit.

The nutritional quality of melon fruit has been associated with the high concentration of ascorbic acid **(Maietti, et al., 2012)**. Cutting, trimming, and peeling may have an impact on the vitamin content of fruits and vegetables. Cutting enhances the production of ethylene, which sequentially accelerates respiration and senescence with the loss of certain vitamins at a faster rate. Among all vitamins, *L*-ascorbic acid is more prone and more sensitive to the various processing procedures **(Asghar, et al., 2022)**.

Zhou, et al. (2022) reported non-significant difference in control and CP treated cut-melon at 40 kV for 90 s and showed that CP treatment significantly inhibited the decrease of ascorbic acids during melon storage. In the present study ascorbic acid content in control cut-melon samples was 704.49 mg.100g^{-1} DW, which is consistent with previous studies **(Mallek-Ayadi, et al., 2022)**. Surprisingly, ascorbic acid concentration increased in all treatment after cold plasma treatment of melon and the increase was statistically significant in presence of high ozone concentrations (Figure 41). Previously, degradation of ascorbic acid post plasma treatment was attributed to the reaction with ozone and other oxidizing plasma species during the processing **(Bagheri, et al., 2020)**. Opposite studies reported that, gaseous ozone is an abiotic elicitor of defence responses in plant materials and fruit exhibiting properties of living organisms. As a result, in presence of ozone a number of biochemical processes could take place in the raw materials, leading to the formation of many primary and secondary metabolites, mainly polyphenols and vitamins as shown in figure 37 **(Piechowiak, et al., 2019)**. For example **(Matłok, et al., 2022)**, reported significant increase in *L*-ascorbic acid content of saskatoon berries exposed to ozone at a rate of 10 ppm for 15 min. which was explained and linked to the response of the fruit, which still exhibits the characteristics of living organisms by generating increased amounts of small-molecule antioxidants that may potentially mitigate the harmful effects of a powerful oxidant such as ozone.

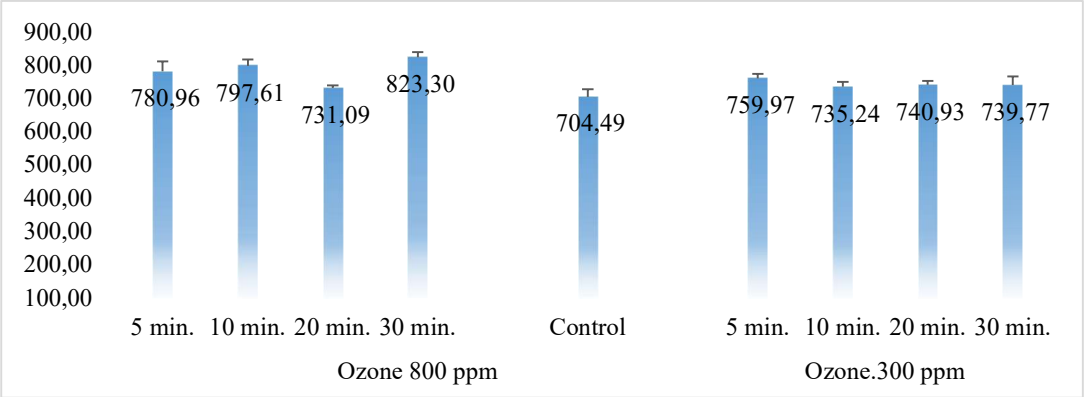

Figure 41: *L*-ascorbic acid determined by HPLC-DAD in control and DBD treated melon samples, processed at different times in presence of two different ozone concentrations. Expressed as (mg.100g^{-1} DW).

3.3.4. Influence of DBD plasma treatment on vitamins B (riboflavin, nicotinamide, and nicotinic acid) contents of cut-melon fruit.

In this study, the contents of different forms of vitamin B were evaluated using UHPLC-ESI–MS/MS system. The contents of the untreated (control) and the CP treated melon at different times and in presence of different ozone concentrations are shown in figure 42 and table 16. Compared to the control sample (0.031 ± 0.003 mg.$100g^{-1}$), CP treated samples at both ozone concentrations and at all times exhibited non-significant increases of riboflavin (B2) content. On the contrary, significant reductions were observed in the contents of both forms of vitamin B3 after plasma treatment. Except for samples treated for short time (5 min.) in presence of ozone.800 ppm which showed non-significant changes in both nicotinic acid and nicotinamide contents (Table 16).

The term niacin (vitamin B3) comprises the two main water-soluble forms nicotinic acid and nicotinamide (niacinamide). In the body, niacin primarily functions as a component of the coenzymes NAD (nicotinamide adenine dinucleotide) and NADP (nicotinamide adenine dinucleotide phosphate) which are present in all cells. These coenzymes play essential roles for the functioning of a wide range of enzymes involved in the metabolism of carbohydrates, amino acids and fat. In addition to its function in coenzymes, niacin is involved in DNA repair and gene stability. Intake of nicotinic acid and nicotinamide from regular foods should be considered to avoid the side effects of high supplemental intake, in which the current maximum limit for niacin added shouldn't exceed 32 mg/day **(Finglas, 2000)**.

However most studies reported the stability of vitamin B3 to the different processing techniques, niacin degradation was previously reported after drying and milling of fruits and vegetables **(Reddy, et al., 1999)**. The effect of plasma treatment on vitamin B is still lacking in available literature, more studies are required to study the impact of different processing methods on the contents of B vitamins and to understand the mechanism of degradation &/or retention.

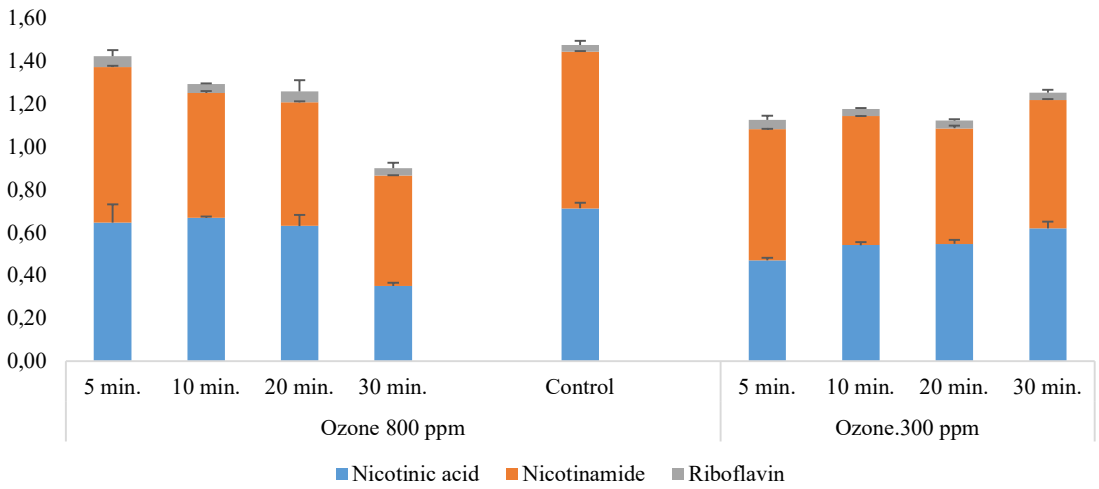

Figure 42: Content of riboflavin, nicotinic acid and nicotinamide in control and DBD treated melon samples, processed at different times in presence of two different ozone concentrations. Expressed as (mg.100g^{-1} DW).

Table 16: Content of vitamin C, riboflavin, nicotinic acid and nicotinamide in control and DBD treated melon samples, processed at different times in presence of two different ozone concentrations. Expressed as (mg.100g^{-1} DW).

Treatment time (min)	Gas type	Nicotinic acid (Vit.B3)	Nicotinamide (Vit.B3)	Riboflavin (Vit.B2)	Total Vitamin B content	Vitamin C
5	**Ozone 800ppm**	0.646 ± 0.086^{ab}	0.727 ± 0.028^{a}	0.051 ± 0.006^{a}	1.42 ± 0.11^{ab}	780.96 ± 29.98^{ab}
10		0.670 ± 0.005^{ab}	0.582 ±0.003^{bc}	0.041 ± 0.008^{a}	1.29 ± 0.02^{bc}	797.61 ± 19.21^{ab}
20		0.631 ± 0.052^{ab}	0.578 ±0.053^{bc}	0.050 ± 0.004^{a}	1.26 ± 0.01^{bc}	731.09 ± 7.22^{ab}
30		0.350 ± 0.015^{d}	0.515 ±0.026^{c}	0.035 ± 0.003^{a}	0.90 ± 0.01^{d}	823.30 ± 15.64^{a}
Control	–	0.713 ± 0.026^{a}	0.731 ± 0.020^{a}	0.031 ± 0.003^{a}	1.48 ± 0.05^{a}	704.49 ± 22.58^{b}
5	**Ozone 300 ppm**	0.470 ± 0.011^{cd}	0.614 ± 0.019^{b}	0.042 ± 0.001^{a}	1.13 ± 0.01^{c}	759.97 ± 13.75^{b}
10		0.541 ± 0.015^{bc}	0.603 ± 0.003^{bc}	0.034 ± 0.001^{a}	1.18 ± 0.01^{c}	735.24 ± 14.07^{b}
20		0.548 ± 0.018^{bc}	0.539 ± 0.006^{bc}	0.034 ± 0.001^{a}	1.12 ± 0.04^{c}	740.93 ± 11.10^{b}
30		0.620 ± 0.030^{b}	0.599 ± 0.014^{bc}	0.036 ± 0.012^{a}	1.25 ± 0.05^{bc}	739.77 ± 25.61^{b}

All the data are expressed as mean ± standard deviations. Means that do not share letters in each column differ significantly ($p < 0.05$) according to Tukey's test.

4 Conclusion

4. Conclusion

Cold plasma (CP) is at a nascent stage but is gaining interest among researchers because of its non-thermal nature. It destroys microorganisms, preserve food, and maintain quality without employing chemical antimicrobial agents. CP has a positive impact on the bioactive components of food as compared to conventional thermal treatment. The low treatment temperature and short treatment time helped maintain the chemical composition, sensory and physicochemical characteristics of the food product. Moreover, CP is chemical-free so it can be used safely for the processing of organic produce. In brief, considering the results of our research, it seems that the type and variety of the plant and the condition of the CP treatment are of the most important and effective parameters in the content of phenolic compounds and vitamins in the treated sample as shown in figure 43.

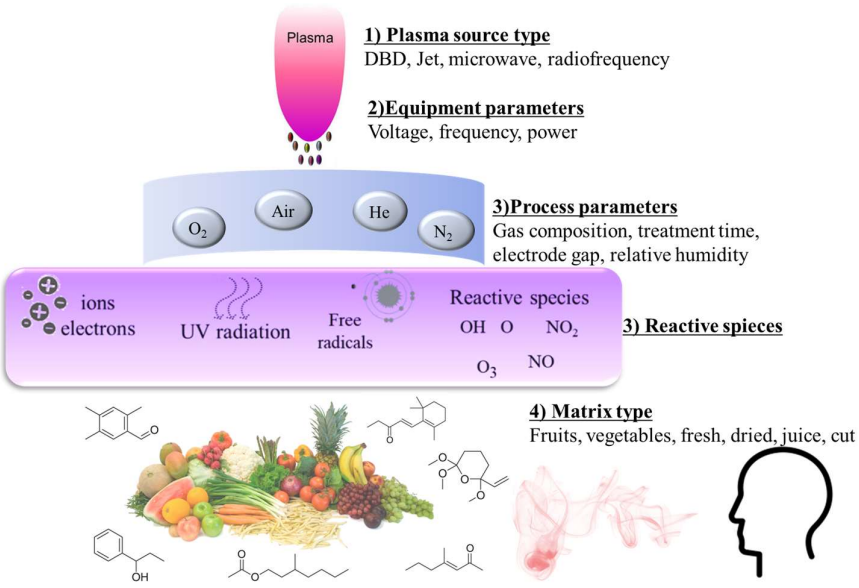

Figure 43: Major parameters responsible for changes of bioactive compounds after cold plasma treatment

The impact of Plasma activated water (PAW) technique on the phytochemical profile, nutritional properties and antioxidant activity of rocket-salad leaves showed that PAW treatment at longer treatment times allowed a good preservation of the investigated vitamins (ascorbic acid, riboflavin, nicotinic acid and nicotinamide) and of polyphenolic compounds. Moreover, the DPPH reducing activity of the treated samples showed the same trend of the content of bioactive compounds, showing a significant increase in the longest treatment. 52 volatile organic compounds of different chemical classes were identified in rocket samples. Glucosinolate hydrolysis products are the major chemical class. PAW application induced

some chemical modifications in the volatile compounds. Changes in the content of the major compounds varied with the increase or decrease in the treatment time. However, PAW-10 and -2 were grouped closely to the control. A significant decrease in the content of β-sitosterol and campesterol was observed after PAW treatment, except for PAW-10, which showed a non-significant reduction in both compounds. A significant increase in β- carotene and luteolin was observed after the shortest treatment time PAW-2.

Then the effect of dielectric barrier discharge (DBD) cold plasma treatment on quality of whole strawberries was studied immediately after processing and during storage at 4 °C. Results showed preservation of total phenolic profile and significant increase in the total phenolic acids (614.2 to 784.4 $mg.kg^{-1}$) and total flavonols (145.2 to 196.4 $mg.kg^{-1}$) contents immediately after DBD treatment. DBD also induced a significant increase in quercetin-3-o-rutinoside, -3-o-glucoside and 3-o-galactoside, in addition to, kaempferol-3-glucoside. Untargeted primary metabolomics using GC-MS analysis showed no discernible differences between the primary metabolite profiles of control and treated strawberries immediately post treatment. However, a trend of separation was reported based only on the consideration of the storage period. Although, ascorbic acid decreased immediately after processing, higher stability during storage was observed. During storage TPC seems to be non-significantly changed, however the DPPH activity was significantly increased by time in the processed samples. These results all together indicated the safety of DBD treatment in preservation of whole strawberries and confirmed the stability of the major bioactive and sensitive compounds or even the increase of some antioxidant phenolic compounds in the processed samples.

Moreover, the impact of ozone concentration and plasma treatment time on quality of DBD treated fresh-cut-melon samples was studied. Total of 14 phenolic compounds were identified and quantified. Total phenolic concentrations analysed by LC-MS/MS, were statistically not changed in short treatment times (5 minutes) for both low and high ozone concentrations. Ascorbic acid concentration increased in all treatment after cold plasma treatment of melon and the increase was statistically significant in presence of high ozone concentrations. Moreover, CP treated samples at both ozone concentrations and at all times exhibited non-significant increases of riboflavin (B2) content. On the contrary, significant reductions were observed in the contents of both forms of vitamin B3 after plasma treatment. Except for samples treated for short time (5 min.) in presence of ozone.800 ppm which showed non-significant changes in both nicotinic acid and nicotinamide contents

Approval of plasma processes for direct and indirect food applications requires considerable data collection, data analysis, and time. An inclusive and in-depth understanding of the influence of plasma-induced reactive species on functional characteristics of food is still in its nascent form, thus necessitating further research in the discipline. Future studies still required to better understand the interactions between the plasma species and various food compounds.

Bibliography

Abouelenein, D., Angeloni, S., Caprioli, G., Genovese, J., Mustafa, A. M., Nzekoue, F. K., Petrelli, R., Rocculi, P., Sagratini, G., & Tappi, S. (2021). Effect of plasma activated water on selected chemical compounds of rocket-salad (*Eruca sativa* Mill.) leaves. *Molecules, 26*(24), 7691.

Abouelenein, D., Caprioli, G., & Mustafa, A. M. (2023). Exploring the impacts of novel cold plasma technology on the volatile profile, flavor, and aroma properties of fruits and vegetables—A review. *Food Safety and Health*.

Abouelenein, D., Mustafa, A. M., Nzekoue, F. K., Caprioli, G., Angeloni, S., Tappi, S., Castagnini, J. M., Dalla Rosa, M., & Vittori, S. (2023). The impact of plasma activated water treatment on the phenolic profile, vitamins content, antioxidant and enzymatic activities of rocket-salad leaves. *Antioxidants, 12*(1), 28.

Adekunte, A., Tiwari, B., Scannell, A., Cullen, P., & O'donnell, C. (2010). Modelling of yeast inactivation in sonicated tomato juice. *International Journal of Food Microbiology, 137*(1), 116-120.

Adhikari, B., Adhikari, M., Ghimire, B., Park, G., & Choi, E. H. (2019). Cold atmospheric plasma-activated water irrigation induces defense hormone and gene expression in tomato seedlings. *Scientific Reports, 9*(1), 1-15.

Agagunduz, D., & Karabudak, E. (2017). Effects of food disinfectants on vitamin C content of rockets: Chlorine, calcium oxide and acetic acid. *CARPATHIAN JOURNAL OF FOOD SCIENCE AND TECHNOLOGY, 9*(2), 77-92.

Ahmadnia, M., Sadeghi, M., Abbaszadeh, R., & Ghomi Marzdashti, H. R. (2021). Decontamination of whole strawberry via dielectric barrier discharge cold plasma and effects on quality attributes. *Journal of Food Processing and Preservation, 45*(1), e15019.

Almeida, F. D. L., Cavalcante, R. S., Cullen, P. J., Frias, J. M., Bourke, P., Fernandes, F. A., & Rodrigues, S. (2015). Effects of atmospheric cold plasma and ozone on prebiotic orange juice. *Innovative Food Science & Emerging Technologies, 32*, 127-135.

Alnaizy, R., & Akgerman, A. (2000). Advanced oxidation of phenolic compounds. *Advances in Environmental Research, 4*(3), 233-244.

Alothman, M., Kaur, B., Fazilah, A., Bhat, R., & Karim, A. A. (2010). Ozone-induced changes of antioxidant capacity of fresh-cut tropical fruits. *Innovative Food Science & Emerging Technologies, 11*(4), 666-671.

Amaro, A. L., Oliveira, A., & Almeida, D. P. (2015). Biologically active compounds in melon: Modulation by preharvest, post-harvest, and processing factors. In *Processing and Impact on Active Components in Food*, (pp. 165-171): Elsevier.

Amini, M., & Ghoranneviss, M. (2016). Effects of cold plasma treatment on antioxidants activity, phenolic contents and shelf life of fresh and dried walnut (Juglans regia L.) cultivars during storage. *Lwt, 73*, 178-184.

Asghar, A., Rashid, M. H., Ahmed, W., Roobab, U., Inam-ur-Raheem, M., Shahid, A., Kafeel, S., Akram, M. S., Anwar, R., & Aadil, R. M. (2022). An in-depth review of novel cold plasma technology for fresh-cut produce. *Journal of Food Processing and Preservation, 46*(7), e16560.

Avato, P., & Argentieri, M. (2015). Brassicaceae: a rich source of health improving phytochemicals. *Phytochemistry Reviews, 14*(6), 1019-1033.

Azarenko, O., Jordan, M. A., & Wilson, L. (2014). Erucin, the major isothiocyanate in arugula (*Eruca sativa*), inhibits proliferation of MCF7 tumor cells by suppressing microtubule dynamics. *PloS One, 9*(6), e100599.

Bagheri, H., & Abbaszadeh, S. (2020). Effect of cold plasma on quality retention of fresh-cut Produce. *Journal of Food Quality, 2020*, 1-8.

Bahrami, N., Bayliss, D., Chope, G., Penson, S., Perehinec, T., & Fisk, I. D. (2016). Cold plasma: A new technology to modify wheat flour functionality. *Food Chemistry, 202*, 247-253.

Bao, Y., Reddivari, L., & Huang, J.-Y. (2020). Enhancement of phenolic compounds extraction from grape pomace by high voltage atmospheric cold plasma. *LWT, 133*, 109970.

Barba, F. J., Esteve, M. J., & Frígola, A. (2012). High pressure treatment effect on physicochemical and nutritional properties of fluid foods during storage: a review. *Comprehensive Reviews in Food Science and Food Safety, 11*(3), 307-322.

Bell, L., Kitsopanou, E., Oloyede, O. O., & Lignou, S. (2021). Important odorants of four brassicaceae species, and discrepancies between glucosinolate profiles and observed hydrolysis products. *Foods, 10*(5), 1055.

Bell, L., Methven, L., Signore, A., Oruna-Concha, M. J., & Wagstaff, C. (2017). Analysis of seven salad rocket (*Eruca sativa*) accessions: The relationships between sensory attributes and volatile and non-volatile compounds. *Food Chemistry, 218*, 181-191.

Bell, L., Spadafora, N. D., Müller, C. T., Wagstaff, C., & Rogers, H. J. (2016). Use of TD-GC–TOF-MS to assess volatile composition during post-harvest storage in seven accessions of rocket salad (*Eruca sativa*). *Food Chemistry, 194*, 626-636.

Bell, L., & Wagstaff, C. (2014). Glucosinolates, myrosinase hydrolysis products, and flavonols found in rocket (*Eruca sativa* and *Diplotaxis tenuifolia*). *Journal of Agricultural and Food Chemistry, 62*(20), 4481-4492.

Bell, L., & Wagstaff, C. (2019). Rocket science: A review of phytochemical & health-related research in *Eruca* & *Diplotaxis* species. *Food Chemistry: X, 1*, 100002.

Bell, L., Yahya, H. N., Oloyede, O. O., Methven, L., & Wagstaff, C. (2017). Changes in rocket salad phytochemicals within the commercial supply chain: Glucosinolates, isothiocyanates, amino acids and bacterial load increase significantly after processing. *Food Chemistry, 221*, 521-534.

Benedetti, A., Comporti, M., Fulceri, R., & Esterbauer, H. (1984). Cytotoxic aldehydes originating from the peroxidation of liver microsomal lipids: identification of 4, 5-dihydroxydecenal. *Biochimica et Biophysica Acta (BBA)-Lipids and Lipid Metabolism, 792*(2), 172-181.

Birania, S., Attkan, A. K., Kumar, S., Kumar, N., & Singh, V. K. (2022). Cold plasma in food processing and preservation: A review. *Journal of Food Process Engineering, 45*(9), e14110.

Blažević, I., & Mastelić, J. (2008). Free and bound volatiles of rocket (*Eruca sativa* Mill.). *Flavour and Fragrance Journal, 23*(4), 278-285.

Bourke, P., Ziuzina, D., Boehm, D., Cullen, P. J., & Keener, K. (2018). The potential of cold plasma for safe and sustainable food production. *Trends in Biotechnology, 36*(6), 615-626.

Buckow, R., Ng, S., & Toepfl, S. (2013). Pulsed electric field processing of orange juice: a review on microbial, enzymatic, nutritional, and sensory quality and stability. *Comprehensive reviews in food science and food safety, 12*(5), 455-467.

Burnett, S., & Beuchat, L. (2000). Human pathogens associated with raw produce and unpasteurized juices, and difficulties in decontamination. *Journal of Industrial Microbiology and Biotechnology, 25*(6), 281-287.

Bußler, S. (2017). *Cold atmospheric pressure plasma treatment of food matrices.* Unpublished Doctoral Thesis, Technische Universität Berlin.

Bußler, S., Herppich, W. B., Neugart, S., Schreiner, M., Ehlbeck, J., Rohn, S., & Schlüter, O. (2015). Impact of cold atmospheric pressure plasma on physiology and flavonol glycoside profile of peas (*Pisum sativum* 'Salamanca'). *Food Research International, 76*, 132-141.

Campelo, P. H., Alves Filho, E. G., Silva, L. M., de Brito, E. S., Rodrigues, S., & Fernandes, F. A. (2020a). Modulation of aroma and flavor using dielectric barrier discharge plasma technology in a juice rich in terpenes and sesquiterpenes. *Lwt, 130*, 109644.

Campelo, P. H., Alves Filho, E. G., Silva, L. M., de Brito, E. S., Rodrigues, S., & Fernandes, F. A. (2020b). Modulation of aroma and flavor using glow discharge plasma technology. *Innovative Food Science & Emerging Technologies, 62*, 102363.

Capelli, F., Tappi, S., Gritti, T., de Aguiar Saldanha Pinheiro, A. C., Laurita, R., Tylewicz, U., Spataro, F., Braschi, G., Lanciotti, R., & Gómez Galindo, F. (2021). Decontamination of food packages from SARS-CoV-2 RNA with a cold plasma-assisted system. *Applied Sciences, 11*(9), 4177.

Caprioli, G., Fiorini, D., Maggi, F., Marangoni, M., Papa, F., Vittori, S., & Sagratini, G. (2014). Ascorbic acid content, fatty acid composition and nutritional value of the neglected vegetable Alexanders (*Smyrnium olusatrum* L., Apiaceae). *Journal of Food Composition and Analysis, 35*(1), 30-36.

Caprioli, G., Kamgang Nzekoue, F., Fiorini, D., Scocco, P., Trabalza-Marinucci, M., Acuti, G., Tardella, F. M., Sagratini, G., & Catorci, A. (2020). The effects of feeding supplementation on the nutritional quality of milk and cheese from sheep grazing on dry pasture. *International Journal of Food Sciences and Nutrition, 71*(1), 50-62.

Caprioli, G., Sagratini, G., Vittori, S., & Torregiani, E. (2018). Optimization of an extraction procedure for the simultaneous quantification of riboflavin, nicotinamide and nicotinic acid in anchovies (*Engraulis enrasicolus)* by high-performance liquid chromatography–tandem mass spectrometry. *Journal of Food Composition and Analysis, 66*, 23-29.

Castro, D. R. G., Mar, J. M., da Silva, L. S., da Silva, K. A., Sanches, E. A., de Araújo Bezerra, J., Rodrigues, S., Fernandes, F. A. N., & Campelo, P. H. (2020). Improvement of the bioavailability of Amazonian juices rich in bioactive compounds using glow plasma technique. *Food and Bioprocess Technology, 13*, 670-679.

Centers for Disease Control and Prevention (CDC). 2011. *Foodborne outbreak online database (FOOD)* [Online]. Available: https://www.cdc.gov/foodsafety/pdfs/foodborne-disease-outbreaks-annual-report-2011-508c.pdf.

Centers for Disease Control and Prevention (CDC). 2019. *Outbreak of Salmonella infections linked to pre-cut melons.* [Online]. Available: https://www.cdc.gov/salmonella/carrau-04-19/index.html.

Chen, C., Liu, C., Jiang, A., Guan, Q., Sun, X., Liu, S., Hao, K., & Hu, W. (2019). The effects of cold plasma-activated water treatment on the microbial growth and antioxidant properties of fresh-cut pears. *Food and Bioprocess Technology, 12*, 1842-1851.

Chen, H. H., Chang, H. C., Chen, Y. K., Hung, C. L., Lin, S. Y., & Chen, Y. S. (2016). An improved process for high nutrition of germinated brown rice production: Low-pressure plasma. *Food Chemistry, 191*, 120-127.

Chen, Y.-Q., Cheng, J.-H., & Sun, D.-W. (2020). Chemical, physical and physiological quality attributes of fruit and vegetables induced by cold plasma treatment:

Mechanisms and application advances. *Critical Reviews in Food Science and Nutrition, 60*(16), 2676-2690.

Chisari, M., Barbagallo, R. N., Spagna, G., & Artes, F. (2011). Improving the quality of fresh-cut melon through inactivation of degradative oxidase and pectinase enzymatic activities by UV-C treatment. *International Journal of Food Science & Technology, 46*(3), 463-468.

Chutia, H., Mahanta, C. L., Ojah, N., & Choudhury, A. J. (2020). Fuzzy logic approach for optimization of blended beverage of cold plasma treated TCW and orange juice. *Journal of Food Measurement and Characterization, 14*, 1926-1938.

Civello, P. M., Martínez, G. A., Chaves, A. R., & Añón, M. C. (1997). Heat treatments delay ripening and postharvest decay of strawberry fruit. *Journal of Agricultural and Food Chemistry, 45*(12), 4589-4594.

Cory, H., Passarelli, S., Szeto, J., Tamez, M., & Mattei, J. (2018). The role of polyphenols in human health and food systems: A mini-review. *Frontiers in nutrition, 5*, 87.

da Silva Marineli, R., Furlan, C. P. B., Marques, A. y. C., Bicas, J., Pastore, G. M., & Maróstica Jr, M. R. (2015). Phytosterols: Biological effects and mechanisms of hypocholesterolemic action. *Biotechnology of Bioactive Compounds: Sources and applications*, 565-581.

Dai, T., Chang, X., Hu, Z., Liang, L., Sun, M., Liu, P., & Liu, X. (2019). Untargeted metabolomics based on GC-MS and chemometrics: A new tool for the early diagnosis of strawberry anthracnose caused by Colletotrichum theobromicola. *Plant Disease, 103*(10), 2541-2547.

de Castro, D. R. G., Mar, J. M., da Silva, L. S., da Silva, K. A., Sanches, E. A., de Araújo Bezerra, J., Rodrigues, S., Fernandes, F. A., & Campelo, P. H. (2020). Dielectric barrier atmospheric cold plasma applied on camu-camu juice processing: Effect of the excitation frequency. *Food Research International, 131*, 109044.

Dharini, M., Jaspin, S., & Mahendran, R. (2022). Cold plasma reactive species: Generation, properties, and interaction with food biomolecules. *Food Chemistry*, 134746.

Di Mascio, P., Kaiser, S., & Sies, H. (1989). Lycopene as the most efficient biological carotenoid singlet oxygen quencher. *Archives of Biochemistry and Biophysics, 274*(2), 532-538.

Dionísio, A. P., Gomes, R. T., & Oetterer, M. (2009). Ionizing radiation effects on food vitamins: a review. *Brazilian Archives of Biology and Technology, 52*(5), 1267-1278.

Domonkos, M., Tichá, P., Trejbal, J., & Demo, P. (2021). Applications of cold atmospheric pressure plasma technology in medicine, agriculture and food industry. *Applied Sciences, 11*(11), 4809.

Dong, X. Y., & Yang, Y. L. (2019). A novel approach to enhance blueberry quality during storage using cold plasma at atmospheric air pressure. *Food and Bioprocess Technology, 12*(8), 1409-1421.

Dvorakova, M., Pumprova, K., Antonínová, Ž., Rezek, J., Haisel, D., Ekrt, L., Vanek, T., & Langhansova, L. (2021). Nutritional and antioxidant potential of fiddleheads from European ferns. *Foods, 10*(2), 460.

Ebadi, M. T., Abbasi, S., Harouni, A., & Sefidkon, F. (2019). Effect of cold plasma on essential oil content and composition of lemon verbena. *Food science & nutrition, 7*(4), 1166-1171.

Ekezie, F.-G. C., Sun, D.-W., & Cheng, J.-H. (2019). Altering the IgE binding capacity of king prawn (*Litopenaeus vannamei*) tropomyosin through conformational changes induced by cold argon-plasma jet. *Food Chemistry, 300*, 125143.

Fan, L., Liu, X., Ma, Y., & Xiang, Q. (2020). Effects of plasma-activated water treatment on seed germination and growth of mung bean sprouts. *Journal of Taibah University for Science, 14*(1), 823-830.

Fang, Z., Qiu, Y., Sun, Y., Wang, H., & Edmund, K. (2008). Experimental study on discharge characteristics and ozone generation of dielectric barrier discharge in a cylinder–cylinder reactor and a wire–cylinder reactor. *Journal of Electrostatics, 66*(7-8), 421-426.

Fernandes, F. A., & Rodrigues, S. (2021). Cold plasma processing on fruits and fruit juices: A review on the effects of plasma on nutritional quality. *Processes, 9*(12), 2098.

Fernandes, F. A., Santos, V. O., & Rodrigues, S. (2019). Effects of glow plasma technology on some bioactive compounds of acerola juice. *Food Research International, 115*, 16-22.

Fernández-Lara, R., Gordillo, B., Rodríguez-Pulido, F. J., González-Miret, M. L., del Villar-Martínez, A. A., Dávila-Ortiz, G., & Heredia, F. J. (2015). Assessment of the differences in the phenolic composition and color characteristics of new strawberry (*Fragaria x ananassa* Duch.) cultivars by HPLC–MS and imaging tristimulus colorimetry. *Food Research International, 76*, 645-653.

Finglas, P. M. (2000). Dietary reference intakes for thiamin, riboflavin, niacin, vitamin B6, folate, vitamin B12, pantothenic acid, biotin and choline. In).

Force, L. E., O'Hare, T. J., Wong, L. S., & Irving, D. E. (2007). Impact of cold storage on glucosinolate levels in seed-sprouts of broccoli, rocket, white radish and kohl-rabi. *Postharvest Biology and Technology, 44*(2), 175-178.

Galanakis, C. M. (2021). *Nutraceutical and functional food components: Effects of innovative processing techniques*: Academic Press.

Gamboa-Santos, J., Soria, A. C., Pérez-Mateos, M., Carrasco, J. A., Montilla, A., & Villamiel, M. (2013). Vitamin C content and sensorial properties of dehydrated carrots blanched conventionally or by ultrasound. *Food Chemistry, 136*(2), 782-788.

Garofulić, I. E., Jambrak, A. R., Milošević, S., Dragović-Uzelac, V., Zorić, Z., & Herceg, Z. (2015). The effect of gas phase plasma treatment on the anthocyanin and phenolic acid content of sour cherry Marasca (*Prunus cerasus* var. Marasca) juice. *LWT-Food Science and Technology, 62*(1), 894-900.

Garzoli, S., Cairone, F., Carradori, S., Mocan, A., Menghini, L., Paolicelli, P., Ak, G., Zengin, G., & Cesa, S. (2020). Effects of processing on polyphenolic and volatile composition and fruit quality of clery strawberries. *Antioxidants, 9*(7), 632.

Giannoglou, M., Xanthou, Z.-M., Chanioti, S., Stergiou, P., Christopoulos, M., Dimitrakellis, P., Efthimiadou, A., Gogolides, E., & Katsaros, G. (2021). Effect of cold atmospheric plasma and pulsed electromagnetic fields on strawberry quality and shelf-life. *Innovative Food Science & Emerging Technologies, 68*, 102631.

Gil, M. I., Holcroft, D. M., & Kader, A. A. (1997). Changes in strawberry anthocyanins and other polyphenols in response to carbon dioxide treatments. *Journal of Agricultural and Food Chemistry, 45*(5), 1662-1667.

Grzegorzewski, F., Ehlbeck, J., Schlüter, O., Kroh, L. W., & Rohn, S. (2011). Treating lamb's lettuce with a cold plasma–Influence of atmospheric pressure Ar plasma immanent species on the phenolic profile of *Valerianella locusta*. *LWT-Food Science and Technology, 44*(10), 2285-2289.

Grzegorzewski, F., Rohn, S., Kroh, L. W., Geyer, M., & Schlüter, O. (2010). Surface morphology and chemical composition of lamb's lettuce (*Valerianella locusta*) after exposure to a low-pressure oxygen plasma. *Food Chemistry, 122*(4), 1145-1152.

Gutiérrez, D. R., Lemos, L., & Rodríguez, S. d. C. (2018a). Effect of UV-C and ozone on the bioactive compounds and antioxidant capacity of minimally processed rocket (*Eruca Sativa* Mill.). *Int. J. New Technol. Res, 4*, 23-29.

Gutiérrez, D. R., Lemos, L., & Rodríguez, S. d. C. (2018b). Effect of UV-C and ozone on the bioactive compounds and antioxidant capacity of minimally processed rocket (Eruca Sativa Mill.). *International Journal of New Technology and Research, 4*(9).

Herceg, Z., Kovačević, D. B., Kljusurić, J. G., Jambrak, A. R., Zorić, Z., & Dragović-Uzelac, V. (2016). Gas phase plasma impact on phenolic compounds in pomegranate juice. *Food Chemistry, 190*, 665-672.

Heredia, J. B., & Cisneros-Zevallos, L. (2009). The effect of exogenous ethylene and methyl jasmonate on pal activity, phenolic profiles and antioxidant capacity of carrots (*Daucus carota*) under different wounding intensities. *Postharvest Biology and Technology, 51*(2), 242-249.

Hou, Y., Wang, R., Gan, Z., Shao, T., Zhang, X., He, M., & Sun, A. (2019). Effect of cold plasma on blueberry juice quality. *Food Chemistry, 290*, 79-86.

Hu, C.-J., Li, D., Ma, Y.-X., Zhang, W., Lin, C., Zheng, X.-Q., Liang, Y.-R., & Lu, J.-L. (2018). Formation mechanism of the oolong tea characteristic aroma during bruising and withering treatment. *Food Chemistry, 269*, 202-211.

Huang, S., Lim, S. Y., Lau, H., Ni, W., & Li, S. F. Y. (2022). Effect of glycinebetaine on metabolite profiles of cold-stored strawberry revealed by 1H NMR-based metabolomics. *Food Chemistry, 393*, 133452.

Idehen, E., Tang, Y., & Sang, S. (2017). Bioactive phytochemicals in barley. *Journal of Food and Drug Analysis, 25*(1), 148-161.

Illera, A., Chaple, S., Sanz, M., Ng, S., Lu, P., Jones, J., Carey, E., & Bourke, P. (2019). Effect of cold plasma on polyphenol oxidase inactivation in cloudy apple juice and on the quality parameters of the juice during storage. *Food Chemistry: X, 3*, 100049.

Ismail, H. I., Chan, K. W., Mariod, A. A., & Ismail, M. (2010). Phenolic content and antioxidant activity of cantaloupe (*Cucumis melo*) methanolic extracts. *Food Chemistry, 119*(2), 643-647.

Jirovetz, L., Smith, D., & Buchbauer, G. (2002). Aroma compound analysis of *Eruca sativa* (Brassicaceae) SPME headspace leaf samples using GC, GC− MS, and olfactometry. *Journal of Agricultural and Food Chemistry, 50*(16), 4643-4646.

Jonvik, K. L., Nyakayiru, J., Pinckaers, P. J., Senden, J. M., van Loon, L. J., & Verdijk, L. B. (2016). Nitrate-rich vegetables increase plasma nitrate and nitrite concentrations and lower blood pressure in healthy adults. *The Journal of nutrition, 146*(5), 986-993.

Kasim, R., & Kasim, M. U. (2014). Biochemical and color changes of fresh-cut melon (*Cucumis melo* L. cv. Galia) treated with UV-C. *Food Science and Technology, 34*, 547-551.

Kaur, K., Pandiselvam, R., Kothakota, A., Ishwarya, S. P., Zalpouri, R., & Mahanti, N. K. (2022). Impact of ozone treatment on food polyphenols–A comprehensive review. *Food Control*, 109207.

Keshavarzi, M., Najafi, G., Ahmadi Gavlighi, H., Seyfi, P., & Ghomi, H. (2020). Enhancement of polyphenolic content extraction rate with maximal antioxidant activity from green tea leaves by cold plasma. *Journal of Food Science, 85*(10), 3415-3422.

Keyata, E. O., Tola, Y. B., Bultosa, G., & Forsido, S. F. (2021). Phytochemical contents, antioxidant activity and functional properties of *Raphanus sativus* L, *Eruca sativa* L. and *Hibiscus sabdariffa* L. growing in Ethiopia. *Heliyon, 7*(1), e05939.

Khoobchandani, M., Ganesh, N., Gabbanini, S., Valgimigli, L., & Srivastava, M. (2011). Phytochemical potential of *Eruca sativa* for inhibition of melanoma tumor growth. *Fitoterapia, 82*(4), 647-653.

Kodama, S., Thawatchaipracha, B., & Sekiguchi, H. (2014). Enhancement of essential oil extraction for steam distillation by DBD surface treatment. *Plasma Processes and Polymers, 11*(2), 126-132.

Kolayli, S., Kara, M., Tezcan, F., Erim, F. B., Sahin, H., Ulusoy, E., & Aliyazicioglu, R. (2010). Comparative study of chemical and biochemical properties of different melon cultivars: Standard, hybrid, and grafted melons. *Journal of Agricultural and Food Chemistry, 58*(17), 9764-9769.

Korachi, M., Ozen, F., Aslan, N., Vannini, L., Guerzoni, M. E., Gottardi, D., & Ekinci, F. Y. (2015). Biochemical changes to milk following treatment by a novel, cold atmospheric plasma system. *International Dairy Journal, 42*, 64-69.

Koukounaras, A., Siomos, A. S., & Sfakiotakis, E. (2007). Postharvest CO2 and ethylene production and quality of rocket (Eruca sativa Mill.) leaves as affected by leaf age and storage temperature. *Postharvest Biology and Technology, 46*(2), 167-173.

Kovačević, D. B., Kljusurić, J. G., Putnik, P., Vukušić, T., Herceg, Z., & Dragović-Uzelac, V. (2016). Stability of polyphenols in chokeberry juice treated with gas phase plasma. *Food Chemistry, 212*, 323-331.

Kovačević, D. B., Putnik, P., Dragović-Uzelac, V., Pedisić, S., Jambrak, A. R., & Herceg, Z. (2016). Effects of cold atmospheric gas phase plasma on anthocyanins and color in pomegranate juice. *Food Chemistry, 190*, 317-323.

Kuchi, V. S., Ilahy, R., & Siddiqui, M. W. (2018). Commercial disinfectants in skirmishing postharvest diseases. *Postharvest Disinfection of Fruits and Vegetables*, 273-292.

Kumar, S., Pipliya, S., & Srivastav, P. P. (2023). Effect of cold plasma on different polyphenol compounds: A review. *Journal of Food Process Engineering, 46*(1), e14203.

Lacombe, A., Niemira, B. A., Gurtler, J. B., Fan, X., Sites, J., Boyd, G., & Chen, H. (2015). Atmospheric cold plasma inactivation of aerobic microorganisms on blueberries and effects on quality attributes. *Food Microbiology, 46*, 479-484.

Laurita, R., Gozzi, G., Tappi, S., Capelli, F., Bisag, A., Laghi, G., Gherardi, M., Cellini, B., Abouelenein, D., & Vittori, S. (2021). Effect of plasma activated water (PAW) on rocket leaves decontamination and nutritional value. *Innovative Food Science & Emerging Technologies*, 102805.

Lee, K. H., Woo, K. S., Yong, H. I., Jo, C., Lee, S. K., Lee, B. W., Oh, S.-K., Lee, Y.-Y., Lee, B., & Kim, H.-J. (2018). Assessment of microbial safety and quality changes of brown and white cooked rice treated with atmospheric pressure plasma. *Food Science and Biotechnology, 27*(3), 661-667.

Lee, L. C., Liong, C.-Y., & Jemain, A. A. (2018). Partial least squares-discriminant analysis (PLS-DA) for classification of high-dimensional (HD) data: a review of contemporary practice strategies and knowledge gaps. *Analyst, 143*(15), 3526-3539.

Leite, A. K., Fonteles, T. V., Miguel, T. B., da Silva, G. S., de Brito, E. S., Alves Filho, E. G., Fernandes, F. A., & Rodrigues, S. (2021). Atmospheric cold plasma frequency imparts changes on cashew apple juice composition and improves vitamin C bioaccessibility. *Food Research International, 147*, 110479.

Leitzke, A., Reisz, E., Flyunt, R., & von Sonntag, C. (2001). The reactions of ozone with cinnamic acids: formation and decay of 2-hydroperoxy-2-hydroxyacetic acid. *Journal of the Chemical Society, Perkin Transactions 2*(5), 793-797.

Leng, C., Zhang, Y., Wang, M., Wang, P., Gu, Z., & Yang, R. (2019). Dynamic variation of glucosinolates and isothiocyanates in broccoli sprouts during hydrolysis. *Scientia Horticulturae, 255*, 128-133.

Leonova, T., Popova, V., Tsarev, A., Henning, C., Antonova, K., Rogovskaya, N., Vikhnina, M., Soboleva, A., Dinastia, E., & Dorn, M. (2019). Drought-related changes in the metabolism and nutritional properties of mature pea (*Pisum sativum* L.) seeds in the context of protein glycation.

Li, L., Wu, Q., Wang, Y., Aghdam, M. S., Ban, Z., Zhang, X., Lu, H., Li, D., Yan, J., & Limwachiranon, J. (2019). Systematically quantitative proteomics and metabolite profiles offer insight into fruit ripening behavior in *Fragaria× ananassa*. *RSC advances, 9*(25), 14093-14108.

Li, M., Li, X., Han, C., Ji, N., Jin, P., & Zheng, Y. (2019). Physiological and metabolomic analysis of cold plasma treated fresh-cut strawberries. *Journal of Agricultural and Food Chemistry, 67*(14), 4043-4053.

Li, X., Li, M., Ji, N., Jin, P., Zhang, J., Zheng, Y., Zhang, X., & Li, F. (2019). Cold plasma treatment induces phenolic accumulation and enhances antioxidant activity in fresh-cut pitaya (*Hylocereus undatus*) fruit. *Lwt, 115*, 108447.

Liao, X., Li, J., Muhammad, A. I., Suo, Y., Chen, S., Ye, X., Liu, D., & Ding, T. (2018). Application of a dielectric barrier discharge atmospheric cold plasma (Dbd-Acp) for Eshcerichia coli inactivation in apple juice. *Journal of Food Science, 83*(2), 401-408.

Liao, X., Muhammad, A. I., Chen, S., Hu, Y., Ye, X., Liu, D., & Ding, T. (2019). Bacterial spore inactivation induced by cold plasma. *Critical Reviews in Food Science and Nutrition, 59*(16), 2562-2572.

Liu, J., Liu, M., He, C., Song, H., Guo, J., Wang, Y., Yang, H., & Su, X. (2015). A comparative study of aroma-active compounds between dark and milk chocolate: relationship to sensory perception. *Journal of the Science of Food and Agriculture, 95*(6), 1362-1372.

Liu, Q., Wu, H., Luo, J., Liu, J., Zhao, S., Hu, Q., & Ding, C. (2021). Effect of dielectric barrier discharge cold plasma treatments on flavor fingerprints of brown rice. *Food Chemistry, 352*, 129402.

López-Gámez, G., Elez-Martínez, P., Martín-Belloso, O., & Soliva-Fortuny, R. (2021). Recent advances toward the application of non-thermal technologies in food processing: An insight on the bioaccessibility of health-related constituents in plant-based products. *Foods, 10*(7), 1538.

Ma, R., Yu, S., Tian, Y., Wang, K., Sun, C., Li, X., Zhang, J., Chen, K., & Fang, J. (2016). Effect of non-thermal plasma-activated water on fruit decay and quality in postharvest Chinese bayberries. *Food and Bioprocess Technology, 9*, 1825-1834.

Ma, T., & Lan, W. (2015). Effects of non-thermal plasma sterilization on volatile components of tomato juice. *International Journal of Environmental Science and Technology, 12*, 3767-3772.

Mahmoud, B. S. (2012). Effects of X-ray treatments on pathogenic bacteria, inherent microflora, color, and firmness on whole cantaloupe. *International Journal of Food Microbiology, 156*(3), 296-300.

Maier-Maercker, U., & Koch, W. (1992). Histological examination of spruce needles from a long-term gas exchange experiment in pure and polluted air in the field. *Trees, 6*, 186-194.

Maietti, A., Tedeschi, P., Stagno, C., Bordiga, M., Travaglia, F., Locatelli, M., Arlorio, M., & Brandolini, V. (2012). Analytical traceability of melon (*Cucumis melo* var reticulatus): Proximate composition, bioactive compounds, and antioxidant capacity

in relation to cultivar, plant physiology state, and seasonal variability. *Journal of Food Science, 77*(6), C646-C652.

Mallek-Ayadi, S., Bahloul, N., Baklouti, S., & Kechaou, N. (2022). Bioactive compounds from *Cucumis melo* L. fruits as potential nutraceutical food ingredients and juice processing using membrane technology. *Food science & nutrition, 10*(9), 2922-2934.

Mandal, R., Singh, A., & Singh, A. P. (2018). Recent developments in cold plasma decontamination technology in the food industry. *Trends in Food Science & Technology, 80*, 93-103.

Manzocco, L., Da Pieve, S., & Maifreni, M. (2011). Impact of UV-C light on safety and quality of fresh-cut melon. *Innovative Food Science & Emerging Technologies, 12*(1), 13-17.

Marszałek, K., Woźniak, Ł., Kruszewski, B., & Skąpska, S. (2017). The effect of high pressure techniques on the stability of anthocyanins in fruit and vegetables. *International Journal of Molecular Sciences, 18*(2), 277.

Martínez-Sánchez, A., Allende, A., Bennett, R. N., Ferreres, F., & Gil, M. I. (2006). Microbial, nutritional and sensory quality of rocket leaves as affected by different sanitizers. *Postharvest Biology and Technology, 42*(1), 86-97.

Martínez, J. M., Delso, C., Angulo, J., Álvarez, I., & Raso, J. (2018). Pulsed electric field-assisted extraction of carotenoids from fresh biomass of *Rhodotorula glutinis*. *Innovative Food Science & Emerging Technologies, 47*, 421-427.

Martiñon, M. E., Moreira, R. G., Castell-Perez, M. E., & Gomes, C. (2014). Development of a multilayered antimicrobial edible coating for shelf-life extension of fresh-cut cantaloupe (*Cucumis melo* L.) stored at 4 C. *LWT-Food Science and Technology, 56*(2), 341-350.

Matłok, N., Piechowiak, T., Zardzewiały, M., & Balawejder, M. (2022). Effects of post-harvest ozone treatment on some molecular stability markers of *Amelanchier alnifolia* Nutt. fruit during cold storage. *International Journal of Molecular Sciences, 23*(19), 11152.

Mead, J. F. (1976). Free radical mechanisms of lipid damage and consequences for cellular membranes. *European Journal of Immunology, 9*, 426-433.

Mehta, D., Sharma, N., Bansal, V., Sangwan, R. S., & Yadav, S. K. (2019). Impact of ultrasonication, ultraviolet and atmospheric cold plasma processing on quality parameters of tomato-based beverage in comparison with thermal processing. *Innovative Food Science & Emerging Technologies, 52*, 343-349.

Mehta, D., & Yadav, S. K. (2020). Impact of atmospheric non-thermal plasma and hydrothermal treatment on bioactive compounds and microbial inactivation of strawberry juice: A hurdle technology approach. *Food Science and Technology International, 26*(1), 3-10.

Melchini, A., & Traka, M. H. (2010). Biological profile of erucin: a new promising anticancer agent from cruciferous vegetables. *Toxins, 2*(4), 593-612.

Mieszczakowska-Frąc, M., Celejewska, K., & Płocharski, W. (2021). Impact of innovative technologies on the content of vitamin C and its bioavailability from processed fruit and vegetable products. *Antioxidants, 10*(1), 54.

Mikulic-Petkovsek, M., Schmitzer, V., Slatnar, A., Weber, N., Veberic, R., Stampar, F., Munda, A., & Koron, D. (2013). Alteration of the content of primary and secondary metabolites in strawberry fruit by *Colletotrichum nymphaeae* infection. *Journal of Agricultural and Food Chemistry, 61*(25), 5987-5995.

Misra, N. (2015). The contribution of non-thermal and advanced oxidation technologies towards dissipation of pesticide residues. *Trends in Food Science & Technology, 45*(2), 229-244.

Misra, N. (2016). Quality of cold plasma treated plant foods. In *Cold plasma in food and agriculture*, (pp. 253-271): Elsevier.

Misra, N., & Jo, C. (2017). Applications of cold plasma technology for microbiological safety in meat industry. *Trends in Food Science & Technology, 64*, 74-86.

Misra, N., Moiseev, T., Patil, S., Pankaj, S., Bourke, P., Mosnier, J., Keener, K., & Cullen, P. (2014). Cold plasma in modified atmospheres for post-harvest treatment of strawberries. *Food and Bioprocess Technology, 7*(10), 3045-3054.

Misra, N., Pankaj, S., Frias, J., Keener, K., & Cullen, P. (2015). The effects of nonthermal plasma on chemical quality of strawberries. *Postharvest Biology and Technology, 110*, 197-202.

Misra, N., Patil, S., Moiseev, T., Bourke, P., Mosnier, J., Keener, K., & Cullen, P. (2014). In-package atmospheric pressure cold plasma treatment of strawberries. *Journal of Food Engineering, 125*, 131-138.

Misra, N., Schlüter, O., & Cullen, P. (2016). Chapter 1—plasma in food and agriculture. *Cold Plasma in Food and Agriculture; Misra, NN, Schlüter, O., Cullen, PJ, Eds*, 1-16.

Misra, N., Tiwari, B., Raghavarao, K., & Cullen, P. (2011). Nonthermal plasma inactivation of food-borne pathogens. *Food Engineering Reviews, 3*, 159-170.

Muhammad, A. I., Liao, X., Cullen, P. J., Liu, D., Xiang, Q., Wang, J., Chen, S., Ye, X., & Ding, T. (2018). Effects of nonthermal plasma technology on functional food components. *Comprehensive reviews in food science and food safety, 17*(5), 1379-1394.

Mullaney, J. A., Kelly, W. J., McGhie, T. K., Ansell, J., & Heyes, J. A. (2013). Lactic acid bacteria convert glucosinolates to nitriles efficiently yet differently from Enterobacteriaceae. *Journal of Agricultural and Food Chemistry, 61*(12), 3039-3046.

Munekata, P. E., Domínguez, R., Pateiro, M., & Lorenzo, J. M. (2020). Influence of Plasma Treatment on the Polyphenols of Food Products—A Review. *Foods, 9*(7), 929.

Mustafa, A. M., Angeloni, S., Abouelenein, D., Acquaticci, L., Xiao, J., Sagratini, G., Maggi, F., Vittori, S., & Caprioli, G. (2022). A new HPLC-MS/MS method for the simultaneous determination of 36 polyphenols in blueberry, strawberry and their commercial products and determination of antioxidant activity. *Food Chemistry, 367*, 130743.

Mustafa, A. M., Mazzara, E., Abouelenein, D., Angeloni, S., Nunez, S., Sagratini, G., López, V., Cespi, M., Vittori, S., & Caprioli, G. (2022). Optimization of Solvent-Free Microwave-Assisted Hydrodiffusion and Gravity Extraction of Morus nigra L. Fruits Maximizing Polyphenols, Sugar Content, and Biological Activities Using Central Composite Design. *Pharmaceuticals, 15*(1), 99.

Nicolau-Lapeña, I., Aguiló-Aguayo, I., Bobo, G., Viñas, I., Anguera, M., & Abadias, M. (2022). Ferulic acid application to control growth *Listeria monocytogenes* and *Salmonella enterica* on fresh-cut apples and melon, and its effect in quality parameters. *Postharvest Biology and Technology, 186*, 111831.

Nunes, T. P., Martins, C. G., Faria, A. F., Bíscola, V., de Oliveira Souza, K. L., Mercadante, A. Z., Cordenunsi, B. R., & Landgraf, M. (2013). Changes in total ascorbic acid and carotenoids in minimally processed irradiated Arugula (*Eruca sativa* Mill) stored under refrigeration. *Radiation Physics and Chemistry, 90*, 125-130.

Nwabor, O. F., Onyeaka, H., Miri, T., Obileke, K., Anumudu, C., & Hart, A. (2022). A cold plasma technology for ensuring the microbiological safety and quality of foods. *Food Engineering Reviews, 14*(4), 535-554.

Nzekoue, F. K., Caprioli, G., Ricciutelli, M., Cortese, M., Alesi, A., Vittori, S., & Sagratini, G. (2020). Development of an innovative phytosterol derivatization method to improve the HPLC-DAD analysis and the ESI-MS detection of plant sterols/stanols. *Food Research International, 131*, 108998.

Odriozola-Serrano, I., Soliva-Fortuny, R., & Martín-Belloso, O. (2008). Phenolic acids, flavonoids, vitamin C and antioxidant capacity of strawberry juices processed by high-intensity pulsed electric fields or heat treatments. *European Food Research and Technology, 228*, 239-248.

Oh, Y. J., Song, A. Y., & Min, S. C. (2017). Inhibition of *Salmonella typhimurium* on radish sprouts using nitrogen-cold plasma. *International Journal of Food Microbiology, 249*, 66-71.

Okmen, Z. A., & Bayindirli, A. L. (1999). Effect of microwave processing on water soluble vitamins: Kinetic parameters. *International Journal of Food Properties, 2*(3), 255-264.

Oms-Oliu, G., Martínez, R. R.-M., Soliva-Fortuny, R., & Martín-Belloso, O. (2008). Effect of superatmospheric and low oxygen modified atmospheres on shelf-life extension of fresh-cut melon. *Food Control, 19*(2), 191-199.

Oulad El Majdoub, Y., Alibrando, F., Cacciola, F., Arena, K., Pagnotta, E., Matteo, R., Micalizzi, G., Dugo, L., Dugo, P., & Mondello, L. (2020). Chemical characterization of three accessions of *Brassica juncea* L. extracts from different plant tissues. *Molecules, 25*(22), 5421.

Paixão, L., Fonteles, T. V., Oliveira, V. S., Fernandes, F. A., & Rodrigues, S. (2019). Cold plasma effects on functional compounds of siriguela juice. *Food and Bioprocess Technology, 12*(1), 110-121.

Pal, P., Kaur, P., Singh, N., Kaur, A., Misra, N., Tiwari, B. K., Cullen, P. J., & Virdi, A. S. (2016). Effect of nonthermal plasma on physico-chemical, amino acid composition, pasting and protein characteristics of short and long grain rice flour. *Food Research International, 81*, 50-57.

Palekar, M. P., Taylor, T. M., Maxim, J. E., & Castillo, A. (2015). Reduction of *Salmonella enterica* serotype Poona and background microbiota on fresh-cut cantaloupe by electron beam irradiation. *International Journal of Food Microbiology, 202*, 66-72.

Pankaj, S. K., Bueno-Ferrer, C., Misra, N., Milosavljević, V., O'donnell, C., Bourke, P., Keener, K., & Cullen, P. (2014). Applications of cold plasma technology in food packaging. *Trends in Food Science & Technology, 35*(1), 5-17.

Pankaj, S. K., Wan, Z., Colonna, W., & Keener, K. M. (2017). Effect of high voltage atmospheric cold plasma on white grape juice quality. *Journal of the Science of Food and Agriculture, 97*(12), 4016-4021.

Pankaj, S. K., Wan, Z., & Keener, K. M. (2018). Effects of cold plasma on food quality: A review. *Foods, 7*(1), 4.

Patra, A., Prasath, V. A., Pandiselvam, R., Sutar, P. P., & Jeevarathinam, G. (2022). Effect of plasma activated water (PAW) on physicochemical and functional properties of foods. *Food Control*, 109268.

Pavlovska, G., Dukovska, E., Antoska-Knights, V., & Jankuloska, V. (2015). Influence of temperature of storage on amount of vitamin C in strawberries". *Journal of Hygienic Engineering and Design, 11*, 15-19.

Pedrosa, M. C., Lima, L., Heleno, S., Carocho, M., Ferreira, I. C., & Barros, L. (2021). Food metabolites as tools for authentication, processing, and nutritive value assessment. *Foods, 10*(9), 2213.

Pérez-Andrés, J. M., Cropotova, J., Harrison, S. M., Brunton, N. P., Cullen, P. J., Rustad, T., & Tiwari, B. K. (2020). Effect of cold plasma on meat cholesterol and lipid oxidation. *Foods, 9*(12), 1786.

Piechowiak, T., & Balawejder, M. (2019). Impact of ozonation process on the level of selected oxidative stress markers in raspberries stored at room temperature. *Food Chemistry, 298*, 125093.

Porto, E., Alves Filho, E. G., Silva, L. M. A., Fonteles, T. V., do Nascimento, R. B. R., Fernandes, F. A., de Brito, E. S., & Rodrigues, S. (2020). Ozone and plasma processing effect on green coconut water. *Food Research International, 131*, 109000.

Pour, A. K., Khorram, S., Ehsani, A., Ostadrahimi, A., & Ghasempour, Z. (2022). Atmospheric cold plasma effect on quality attributes of banana slices: Its potential use in blanching process. *Innovative Food Science & Emerging Technologies, 76*, 102945.

Puligundla, P., Lee, T., & Mok, C. (2020). Effect of corona discharge plasma jet treatment on the degradation of aflatoxin B1 on glass slides and in spiked food commodities. *Lwt, 124*, 108333.

Punia Bangar, S., Suri, S., Nayi, P., & Phimolsiripol, Y. (2022). Cold plasma for microbial safety: Principle, mechanism, and factors responsible. *Journal of Food Processing and Preservation*, e16850.

Raffo, A., Masci, M., Moneta, E., Nicoli, S., Del Pulgar, J. S., & Paoletti, F. (2018). Characterization of volatiles and identification of odor-active compounds of rocket leaves. *Food Chemistry, 240*, 1161-1170.

Ramazzina, I., Berardinelli, A., Rizzi, F., Tappi, S., Ragni, L., Sacchetti, G., & Rocculi, P. (2015). Effect of cold plasma treatment on physico-chemical parameters and antioxidant activity of minimally processed kiwifruit. *Postharvest Biology and Technology, 107*, 55-65.

Ramazzina, I., Tappi, S., Rocculi, P., Sacchetti, G., Berardinelli, A., Marseglia, A., & Rizzi, F. (2016). Effect of cold plasma treatment on the functional properties of fresh-cut apples. *Journal of Agricultural and Food Chemistry, 64*(42), 8010-8018.

Reddy, M. B., & Love, M. (1999). The impact of food processing on the nutritional quality of vitamins and minerals. *Impact of processing on food safety*, 99-106.

Richards, G. M., & Beuchat, L. R. (2004). Attachment of *Salmonella Poona* to cantaloupe rind and stem scar tissues as affected by temperature of fruit and inoculum. *Journal of Food Protection, 67*(7), 1359-1364.

Rodríguez, Ó., Gomes, W. F., Rodrigues, S., & Fernandes, F. A. (2017). Effect of indirect cold plasma treatment on cashew apple juice (*Anacardium occidentale* L.). *Lwt, 84*, 457-463.

Ruther, J., & Kleier, S. (2005). Plant–plant signaling: ethylene synergizes volatile emission in *Zea mays* induced by exposure to (Z)-3-hexen-1-ol. *Journal of Chemical Ecology, 31*(9), 2217-2222.

Sadiq, A., Hayat, M. Q., & Mall, S. M. (2014). Qualitative and quantitative determination of secondary metabolites and antioxidant potential of *Eruca sativa*. *Nat. Prod. Chem. Res, 2*(4), 137.

Saengha, W., Karirat, T., Buranrat, B., Matra, K., Deeseenthum, S., Katisart, T., & Luang-In, V. (2021). Cold plasma treatment on mustard green seeds and its effect on

growth, isothiocyanates, antioxidant activity and anticancer activity of microgreens. *Int. J. Agric. Biol, 25*(3).

Sakudo, A., Misawa, T., & Yagyu, Y. (2020). Equipment design for cold plasma disinfection of food products. In *Advances in cold plasma applications for food safety and preservation*, (pp. 289-307): Elsevier.

Salazar-Orbea, G. L., García-Villalba, R., Bernal, M. J., Hernández, A., Tomás-Barberán, F. A., & Sánchez-Siles, L. M. (2023). Stability of phenolic compounds in apple and strawberry: Effect of different processing techniques in industrial set up. *Food Chemistry, 401*, 134099.

Santos Jr, L., Cubas, A., Moecke, E., Ribeiro, D., & Amante, E. (2018). Use of cold plasma to inactivate *Escherichia coli* and physicochemical evaluation in pumpkin puree. *Journal of Food Protection, 81*(11), 1897-1905.

Sarangapani, C., O'Toole, G., Cullen, P., & Bourke, P. (2017). Atmospheric cold plasma dissipation efficiency of agrochemicals on blueberries. *Innovative Food Science & Emerging Technologies, 44*, 235-241.

Saremnezhad, S., Soltani, M., Faraji, A., & Hayaloglu, A. A. (2021). Chemical changes of food constituents during cold plasma processing: A review. *Food Research International, 147*, 110552.

Schnabel, U., Niquet, R., Schlüter, O., Gniffke, H., & Ehlbeck, J. (2015). Decontamination and sensory properties of microbiologically contaminated fresh fruits and vegetables by microwave plasma processed air (PPA). *Journal of Food Processing and Preservation, 39*(6), 653-662.

Scholtz, V., Pazlarova, J., Souskova, H., Khun, J., & Julak, J. (2015). Nonthermal plasma—A tool for decontamination and disinfection. *Biotechnology Advances, 33*(6), 1108-1119.

Selma, M. V., Ibáñez, A. M., Cantwell, M., & Suslow, T. (2008). Reduction by gaseous ozone of Salmonella and microbial flora associated with fresh-cut cantaloupe. *Food Microbiology, 25*(4), 558-565.

Setsuhara, Y., Cho, K., Shiratani, M., Sekine, M., & Hori, M. (2013). Plasma interactions with aminoacid (l-alanine) as a basis of fundamental processes in plasma medicine. *Current Applied Physics, 13*, S59-S63.

Shirani, K., Shahidi, F., & Mortazavi, S. A. (2020). Investigation of decontamination effect of argon cold plasma on physicochemical and sensory properties of almond slices. *International Journal of Food Microbiology, 335*, 108892.

Silveira, A., Aguayo, E., & Artés, F. (2010). Emerging sanitizers and clean room packaging for improving the microbial quality of fresh-cut 'Galia'melon. *Food Control, 21*(6), 863-871.

Silveira, M. R., Coutinho, N. M., Esmerino, E. A., Moraes, J., Fernandes, L. M., Pimentel, T. C., Freitas, M. Q., Silva, M. C., Raices, R. S., & Ranadheera, C. S. (2019). Guava-flavored whey beverage processed by cold plasma technology: Bioactive compounds, fatty acid profile and volatile compounds. *Food Chemistry, 279*, 120-127.

Song, A. Y., Oh, Y. J., Kim, J. E., Song, K. B., Oh, D. H., & Min, S. C. (2015). Cold plasma treatment for microbial safety and preservation of fresh lettuce. *Food Science and Biotechnology, 24*, 1717-1724.

Spadafora, N. D., Amaro, A. L., Pereira, M. J., Müller, C. T., Pintado, M., & Rogers, H. J. (2016). Multi-trait analysis of post-harvest storage in rocket salad (*Diplotaxis tenuifolia*) links sensorial, volatile and nutritional data. *Food Chemistry, 211*, 114-123.

Sruthi, N., Josna, K., Pandiselvam, R., Kothakota, A., Gavahian, M., & Khaneghah, A. M. (2021). Impacts of cold plasma treatment on physicochemical, functional, bioactive, textural, and sensory attributes of food: a comprehensive review. *Food Chemistry*, 130809.

Starek, A., Pawłat, J., Chudzik, B., Kwiatkowski, M., Terebun, P., Sagan, A., & Andrejko, D. (2019). Evaluation of selected microbial and physicochemical parameters of fresh tomato juice after cold atmospheric pressure plasma treatment during refrigerated storage. *Scientific Reports, 9*(1), 1-11.

Stübler, A.-S., Lesmes, U., Juadjur, A., Heinz, V., Rauh, C., Shpigelman, A., & Aganovic, K. (2020). Impact of pilot-scale processing (thermal, PEF, HPP) on the stability and bioaccessibility of polyphenols and proteins in mixed protein-and polyphenol-rich juice systems. *Innovative Food Science & Emerging Technologies, 64*, 102426.

Sut, S., Boschiero, I., Solana, M., Malagoli, M., Bertucco, A., & Dall'Acqua, S. (2018). Supercritical CO2 extraction of *Eruca sativa* using cosolvents: Phytochemical composition by LC-MS analysis. *Molecules, 23*(12), 3240.

Tappi, S., Gozzi, G., Vannini, L., Berardinelli, A., Romani, S., Ragni, L., & Rocculi, P. (2016). Cold plasma treatment for fresh-cut melon stabilization. *Innovative Food Science & Emerging Technologies, 33*, 225-233.

Tappi, S., Ramazzina, I., Rizzi, F., Sacchetti, G., Ragni, L., & Rocculi, P. (2018). Effect of plasma exposure time on the polyphenolic profile and antioxidant activity of fresh-cut apples. *Applied Sciences, 8*(10), 1939.

Taviano, M. F., Cavò, E., Spadaro, V., Raimondo, F. M., Musolino, V., Cacciola, F., El Majdoub, Y. O., Mondello, L., Condurso, C., & Cincotta, F. (2021). Phytochemical constituents, antioxidant activity, and toxicity assessment of the aerial part extracts from the infraspecific taxa of *Matthiola fruticulosa* (Brassicaceae) endemic to Sicily. *Molecules, 26*(14), 4114.

Tawfik, M. M., Yamato, K. T., Kohchi, T., Koeduka, T., & Matsui, K. (2017). *n*-Hexanal and (Z)-3-hexenal are generated from arachidonic acid and linolenic acid by a lipoxygenase in *Marchantia polymorpha* L. *Bioscience, Biotechnology, and Biochemistry, 81*(6), 1148-1155.

Thirumdas, R., Deshmukh, R., & Annapure, U. (2016). Effect of low temperature plasma on the functional properties of basmati rice flour. *Journal of food science and technology, 53*, 2742-2751.

Tremarin, A., Brandão, T. R., & Silva, C. L. (2017). Inactivation kinetics of *Alicyclobacillus acidoterrestris* in apple juice submitted to ultraviolet radiation. *Food Control, 73*, 18-23.

Uarrota, V. G., Fuentealba, C., Hernández, I., Defilippi-Bruzzone, B., Meneses, C., Campos-Vargas, R., Lurie, S., Hertog, M., Carpentier, S., & Poblete-Echeverría, C. (2019). Integration of proteomics and metabolomics data of early and middle season *Hass avocados* under heat treatment. *Food Chemistry, 289*, 512-521.

Uddin, M., Hawlader, M., Ding, L., & Mujumdar, A. (2002). Degradation of ascorbic acid in dried guava during storage. *Journal of Food Engineering, 51*(1), 21-26.

Ukuku, D. O., Huang, L., & Sommers, C. (2015). Efficacy of sanitizer treatments on survival and growth parameters of *Escherichia coli* O157: H7, Salmonella, and *Listeria monocytogene*s on fresh-cut pieces of cantaloupe during storage. *Journal of Food Protection, 78*(7), 1288-1295.

Van Durme, J., & Vandamme, J. (2016). Non-thermal plasma as preparative technique to evaluate olive oil adulteration. *Food Chemistry, 208*, 185-191.

Vaughn, S. F., & Berhow, M. A. (2005). Glucosinolate hydrolysis products from various plant sources: pH effects, isolation, and purification. *Industrial Crops and Products, 21*(2), 193-202.

Villarreal, N. M., Bustamante, C. A., Civello, P. M., & Martínez, G. A. (2010). Effect of ethylene and 1-MCP treatments on strawberry fruit ripening. *Journal of the Science of Food and Agriculture, 90*(4), 683-689.

Villatoro-Pulido, M., Priego-Capote, F., Álvarez-Sánchez, B., Saha, S., Philo, M., Obregón-Cano, S., De Haro-Bailón, A., Font, R., & Del Río-Celestino, M. (2013). An approach to the phytochemical profiling of rocket [*Eruca sativa* (Mill.) Thell]. *Journal of the Science of Food and Agriculture, 93*(15), 3809-3819.

Wang, Q., & Salvi, D. (2021). Recent progress in the application of plasma-activated water (PAW) for food decontamination. *Current Opinion in Food Science, 42*, 51-60.

Wang, R., Nian, W., Wu, H., Feng, H., Zhang, K., Zhang, J., Zhu, W., Becker, K., & Fang, J. (2012). Atmospheric-pressure cold plasma treatment of contaminated fresh fruit and vegetable slices: inactivation and physiochemical properties evaluation. *The European Physical Journal D, 66*(10), 1-7.

Wang, Y., Wang, Z., Zhu, X., Yuan, Y., Gao, Z., & Yue, T. (2020). Application of electrical discharge plasma on the inactivation of *Zygosaccharomyces rouxii* in apple juice. *Lwt, 121*, 108974.

Wąsowicz, E., Gramza, A., Hęś, M., Jeleń, H. H., Korczak, J., Małecka, M., Mildner-Szkudlarz, S., Rudziñska, M., Samotyja, U., & Zawirska-Wojtasiak, R. (2004). Oxidation of lipids in food. *Pol J Food Nutr Sci, 13*(54), 87-100.

Wojtasik-Kalinowska, I., Szpicer, A., Binkowska, W., Hanula, M., Marcinkowska-Lesiak, M., & Poltorak, A. (2023). Effect of processing on volatile organic compounds formation of meat. *Applied Sciences, 13*(2), 705.

Won, M. Y., Lee, S. J., & Min, S. C. (2017). Mandarin preservation by microwave-powered cold plasma treatment. *Innovative Food Science & Emerging Technologies, 39*, 25-32.

Worley, B., & Powers, R. (2013). Multivariate analysis in metabolomics. *Current metabolomics, 1*(1), 92-107.

Xu, L., Garner, A. L., Tao, B., & Keener, K. M. (2017). Microbial inactivation and quality changes in orange juice treated by high voltage atmospheric cold plasma. *Food and Bioprocess Technology, 10*(10), 1778-1791.

Xu, W., Mann, S., Curone, G., & Kenéz, Á. (2021). Heat treatment of bovine colostrum: effects on colostrum metabolome and serum metabolome of calves. *Animal, 15*(4), 100180.

Xu, Y., Tian, Y., Ma, R., Liu, Q., & Zhang, J. (2016). Effect of plasma activated water on the postharvest quality of button mushrooms, *Agaricus bisporus*. *Food Chemistry, 197*, 436-444.

Yodpitak, S., Mahatheeranont, S., Boonyawan, D., Sookwong, P., Roytrakul, S., & Norkaew, O. (2019). Cold plasma treatment to improve germination and enhance the bioactive phytochemical content of germinated brown rice. *Food Chemistry, 289*, 328-339.

Zargarchi, S., & Saremnezhad, S. (2019). Gamma-aminobutyric acid, phenolics and antioxidant capacity of germinated indica paddy rice as affected by low-pressure plasma treatment. *Lwt, 102*, 291-294.

Zhang, B.-Y., Samapundo, S., Pothakos, V., Sürengil, G., & Devlieghere, F. (2013). Effect of high oxygen and high carbon dioxide atmosphere packaging on the microbial spoilage and shelf-life of fresh-cut honeydew melon. *International Journal of Food Microbiology, 166*(3), 378-390.

Zhang, B., Tan, C., Zou, F., Sun, Y., Shang, N., & Wu, W. (2022). Impacts of cold plasma technology on sensory, nutritional and safety quality of food: A review. *Foods, 11*(18), 2818.

Zhang, Z. H., Wang, L. H., Zeng, X. A., Han, Z., & Brennan, C. S. (2019). Non-thermal technologies and its current and future application in the food industry: a review. *International Journal of Food Science & Technology, 54*(1), 1-13.

Zheng, H.-z., Hwang, I.-W., & Chung, S.-K. (2009). Enhancing polyphenol extraction from unripe apples by carbohydrate-hydrolyzing enzymes. *Journal of Zhejiang University Science B, 10*(12), 912.

Zhou, D., Li, T., Cong, K., Suo, A., & Wu, C. (2022). Influence of cold plasma on quality attributes and aroma compounds in fresh-cut cantaloupe during low temperature storage. *Lwt, 154*, 112893.

Zhou, D., Sun, R., Zhu, W., Shi, Y., Ni, S., Wu, C., & Li, T. (2023). Impact of dielectric barrier discharge cold plasma on the quality and phenolic metabolism in blueberries based on metabonomic analysis. *Postharvest Biology and Technology, 197*, 112208.

Zhu, L., Wei, Q., Porchas, M., Brierley, P., Friedman, M., Crosby, K., Patil, B., & Ravishankar, S. (2022). Plant-based antimicrobials inactivate *Listeria monocytogenes* and *Salmonella enterica* on melons grown in different regions of the United States. *Food Microbiology, 101*, 103876.

Zhu, X., Jiang, J., Yin, C., Li, G., Jiang, Y., & Shan, Y. (2019). Effect of ozone treatment on flavonoid accumulation of Satsuma mandarin (*Citrus unshiu* Marc.) during ambient storage. *Biomolecules, 9*(12), 821.

Žnidarčič, D., Ban, D., & Šircelj, H. (2011). Carotenoid and chlorophyll composition of commonly consumed leafy vegetables in Mediterranean countries. *Food Chemistry, 129*(3), 1164-1168.